Revêtements UV-aqueux pour le bois renforcés par la Cellulose Nano-Cristalline

Thèse

Vahe Vardanyan

Doctorat en sciences du bois
Philosophiae Doctor (Ph.D.)

Québec, Canada

© Vahe Vardanyan, 2015

Résumé

La présente thèse vise à augmenter la performance de revêtements UV-aqueux pour le bois, en utilisant la ressource forestière. Dans ce but, nous pensons remplacer les nanoparticules étudiées précédemment par de la cellulose nanocristalline (CNC), un produit canadien et québécois, issu de la forêt. Il existe plusieurs cas dans la littérature de composites de nanocellulose-thermoplastique, mais il y a peu d'études sur les revêtements renforcés par des CNC. L'un des aspects clés de la technologie des nanocomposites reste la dispersion des nanoparticules dans la matrice. Pour quantifier la qualité de la dispersion, des méthodes efficaces de caractérisation sont nécessaires. Dans cette thèse, deux nouvelles méthodes de caractérisation basées sur la microscopie à force atomique et la rétrodiffusion de la lumière laser (He-Ne 632,8 nm) sont appliquées pour caractériser ces revêtements nanocomposites. Une forte corrélation entre la nano-rugosité de surface du revêtement et la distribution angulaire de la lumière du laser rétrodiffusée a été constatée.

L'objectif général de cette recherche est de développer des revêtements UV-aqueux renforcées par les nanoparticules pour les applications sur le bois, et d'étudier l'effet, principalement sur les propriétés d'usure, des revêtements composites. Les CNC ont été mélangées à la formulation de revêtements dans le but d'améliorer les propriétés mécaniques des revêtements secs. Les formulations de revêtements ont été pulvérisées sur des planches d'érable à sucre, qui ont été ensuite placées dans un four pour évaporer l'eau et cuire le revêtement par rayonnement UV. Les CNC ont été modifiées soit par les bromures d'ammonium quaternaire alkylés ou le chlorure d'acryloyle. Les propriétés mécaniques (résistances à l'abrasion et égratignure, la dureté et l'adhérence) ont été analysées et comparées à celles des vernis de référence sans nanoparticules. L'ajout de la CNC modifiée dans les revêtements UV-aqueux a entraîné une augmentation de 30-40% de la résistance à l'usure (abrasion et égratignure), sans perte d'apparence. Ces revêtements sur substrat de bois, avec et CNC ajoutée, ont été soumis à un vieillissement accéléré pendant 1200 h. Les résultats montrent que l'ajout de CNC dans les revêtements non seulement augmente les propriétés mécaniques, mais augmente également la stabilité de la couleur des bois ainsi peints.

Abstract

This thesis is aimed to increase the performance of UV - waterborne coatings for wood, using the forest resources. For this purpose, we believe replacing nanoparticles studied previously by the cellulose nanocrystals (CNC), a Canadian and Quebec product from the forest. There are several instances in the literature of nanocellulose-thermoplastic composites, but there are few studies on coatings reinforced by CNC. One of the key aspects in the technology of nanocomposites remains the dispersion of the nanoparticles within the matrix. To quantify the dispersion, efficient methods of characterization are needed. In this thesis two new characterization methods based on atomic force microscopy and back scattering of laser light (He-Ne 632.8 nm) are applied to characterize such nanocomposite coatings. A strong correlation between surface nano-roughness of coatings and angular distribution of backscattered laser light was found.

The overall objective of the research is to develop nanoparticles reinforced UV-water-based coatings for wood applications, and to study the effect mainly on wear properties of the final composite coatings. CNC were mixed to the coating formulation in order to improve the mechanical properties of the coatings. The coating formulations were sprayed on sugar maple boards, which were then placed in an oven to evaporate the water to finally be UV-cured. CNC was modified by either alkyl quaternary ammonium bromides or acryloyl chloride. The mechanical properties (abrasion and scratch resistances, hardness and adhesion) were analyzed and compared to the reference varnish without nanoparticles. The modified CNC addition in UV-water-based coatings results in a ca 30 - 40% increase in wear resistance (abrasion and scratch), without any loss of appearance. These coatings on wood substrate, with and without added CNC, were submitted to accelerated weathering during 1200 h. The results show that the addition of CNC to coatings not only increases mechanical properties but also increases color stability of coated wood.

Table des matières

Liste des tableaux

Liste des figures

À toi Papa

Remerciements

Mes remerciements vont tout d'abord mes directeurs de thèse Prof. Bernard Riedl et Prof. Tigran Galstian, qui par leur collaboration ont permis la naissance de ce projet.

Je remercie Prof. Riedl pour son support constant dans tous les aspects, particulièrement pour son accueil chaleureux et pour m'avoir aidé à passer facilement à un tout nouveau domaine d'étude pour moi. Je le remercie pour sa grande patience et pour m'avoir enseigné à faire du ski et survivre dans le pays d'hiver. ☺

Je remercie Prof. Galstian qui m'a invité à faire une recherche à l'Université Laval et qui m'a bien montré qu'un physicien peut travailler sur n'importe quel domaine de science.

Je tiens à remercier le Fond Québécois de Recherche sur la Nature et les Technologies (FQRNT) et NanoQuébec pour leur soutien financier. Je remercie le Centre d'Optique, Photonique et Laser (COPL), le Centre de Recherche sur les Matériaux Renouvelables (CRMR), FPInnovations et l'Université Laval pour le soutien matériel et administratif qu'ils m'ont apporté.

Je remercie Dr. Bouddah Poaty-Poaty, qui m'a bien aidé à commencer ce projet, pour l'orientation et dévouement consacrés à cette étude. Je remercie Dr. Gregory Chauve et Dr. Véronic Landry, les chercheurs de FPInnovations, pour leur grande aide pendant les rédactions des articles. J'exprime également mes remerciements à Luana Wilczak, stagiaire d'été, qui m'a grandement aidé dans l'avancement de mes travaux.

Je ne pouvais oublier de remercier tous les techniciens du COPL et CRMR et tout particulièrement Patrick Larochelle, Yves Bédard, Benoit St-Pierre, Hugues Auger, Daniel Bourgault, Luc Germain, Sylvain Auger, Daniel Gingras, Rodica Neagu Plesu, Daniel Gingras et notre informaticien Martin Blouin. Et bien sûr je remercie Mme Guylaine Bélanger, qui est toujours très gentille et toujours prête pour résoudre les problèmes …

Je remercie tous mes amis et collègues de travail, je voudrais exprimer ma satisfaction de pouvoir étudier et travailler avec eux pendant la durée de ce projet. Leur soutien a été indispensable.

Mes grands remerciements vont à Anush Stepanyan, mon amour, qui a été toujours à côté de moi et m'a donné l'énergie pour continuer les travaux. Je t'aime beaucoup!

Enfin, toute ma profonde gratitude va à mes parents et mon frère qui m'ont vraiment encouragé dans mes études universitaires. Merci à toi Papa d'avoir toujours eu confiance en moi, d'avoir cru en moi, de m'avoir toujours soutenu tout au long de mon parcours scolaire et tout particulièrement lors de mon doctorat. Merci pour tout!

Avant-propos

Le présent travail a été réalisé sous la direction de M. Bernard Riedl, professeur titulaire au Département des Sciences du Bois et de la Forêt de l'Université Laval et sous la codirection de M. Tigran Galstian, professeur titulaire au Département de Physique, de Génie Physique et d'Optique de l'Université Laval. Ce travail de recherche a été effectué dans plusieurs laboratoires à Québec (Centre d'Optique Photonique et Laser (COPL), Centre de Recherche sur les Matériaux Renouvelables (CRMR) et FPInnovations) et à Montréal (FPInnovations) grâce aux financements offerts par le Fonds de Recherche Nature et Technologie du Québec (FRNTQ), Conseil de Recherches en Sciences Naturelles et Génie du Canada (CRSNG), ArboraNano et NanoQuébec.

Ce document est présenté sous un format de thèse de publication. Il a été conçu selon les critères de présentation adoptés par la Faculté des études supérieures et postdoctorales (FESP) de l'Université Laval.

Dans cette thèse sont présentés quatre articles scientifiques et deux chapitres de livres rédigés en anglais.

Chapitre de livre 1 *(Chapitre 2)*.

Vardanyan V., Poaty B., Landry V., Chauve G., Galstian T. and Riedl B., *Wear resistance of nanocomposite coatings*, dans : *Anti-Abrasive Nanocoatings: Current and future applications*, Woodhead Publishing, 2014, Elsevier. En impression.

Contributions des auteurs:

Vahe Vardanyan – planification et réalisation expérimentale, interprétation et analyse des résultats et rédaction de chapitre.

Bouddah Poaty – aide dans la planification et réalisation expérimentale, conseiller pendant l'interprétation des résultats et la rédaction de chapitre.

Véronic Landy et Grégory Chauve – conseillers pendant la rédaction de chapitre.

Tigran Galstian et Bernard Riedl – vérifier l'ensemble des résultats préliminaires avant le début des essais finaux, aider l'auteur principal à interpréter certains résultats et apporter des corrections nécessaires aux chapitre avant leur soumission dans le livre.

Article 1 ***(Chapitre 3)*****.**

Poaty B., Vardanyan V., Wilczak L., Chauve G., and Riedl B. *Modification of cellulose nanocrystals as reinforcement derivatives for wood coatings.* Progress in Organic Coatings, 2014. **77**(4): p. 813-820.

Bouddah Poaty – planification et réalisation expérimentale, interprétation et analyse des résultats et rédaction de l'article.

Vahe Vardanyan – aide dans la planification et réalisation expérimentale, conseiller pendant l'interprétation et analyse des résultats et la rédaction de l'article.

Luana Wilczak – stagiaire d'été, planification et réalisation certaines travaux expérimentales.

Grégory Chauve – conseiller pendant la rédaction de l'article.

Bernard Riedl – vérifier l'ensemble des résultats préliminaires avant le début des essais finaux, aider l'auteur principal à interpréter certains résultats et apporter des corrections nécessaires aux articles avant leur soumission dans la revue scientifique.

Article 2 ***(Chapitre 4)*****.**

Vardanyan V., Poaty B., Chauve G., Landry V., Galstian T. and Riedl B., *Mechanical properties of UV-waterborne varnishes reinforced by cellulose nanocrystals.* Journal of Coatings Technology and Research, 2014. **11**(6): p. 841-852.

Contributions des auteurs:

Vahe Vardanyan – planification et réalisation expérimentale, interprétation et analyse des résultats et rédaction de l'article.

Bouddah Poaty – aide dans la planification et réalisation expérimentale, conseiller pendant l'interprétation des résultats et la rédaction de l'article.

Véronic Landy et Grégory Chauve – conseillers pendant la rédaction de l'article.

Tigran Galstian et Bernard Riedl – vérifier l'ensemble des résultats préliminaires avant le début des essais finaux, aider l'auteur principal à interpréter certains résultats et apporter des corrections nécessaires aux chapitre avant leur soumission la revue scientifique.

Article 3 ***(Chapitre 5).***

Vardanyan V., Galstian T. and Riedl B., *Characterization of cellulose nanocrystals dispersion in varnishes by back scattering of laser light,* Journal of Coatings Technology and Research, 2014, soumis.

Contributions des auteurs:

Vahe Vardanyan – planification et réalisation expérimentale, interprétation et analyse des résultats et rédaction de l'article.

Tigran Galstian et Bernard Riedl – vérifier l'ensemble des résultats préliminaires avant le début des essais finaux, aider l'auteur principal à interpréter certains résultats et apporter des corrections nécessaires aux chapitre avant leur soumission dans la revue scientifique.

Article 4 ***(Chapitre 6).***

Vardanyan V., Galstian T. and Riedl B., *Effect of addition of cellulose nanocrystals to wood coatings on color changes and surface roughness due to accelerated weathering,* Journal of Coatings Technology and Research, 2014, en impression.

Contributions des auteurs:

Vahe Vardanyan – planification et réalisation expérimentale, interprétation et analyse des résultats et rédaction de l'article.

Tigran Galstian et Bernard Riedl – vérifier l'ensemble des résultats préliminaires avant le début des essais finaux, aider l'auteur principal à interpréter certains résultats et apporter des corrections nécessaires aux chapitre avant leur soumission dans la revue scientifique.

Chapitre de livre 2 ***(Annexe A).***

Riedl B. Vardanyan V., Nguengang W., Kaboorani A., Landry V., Poaty B., Vlad Cristea M., Sow C., *Nanocomposite coatings*, dans: *Functional Materials: Energy, Sustainable Development and Biomedical Sciences*. 2014, M. Leclerc, R. Gauvin, Ed., De Gruiter. p. 443-464 (2014).

Contributions des auteurs:

Bernard Riedl – planification, interprétation et analyse des résultats et rédaction de chapitre.

Vahe Vardanyan, William Nguegang, Ali Kaboorani, Véronic Landry, Bouddah Poaty, Mirela Vlad Cristea et Caroline Sow – présentation des résultats et conseillers pendant la rédaction du chapitre.

Les résultats issus de ce travail de recherche ont également fait l'objet de présentations orales et d'affiches techniques lors de congrès scientifiques.

Présentations orales

1. *Inclusion of nanocellulose in coatings for wood,* TAPPI international conference on nanotechnology, 12 mai 2012, Montréal, Canada.

2. *Revêtements nanocomposites UV-aqueux pour le bois,* Colloque du CRB, 30 novembre 2012, Québec, Canada.

3. *Les propriétés mécaniques des revêtements UV-aqueux renforcées par la nanocristalline cellulose,* Colloque Etudiant du CERMA, 13 septembre 2013, Québec, Canada.

4. *Revêtements nanocomposites UV-aqueux pour le bois,* 2e Colloque étudiant du CRIBIQ, 24 septembre 2013, Trois-Rivières, Canada.

5. *Wear and weathering resistance of UV-curable of wood water-based coatings with added cellulose nanocrystals,* FIBRE Cross-Country/Cross-Linking Workshop, 1 novembre 2013, Montréal, Canada.

Présentations affiches

1. *Intégration de nanocellulose cristalline dans des revêtements pour le bois,* NanoQuebec 2012 "Nanotechnologies: sources of innovation and competitiveness", 21 mars 2012, Montréal, Canada.

2. *Caractérisation de la dispersion de la nanocellulose cristalline dans les revêtements par microscopie à force atomique,* 5^{e} Colloque annuel du CQMF, 2 novembre 2012, Trois-Rivières, Canada.

3. *Caractérisation de la dispersion de la nanocellulose cristalline dans les revêtements par rétrodiffusion de la lumière,* Journée du COPL, 13 mai 2013, Montréal, Canada.

4. *Wear resistance of UV-curable of wood water-based coatings with added cellulose nanocrystals,* NANOCON 2013, 16-18 octobre 2013, Brno, République Tchèque.

5. *Characterization of nanocrystalline cellulose dispersion in varnishes by back scattering of laser light,* IONS-2014, 24-27 mai 2014, Montréal, Canada.

6. *Caractérisation de la dispersion de la nanocellulose cristalline dans les revêtements par rétrodiffusion de la lumière,* Colloque Etudiant du CERMA, 28 octobre 2014, Québec, Canada.

Introduction générale

La nature est parfaite! Depuis l'enfance en disant « la nature », j'avais toujours imaginé une forêt et des arbres. C'est magnifique! On a beaucoup des choses à apprendre de la nature et c'est pour ça qu'on a créé des sciences de la nature. Pendant milliards des années d'évolution (3,5-3,8 milliard [1, 2]) la nature a créé des mécanismes de protection pour continuer son existence. Comme une des beaux représentants de la chaîne de l'évolution, le bois, lui aussi, a bien avancé dans l'art de survivre. L'écorce du bois protège l'arbre contre des impacts mécaniques (par exemple contre les animaux), chimiques et bien sûr des rayonnements ultraviolets (UV) du soleil [3, 4].

Il existe une énorme quantité de type d'arbres. Les arbres sont notre source principale d'oxygène, sans lequel on ne peut pas vivre. Mais les arbres ne sont pas seulement source d'oxygène et énergie. Dans notre milieu de vie, on utilise différents produits du bois: meubles, panneaux, des planches, des portes et des fenêtres; bien sûr, il y a même des maisons construites entièrement de bois. Mais nous utilisons plutôt le bois, sans son écorce, du point vue esthétique (on aime la texture) et on doit alors créer notre propre protection de surface pour pouvoir utiliser les produits du bois à plus long terme. Dans ce but, nous avons développé différents types de revêtements. Il y deux grands groupes de revêtements : intérieur et extérieur. Le rôle des revêtements intérieurs est de protéger les produits du bois contre l'influence mécanique (abrasion, égratignure etc.). Les revêtements extérieurs servent plus comme des protecteurs contre le rayonnement UV et des champignons. Mais bien sûr il y a des revêtements qui sont capables de jouer les deux rôles en même temps. Nous allons discuter dans ce présent travail, sur de tels revêtements, dits 'UV-aqueux', pour le bois.

Le secteur forestier a toujours été très majeur au Québec et généralement partout au Canada. L'industrie des lambris extérieurs et autres composantes en bois pour portes et fenêtres est très importante au Québec. Ces industries utilisent une quantité importante de revêtements. Les revêtements aqueux, bien qu'avantageux pour l'environnement et la santé des travailleurs et utilisateurs présentent encore plusieurs lacunes de performance [5].

L’amélioration de la durabilité et de la performance du bois par l’utilisation de produits en phase aqueuse (à faible teneur en solvant) permettra d’augmenter l’utilisation des produits forestiers dans la construction, à l’intérieur comme à l’extérieur, tout en stimulant la croissance du marché, tributaire des normes de l’environnement.

Le présent projet consiste à augmenter la performance de revêtements UV-aqueux pour le bois, en utilisant la ressource forestière. Dans ce but, nous pensons remplacer les nanoparticules étudiées précédemment ([6-9]) par de la cellulose nanocristalline (CNC), un produit canadien et québécois, issu de la forêt. L'objectif principal du projet est la formulation des revêtements aqueux nanocomposites (renforcés par la CNC) opaques et transparent pour le bois à usage extérieur et intérieur, et étudier l’effet des nanoparticules essentiellement sur les propriétés d’usure des revêtements. Pour garder la texture du bois, on utilise souvent des revêtements transparents (des vernis), mais l’industrie des armoires de cuisine et du meuble utilisent également des finitions opaques (des peintures), dans ce cas-ci adaptées pour des applications intérieures.

La présente thèse est la continuation de quatre thèses-mémoires complétés. Ils concernent la dispersion de nanoargiles et autres renforts inorganiques dans les revêtements non-aqueux [7], les nanorenforts dans les revêtements intérieurs aqueux [6], les nanorenforts dans les revêtements extérieurs architecturaux [8], et la résistance aux UV des revêtements extérieurs [9]. Ces travaux indiquent que les nanorenforts apportent une meilleure résistance à l’usure et aux UV aux revêtements en autant que les nanoparticules soient bien dispersées. Cette variabilité dans la qualité de la dispersion dépend de la chimie du système utilisé mais aussi fortement des appareils utilisés pour effectuer la dispersion. Il a été aussi démontré que la dispersion en milieu aqueux constitue un défi important étant donné la faible viscosité des produits de finition aqueux, des effets du pH et de la force ionique en milieu aqueux, alliés à la très grande surface spécifique des nanorenforts.

L’originalité de cette thèse consiste en l’ajout de la CNC dans les revêtements pour améliorer leurs résistances mécaniques, qui n’a jamais été fait avant.

Les nanoparticules sont connues pour leur difficulté de dispersion, plus particulièrement dans les milieux aqueux. Puisqu’il est difficile d’intégrer les nanoparticules inorganiques

dans une matrice polymère (organique), ce sera possiblement plus facile d'utiliser des nanoparticules organiques. L'hypothèse de recherche suppose que la nature cellulosique et, éventuellement, la modification appropriée de la surface des nanoparticules aidera à la haute dispersion et stabilité des nanoparticules CNC dans ces revêtements nanocomposites. Pour encore améliorer la dispersion de la CNC dans la matrice, les nanoparticules ont été chimiquement modifiées soit par les bromures d'ammonium quaternaire alkylés ou le chlorure d'acryloyle. La modification de la surface doit mener simultanément à une haute compatibilité avec la résine acrylique ou toute autre résine utilisée. Comparativement aux revêtements sans nanoparticules, les revêtements nanocomposites préparés devraient présenter une meilleure protection contre les UV et une meilleure résistance à l'usure (augmentation de 30-40% de la résistance [10], *Chapitre 4*), respectivement, en milieux extérieur et intérieur.

Chapitre 1. Revue de littérature, matériaux et méthodes

1.1. Généralités

Note : Dans le présent chapitre nous avons présenté la revue de littérature et donné des détails sur les matériaux et méthodes en alternance, pour faciliter la compréhension et éviter les répetitions. Ainsi, par exemple, lorsqu'il est question des méthodes existant pour caractériser la dispersion des nanoparticules, nous avons aussi discuté notre choix d'appareils. Chaque chapitre sous forme de publication (chapitres 2-6, plus les annexes) comporte sa propre revue de littérature et ces revues ne seront pas répétées ici.

La plupart des objets autour de nous sont couverts d'un revêtement. Bien qu'une des propriétés principales des revêtements consiste à décorer les objets, les peintures ont également pour fonction de protéger les objets des dégradations causées par l'humidité, l'oxydation ou bien encore les radiations ultraviolettes (UV). Les peintures et vernis sont des substances liquides ou pulvérulentes qui, une fois appliquées sur un substrat (métal, bois, verre, matériaux plastiques), donnent après diverses transformations physiques et/ou chimiques un revêtement pelliculaire. Ce revêtement, aussi appelé film, a pour fonction de protéger et/ou d'embellir les substrats. Une peinture est un produit de revêtement pigmenté opaque tandis qu'un vernis est un produit de revêtement non-pigmenté transparent. L'industrie des peintures et des vernis consomme d'importantes quantités de produits de finition qui sont le plus souvent à base de solvant : généralement un composé organique hydrocarboné, dérivé du pétrole, en raison de leur grande versatilité [11]. L'usage de revêtements en phase solvant s'accompagne donc d'une émission importante de composés organiques volatils (COV), néfaste pour l'environnement. L'importance grandissante de «l'écodesign» et des produits «verts» pousse les gouvernements à modifier les lois relatives aux émissions de COV (États-Unis et Canada), à l'instar de l'Europe. De tels changements ont amené l'industrie des produits du bois à développer de nouveaux revêtements plus en accord avec l'environnement tels que les revêtements aqueux, à cuisson ultraviolette (UV) ou en poudre.

Les peintures en phase aqueuse présentent de très faibles teneurs en solvant organique et permettent donc de réduire les émissions de COV. Ainsi, la technologie aqueuse permet donc de réduire les risques toxicologiques et d'inflammabilités liés à l'emploi de solvants organiques [11]. Les peintures en phase aqueuse ont été initialement développées dans les années 1950 mais ont connu un essor majeur dans les années 1970 lorsque les réglementations environnementales sont devenues beaucoup plus sévères.

Selon Hosker [12], les revêtements utilisés pour des applications extérieures (meubles de jardin, bardage, terrasse etc.) doivent être formulés pour obtenir une bonne résistance aux rayons UV, changements de température et d'humidité, les insectes ainsi que la pourriture et la moisissure. En revanche, les revêtements de sol doivent résister aux contraintes mécaniques car ils sont constamment sollicités. En fait, les finitions utilisées pour des applications intérieures tels que les meubles, armoires de cuisine et les planchers doivent avoir une bonne résistance mécanique (abrasion, égratignures, l'impact et la dureté), thermique (incendie et flamme, la stabilité thermique) et une résistance aux produits chimiques (détergents, alimentaire etc.) [12]. La sélection de la peinture/vernis doit également être faite en fonction du substrat à revêtir. Les matières plastiques sont connues en tant que matériaux à faible énergie de surface et pour cette raison, le revêtement d'adhérence est une des préoccupations majeures associées aux plastiques. D'un autre côté, les revêtements appliqués sur les métaux doivent être résistants à la corrosion lorsqu'ils sont destinés à des applications extérieures. Les revêtements de bois ne font pas exception; ces revêtements doivent être adaptés à ses particularités nombreuses.

1.1.1. L'importance de revêtements dans l'industrie du bois

Le bois est un matériau naturellement durable, reconnu depuis longtemps pour sa polyvalence ainsi que ses propriétés structurelles exceptionnelles [3, 4, 13]. Toutefois, afin de conserver son aspect et ses propriétés mécaniques, il doit être maintenu dans des conditions favorables. Selon Feist [13], comme n'importe quel matériau biologique, le bois est soumis à la dégradation causée par l'humidité, la lumière et de l'oxydation. Pour cette

raison, les produits fabriqués à partir de bois devraient généralement être traités afin de préserver leurs propriétés.

Parmi les caractéristiques les plus souhaitables pour les revêtements de bois à l'intérieur, à l'abrasion ou résistance à l'usure sont certainement parmi les premiers [6, 7]. Il se produit généralement lorsque la peinture ou du vernis est exposé à l'érosion mécanique, frottement ou friction, par exemple dans les revêtements de sol. Un revêtement peu résistant à l'abrasion conduira à de nombreux défauts de surface après un court laps de temps. Le bois étant un matériau souple soumis à l'indentation, un système de revêtement doit avoir une bonne performance mécanique.

1.1.2. Revêtements intelligents

Lauzon, une compagnie québécoise, utilise les revêtements 'intelligents' (http://plancherslauzon.com/). La technologie 'Pure Genius'de Lauzon révèle les propriétés purifiantes du bois ainsi traité. Après trente jours, le taux de formaldéhyde présent dans les pièces comportant ce matériau, n'est plus que de cinq parties par milliard (5 ppb), comparativement à 16 à 32,5 ppb dans une maison standard. Selon Santé Canada, un taux de 40 ppb et plus représente un risque pour la santé. Le fonctionnement de cette technologie s'apparente à celui d'un arbre. En plus de générer de l'oxygène (O_2) issu de la décomposition du dioxyde de carbone (CO_2), un arbre peut éliminer une partie des oxydes d'azote (NO_X). Le plancher 'Pure Genius' agit de façon semblable, par photocatalyse, et décompose également d'autres composés organiques volatils (COV) nocifs présents à l'intérieur de maison. Il décompose les COVs et les transforme en molécules d'eau et de dioxyde de carbone inoffensives. Le dioxyde de titane réagit à la lumière naturelle ou artificielle. Dans l'obscurité, les molécules agissent encore un certain temps, puis se «rechargent» au retour de la lumière. Exposé à la lumière, le plancher tout entier fonctionne comme un immense filtre naturel. Au contact des nanoparticules actives, les molécules toxiques (COV) se décomposent et se transforment en molécules d'eau et de dioxyde de carbone, inoffensives et imperceptibles. Ceci est donc un exemple d'injection de technologie avancée dans un domaine où c'est certainement une approche novatrice. Nous

pensons que nos présents travaux sont dans cette ligne de pensée. Le chapitre en annexe de cette thèse constitue une introduction à certains aspects généraux des nanorevêtements 'intelligents'.

1.2. Revêtements UV-aqueux

Le marché mondial des revêtements est estimé à 30 millions de tonnes par an et d'une valeur d'environ 120 milliards de dollars américains. L'importance de la technologie UV grandit de jour en jour et les revêtements à base d'eau gagnent des parts de marché. Le succès de cette technologie peut se résumer en quatre points:

1. le mécanisme de cuisson est si rapide qu'il permet d'augmenter la productivité
2. c'est une technologie verte exempte de solvant et n'émettant pas de COV
3. elle permet le traitement de matériaux sensibles à la chaleur tels que le bois et le plastique
4. la très haute densité de réticulation conduit à des films aux propriétés remarquables (propriétés mécaniques, résistance aux produits chimiques) [11, 14].

À cause des restrictions gouvernementales concernant l'émission de COV dans l'atmosphère les industriels n'ont eu d'autres choix que de développer des revêtements plus «verts». Dans cette optique, les revêtements UV-aqueux se sont présentés comme une alternative très intéressante aux problèmes des revêtements en phase solvant. La polymérisation ultraviolette est très rapide, en quelques secondes la cuisson est terminée et la réaction a lieu sans émission de COV. Le choix de l'eau en tant que solvant permet d'éviter les problèmes de toxicité et d'inflammabilité liés à l'utilisation de solvants. Enfin la viscosité des formulations UV-aqueuse facilite grandement leur emploi et leur application.

Les matrices des revêtements UV-aqueux sont des résines photopolymérisables. Les systèmes radicalaires présentent quatre types de résines photopolymérisables : les résines polyester insaturé-styrène, les résines thiol-polyènes, les couples de monomères donneur-accepteur et enfin les résines acrylates.

Dans les résines polyester insaturé-styrène, la réticulation se fait par copolymérisation d'un monomère vinylique avec une double liaison de type maléique ou fumarique située sur la chaîne polymère en présence d'un photoamorceur [14]. Ces résines sont principalement utilisées en tant que vernis dans le secteur de l'ameublement.

Dans les résines thiol-polyènes, le groupement thiol joue le rôle d'un co-amorceur. Sous l'action de la lumière, l'amorceur réagit avec le thiol pour former deux radicaux dont un radical thiol [14].

Dans le cas des couples de monomères donneur-accepteur, l'exposition au rayonnement UV d'un mélange stœchiométrique de deux monomères, l'un ayant un caractère donneur d'électron et l'autre ayant un caractère accepteur d'électron, en présence d'un photoamorceur permet de synthétiser rapidement des copolymères alternés [14].

Les résines acrylates sont de loin les plus couramment employées en tant que résines photopolymérisables compte tenu de la très grande réactivité de la fonction acrylate [14]. Il existe une très large gamme de résines acrylates selon la nature de la fonction acrylate (acrylate ou méthacrylate) et la nature du groupement téléchélique (époxy, polyester, polyéther, uréthane). Cependant, la constante de vitesse de propagation de la fonction méthacrylate étant beaucoup plus faible que celle de la fonction acrylate, la grande majorité des résines acrylates utilisées à l'heure actuelle dans le domaine des revêtements UV sont de type acrylate et non méthacrylate [14].

Dans la présente thèse nous utilisons une résine photopolymérisable à base de polyuréthane-acrylate (PUA). Les liens de type PUA sont idéals pour les applications dans le domaine des revêtements pour le bois. En plus de démontrer une très bonne résistance en tension et aux impacts, les oligomères PUA apportent au revêtement une excellent résistance à l'abrasion et aux égratignures ainsi qu'une très bonne résistance aux changements climatiques [15, 16].

1.3. Photopolymérisation des revêtements UV-aqueux

Il existe deux systèmes de polymérisation selon que les espèces réactives sont de nature radicalaire ou cationique [11, 14, 17]. Cependant les systèmes de polymérisation radicalaire

sont les plus utilisés compte tenu de leur grande réactivité. Le mécanisme de polymérisation radicalaire est constitué de trois étapes principales : l'amorçage, la propagation et la terminaison. Au cours de l'étape d'amorçage, le photoinitiateur exposé à un rayonnement UV, de longueur d'onde située entre 200 et 380 nm, libère des radicaux dits primaires par coupure homolytique d'une liaison covalente. Au cours de l'étape de propagation, la chaîne polymère croît par addition successive d'unités monomères/oligomères sur la macromolécule radicalaire en croissance. C'est l'étape la plus importante de la polymérisation radicalaire puisqu'elle détermine non seulement le degré de polymérisation et la masse moléculaire de la macromolécule, mais également sa configuration de chaîne. L'étape de terminaison, qui met en jeu deux macromolécules radicalaires, provoque la fin de la polymérisation. Il y a soit recombinaison de deux macromolécules radicalaires pour former une seule macromolécule par liaison covalente –C–C–, soit transfert d'un atome d'hydrogène donnant lieu à deux macromolécules par phénomène de dismutation [16].

Dans les systèmes UV-aqueux, qui nécessitent une étape préalable d'évaporation de l'eau par séchage, la photopolymérisation se réalise dans le film sec donc à l'état solide où la mobilité moléculaire est très restreinte [18]. Il est possible d'augmenter le taux de réticulation en maîtrisant plusieurs paramètres tels que la nature du photoinitiateur, celle de la résine, ou bien encore l'intensité lumineuse et la température [18-20].

1.4. Formulation des revêtements UV-aqueux

La formulation des peintures/vernis constitue l'une des étapes les plus importantes pour le formateur. Les propriétés finales du revêtement étant gouvernées par la nature des constituants, le formulateur aura pour mission de choisir judicieusement les constituants adéquats pour la formulation. Une formulation est généralement constituée de 3 ou 4 groupes de composants selon qu'elle soit destinée à un vernis ou une peinture respectivement : la résine (ou liant), le solvant (eau), le pigment (pour les peintures uniquement) et les additifs [6]. Chaque groupe de composants présente un vaste choix de produits présentant des propriétés et des compatibilités spécifiques, aussi une connaissance

avancée dans la formulation des peintures et des vernis est indispensable afin de développer une formulation efficace. Les compositions de la formulation UV-aqueuse sont présentées au *Tableau 1.1*.

La **Résine** constitue l'élément principal d'une formulation de peinture. D'un point de vue chimique, il s'agit de polymères ou d'oligomères polymérisant lors du séchage de la peinture. Son rôle est de former une pellicule continue qui après séchage formera un film sec adhérant au substrat, c'est donc pour cette raison qu'on la qualifie de matériau filmogène [11, 21]. Le liant confère au revêtement ses principales caractéristiques physico-chimiques, c'est donc une matière première essentielle dans la composition d'une peinture [16].

Tableau 1.1. Compositions de la formulation UV-aqueuse

Composant	Structure chimique	Nom commercial
Résine	Polyuréthane-acrylate	Bayhydrol UV 2282
Agent antimoussant	Copolymère polyétherdiméthylsiloxane	Foamex 822
Agent de surface	Copolymère polyéthersiloxane	Byk 348
Dispersant	Solution de bloc de copolymère de haut poids moléculaire	Byk 190
Photoinitiateur	Oxyde de bis-acylphosphine	Irgacure 819DW
Agent épaississant	Polyuréthane	RM 2020
Solvant	Eau déionisée	_
Pigment	TiO_2	_

Le Bayhydrol UV 2282 (Bayer Material Science), oligomère polyuréthane-acrylate en émulsion dans l'eau développée essentiellement pour des applications sur le bois ou ses dérivés, a été employé en tant que liant. Cette résine est caractérisée par un aspect laiteux, propre aux émulsions aqueuses et son taux d'extrait sec est de 43%.

1.4.1. Les additifs

L'oxyde de titane (TiO_2) est bien connu comme un **pigment** blanc. Après plusieurs mesures on a constaté, que ~30% (à la masse sec) de TiO_2 nous donne une opacité de plus que 80%, suffisante pour la peinture opaque.

La formation de mousse au cours de la formulation peut nuire aux propriétés d'apparence du revêtement mais aussi réduire sa fonction de protection. Il est donc nécessaire d'ajouter un **agent antimoussant** dans la formulation afin d'éviter la formation de mousse. Les agents antimoussants sont des liquides de faible tension de surface, insolubles dans le milieu dans lequel ils sont introduits, possédant un coefficient d'entrée et un coefficient d'étalement positifs [11, 21]. Le Foamex 822, copolymère polyétherdiméthylsiloxane, a été utilisé dans ce projet.

L'utilisation du Byk 348 (Byk-Chemie) en tant que **surfactant** permet d'une part d'abaisser la tension de surface des formulations aqueuses et d'autre part de favoriser un meilleur étalement de la formulation sur le bois [11, 21, 22].

L'agent épaississant (agent rhéologique) RM 2020 (Rohm and Haas Company) a été introduit afin d'ajuster la viscosité de la formulation UV-aqueuse. Les propriétés rhéologiques d'une formulation dépendent non seulement de la nature du liant (structure chimique, poids moléculaire, solubilité), mais aussi du solvant et de la concentration en pigments/matières de charges [6, 11, 21, 22].

Le choix du **photoinitiateur** joue un rôle prépondérant dans les systèmes UV puisque la vitesse et l'efficacité de la polymérisation, ainsi que les propriétés des revêtements en dépendent. Le photoinitiateur est un élément indispensable dans une formulation à cuisson ultraviolette puisque c'est lui qui va permettre d'amorcer la réaction de polymérisation

radicalaire par absorption du rayon ultraviolet incident [6, 14]. Les photoinitiateurs de type Norrish I (coupure homolytique au niveau du carbonyle), qui consistent en des cétones aromatiques, sont les plus utilisés compte tenu de leur grande réactivité [6]. Les dicétals benzyliques, les oxydes d'acylphosphine et les α-aminocétones, dont les structures sont présentées à la Figure 1.1, qui se distinguent par une plus grande capacité d'absorbance dans le proche UV, sont les photoinitiateurs de type Norrish I les plus performants [14]. Le photoinitiateur utilisé dans notre recherche est un oxyde de bisacylphosphine en dispersion dans l'eau (45% en poids) de couleur jaunâtre à savoir l'Irgacure 819 DW (Mississauga, Canada).

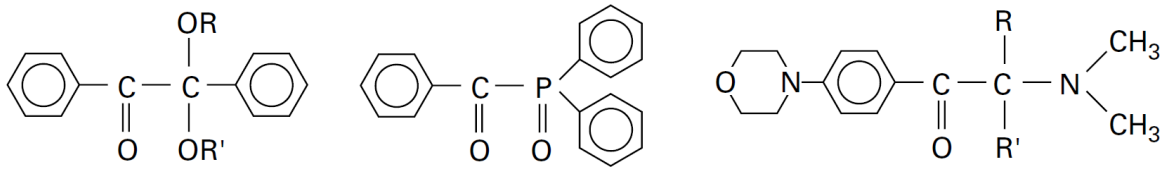

Dicétal benzylique Oxyde d'acylphosphine α-aminocétone

Figure 1.1 Structure chimique des photoinitiateurs de type Norrish I les plus performants [14].

1.4.2. Les agents des renforts

Malgré les nombreux avantages que présentent les revêtements UV-aqueux, la popularité de ces derniers est limitée car leurs propriétés mécaniques sont souvent inférieures à celles de leurs homologues en phase solvant [23]. Un des objectifs de notre recherche consiste à tenter de mettre en valeur les revêtements UV-aqueux en ajoutant des nanoparticules afin de renforcer leurs propriétés. Les nanoparticules permettent d'améliorer certaines propriétés et/ou d'apporter des propriétés spécifiques aux revêtements [6, 7]. Afin d'améliorer la performance des revêtements aqueux pour le bois, on a, par le passé, étudié l'intégration des nanoparticules de ZnO, TiO_2, CeO_2, Al_2O_3, SiO_2 et nanoargiles dans une matrice polymère, sous forme d'un film de revêtement. Ces nanoparticules ont permis d'améliorer

la résistance à l'usure (abrasion et égratignures), la protection contre les UV et les champignons [6-9]. Ils concernent la dispersion de nanoargiles et autres renforts inorganiques dans les revêtements non-aqueux [7], les nanorenforts dans les revêtements intérieurs aqueux [6], les nanorenforts dans les revêtements extérieurs architecturaux [8], et la résistance aux UV des revêtements extérieurs [9]. Ces travaux indiquent que les nanorenforts apportent une meilleure résistance à l'usure et aux UV aux revêtements en autant que les nanoparticules soient bien dispersées. Cette variabilité dans la qualité de la dispersion dépend de la chimie du système utilisé mais aussi fortement des appareils utilisés pour effectuer la dispersion. Il a été aussi démontré que la dispersion en milieu aqueux constitue un défi important étant donné la faible viscosité des produits de finition aqueux, des effets du pH et de la force ionique en milieu aqueux, alliées à la très grande surface spécifique des nanorenforts.

1.5. Hypothèses et objectifs de la recherche

1.5.1. Hypothèses de la recherche

Puisqu'il est difficile d'intégrer les nanoparticules inorganiques dans une matrice polymère (organique), ce sera possiblement plus facile d'utiliser des nanoparticules organiques. Dans ce but, nous pensons remplacer les nanoparticules étudiées précédemment par de la cellulose nanocristalline (CNC). L'hypothèse de recherche suppose que la nature cellulosique et, éventuellement, la modification appropriée de la surface des nanoparticules aidera à la haute dispersion et la stabilité des nanoparticules CNC dans ces revêtements nanocomposites. La modification de la surface doit mener simultanément à une haute compatibilité avec la résine acrylique ou toute autre résine utilisée. Comparativement aux revêtements sans nanoparticules, les revêtements nanocomposites préparés devraient présenter une meilleure protection contre les UV et une meilleure résistance à l'usure, respectivement, en milieux extérieur et intérieur.

1.5.2. Objectifs de la recherche

L'objectif principal du projet est la formulation des revêtements aqueux nanocomposites CNC opaques et transparent pour le bois à usage extérieur et intérieur. Les objectifs spécifiques sont :

1. La dispersion efficace et stable des nanoparticules de CNC comme agent de renfort.
2. La caractérisation physico-chimique des formulations, liquides et solides;
3. La caractérisation de la performance du bois avec les nouveaux revêtements nanocomposites en ce qui concerne la résistance mécanique (résistance à l'abrasion, résistance aux égratignures), la dégradation aux UV, la stabilité de la couleur, ainsi que l'adhésion du film au substrat bois.
4. Obtenir des peintures/vernis plus durs, plus résistants, plus minces, et possiblement, avec des propriétés optiques nouvelles.

1.6. La cellulose nanocristalline

La cellulose (Figure 1.2) est un glucide constitué d'une chaîne linéaire de molécules de D-glucose et le constituant principal des végétaux et en particulier de la paroi de leurs cellules [24]. Les macromolécules de cellulose associées forment des micro-fibrilles, qui elles-mêmes sont associées en couches, forment les parois des fibres végétales. Il s'établit des liaisons hydrogène entre les molécules de glucose des différents chaînes [24]. Les monomères de glucose sont liés par des liaisons β-(1→4), conduisant à des polymères linéaires [25]. Ces polymères s'associent par des liaisons intermoléculaires de type liaisons hydrogène, conférant ainsi une structure fibreuse à la cellulose. L'association de 6 chaînes de cellulose forme une microfibrille de cellulose. L'association de 6 microfibrilles de cellulose forme une macrofibrille et un agencement de plusieurs macrofibrilles forme ce qui est généralement appelé une fibre de cellulose.

C'est le principal constituant du bois. La cellulose constitue la matière organique la plus abondante sur la Terre (plus de 50% de la biomasse). La quantité synthétisée par les végétaux est estimée à 50-100 milliards de tonnes par an.

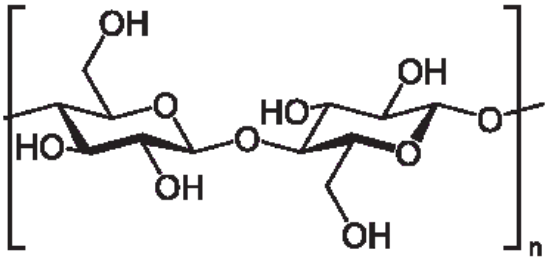

Figure 1.2. Structure de la cellulose (conformation de chaîne).

De nombreux produits sont dérivés de la cellulose, y compris la nanocellulose. 'Nanocellulose' est un terme faisant référence à la cellulose nano-structurée. Cela peut être soit des nanofibres de cellulose (NFC) également appelées 'cellulose microfibrillée' (CMF), la cellulose nanocristalline (CNC), ou la nanocellulose bactérienne, qui se réfère à la cellulose nano-structurée produite par des bactéries.

Les NFC/CMF sont des matériaux constitués de fibrilles de cellulose de taille nanométrique avec un rapport d'aspect élevé (rapport longueur sur largeur). Les dimensions latérales typiques sont de 5 à 20 nanomètres et la dimension longitudinale est dans une large gamme, typiquement quelques micromètres. Les fibrilles sont isolées de sources et procédés variés, y compris contenant de la cellulose des fibres à base de bois (fibres de pâte) par traitements à haute pression, haute température et haute vitesse, homogénéisation, broyage ou microfluidisation.

La nanocellulose peut également être obtenue à partir de fibres indigènes par une hydrolyse acide, donnant lieu à des nanoparticules hautement cristallines et rigides (souvent appelées nanowhiskers) qui sont plus courtes (100 à 1000 nanomètres) que les nanofibrilles obtenues grâce à l'homogénéisation, microfluidisation ou des routes de broyage [26]. Le matériau résultant est connu comme la 'cellulose nanocristalline' (Figure 1.3).

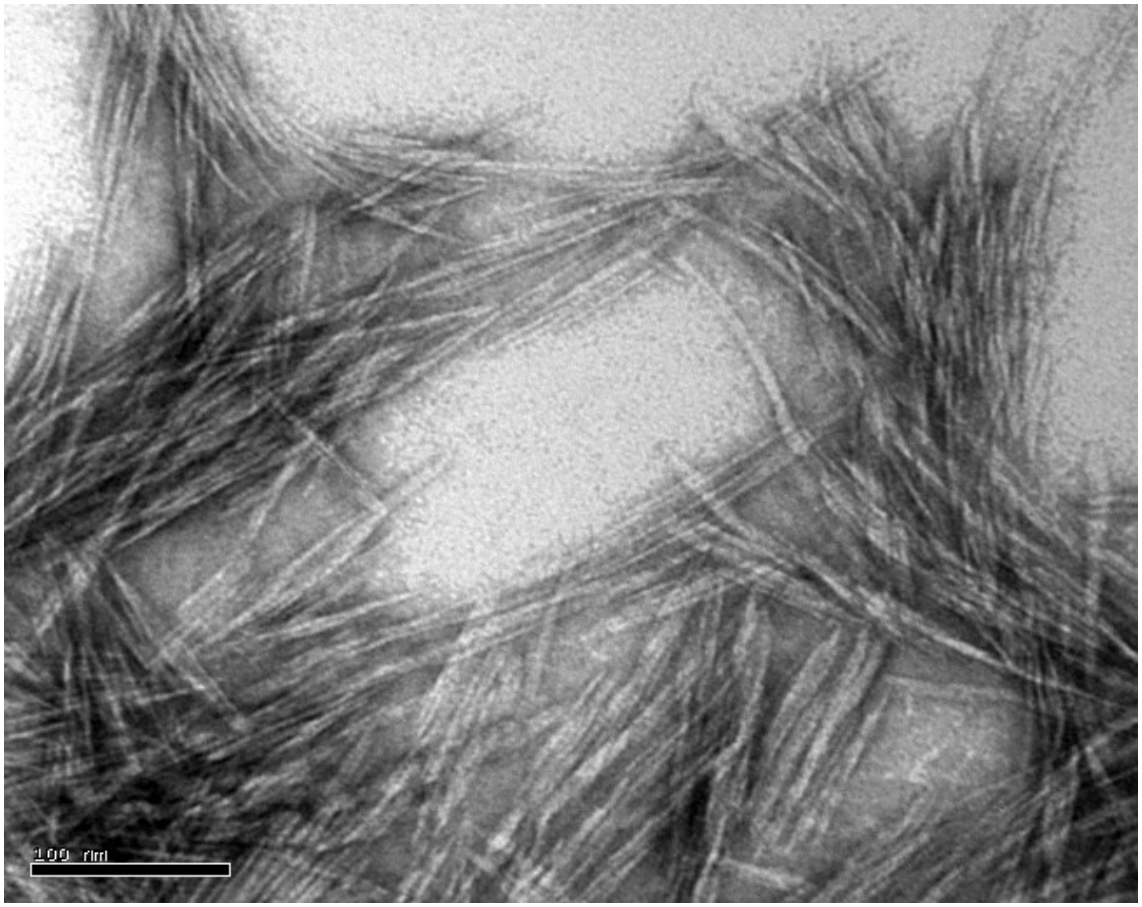

Figure 1.3. Micrographie de CNC dispersée dans l'eau (0.5%) et séchée.

Souvent la CNC est obtenue du bois. La séquence de ce procédé est schématiquement présentée à la Figure 1.4. Bien sûr, il y a aussi les autres types que la CNC du bois: CNC du coton [27], CNC des algues vertes [28], CNC de la pomme de terre [29], CNC de la betterave à sucre [30] et les autres végétaux.

La CNC que nous avons utilisée dans ce projet est développée par FPInnovations et Celluforce. La CNC a été extraitée du bois par un procédé d'hydrolyse acide (H_2SO_4), avec un contrôle strict des conditions de temps et de la température [26, 31] (Figure 1.5). L'action de l'acide enlève la matière initiale de type polysaccharide, étroitement lié à la surface des microfibrilles, résultant en une génération d'un matériau sous-produit amorphe. L'hydrolyse subséquente décompose les parties des chaînes de glucose dans les régions non cristallines. Il reste les zones résiduelles hautement cristallines de la fibre de la cellulose

d'origine. Lorsque ce niveau est atteint, l'hydrolyse est terminée par une dilution rapide de l'acide. Une combinaison de centrifugation et dialyse extensive est utilisée pour enlever complètement l'acide, et un traitement aux ultrasons complète le processus pour disperser les particules individuelles de la cellulose et produire une suspension aqueuse [32].

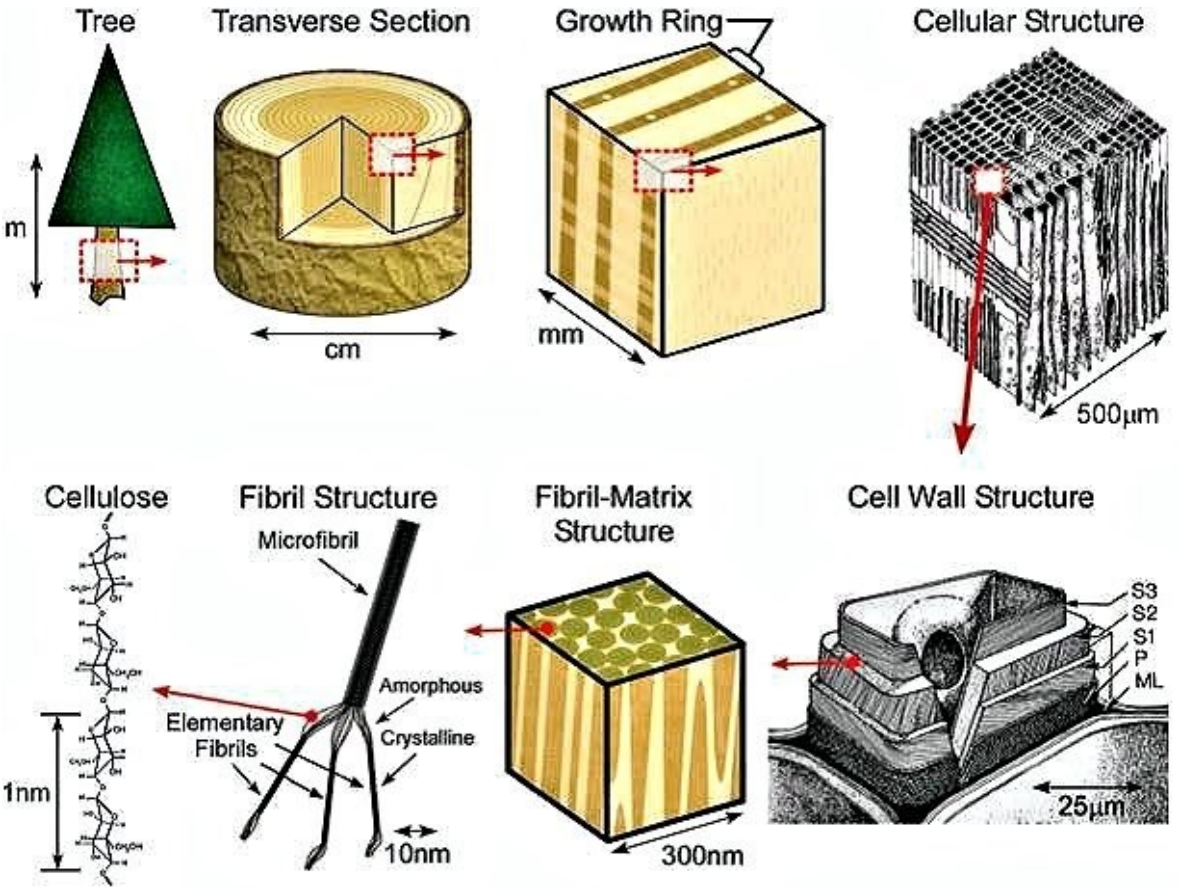

Figure 1.4. Structures de cellulose dans les arbres à partir de grumes jusqu'aux molécules (http://www.gizmag.com/cellulose-nanocrystals-stronger-carbon-fiber-kevlar/23959/).

Des échantillons de la suspension de la CNC ont été soniquées l'aide d'un Sonics vibra-cellule 130 W processeur 20 kHz à ultrasons avec une sonde de diamètre 6 mm. Typiquement, 15 ml d'une suspension de 2-3% en poids de la CNC ont été placés dans un tube en plastique de 50 ml et soniquées à 60% de la puissance maximale. Cette sonication

prolongée (à une entrée d'énergie de plus de 3600 J/g) a été réalisée dans un bain de glace pour empêcher la dégradation provoquée par le chauffage de la suspension [33, 34].

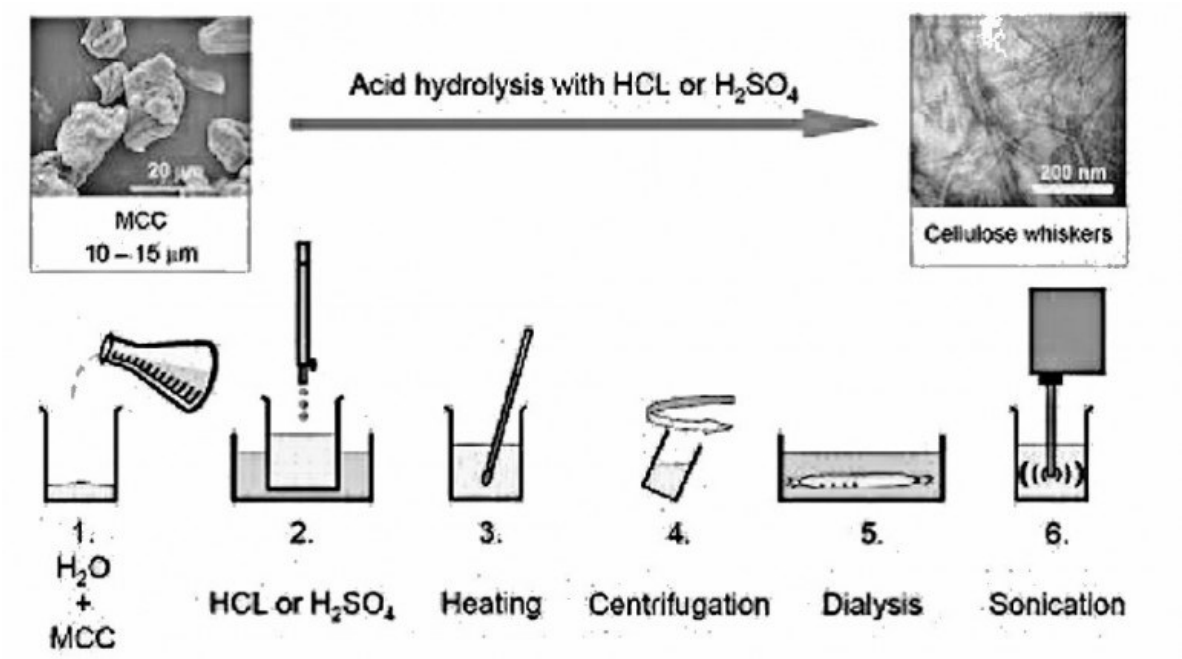

Figure 1.5. De la cellulose microcristalline à cellulose nanocristalline (http://www.gizmag.com/cellulose-nanocrystals-stronger-carbon-fiber-kevlar/23959/).

Suite à ce procédé (Figure 1.4, Figure 1.5), on récupère des nanofibres d'une surface spécifique de 600 m^2/g, un module de Young de 150 GPa et une résistance à la rupture de 10 GPa [35]. Les fibres de cellulose qui restent après ce traitement sont presqu'entièrement cristallines et en tant que telles sont appelés «cristallines». Les dimensions physiques précises des cristallites dépendent de plusieurs facteurs, y compris la source de la cellulose, les conditions d'hydrolyse exactes et la force ionique. Dans notre cas, les dimensions caractéristiques sont: 6-10 nm (largeur) et 100-130 nm (longueur, Figure 1.6), mesurée par un appareil Malvern Zetasizer Nano ZS (Malvern Instruments Ltd).

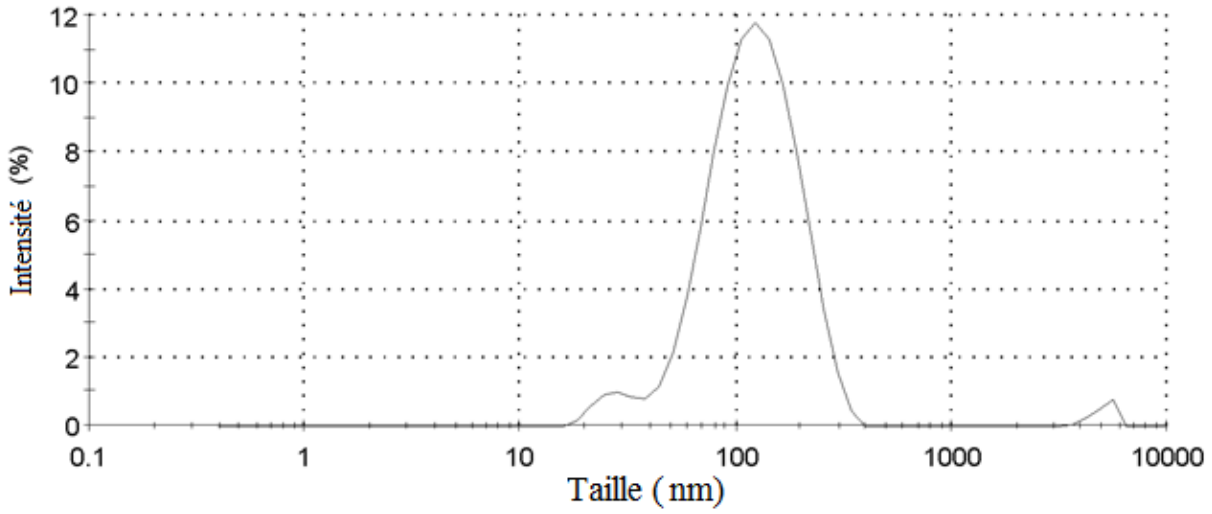

Figure 1.6. Le profil de distribution de taille de 0.05% w/w CNC en suspension dans l'eau.

Il y a très peu de projets présentés dans la littérature sur les revêtements à base d'eau avec la CNC. Quelque travaux ont été réalisés par le groupe européen de A. Dufresne, lequel utilise des 'whiskers' de cellulose [35-37]. En général, ces chercheurs ont constaté que les CNC se dispersent bien en milieu aqueux, ce qui selon notre expérience n'est pas toujours le cas des nanorenforts d'oxydes métalliques et d'argiles. Par contre, ces derniers produits donnent d'excellents contrastes en microscopie électronique de films. Les travaux de Kvien et al. illustrent bien les difficultés encourues lors de la caractérisation par microscopie électronique à transmission (TEM) et à force atomique (AFM) de films polylactide-whiskers [37]. En effet, la CNC est un produit organique sans contraste en TEM/SEM lorsque dispersée dans des matrices polymères organiques [38] (*Chapitre 2*).

Dans le présent projet nous avons utilisé l'AFM comme l'appareil principal pour caractériser la dispersion de la CNC dans les vernis. La microscopie AFM a déjà été utilisée par d'autres auteurs pour étudier la qualité des dispersions de pigments et renforts. Karakas et al. ont montré l'étendue de la distribution et l'agrégation des particules dans 7 formulations différents à la surface des films de peintures [39]. Les résultats expérimentaux ont révélé qu'on peut diminuer l'ajout de TiO_2 de 4% en le remplaçant par la calcite d'une taille optimisée. Farrokhpay a effectué une revue de littérature sur les nouvelles techniques

d'évaluation des surfaces peintes et décrit l'obtention de résultats quantitatifs sur la rugosité de surface par AFM [40]. Thometzek et al. ont aussi utilisé le TEM et l'AFM pour quantifier la qualité de surface des peintures et corréler le degré d'hydrophobicité des particules avec la qualité de la dispersion [41]. Nous pensons donc que l'AFM peut nous aider à caractériser la dispersion de la CNC.

1.7. Préparation des formulations et les échantillons

1.7.1 Méthode de dispersion

Le choix de la méthode de dispersion joue un rôle important quant à l'état de dispersion des nanoparticules. On distingue trois types d'appareillage couramment employés en industrie : le mélangeur à haute vitesse, le broyeur tri-cylindres et le broyeur à billes [42]. Bien que les deux dernières méthodes, mettant en jeu des taux de cisaillement très élevés, aboutissent la plupart du temps à des degrés de dispersion élevés, notre choix s'est arrêté sur le mélangeur à haute vitesse (Figure 1.7).

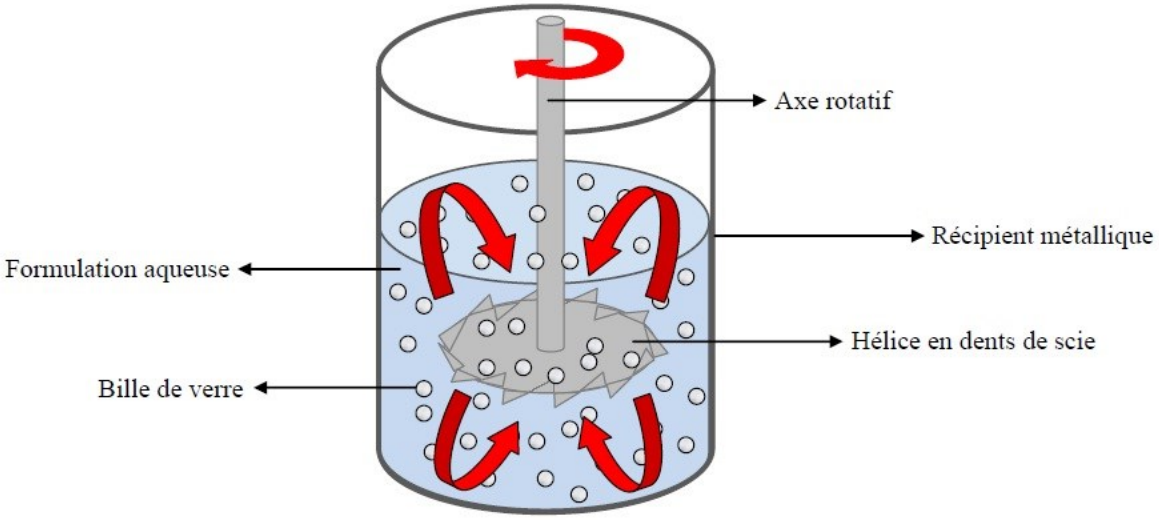

Figure 1.7. Principe de dispersion du mélangeur à haute vitesse [6].

Cet appareillage peu dispendieux permet de reproduire des taux de cisaillements comparables à ceux des mélangeurs industriels. Le mélangeur à haute vitesse consiste en un axe rotatif vertical avec une hélice en dentes de scies à son extrémité tournant à haute vitesse dans une cuve contenant la formulation à disperser.

Pour améliorer la dispersion du TiO_2, nous avons choisi la méthode de dispersion aux ultrasons (Figure 1.8); la formulation est transvasée dans un erlenmeyer de 1 L puis placée dans un bain réfrigérant contenant de l'éthylène glycol et maintenu à 5°C. Une sonde à ultrasons de 750 Watts (Ultrasonic processor, Cole Palmer) et un thermomètre, pour contrôler la température au sein de la dispersion, sont plongés dans la formulation aqueuse. La fréquence des ultrasons utilisée pour la dispersion est de 20 kHz. Le traitement aux ultrasons est réalisé pendant 2 min en fixant la température maximale pouvant être atteinte au sein de la formulation à 40°C [6].

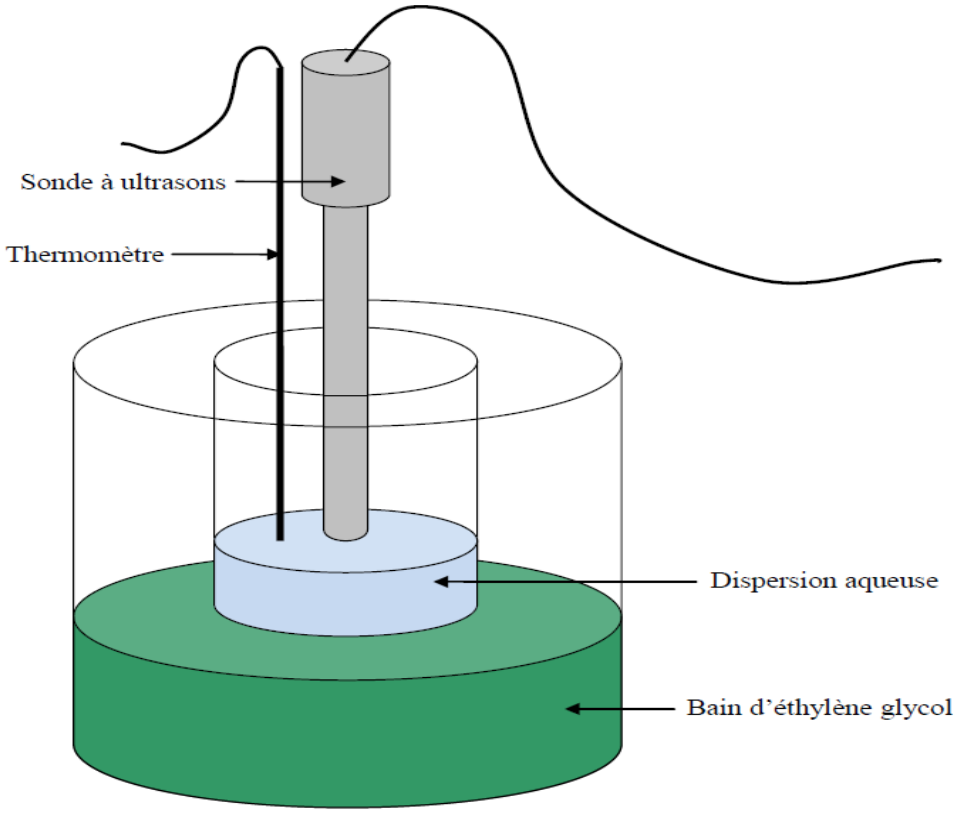

Figure 1.8. Principe de dispersion aux ultrasons [6].

1.7.2. Préparations des formulations

Puisque dans notre formulation il y a différent types des produits, il est très important de respecter l'ordre des ajouts. Il faut toujours préparer les formulations de la même manière, pour avoir les formulations comparables. Donc voici le protocole (Figure 1.9) pour la peinture avec la CNC (vitesse d'agitation 400 rpm).

1. Ajout d'agent antimousse (defoamer) à la résine (dans un contenant métallique), agitation pendant 4 min.

2. Ajout du surfactant au mélange précédent, agitation pendant 4 min.

3. Ajout de 2 g de dispersant au mélange précédent, agitation pendant 4 min.

4. Ajout de TiO_2 graduellement avec 320 g de billes (en verre, diamètre est ~2mm) dans le mélange précédent, agitation pendant 15 min (pendant l'ajout, on augmente la vitesse jusqu'à 950 rpm, pour éviter que la formulation devienne plus visqueuse).

5. Ajout du reste de dispersant (exemple 1.97 g dans le cas de formulation avec 1% de CNC) au mélange précédent, agitation pendant 15 min.

6. Ajout de la quantité d'eau déionisée ''libre'' dans le mélange précédent, agitation pendant 4 min.

7. Ajout du gel (14% dans eau) de CNC, agitation pendant 10 min.

8. Ajout de l'agent rhéologique, agitation pendant 4 min.

9. Ajout du photoinitiateur, agitation pendant 6 min.

Après le processus de la dispersion il nous reste seulement de filtrer les billes.

Dans les formulations de base avec et sans pigment (TiO_2) nous avons ajouté la CNC en concentrations de 0.5, 1, 1.5, 2 et 3% (à la masse sec). Un exemple de formulation opaque avec 1% de CNC est présenté dans le *Tableau 1.2*.

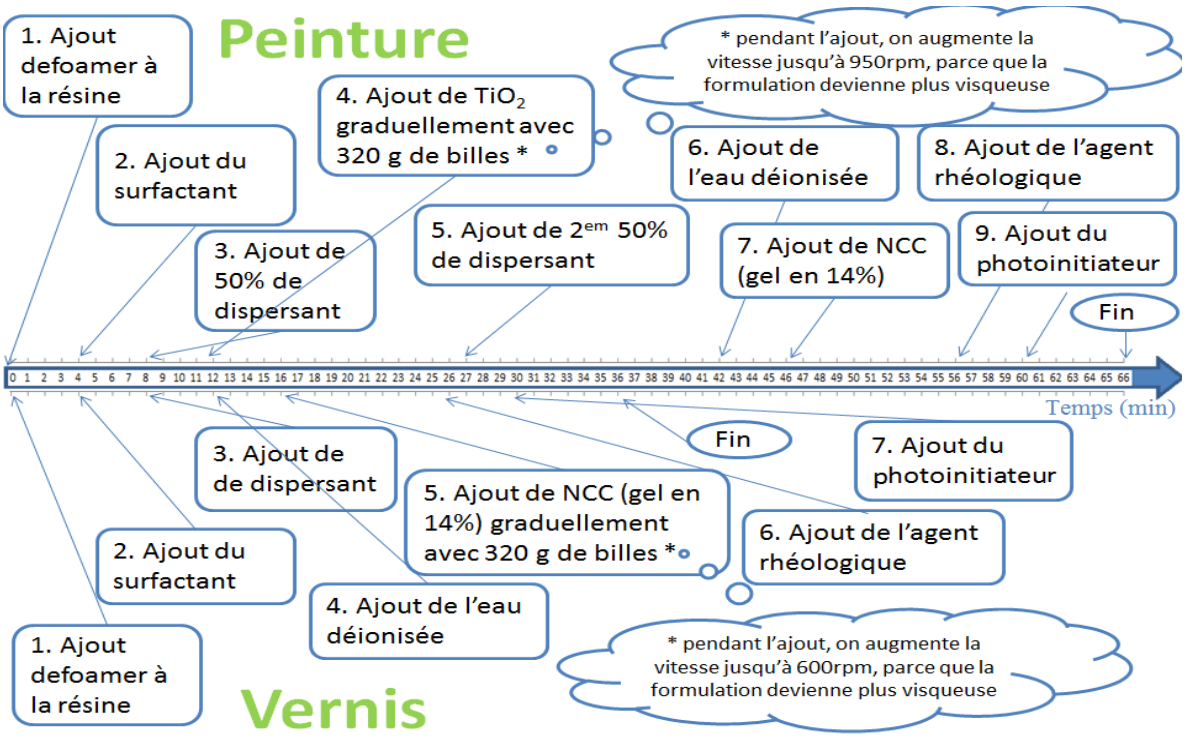

Figure 1.9. Protocole de préparation des formulations.

Tableau 1.2. Liste des produits pour la formulation opaque avec 1% de CNC (274.15 g).

	masse (g)	% sec
- Résine	**210.57**	68.34
- Defoamer	**1.99**	0.41
- Surfactant	**1.23**	0.97
- Dispersant	**3.97**	1.30
- Pigment	**33.10**	26.86
- Eau déionisée	**11.56**	-
- CNC (en gel à 14%)	**8.80**	1.00

- Agent rhéologique	**1.32**	0.22
- Photoinitiateur	**1.61**	0.90
Total	**274,15**	

1.7.3. Choix du substrat

Le bois est un matériau qui possède des caractéristiques uniques tant du point de vue technique qu'esthétique. Il est un matériau biologique considéré complexe par la variabilité de ses propriétés et par sa structure qui varie selon l'espèce et ses conditions de croissance. Par ce fait, il est grandement influencé par les phénomènes naturels comme la pluie, le soleil, la température et les microorganismes. Ainsi, il est essentiel de protéger sa surface en lui appliquant par exemple un revêtement efficace et durable dans le temps. Pour prévoir de bons résultats, il est nécessaire de connaître la structure du bois et ses interactions avec le produit de finition.

Pour ce projet nous avons choisi de travailler sur deux types des bois : l'érable à sucre (*Acer Saccharum*) pour les applications intérieures et l'épinette noire (*Picea Mariana*) pour les applications extérieures.

1.7.3.1. L'érable à sucre

L'érable à sucre (Figure 1.10) est une espèce d'arbres nord-américains, un feuillu de la famille des acéracées, qui peut vivre jusqu'à 250 ans. C'est un arbre pouvant atteindre 35 m de hauteur, et exceptionnellement jusqu'à 45 mètres. L'érable à sucre se retrouve principalement en Amérique du Nord et surtout au Québec vers la côte Est. On en retrouve aussi dans le nord-est des États-Unis ou en Europe, continent où les spécimens sont généralement de moindre taille (25 mètres, contre 40 en Amérique). L'érable à sucre est l'arbre qui nous donne le sirop d'érable et sa feuille apparaît sur le drapeau du Canada.

Le bois d'érable à sucre, caractérisé par un grain fermé, entre dans la fabrication de nombreux produits tels que les meubles, les revêtements de sol, les jouets, etc. Par comparaison aux autres essences de feuillus présents en Amérique du Nord, on constate que l'érable, qui est très dense, possède une très bonne résistance en flexion et en compression. En plus d'être apprécié par les industriels pour sa facilité d'usinage et de sablage et ses bonnes propriétés de tenue des peintures et teintures, le bois d'érable à sucre connaît un franc succès du côté des consommateurs grâce à sa couleur d'un blanc ivoire [6, 9]. D'un point de vue chimique, les proportions en lignine, cellulose et hémicelluloses de l'érable sont respectivement de 21,1%, 46,8% et 22,2% [43].

Figure 1.10. Érable à sucre (www.all-free-download.com/free-photos/yellow_maple_tree_196234.html).

1.7.3.2. L'épinette noire

L'épinette noire ou sapinette noire (Figure 1.11) est une espèce de conifère commun au nord-est des États-Unis et surtout au Canada. C'est une des près de 40 espèces d'épicéas, et l'une des plus résistantes aux climats rudes (toundra) de l'arctique, avec l'épinette rouge (*Picea rubens*), et l'épinette blanche (*Picea glauca*). Elle est pour cette raison le symbole de la forêt boréale d'Amérique, où elle pousse jusqu'à la limite de la toundra.

Au Canada, son premier usage actuel est l'exploitation, souvent en coupe rase, pour la production de pâte à papier. L'épinette noire est un arbre résineux important au Canada pour la production du bois utilisé en structure (charpentes, toitures, échafaudages, faux – planchers, lambris), de contre-plaqués et de panneaux de particules etc. [43]. Le bois d'épinette noir a une masse volumique basale de 406 kg/m^3 et une masse volumique anhydre de 445 kg/m^3. Il sèche assez facilement et la qualité d'usinage est assez bonne. C'est une très bonne source pour l'utilisation à l'extérieur [8].

1.7.4. Préparation des échantillons

Une fois que la formulation est prête, on peut l'appliquer sur le bois. Les dimensions des échantillons de bois sont 96×96×15 mm (l'érable à sucre, Figure 1.12) et 130×60×9 mm (l'épinette noire) dans les directions longitudinales, radiales et tangentielles, respectivement. Les échantillons ont été stockés dans une chambre de conditionnement à 20°C et 65% d'humidité relative jusqu'à masse constante, pour une teneur finale en humidité du bois à l'équilibre de 12%. Avant chaque application, ils ont été sablés avec un papier abrasif (150). Cette procédure de sablage a contribué à l'enlèvement de la faible couche (à la frontière de la surface), pour obtenir une couche de bois frais et maximiser l'adhésion. Comme méthode d'application de la formulation sur le bois on utilise la pulvérisation (Figure 1.13)**.** Après l'application (épaisseur pour le vernis ~127 µm et ~152 µm pour le peinture) on met les échantillons dans une étuve 10 min en 60°C pour évaporer l'eau graduellement. Au cours de cette étape, le film de vernis passe d'un état liquide blanc à un état solide transparent. La cuisson des films est ensuite réalisée à l'aide d'un four UV munie d'une lampe au mercure moyenne pression (600 W·cm^{-1}). C'est une polymérisation

radicalaire. L'intensité de la lumière incidente mesurée à l'aide d'un radiomètre est de l'ordre de 570 $mJ \cdot cm^{-2}$ et la température perçue au cours de la cuisson est située entre 25 et 30°C. Ensuite il faut répéter ces étapes encore une fois, pour obtenir une couche de revêtement ~100 µm (film solide).

Figure 1.11. Épinette noire (www.thinktrees.org/available_tree_species.aspx).

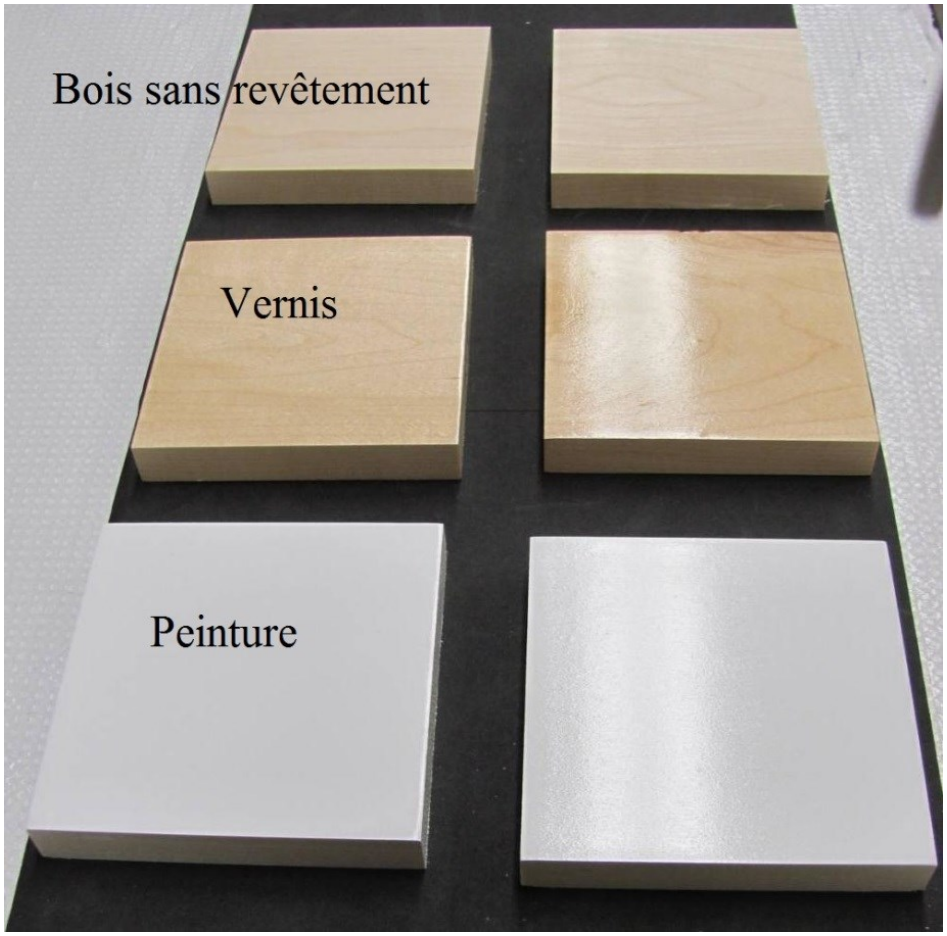

Figure 1.12. Les échantillons du bois sans et avec les revêtements.

À la Figure 1.12, l'apparence des revêtements est présentée. En haut sont des surfaces de bois non revêtu. Au centre, l'effet des vernis sur l'apparence est illustré: la surface est brillante, et il n'y a pas de différence discernable entre la gauche et la droite, qui sont, respectivement, sans et avec 2% de CNC. Au fond, l'effet de la peinture, qui devient blanc et opaque avec ajout de TiO_2, est également considéré, sans différence entre les revêtements avec et sans ajoute de la CNC. Il y a des différences au niveau nanométrique, mais ce n'est pas visible avec les yeux humains.

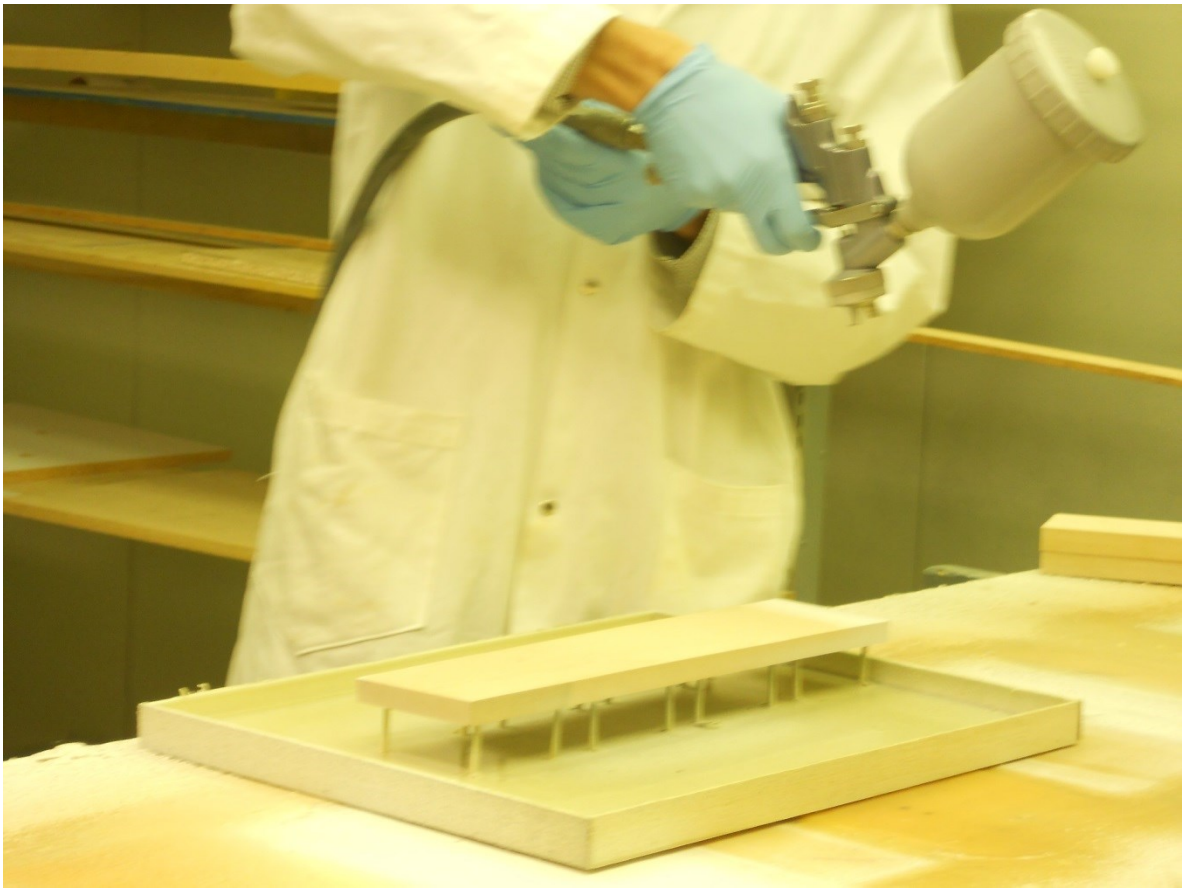

Figure 1.13. Application de la formulation sur le bois par la méthode de pulvérisation.

1.8. Caractérisation des revêtements UV-aqueux

1.8.1. Cinétiques de cuisson

Les mesures par photo-DSC ont été réalisées à l'aide d'un calorimètre différentiel à balayage (DSC822e, Mettler-Toledo) équipé d'une lampe au mercure-xénon en tant que source lumineuse. Préalablement à l'étape de cuisson, les échantillons d'environ 5.6 mg, ont été placés dans des cuves métalliques et chauffées à 80°C pendant 10 min pour éliminer l'eau contenue dans les formulations aqueuses. Les échantillons ont ensuite été irradiés pendant 3 min à une intensité de 47 mW/cm², mesurée à l'aide d'un radiomètre. Les cuissons ultraviolettes ont été réalisées dans des conditions isothermes à 30°C sous flux d'air. Les résultats se présentent sous forme de graphiques représentant les flux de chaleur

issus des réactions de photopolymérisation en fonction du temps de réaction, aussi appelés courbes DSC ou bien encore courbes exothermiques.

Les réactions de photopolymérisation sont basées sur deux types de modèles : ordre n et autocatalytique. Dans une réaction d'ordre n, le taux de conversion est proportionnel à la concentration de monomères n'ayant pas réagi d'après l'équation 1.1 suivante :

$$\frac{d\alpha}{dt}=k(1-\alpha)^n \qquad (1.1)$$

où $d\alpha/dt$ représente le taux de réaction, k la constante de réaction, α le taux de conversion et n l'ordre de la réaction. Dans une réaction autocatalytique, au moins un produit de la réaction contribue à l'augmentation du taux de réaction. La cinétique de cuisson d'une telle réaction peut s'exprimer de la façon suivante :

$$\frac{d\alpha}{dt}=k\alpha^m(1-\alpha)^n \qquad (1.2)$$

où m représente également un ordre de réaction et $m+n$ représente l'ordre total de la réaction.

D'après la loi d'Arrhenius, la constante de réaction k dépend généralement de la température selon l'équation 1.3 suivante :

$$k=A\exp\left(-\frac{E_a}{RT}\right) \qquad (1.3)$$

où A représente le facteur pré-exponentiel, E_a l'énergie d'activation indépendante de la température, R la constante des gaz parfait et T la température.

Le modèle autocatalytique est habituellement employé pour décrire la cinétique de cuisson d'une photopolymérisation. Les courbes DSC présentent les flux de chaleur (dH/dt) en fonction du temps de réaction. Le taux de conversion est alors déterminé de la façon suivante :

$$\alpha = \frac{\Delta H_t}{\Delta H_0} \tag{1.4}$$

où ΔH_t représente la chaleur de réaction dégagée au temps t calculée par intégration de l'aire sous le pic exothermique et ΔH_0 l'enthalpie totale de la réaction. Enfin, le taux de réaction $d\alpha/dt$ est déterminé d'après la relation 1.5 suivante :

$$\frac{d\alpha}{dt} = \frac{1}{\Delta H_0}\frac{dH}{dt} \tag{1.5}$$

1.8.2. Spectroscopie infrarouge

Nous avons étudié la photopolymérisation des formulations PUA aqueuses au moyen de la spectroscopie infrarouge (IR-ATR, PerkinElmer Spectrum 400 Series, Figure 1.14) en suivant la diminution de la bande à 1636 cm^{-1} caractéristique des liaisons doubles acrylates C=C. La bande située à 1724 cm^{-1}, bande invariante caractéristique du groupement carbonyle C=O, a été utilisée afin de normaliser les courbes [44].

Figure 1.14. Appareil FTIR.

Cette propriété physico-chimique permettra de mettre en évidence la cuisson de la résine se traduisant par la conversion des liaisons doubles acrylates en liaisons simples selon le mécanisme de polymérisation radicalaire présenté à la Figure 1.15.

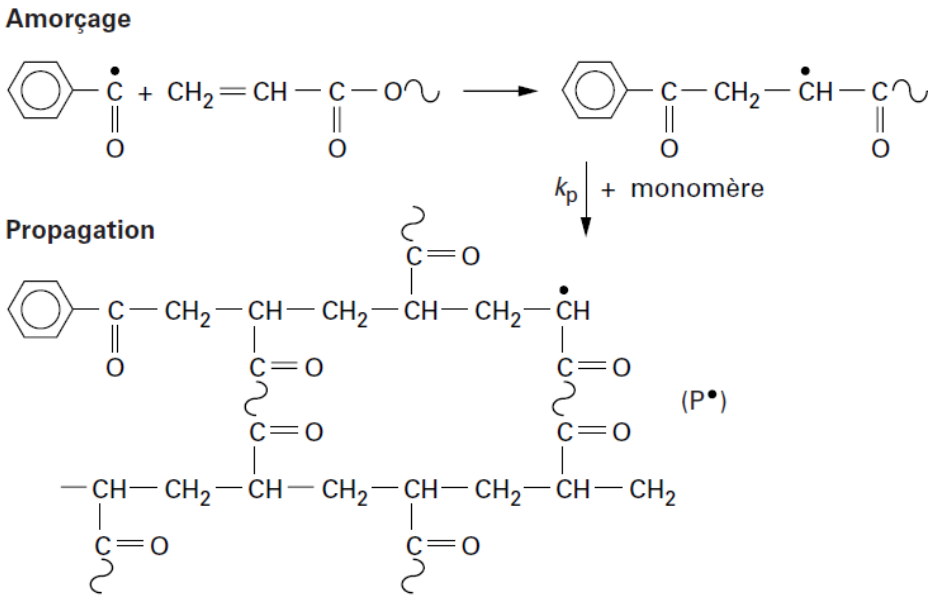

Figure 1.15. Mécanisme de polymérisation radicalaire de la résine PUA UV-aqueuse [14].

1.8.3. Viscosité

Les viscosités des formulations ont été mesurées à l'aide de DV2T Viscosimètre (Figure 1.16) à la température 27°C (Brookfield engineering laboratories, inc., Middleboro, USA). La mesure de la viscosité nous permet d'évaluer jusqu'à combien de pourcent de CNC on peut ajouter dans les formulations, parce que des formulations trop visqueuse ne peuvent pas être appliquée par la méthode de pulvérisation. Selon nos expériences on peut aller jusqu'à 2% de la CNC dans le cas des vernis et jusqu'à 1% de la CNC dans les cas des peintures (le pigment TiO_2 augmente la viscosité de la formulation aussi).

Figure 1.16. Viscosimètre DV2T (Brookfield engineering laboratories, inc.).

1.8.4. Angle de contact

L'angle de contact a été mesuré à l'aide de FTA200 Dynamic Contact Angle Analyzer (First Ten Angstroms, Inc., Portsmouth, USA). La mesure de l'angle de contact (Figure 1.17) rend compte de l'aptitude d'un liquide à s'étaler sur une surface par mouillabilité. L'angle de contact est celui de la tangente du profil d'une goutte déposée sur un substrat, avec la surface du substrat. Dans le présent travail l'angle de contact permet d'évaluer le caractère hydrophile (non-modifiée) ou hydrophobe (modifiée) du film préparé avec la CNC.

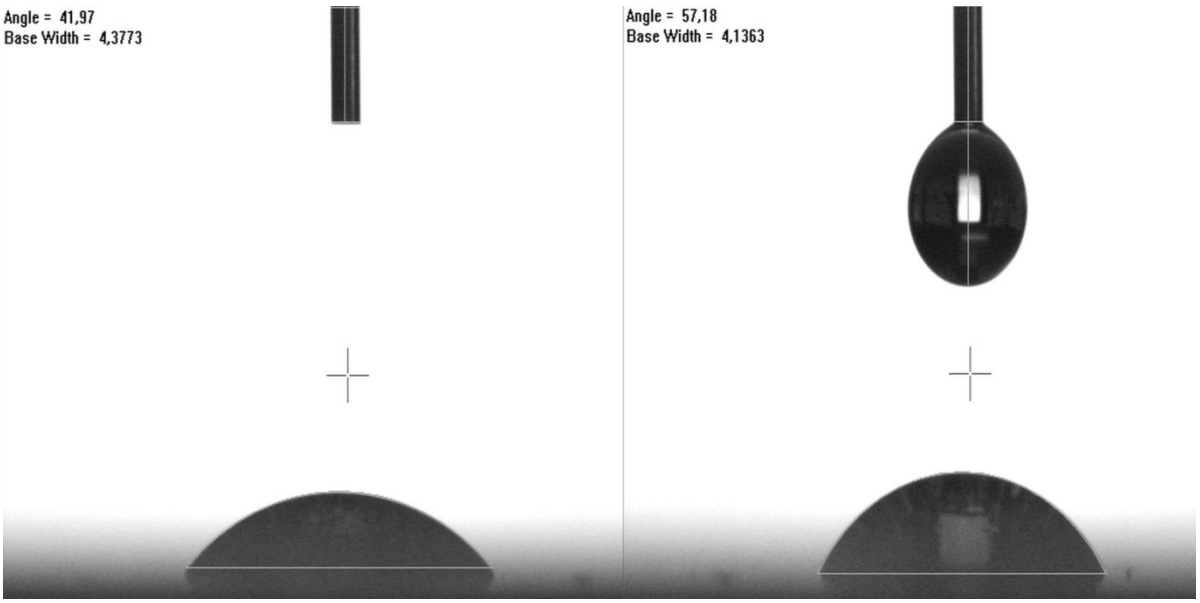

a) b)

Figure 1.17. Angle de contact sur les vernis avec a) CNC hydrophile (non-modifiée) et b) CNC hydrophobe (modifiée).

1.8.5. Microscopie à force atomique

Les observations AFM (ou MFA) ont été effectuées en utilisant un NanoScope V (Figure 1.18), équipé d'un Hybrid XYZ scanner (Veeco Instruments Inc., Santa Barbara, USA). Les mesures AFM ont été réalisées dans des conditions d'air ambiant en tapping mode (radius de la pointe est de 8 nm). La résolution a été fixée à 256 lignes par 256 lignes pour toutes les observations. La rugosité de surface a été calculée dans des zones de balayage de 10×10 μm, en utilisant le paramètre classique rugosité de surface moyenne. Les paramètres ont été calculés par le logiciel Research Nanoscope 7.2:

$$R_a = \frac{1}{n}\sum_{i=1}^{n}\left|Z_i - Z_{ave}\right| \qquad (1.6)$$

où R_a est la rugosité moyenne (Figure 1.19), la moyenne arithmétique des valeurs absolues des écarts de hauteur de surface, Z_i est la valeur actuelle Z, Z_{ave} est la moyenne des valeurs

de Z à l'intérieur de la zone proposée et n est le nombre de points à l'intérieur de la zone proposée (256×256).

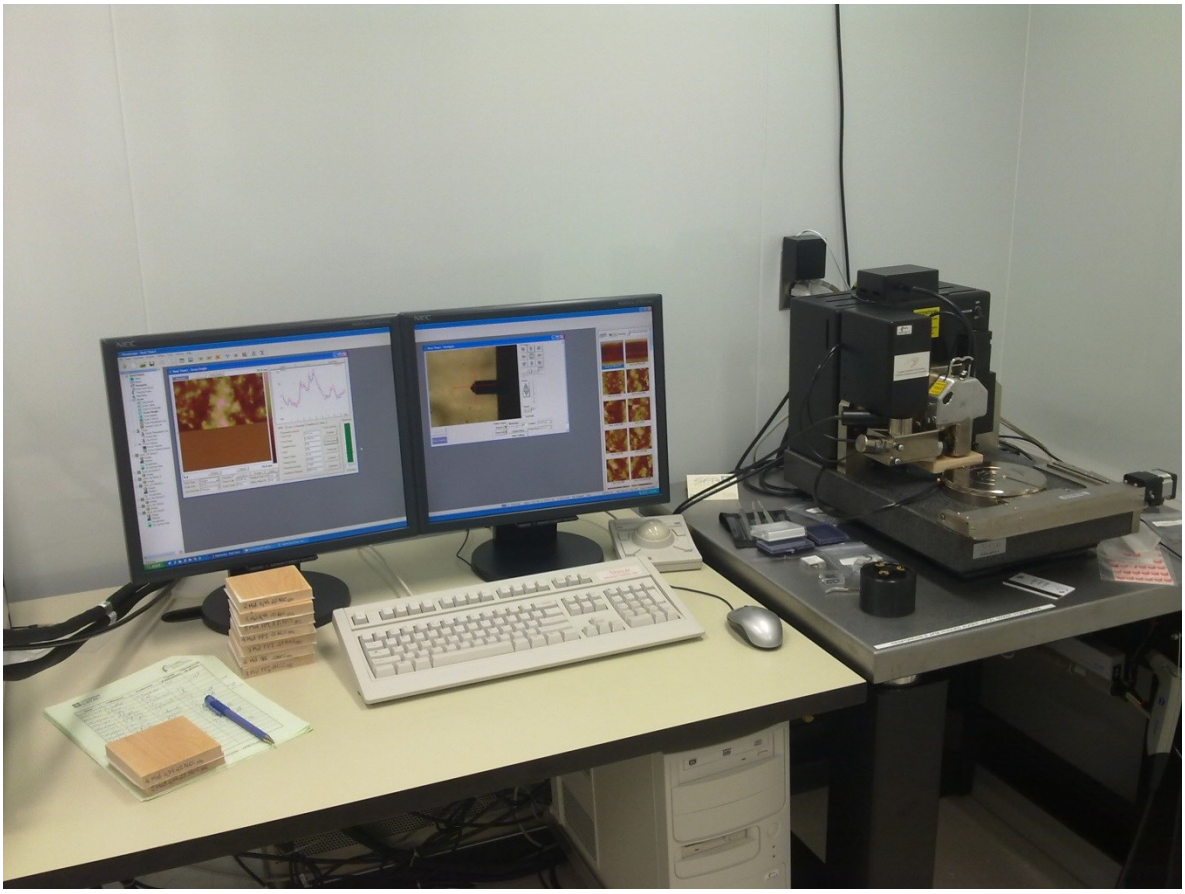

Figure 1.18. Microscopie à force atomique NanoScope V, Veeco Instruments Inc.

Cette rugosité croit-on, est un reflet de la qualité de la dispersion, donc si on a une surface lisse au niveau nanométrique, il y aurait peu d'agrégats.

Il y a différents méthodes pour évaluer le degré de la dispersion. La méthode la plus efficace serait l'analyse avec SEM/TEM. Mais dans notre cas cela est difficile à réaliser, parce que notre matrice (résine) est organique et en même temps les nanoparticules de CNC sont aussi organiques, ainsi malheureusement nous n'avons pas de contraste dans le cas de vernis.

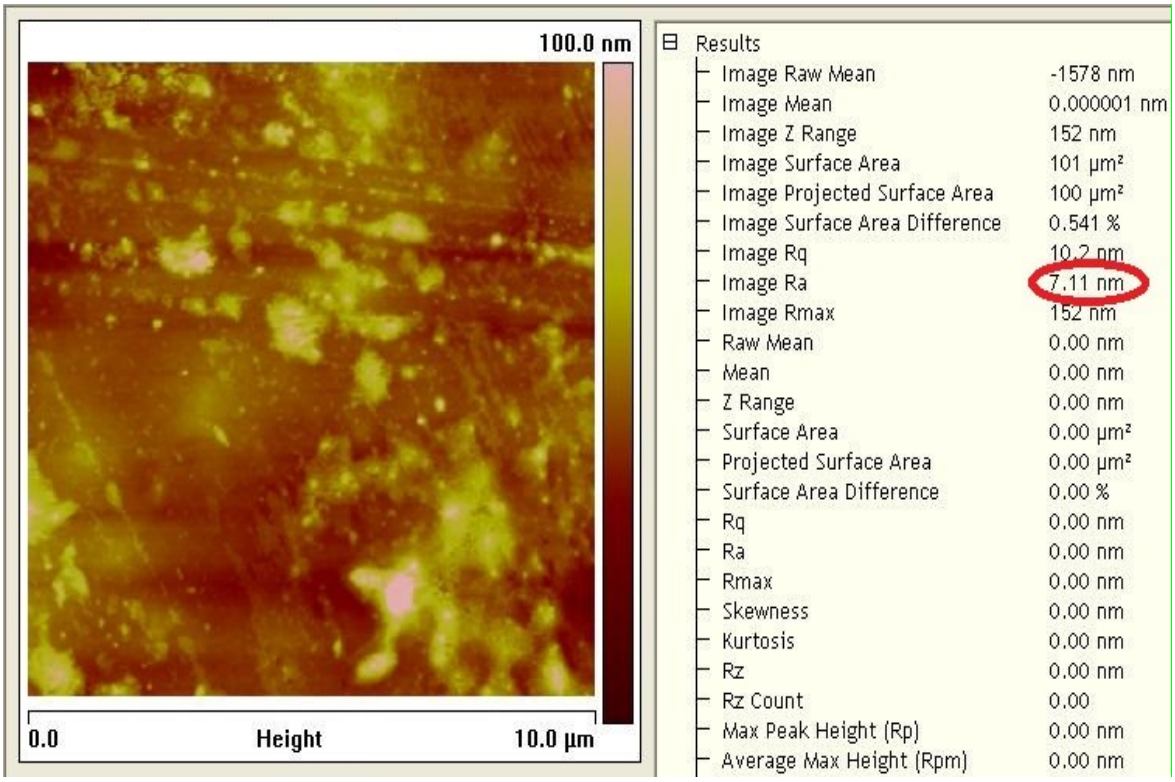

Figure 1.19. Mesure de la rugosité des revêtements par AFM.

1.8.6. Microscopie électronique à balayage

Les observations au SEM (ou MEB) ont été réalisées en utilisant un Quanta FEG 3D (Figure 1.20), microscope électronique à balayage (FEI Company, Hillsboro, USA) à haute résolution. Ce système permet de graver des structures photoniques à l'échelle nanométrique et de les analyser en temps réel. Les observations ont été réalisées sur sec (UV-cuit) films pour étudier la dispersion de TiO_2 et de la CNC dans les revêtements.

Figure 1.20. Le microscope électronique à balayage à haute résolution Quanta FEG 3D.

1.8.7. La spectroscopie de Résonance Magnétique Nucléaire

La spectroscopie de Résonance Magnétique Nucléaire (RMN) est une technique qui exploite les propriétés magnétiques de certains noyaux atomiques. Elle est basée sur le phénomène de résonance magnétique nucléaire [45-47]. Les applications les plus importantes pour la chimie organique sont la RMN du proton et du ^{13}C effectuées sur des solutions liquides. Mais la RMN est aussi applicable à tout noyau possédant un spin non nul, que ce soit dans les solutions liquides ou dans les solides. Certains gaz comme le xénon peuvent aussi être mesurés lorsqu'ils sont adsorbés dans des matériaux poreux par exemple.

La spectroscopie RMN repose sur la détection du phénomène RMN, qui se produit lorsque des noyaux atomiques de spin non nuls sont placés dans un champ magnétique externe

généralement uniforme et qu'ils sont excités par un rayonnement radiofréquence accordé sur les différences d'énergie entre les différents états possibles du spin nucléaire. La fréquence de résonance ν_0 (appelée fréquence de Larmor) est en première approximation directement proportionnelle au champ appliqué B_0 :

$$\nu_0 = \frac{\gamma}{2\pi} B_0 \qquad (1.7)$$

où γ est le rapport gyromagnétique (ou magnétogyrique).

Figure 1.21. Un spectromètre RMN 200 MHz.

Les analyses RNM ont été effectuées avec un spectromètre Bruker Avance 300 (Figure 1.21) à l'état solide à une fréquence de 75 MHz. Tous les spectres ont été enregistrés en utilisant la technique de polarisation croisée et rotation à l'angle magique avec des tubes 7mm. Les échantillons ont été centrifugés à 4000 Hz. Le temps de contact de polarisation croisée a été ajusté à 1 ms et 3000 balayages ont été enregistrés. L'avantage de cette méthode en comparaison à la spectroscopie infra-rouge est que les pics sont bien distincts.

1.8.8. Propriétés mécaniques

Il existe beaucoup des tests et expériences pour mesurer les propriétés mécaniques, mais il faut choisir les méthodes plus appropriées pour notre type de revêtement et pour notre but. Puisque généralement ce sont les formulations pour le meuble, il est très important que les revêtements soient résistants à l'abrasion et aux égratignures, mais il ne faut pas oublier la dureté.

La résistance à **l'abrasion** a été mesurée à l'aide de l'abrasimètre Taber (Figure 1.22, Taber® Abraser 5150, TABER Industries) selon la norme ASTM D4060-01. Deux disques verticaux de 500 g chacun, garnis de papier abrasif de type S-42, frottent sur l'échantillon de bois vernis/peinture, ce dernier étant animé d'une rotation. Un dispositif d'aspiration élimine le vernis/peinture érodé et empêche l'encrassement du papier abrasif. La résistance à l'abrasion est exprimée en perte de masse, causée par le passage des surfaces abrasives, après un cycle de 100 rotations, selon la relation suivant :

$$M_{perdu} = M_0 - M_{100} \qquad (1.8)$$

où M_{perdu} représente la perte de masse de l'échantillon après un cycle de 100 rotations, M_0 correspond à la masse initiale de l'échantillon et M_{100} correspond à la masse de l'échantillon après un cycle de 100 rotations.

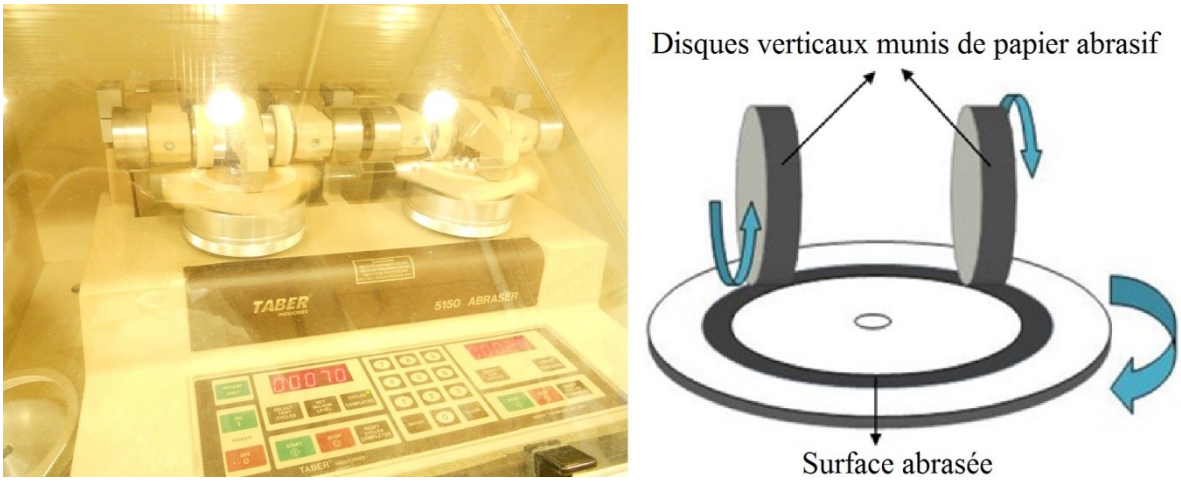

Figure 1.22. Principe de mesure de la résistance à l'abrasion à l'aide de l'abrasimètre Taber.

Pour mesurer la résistance aux **égratignures** il faut d'abord gratter la surface avec une charge standard pour tous les échantillons. Ce test a été réalisé selon la norme ASTM D7027-05, avec un appareil Multi-finger Scratch / Mar Tester, modèle 710, TABER (Figure 1.23). On gratte les échantillons avec la charge de 10 N et ensuite on mesure la profondeur par le profilomètre.

Les mesures de **dureté** ont été réalisées à l'aide d'un pendule de type de König (Pendulum Hardness Tester with König Pendulum, BYK-Gardner) selon la norme ASTM D4366-94 (Figure 1.24). Un film de vernis, d'épaisseur contrôlée et suffisante (>30 µm), est formé sur un échantillon de verre. On mesure l'amortissement des oscillations du pendule qui repose par deux billes d'acier sur le film de vernis. La dureté des revêtements représente donc le nombre d'oscillations du pendule d'un angle de 6° à 3° : le nombre d'oscillations élevé reflète un film dur tandis que le nombre des oscillations faible reflète un film mou. La mesure a été réalisée pour les films vernis: sans et avec 2% CNC.

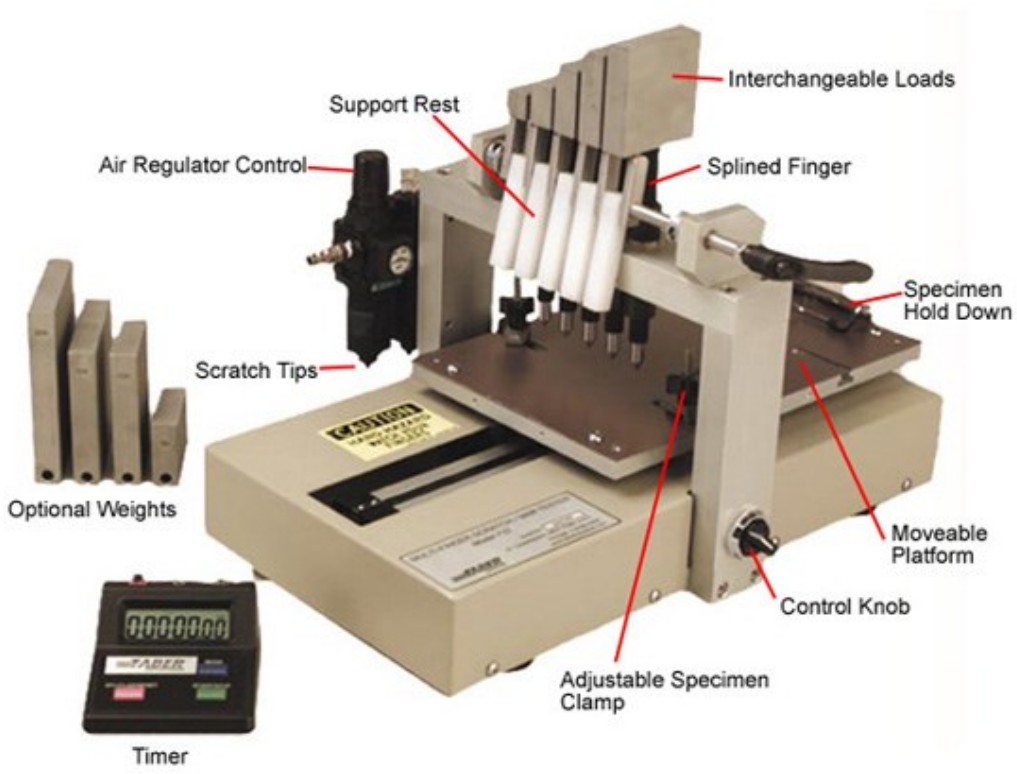

Figure 1.23. Multi-finger Scratch / Mar Tester, modèle 710, TABER.

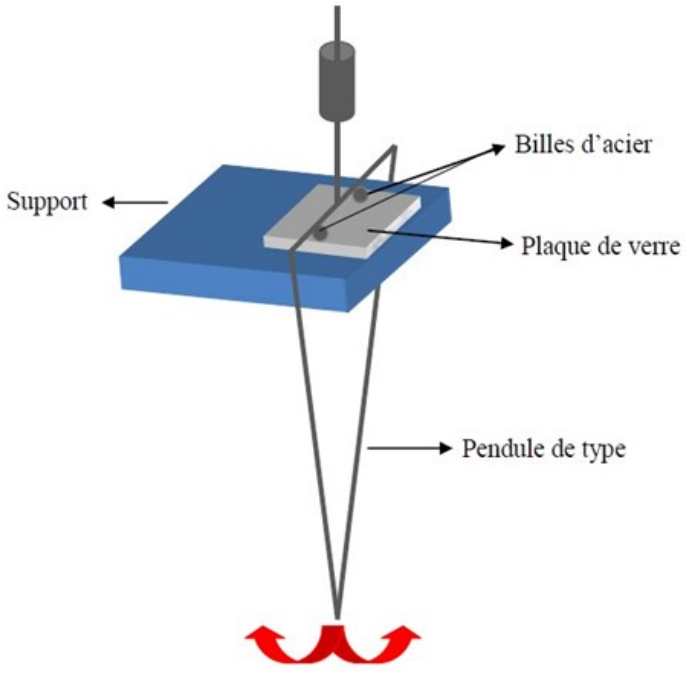

Figure 1.24. Principe de mesure de la dureté à l'aide du pendule de type König.

Les essais de traction permettent d'évaluer le niveau **d'adhésion** des revêtements composites UV-aqueux sur le substrat d'érable à sucre. Des pions métalliques (dollies) de 20 mm de diamètre sont collés à la surface propre du bois avec revêtement à l'aide d'une colle époxy bi-composante puis laissés à sécher pendant un minimum de 24 h (ASTM D4541-93). La méthode consiste à appliquer une force perpendiculaire à la surface du bois (Figure 1.25) par pression hydraulique et à évaluer, à l'aide d'un appareil de précision, la force nécessaire à l'arrachement des pions (Positest Pull-Off Adhesion Tester, DeFelsko®).

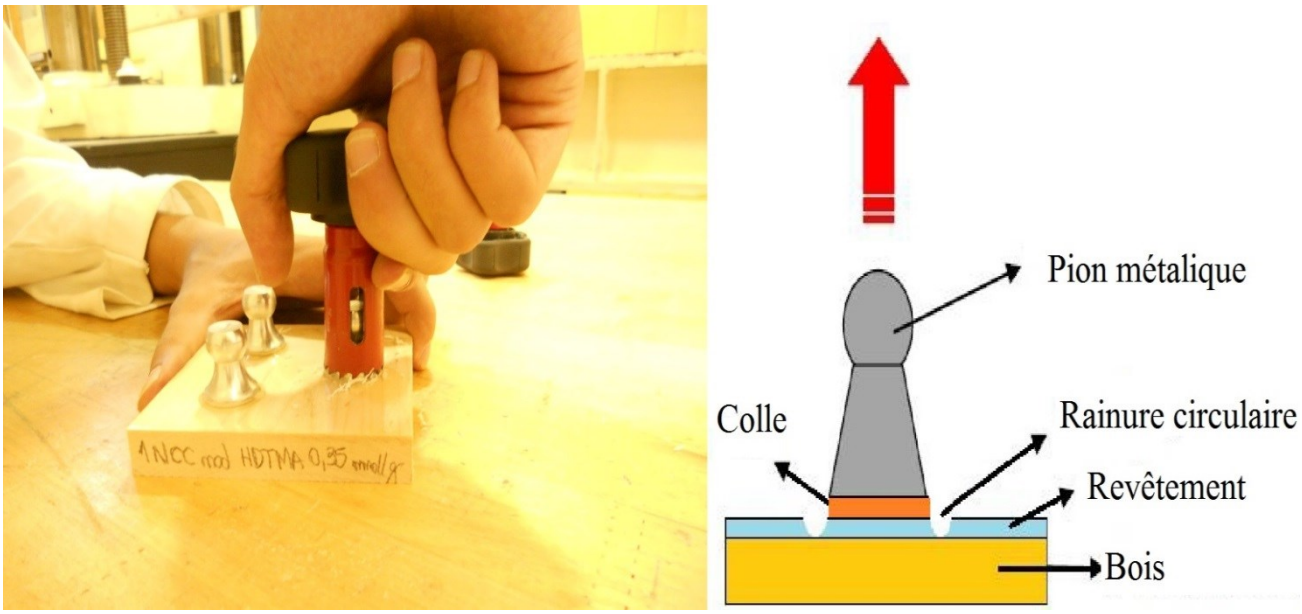

Figure 1.25. Schéma du principe de mesure de l'adhésion.

1.8.9. Propriétés optiques

D'un autre côté, il faut être sûr, que l'ajout de nanoparticules dans la formulation ne change pas les propriétés optiques : brillance et couleur, parce qu'il ne faut pas oublier les aspects esthétiques des revêtements.

La couleur a été mesurée selon le système CIE L*a*b* (Figure 1.26). C'est le système de couleur le plus couramment employé dans le domaine de l'industrie. Ce modèle de couleur

est composé de deux axes a* (composante rouge/verte) et b* (composante jaune/bleu) perpendiculaires déterminant la teinte et d'un axe L*, perpendiculaire au plan a*b*, définissant la clarté (composante de luminosité). Les mesures de couleur ont été effectuées à l'aide du colorimètre Spectro-guide de Byk-Gardner (ASTM D2244) et les valeurs sont exprimées en unités arbitraires. Pour les échantillons vernis et peintures sans et avec CNC la couleur ne change presque pas (Figure 1.12). Tout les point au sein de ces coordonnées peuvent être combinés dans un indice global de la couleur ΔE :

$$\Delta E=\sqrt{(L_2-L_1)^2+(a_2-a_1)^2+(b_2-b_1)^2} \qquad (1.9)$$

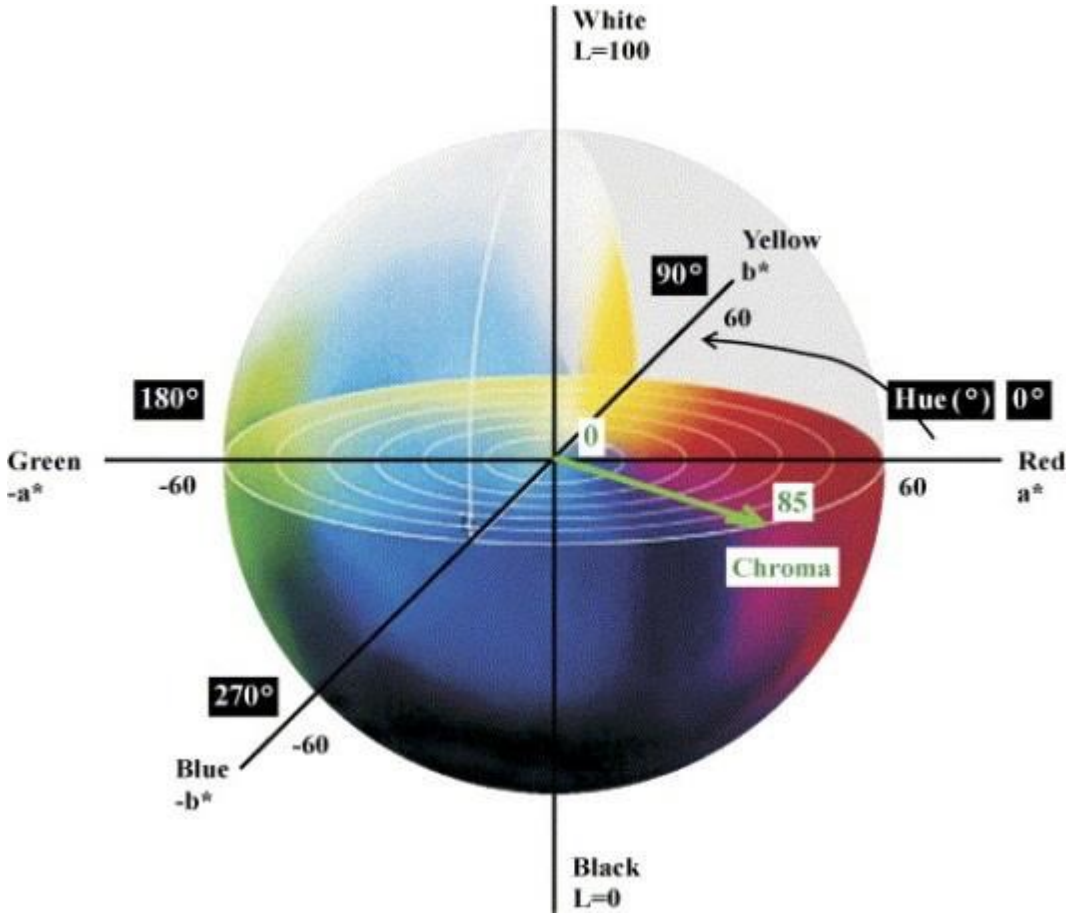

Figure 1.26. Espace de couleur CIE L*a*b*.

La mesure de **la brillance/haze** s'effectue à l'aide d'un brillancemètre/réflectomètre (micro-TRI-gloss, BYK-Gardner). C'est la principale méthode de mesure de brillance/haze employée en industrie (ASTM D523). Le principe de l'appareillage consiste à illuminer la surface du revêtement à l'aide d'une source lumineuse constante à un angle défini puis à mesurer l'intensité de la lumière réfléchie (Figure 1.27). Étant donné que la brillance dépend entre autre de la surface du revêtement (lisse ou rugueuse), nous avons observé un certain changement de la brillance, mais ces niveaux sont satisfaisants pour les vernis et les peintures (Figure 1.12).

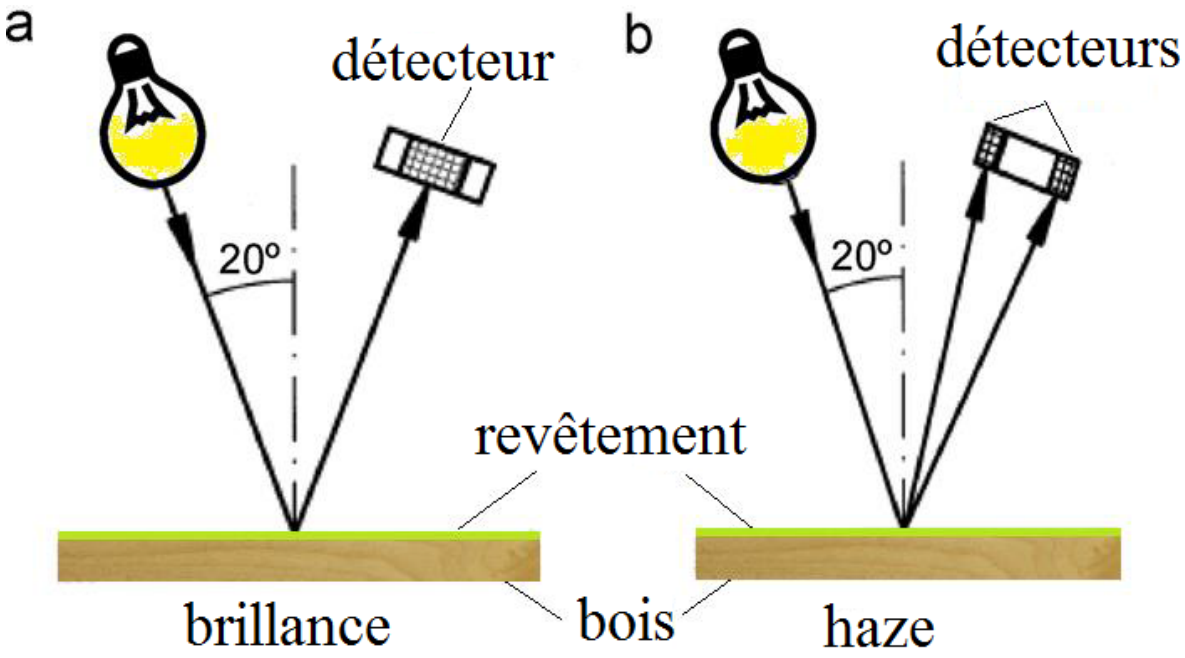

Figure 1.27. Principe de mesure a) brillance et b) haze.

Dans cette étude, une nouvelle méthode de caractérisation basée sur la microscopie à force atomique (AFM) et **la rétrodiffusion de la lumière** de laser (He-Ne 632,8 nm) est appliquée pour caractériser ces revêtements nanocomposites. La distribution angulaire de l'intensité lumineuse rétrodiffusée a été représentée par une distribution de Gauss et son écart-type a été utilisé pour les analyses de la rugosité de surface. Cette caractérisation de laser est plus rapide

et peut se faire sans contact direct sur une surface plus large que celle de l'AFM, et peut nous donner une idée sur les propriétés mécaniques des revêtements.

La rétrodiffusion de la lumière de laser He-Ne a été mesurée par un montage optique (Figure 1.28). La même géométrie (Figure 1.27) de mesure brillant/haze a été utilisée pour construire la configuration optique (angle d'incidence est de 20°). Le faisceau de laser He-Ne, fonctionnant à 632,8 nm (rouge), a été utilisé pour sonder l'échantillon de revêtement, qui est fixé au centre de la table optique principale. Pour mesurer la dépendance angulaire de la lumière diffusée, la base rotative tournée de -30° à 30° de la position initiale du photodétecteur, qui est de 20° à la normale de la surface de l'échantillon (la position de la réflexion spéculaire).

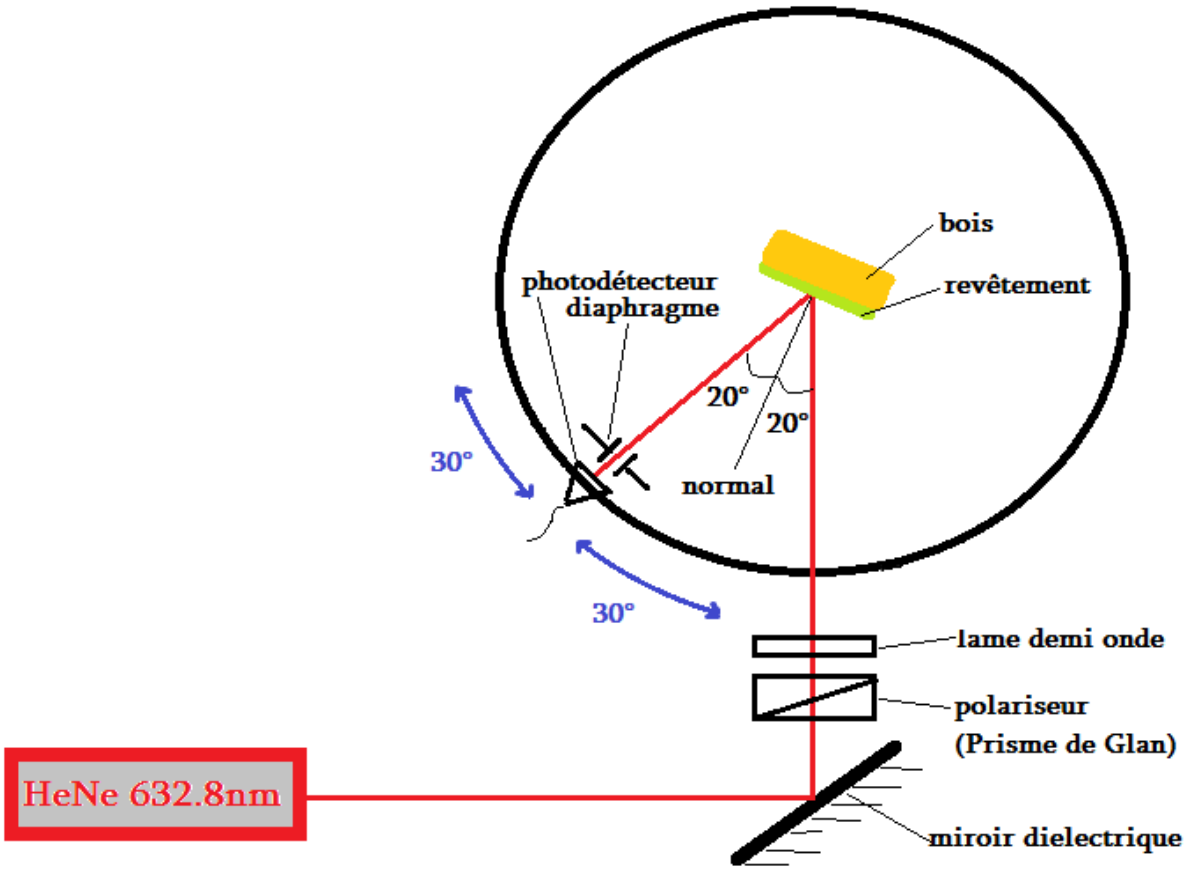

Figure 1.28. Le montage optique pour mesure de la rétrodiffusion de la lumière des revêtements.

1.8.10. Vieillissement accéléré

Les essais à réaliser afin d'évaluer la performance des revêtements extérieurs et intérieurs sont différents. Dans le cas de revêtements extérieurs, la protection contre la radiation UV est très importante. La performance des systèmes bois-revêtement a été testée grâce à une chambre de vieillissement accéléré de type WheaterOmeter Atlas Ci3000+ (Figure 1.29) équipé avec une lampe Xénon et des filtres spéciaux afin d'obtenir une meilleure simulation de la radiation solaire, une distribution uniforme et une stabilité de la lumière. Les échantillons ont été exposés à un rayonnement UV (290 à 400 nm) à différents températures et différents taux d'humidité relative (ASTM G155) durant 1200 heures. Suite à ces essais, la variation de la couleur de l'état de la surface avec le temps d'exposition a été déterminée. Les changements de rugosité des revêtements ont été également évalués afin d'évaluer leur dégradation. La dégradation par le vieillissement climatique a été suivie par l'AFM.

Figure 1.29. La chambre de vieillissement accéléré WheaterOmeter Atlas Ci3000+.

1.9. Introduction aux cinq articles - chapitres prochains

Dans le ***Chapitre 2***, une nouvelle méthode de caractérisation basée sur la microscopie à force atomique est appliquée pour caractériser ces revêtements nanocomposites. L'analyse de la dispersion a été réalisée par microscopie à force atomique en mesurant la rugosité de surface. Une analyse élémentaire a été faite pour mesurer la quantité de pigment blanc de TiO_2 dans les agrégats de peinture. L'addition de la CNC dans les revêtements résulte en une augmentation de 20-30% environ de la résistance à l'usure, sans perte d'apparence. Lorsque le vernis a été appliqué sur une couche de peinture opaque, plutôt que sur du bois, le même renforcement a eu lieu.

Dans le ***Chapitre 3***, les CNC, un nanomatériau renouvelable émergent, ont été soumises à un greffage de chaînes carbonées afin d'améliorer leur dispersion et leur capacité à transférer leur propriété de rigidité à des matrices moins polaires, en particulier les revêtements acryliques pour le bois. Ces modifications ont été réalisées en utilisant soit des bromures d'ammonium quaternaire alkylés ou du chlorure d'acryloyle. Ces nouvelles fonctionnalités chimiques, n'induisant pas de profonds changements structurels de la CNC modifiées, ont été mises en évidence par la résonance magnétique nucléaire, la spectroscopie infrarouge et l'analyse élémentaire en azote. Les dérivés de CNC se sont mieux dispersés dans le revêtement acrylique aqueux tel que suggéré par l'AFM, avec une rugosité de surface moyenne réduite de 9 à 6 nm sur les revêtements contenant les CNC non modifiées et modifiées, respectivement.

Le ***Chapitre 4*** est le chapitre principal de cette thèse, parce qu'ici on a réussi l'objectif général de cette recherche : développer des revêtements UV-aqueux renforcés par les nanoparticules pour les applications de bois, et étudier leur effet principalement sur les propriétés d'usure des revêtements composites. Les propriétés mécaniques (résistances à l'abrasion et égratignure, la dureté et l'adhérence) ont été analysées et comparées à celles des vernis de référence sans nanoparticules. L'ajout de la CNC modifiée dans les revêtements UV-aqueux a entraîné une augmentation de 30-40% de la résistance à l'usure (abrasion et égratignure), sans perte de l'apparence.

Dans le ***Chapitre 5***, une nouvelle méthode de caractérisation basée sur l'AFM et la rétrodiffusion de la lumière de laser rouge (He-Ne 632,8 nm) est appliquée pour caractériser ces revêtements nanocomposites. La distribution angulaire de l'intensité lumineuse rétrodiffusée a

été représentée par une distribution de Gauss et son écart-type a été utilisé pour les analyses de la rugosité de surface. Une forte corrélation entre la nano-rugosité de surface du revêtement et la distribution angulaire (demi-largeur de l'étalement angulaire) de la lumière du laser rétrodiffusée a été constatée. Cette caractérisation laser est plus rapide et peut se faire sans contact direct sur une surface plus large que celle de l'AFM, et peut nous donner une idée sur les propriétés mécaniques des revêtements.

Dans le ***Chapitre 6***, la formulation aqueuse d'acrylate polyuréthane translucide cuite sous rayonnement ultra-violet a été soumise au vieillissement accéléré pendant 1200 h, sur un substrat de bois, avec et sans cellulose nanocristalline (CNC) ajoutée dans les revêtements. Des mesures de nano-rugosité ont été effectuées avec la microscopie à force atomique sur une surface recouverte ainsi vieillie. La rugosité de surface a augmenté 8-10 fois après le vieillissement. Des mesures de couleur et luminosité ont été effectuées périodiquement, chaque 100 h, au cours du vieillissement. Les tests ont été faits aussi pour un revêtement multicouche, soit un vernis sur un revêtement opaque sur bois.

Chapitre 2. Wear resistance of nanocomposite coatings

2.1. Résumé

Il existe plusieurs cas dans la littérature de composites de nanocellulose-thermoplastique, mais il y a peu d'études sur les revêtements renforcés par des celluloses nanocristallines (CNC). L'un des aspects clés de la technologie des nanocomposites reste la dispersion de nanoparticules dans la matrice. Pour quantifier la dispersion, des méthodes efficaces de caractérisation sont nécessaires. Dans cet article, une nouvelle méthode de caractérisation basée sur la microscopie à force atomique est appliquée pour caractériser ces revêtements nanocomposites. L'objectif général de cette recherche est de développer des revêtements UV-aqueux renforcées par les nanoparticules pour les applications sur le bois, et d'étudier l'effet, principalement sur les propriétés d'usure, des revêtements composites. Les CNC ont été mélangées à la formulation de revêtements dans le but d'améliorer les propriétés mécaniques des revêtements secs. Les formulations de revêtements ont été pulvérisées sur des planches d'érable à sucre, qui ont été ensuite placées dans un four pour évaporer l'eau et cuire le revêtement par rayonnement UV. L'analyse de la dispersion a été réalisée par microscopie à force atomique en mesurant la rugosité de surface. Une analyse élémentaire a été faite pour mesurer la quantité de pigment blanc de TiO_2 dans les agrégats de peinture. L'addition de la CNC dans les revêtements résulte en une augmentation d'environ 20-30% de la résistance à l'usure, sans perte d'apparence. Lorsque le vernis a été appliqué sur une couche de peinture opaque, plutôt que sur du bois, le même renforcement a eu lieu.

2.2. Abstract

There are several instances in the literature of nanocellulose-thermoplastic composites, but there are few studies on coatings reinforced by cellulose nanocrystals (CNC). One of the key aspects in the technology of nanocomposites remains the dispersion of the nanoparticles within the matrix. To quantify the dispersion, efficient methods of characterization are needed. In this paper a new characterization method based on atomic force microscopy is applied to characterize such nanocomposite coatings. The overall objective of the research is to develop nanoparticles reinforced UV-water-based coatings for wood applications, and to study the effect mainly on wear properties of the final composite coatings. CNC were mixed to the coating formulation in order to improve the mechanical properties of the coatings. The coating formulations were sprayed on sugar maple boards, which were then placed in an oven to evaporate the water to finally be UV-cured. The dispersion analysis was done by atomic force microscopy by measuring roughness. Elemental analysis was done to measure the amount of TiO_2 white pigment in paint aggregates. CNC addition in coatings results in a ca 20-30% increase in wear resistance, without loss of appearance. When the reinforced varnish was applied to an opaque paint layer, rather than the wood, the same reinforcement took place.

Keywords: UV-water-based coatings; Cellulose nanocrystals; dispersion; atomic force microscopy; scanning electron microscopy; characterization; ultrasound; elemental analysis; roughness; wood

2.3. Introduction

Coatings are generally employed for two main reasons: to modify the appearance (color, texture, etc.) of materials (decorative coatings) or to protect them against numerous stresses (UV light, mechanical, chemical or thermal stresses). Coatings have to be selected according to the intended application.

According to Hosker [12], coatings used for exterior applications (garden furniture, siding, patio, etc.) must be formulated to achieve good resistance to UV rays, changes in temperature and humidity, insects as well as rot and mildew. In contrast, floor coatings must be resilient to mechanical stresses as they are constantly solicited. In fact, finishes used for interior applications such as furniture, kitchen cabinets and floors must have good mechanical (abrasion, scratches, impact and hardness), thermal (fire and flame, thermal stability) and chemical resistance (detergent, food, etc.) [12]. Coatings selection must also be made according to the substrate to be coated. Plastic materials are known as low surface energy materials and for this reason, coating adhesion is one of the major concerns associated with plastic. On the other side, coatings applied on metals have to be corrosion resistant if intended for exterior applications. Wood coatings are no exception; coatings must be adapted to its numerous particularities.

2.3.1. The importance of coatings in the wood industry

Wood is a naturally durable material, long recognized for its versatility as well as its exceptional structural properties [13]. However, to maintain its appearance as well as its mechanical properties, it must be kept under favorable conditions. According to Feist [13], like any biological material, wood is subject to degradation caused by light, moisture and oxidation. For this reason, products made from wood should generally be treated in order to preserve their properties. The use of finishing products is often the preferred avenue. Among the most desirable characteristics for interior wood coatings, abrasion or wear resistance is certainly among the first. Abrasion is a degradation due to mechanical wear by hard and rough objects. It generally occurs when paint or varnish is exposed to mechanical erosion, rubbing or friction, such as in floor finishes. A low abrasion resistant coating will lead to many surface defects after a short period of time (Surface Modification Center, 2013). Resistance to abrasion is related to coating's toughness and depends on its ability to dissipate the mechanical energy. Wood being a soft material subject to indentation, coating system must have a good mechanical performance.

Abrasion resistance of a coating will depend on the type of coatings used and of the fillers added. Different type of coatings can be used for interior wood products, the most frequently used being nitrocellulose, pre- and post-catalyzed lacquer, conversion varnish, catalyzed polyurethane, polyester and UV curable coatings (high solids and water-based). Besides performance criteria, drying time, costs per volume, application methods, drying methods and equipments required are important factors to consider when selecting a coating. Since it is not a decision based on a single criterion, one might choose a less efficient coating in terms of mechanical performance but which is more suitable taking into consideration the facilities of the industry or the coating costs per volume. For this reason, reinforcing fillers are often added to the coating formulation in order to reach better mechanical performance. Water-based coatings, which are becoming increasingly used by wood industries, are no exception.

2.3.2. Water-based coatings

Year after year, water-based coatings gain market share due to new regulations on volatile organic compound emissions and the numerous voluntary certification programs to which specifiers (architects, engineers, etc.) subscribe. Organic solvents used in most coatings generate issues with respect to the environment and human health, not to mention handling and storage. As a result, regulations on Volatile Organic Compounds (VOC) are becoming tighter in several countries. In fact, European, American and Canadian architectural regulations have recently been modified to restrict usage and encourage less hazardous alternatives. On the basis of their broad experience with solvent-borne coatings over several decades, the woodworking industries and consumers expect to meet these new VOC requirements while maintaining coating quality (performance and aspect) achieved with solvent-borne coatings.

The proposed alternatives to solvent-based coatings include water-based coatings. Even if they are gaining significant market shares, they entail significant disadvantages, and these still restrict their adoption by a portion of the wood industry. One major disadvantage relates to the mechanical performance of water-based coatings, which typically differs from

that of solvent-based coatings. One way to overcome the lack of performance of water-based coatings is to add to the coating formulation different fillers that will improve the mechanical performance and more specifically the abrasion resistance.

2.3.3. Reinforcing fillers

Reinforcing fillers are often used in order to increase the performance thus the service life of coatings. In the wood industry, silica (SiO_2) and alumina (Al_2O_3) are used at the micrometer scale to get a good abrasion and scratch resistance. These metal oxides are relatively cheap, abundant, and they possess a relatively low refractive index compared for example with titanium and zinc oxides which are used as UV absorbers. Silica and alumina are hard materials, silica being around 6-7 on the Moh's scale and alumina (corundum) being 9. However, the addition of micrometric particles, even if their refractive index is relatively low and near the one of the resin, diffracts light which leads to a reduced transparency of the coating. For UV-curable coatings, it can also interfere with the curing process. Light scattering is one of the reasons among others explaining why over the last few years several coating suppliers have switched to nanosize fillers.

2.3.3.1. Special case of nanosize fillers

Nanocomposites can be defined as multiphase materials comprising minimally a phase size of less than 100 nanometers. This well-accepted definition is not based on an arbitrary choice. In fact, as the size scale of matter becomes smaller, down to the nano-scale, the principles which govern macroscopic materials become non-scalable. This could be explained on the basis of intermolecular forces that govern material behavior [48]. Although gels, colloids and copolymers can be included in the nanocomposite definition, the term nanocomposite generally refers to the addition of a nano-sized phase in a matrix, both with different properties as well as a different structure. In general, nanoparticles are used for their optical, magnetic or conductive properties, rather than for their quality of mechanical reinforcement. However, some nanoparticles such as aluminum oxide (Al_2O_3)

and silica (SiO_2) are used, similarly to their micrometric counterparts, to improve the mechanical properties of polymer matrices. Coatings containing well dispersed nano-size inorganic materials can be considered as nanocomposites [49-51]. *Table 2.1* summarizes studies performed to improve different properties using nanoparticles.

Table 2.1. Summary of the most frequently used nanoparticle in coatings

Nanoparticle		Property achieved	Reference
Type	Geometry		
Clay	Lamellar	Barrier properties	Asif et al. [52] Park et al. [53]
Silica (SiO_2)	Spherical	Hardness Wear resistance Impact resistance Scratch resistance	Jailli et al. [54] Amerio et al. [55] Ranjbar et al. [56] Sow et al. [57] Sangermano et al. [58]
Aluminum oxide (Al_2O_3)			
Zinc oxide	Spherical	Resistance to UV light	Cristea et al. [59]
Titanium dioxide			

A number of studies have already been conducted on UV-curable acrylate coatings with nano-size aluminum oxide and silicon oxide. One of the major issues related to nanocomposite coatings is to achieve a good dispersion of the nanoparticles in the polymer matrix. For this reason, Bauer et al. [60] have grafted different silanes at the surface of nanoparticles. 3-(methacryloxy) propyl-triethoxysilane (MEMO) was grafted at the surface of silica nanoparticles and nano alumina. The addition of 35% by weight of the acrylate monomer modified nanoparticles led to a significant increase in scratch resistance. The polymer nanocomposite with and without nanoparticles have also been subjected to wear resistance experiments (steel wool, 60 cycles). The nanocomposite coating was found to have a mechanical strength much greater than the one of the coating without nanoparticles. The nanocomposite remained intact while the unmodified coating was severely affected by these tests.

In another paper Bauer et al. [61] have expanded the range of nanosize fillers and silane coupling agents added to polyacrylates. They compared the nanocomposites prepared with MEMO with nanocomposite prepared with two other coupling agents: trimethoxysilane vinyl (VTMO) and propyl trimethoxysilane (PTMO). These coupling agents were grafted onto the same silica nanoparticles and also on aluminum oxide nanoparticles (Al_2O_3), zirconium oxide (ZrO_2) and titanium oxide (TiO_2). Taber rotary platform experiments were performed and mass losses were measured. These tests were performed with the use of the coupling agent VTMO in the resin. For all nanocomposites, it was possible to note a significant increase of the wear resistance. The results were closely related to the hardness of the nanofiller as well as its refractive index. The high refractive indices of the zirconium and titanium oxide led to a decrease in curing efficiency. Ultraviolet penetration decreases because of light scattering. Bauer et al. [62] also published results on the improvement of polyacrylates by adding both nanoparticles and microparticles. Abrasion resistance tests have been carried out and showed that the mixture of two types of particles leads to a significant increase in resistance to abrasion. Indeed, the abrasion resistance is much higher than for the formulation with the same concentration of microparticles or nanoparticles. In a second article on the subject they concluded on the importance of the micrometer aluminum oxide size [63]. Using the same proportions of silica and alumina as in the previous article, they varied the size of the aluminum oxide and determined the abrasion

resistance. The results obtained show that the 16 microns aluminum oxide combined with nanoscale silica leads to excellent abrasion resistance. The work realized by Bauer demonstrated the importance of the chemical composition, the size of nanoparticles and microparticles chosen as well as the nature of the coupling agent. Sow et al. [57] have also demonstrated in their work on UV-curable water-based nanocomposites the importance of good nanoparticles dispersion on the final mechanical properties. Aggregates were found to decrease the hardness of the coating films. Dispersing nanoparticles is a real challenge. Their high surface area, promoting agglomeration and aggregation, makes it necessary to modify the surfaces of the inorganic nanoparticles in order to make them compatible with the organic matrix. Using an organic filler could help to limit the dispersion issues.

2.3.3.2. Nanocrystalline cellulose: a potential reinforcing filler for coatings

Cellulose is the most abundant organic material on earth (more than 50% of the biomass). It is the main component of wood and other woody plants. Cellulose macromolecules associated form microfibrils, which themselves are associated in layers, form the cell walls of plant fiber. Strong hydrogen bonds are present between the anhydroglucose molecules of the different cellulose chains.

Many products in everyday life are cellulose derivatives, including a new product, cellulose nanocrystals (CNC), also called whiskers. CNC are extracted from native cellulose sources such as wood pulp by controlled acid hydrolysis [29]. The resulting rod-like shape and negative surface charge of CNC's give rise to electrostatically stable colloidal suspensions. Wood is the not only source of CNC, to name a few: cotton [27], green algae [28], beet sugar [30] are sources of CNC. Bacterial CNC can also be produced [64]. There are very few studies in the literature on water-based coatings with the CNC since it is a rather new product. Some work has been done by the Dufresne's group, which uses 'whiskers' of cellulose [35]. Several particles were mixed with waterborne coatings for wood-derived products in order to improve their performance. CNC was found to be good reinforcing filler when mixed with aqueous latex matrices [65]. Similarly to the inorganic fillers, the main challenge of mixing CNC particles into a host matrix is to achieve a homogeneous

dispersion in order to maximize the macroscopic effects on the mechanical reinforcement. Landry et al. [42, 66] have shown that the addition of small concentrations of CNC particles to clear water-based coatings could help improving mechanical properties (abrasion and scratch resistance, hardness).

Since it is difficult to incorporate inorganic nanoparticles in a polymer matrix (organic), it will possibly be easier to use organic nanoparticles. For this purpose, we investigated the replacement of the inorganic nanoparticles, studied previously, by CNC particles. In addition, these have high aspect ratio, as opposed to inorganic nanoparticles which are usually spherical and they are also bio-based. The research hypothesis assumes that CNC as such, and possibly with appropriate modification of its surface, will show high dispersion and stability of the nanoparticles of CNC in the nanocomposite coatings.

The atomic force microscope (AFM) has been used to study the quality of pigment dispersions and reinforcements. Karakas et al. [39] have shown the extent of the distribution and particle aggregation in seven different formulations in relation to the surface of the paint films. The experimental results showed that the addition of TiO_2 can be reduced by 4% by optimizing the calcite optimum size. Farrokhpay [40] conducted a literature review on the new assessment techniques of painted surfaces and obtained quantitative results on the surface roughness characterization by AFM. Thometzek et al. [41] also used TEM and AFM to quantify the surface quality of paintings and correlated the degree of hydrophobicity of the particles with the quality of the dispersion. This chapter aims to qualify the dispersion of CNC in varnish/paint coatings, determine the surface roughness of the nanocomposite coatings by AFM and link these results with the abrasion resistance performance.

2.4. Materials and methods

UV-curable clear and opaque coatings were prepared minimally from a water-based emulsified polyurethane acrylate resin, a defoaming agent, a surfactant, a dispersant, a

thickener, nanocrystalline cellulose and a photoinitiator. Opaque formulations also include titanium dioxide (TiO_2) (*Table 2.2*).

Table 2.2. Varnish and paint formulations

	% NCC dry w/w	Binder	Antifoaming agent	Surfactant	Dispersant	Pigment	Solvent	NCC	Thickener	Photoinitiator	TOTAL
		Liquid mass (g)									
Varnish	0	274.73	1.86	1.15	3.72	-	25.50	-	1.24	2.30	**310.50**
	0.5	273.36	1.85	1.14	3.70	-	22.84	4.08	1.23	2.29	**310.49**
	1	271.98	1.84	1.14	3.68	-	20.19	8.16	1.23	2.28	**310.50**
	1.5	270.61	1.83	1.13	3.66	-	17.53	12.24	1.22	2.27	**310.49**
	2	269.24	1.82	1.13	3.65	-	14.87	16.33	1.21	2.26	**310.51**
	3	266.49	1.80	1.12	3,61	-	9.56	24.49	1.20	2.23	**310.50**
Paint	0	197.23	1.86	1.15	3.72	31	26.5	-	1.24	2.3	**265.00**
	0.5	196.24	1.85	1.14	3.70	30.85	23.61	4.08	1.23	2.29	**264.99**
	1	195.26	1.84	1.14	3.68	30.69	20.72	8.16	1.23	2.28	**264.99**
	1.5	194.27	1.83	1.13	3.66	30.54	17.83	12.24	1.22	2.27	**265.01**
	2	193.29	1.82	1.13	3.65	30.38	14.94	16.33	1.22	2.25	**264.99**
	Initial concentration (%)	**40**	**25.5**	**97.8**	**40.5**	**100**	-	**14**	**20.1**	**45**	

The resin selected is the Bayhydrol UV 2282 (Bayer Material Science), a polyurethane acrylate (PUA) oligomer emulsified in water that was primarily developed for applications on wood. The photoinitiator used is a bis-acyl phosphine oxide (Irgacure 819DW, BASF Resins - Inks and OPV) dispersed in water (45 wt %). Titanium oxide (TiO_2) was used as a pigment. After trials, it was found that ~ 30% (dry weight) of TiO_2 gives an opacity of 80%.

Table 2.2 summarizes the weight of each chemical used to prepare the different formulations. CNC concentrations were set to 0.5, 1, 1.5, 2 and 3% (dry weight).

In *Table 2.2*, the initial concentration of each ingredient can be described as follows:

$$I = \frac{M_{dry}}{M_{liquid}} \times 100\% \qquad (2.1)$$

where M_{dry} and M_{liquid} are the dry and liquid weight of each ingredient when added to the formulation. The CNC used in this research is in gel state (14% w/w in water). Final liquid weight of formulations is different, approximately 310.5 g for varnishes and 265.5 g for paints. In both cases, the dry weight of coatings equals 114.28 g. This was done to have comparative formulations. So, overall initial concentration, as solids content, for varnishes is about 37% and about 43% for paints.

2.4.1. Cellulose nanocrystals

Aqueous CNC suspensions were prepared in FPInnovations pilot plant by sulfuric acid hydrolysis of a commercial bleached softwood kraft pulp according to a procedure modified from the literature [67]. Samples of the suspension of CNC were sonicated using a Sonics Vibra-cell 130W, 20 kHz ultrasonic processor with a 6 mm diameter probe. Typically, 15 ml of a 2-3%w/w CNC suspension were placed in a plastic tube of 50 ml and sonicated at 60% of the maximum power. This sonication treatment (corresponding to a total energy input of ~ 3600 J / g CNC) was performed in an ice bath to prevent the CNC degradation caused by the heating. Following this process, retrieved nanofibers have the following properties: specific surface area of 600 m^2/g, a Young's modulus of 150 GPa and a tensile strength of 10 GPa [67].

Cellulose fibers that remain after this treatment are almost entirely crystalline and as such are called "crystalline". The precise physical dimensions of the crystallites depend on several factors, including the source of cellulose hydrolysis accurate conditions, and ionic strength.

The aqueous CNC suspension was then concentrated in a Labconco RapidVap (Labconco, Kansas City, USA) down to 14% w/w. Such high CNC concentration is required to adjust the CNC loading within the formulation and avoid excessive dilution.

2.4.2. CNC particle size measurement by light scattering

Particle size or aggregate size was determined by photon correlation spectroscopy (PCS) using a Malvern Zetasizer Nano ZS (Malvern Instruments Ltd, Malvern, United Kingdom). To avoid excess light scattering in the spectrometer, the samples were diluted to 0.05 wt % CNC in the presence of 5 mM NaCl. Samples were filtered with 0.45 μm nylon or 0.7 μm GF/F Whatman syringe filters prior to measurement. No significant loss of CNC occurred as proven by gravimetry measurements after filtration. Measurements were performed in triplicate at 25 °C.

Because PCS is a light-scattering method, the measured CNC particle size values quoted are the z-average (intensity mean) hydrodynamic diameters of equivalent spheres and do not represent actual physical dimensions of the rodlike CNC particles. However, they are valid for comparison purposes.

2.4.3. Coating formulations preparation; dispersion method

The choice of the dispersion method plays an important role in the final dispersion state of nanoparticles [42]. Several types of apparatus are commonly used in the industry, among those: high speed mixer, three-cylinder mill and ball mill. Although the last two methods lead to very high shear rates and high degree of dispersion, high-speed mixer (Dispermat, VMA-Getzmann GMBH D-51580 Reichshof) was preferred as it is most commonly encountered in the industry. The mixer used can reproduce shear rates comparable to those of industrial mixers.

To achieve good TiO_2 dispersion, ultrasonication was used after high speed mixing, the formulation was transferred to a 1 L Erlenmeyer flask and placed in a cooling bath containing ethylene glycol maintained at 5°C. An ultrasonic probe of 750 Watts (Ultrasonic processor, Cole Palmer) and a thermometer were immersed in the aqueous formulation. The ultrasonic frequency used for the dispersion was set to 20 kHz. The ultrasonic treatment was carried out for 2 min by setting the maximum temperature attainable in the formulation at 40 °C [57].

2.4.4. Preparation of the formulations

The protocols followed to prepare the paint and varnish formulations are presented in Figure 2.1. To ensure reproducible results, the order of addition of the different ingredients was closely followed. The stirring speed was set to 400 rpm. After the dispersion of the nanoparticles and the TiO_2, formulations were filtered to remove the glass beads.

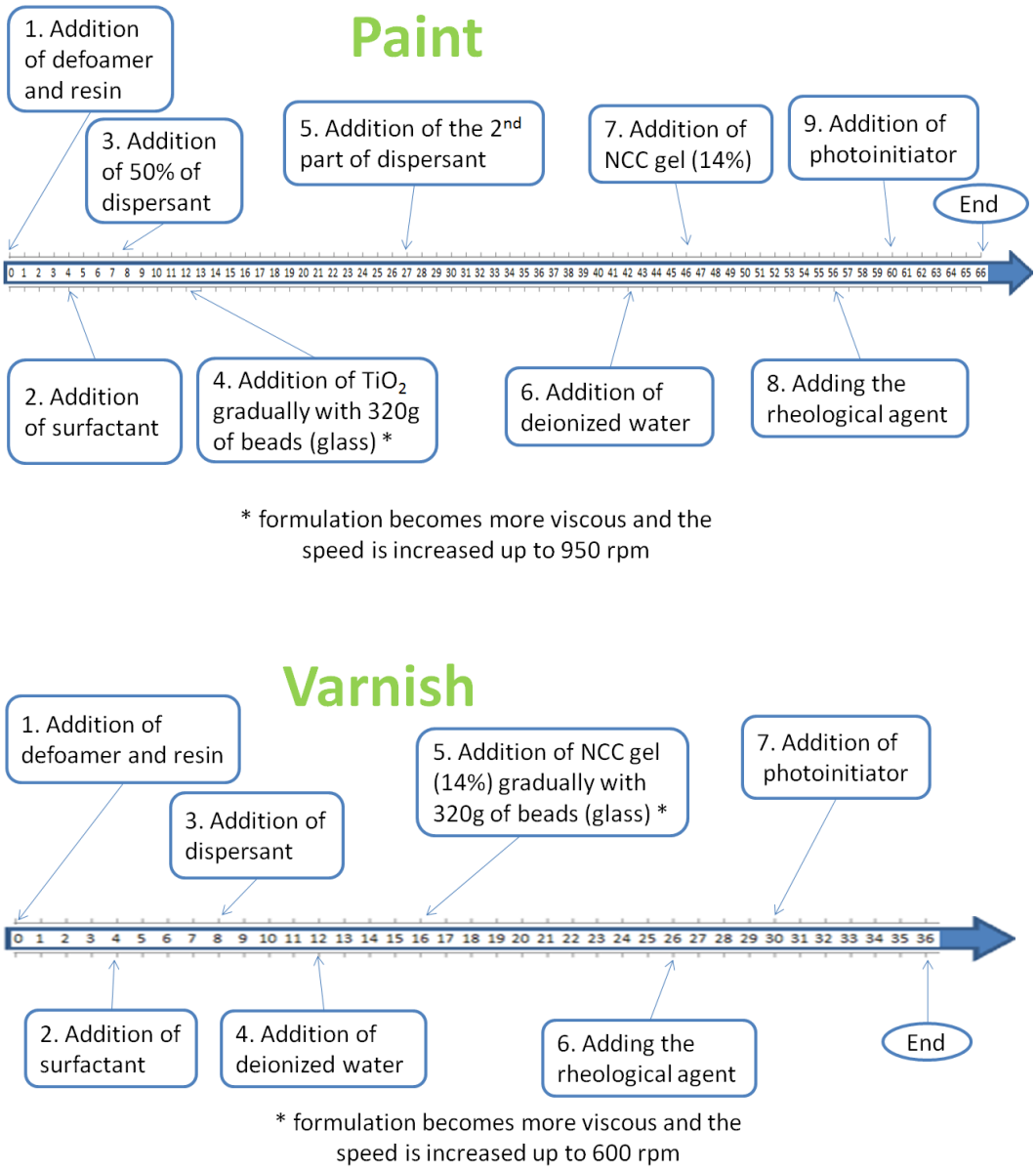

Figure 2.1. Formulations preparation protocol: paint and varnish.

2.4.5. Wood samples preparation

The dimensions of the sanded Sugar Maple (*Acer Saccharum*) wood samples used in this project are 96 × 96 × 15 mm (Figure 2.2). Samples were conditioned at 60% relative humidity prior to coating application. Paint and varnish formulations were applied by pulverization. After application (dry film thickness of 127±20 µm for varnish and 152±20 µm for paint formulations), samples were placed in an oven for 10 minutes at 60°C to evaporate water. After complete water evaporation, the ultraviolet curing was carried out using a UV oven equipped with a medium pressure mercury lamp (600 W/cm). The intensity of the UV light, with complete UV range beginning at 184.9 nm, was 570 mJ/cm^2 and the perceived temperature during curing ranges between 25 and 30°C. These steps gave a final dry coating thickness (solid film) of about 100 microns.

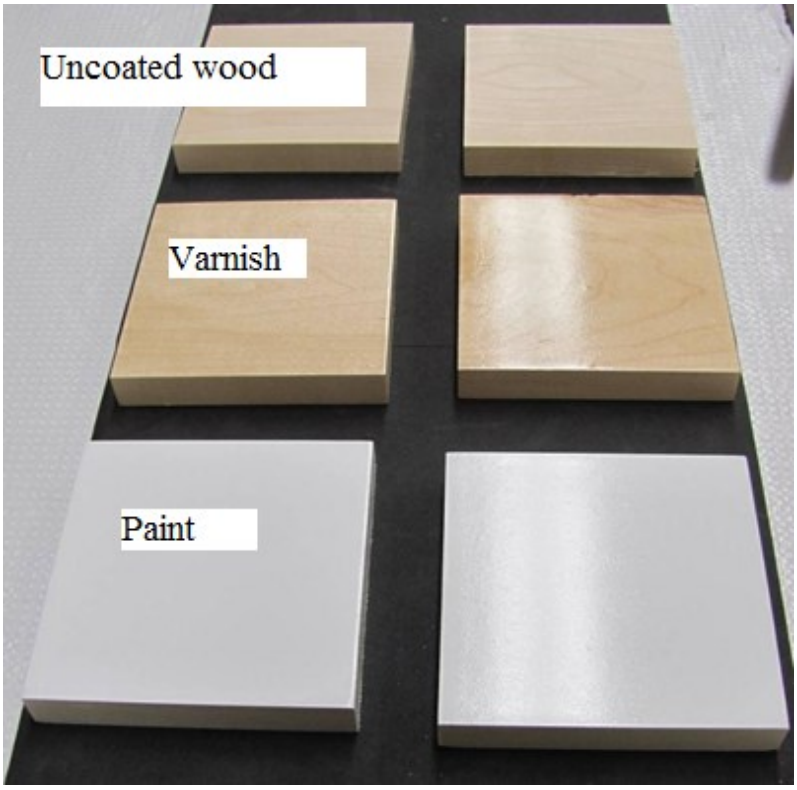

Figure 2.2. Samples with and without coatings (without CNC (left) and with CNC (right)).

In Figure 2.2, appearance of the coatings, discussed in this paper, are shown. At the top are uncoated wood surfaces. In the middle, varnishes are presented: the surface is shiny, and there is no discernible difference between left and right, which are, respectively, the varnish without CNC and the varnish with 1% CNC. At the bottom, painted samples are presented. They are white and opaque thanks to the TiO_2 particles. Again, there is no major difference between coatings with and without CNC.

2.4.6. Atomic force microscopy

AFM observations were carried out using a NanoScope V, fitted with a Hybrid XYZ scanner (Veeco Instruments Inc., Santa Barbara, USA). AFM measurements were performed under ambient air conditions in tapping mode (tip radius is 8 nm). The resolution was set to 256 lines by 256 pixels for all observations. Surface roughness was calculated in 10 × 10 μm scan areas, using the classical mean surface roughness parameter. The parameters were calculated by the Research Nanoscope 7.2 software using this equation:

$$R_a = \frac{1}{n}\sum_{i=1}^{n}\left|Z_i - Z_{ave}\right| \tag{2.2}$$

where R_a is the mean roughness, the arithmetic average of the absolute values of the surface height deviations, Z_i is the current Z value, Z_{ave} is the average of the Z values within the given area and n is the number of points within the given area (256 × 256).

2.4.7. Scanning electron microscopy (SEM) and elemental analysis

SEM observations were carried out using a Quanta 3D FEG high-resolution scanning electron microscope (FEI Company, Hillsboro, USA). UV-cured waterborne films were analyzed to investigate the dispersion of TiO_2 and CNC in the films.

The elemental analysis of the UV-cured waterborne films was studied using an EDAX's Sapphire Si (Li) Energy Dispersive Spectroscopy (EDS) Detector for the SEM with classic 10-Liter Dewar.

2.4.8. Abrasion resistance

Abrasion resistance of the paint and varnish formulations was studied using a Taber Abraser (Taber Abraser 5135, TABER Industries, North Tonawanda, NY, USA) following ASTM D4060 standard. Mass loss was recorded after 100 rotations, with 500 g discs, with type S-42 sanded paper.

2.4.9. Scratch resistance

To measure the scratch resistance, the surface must be scraped with a standard load for all samples. This test was performed according to ASTM D7027-05 standard, using a Maluti-finger Scratch / Mar Tester, model 710, (TABER Industries, North Tonawanda, NY, USA). The samples were scratched with a 10 N load, followed by depth profiling with the profilometer.

2.5. Results and discussion

2.5.1. CNC samples characterization

Prior to investigation of the surface roughness of the nanocomposite coatings, the average size of the CNC particles in water was measured. Figure 2.3 displays the particle size distribution profile by intensity, with logarithmic X-axis and linear Y-axis. These experiments were performed in water, as it is not possible to perform the particle size analysis with this equipment in presence of resin.

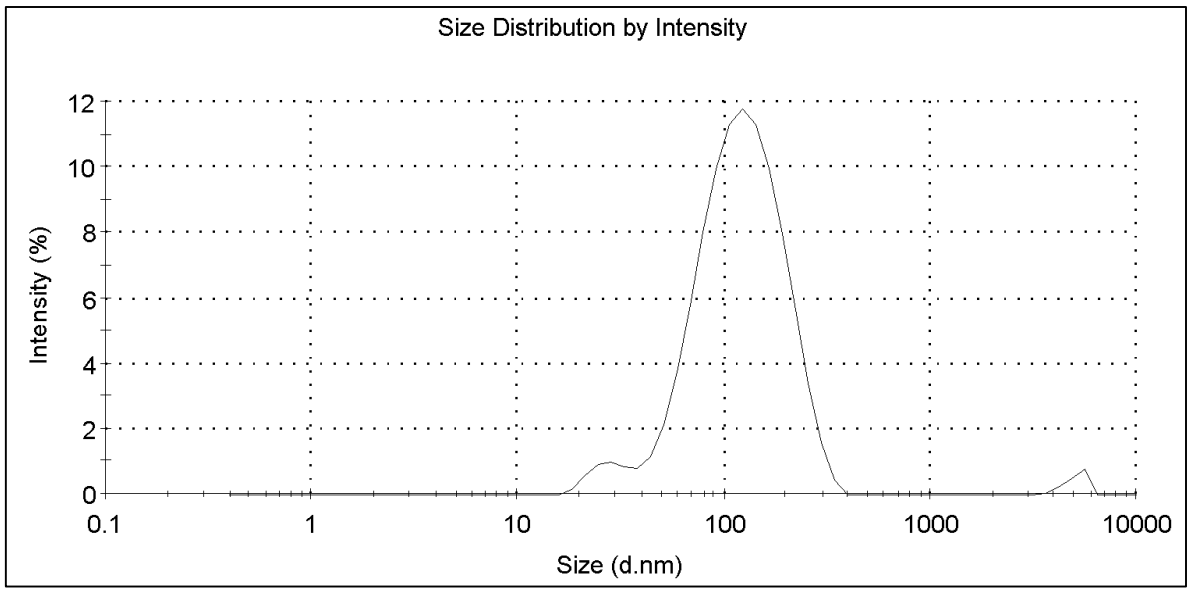

Figure 2.3. Size distribution profile of the 0.05% w/w CNC suspension in water.

This technique, as mentioned previously, does not recognize the fiber-like nature of CNC and gives a value equivalent to a hydrodynamic volume size. The characteristic dimension of CNC, assimilated to a hydrodynamic volume size, as measured in aqueous suspension gives an averaged particle diameter of 110 nm (+/- 5 nm). According to measurements performed by FPInnovations, the dimensions of CNC particles are 6-10 nm (width) and 100-130 nm (length).

2.5.2. Polymerized coating formulations characterization

The most widely used method to analyze the dispersion state of nanoparticles in dry films electron microscopy, scanning (SEM) or transmission (TEM). However, in this project, it is difficult to do so as the polymer matrix (resin) and the CNC particles are both organic which leads to a very low contrast between the resin and the particles. SEM images of the clear coatings (varnish) with or without CNC (Figure 2.4 a-b) show no significant differences. In fact, varnish surfaces are very homogeneous, and the presence of CNC does not impact the surface. Other workers have shown that wood surfaces are rather rough at

the nanoscale, since wood is a porous substrate, but once covered with a coating, even with only 30 microns thickness, it becomes highly even at nanoscale [68].

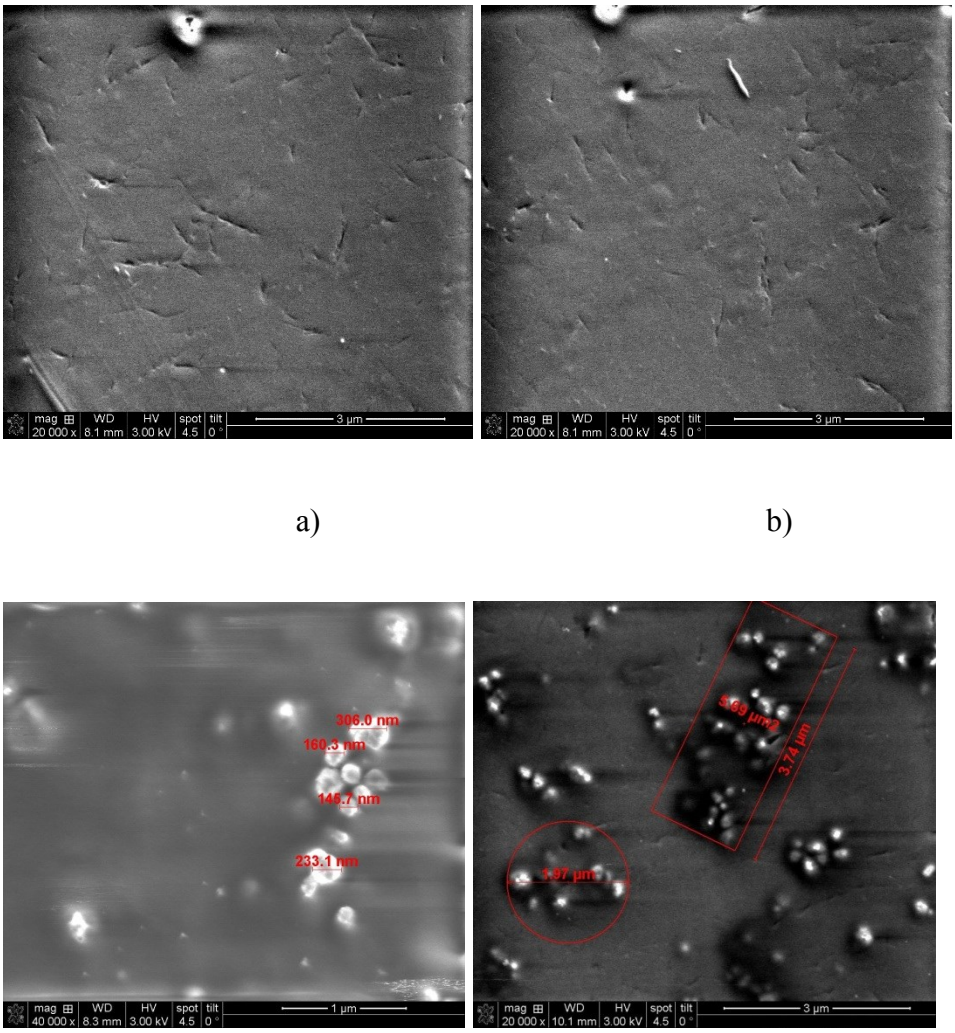

Figure 2.4. SEM imaging (a) varnish without CNC, (b) varnish with 1.5% CNC, (c) paint without CNC, (d) painting with 1.5% CNC.

In the case of paint formulations, a good contrast between the resin and the titanium oxide was observed, but not for the CNC particles (Figure 2.4 c-d). For the paint formulations,

TiO_2 particles clearly appear as white dots on the micrographs. To make sure that the white dots are indeed microparticles of TiO_2, elemental analysis was performed. Two points were selected and studied on Figure 2.5; a) where aggregates were observed and b) on a smooth part of the film without aggregates. Thanks to this analysis, the presence of TiO_2 microparticles has been shown in the aggregates.

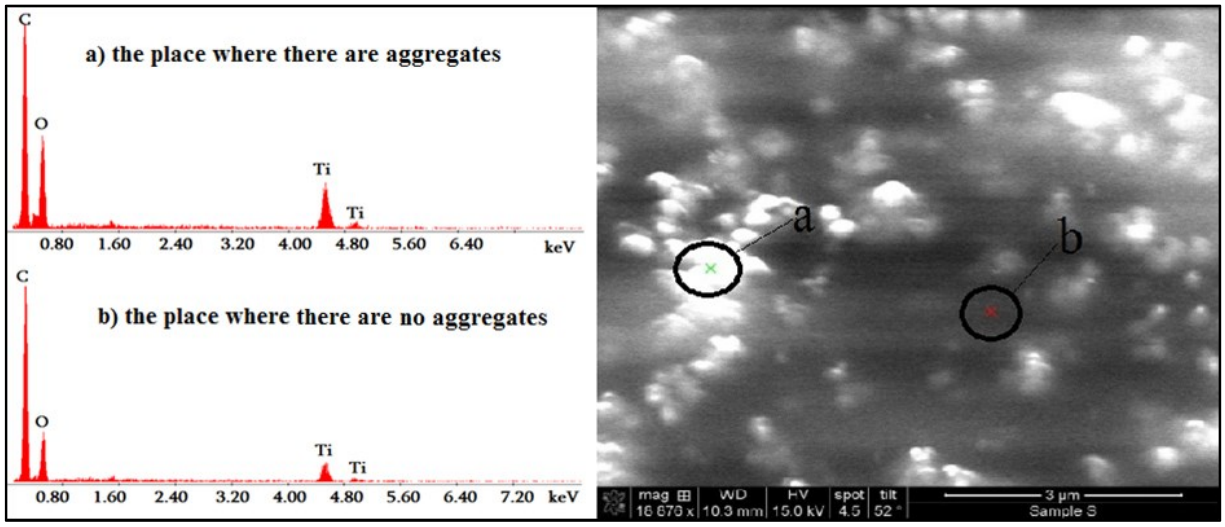

Figure 2.5. Elemental analysis of paint surface: (a) where there are aggregates and (b) where there are no aggregates.

The small peaks (Figure 2.5-b) are due to the presence of TiO_2 nanoparticles, invisible in this micrograph at this scale, but probably present in all film volume. It is not possible to perform a similar analysis for the varnish films as no aggregates can be observed. To overcome this issue, AFM experiments were performed and results are presented in Figure 2.6. Nanoscopic roughness is a reflection of the quality of the CNC dispersion within the formulations. If surface is smooth at the nanometer level, CNC particles are well dispersed and aggregates are small.

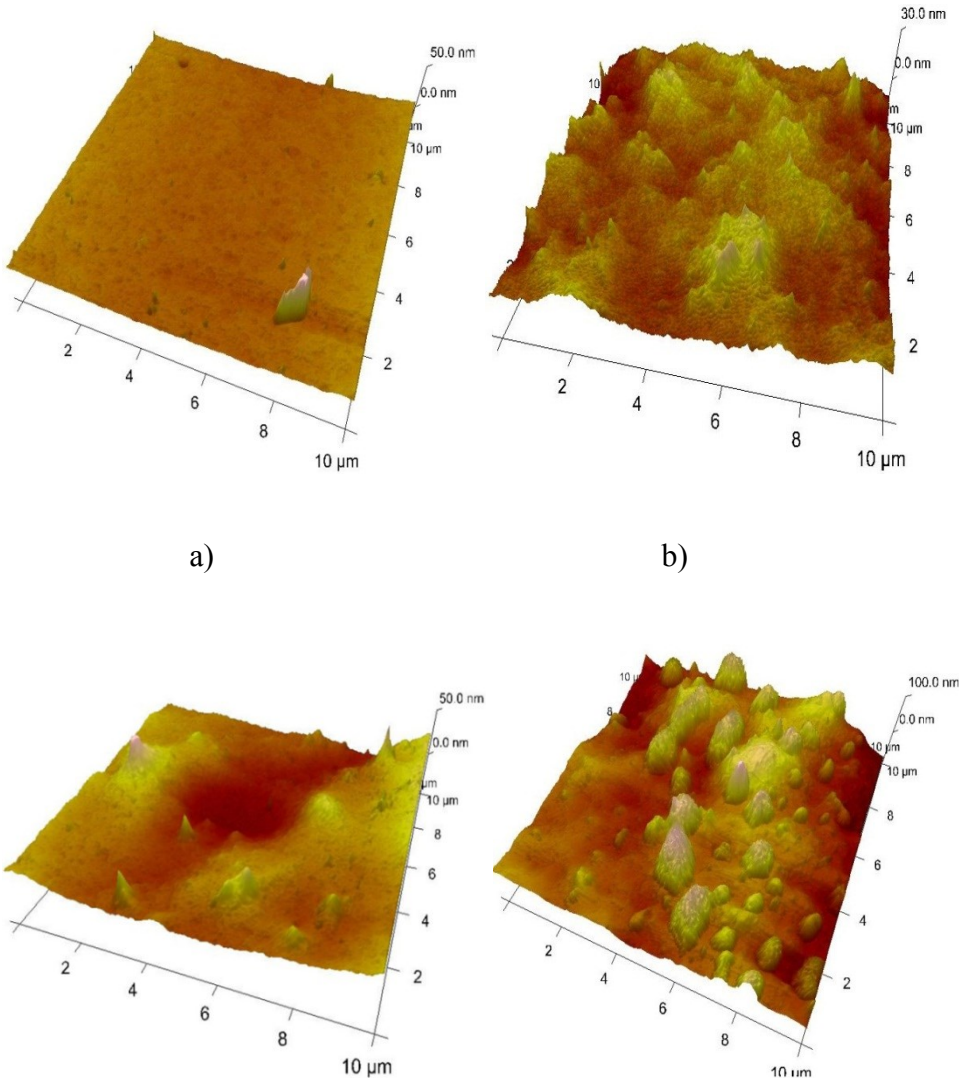

Figure 2.6. AFM profile images of: (a) varnish without CNC, (b) varnish with 1.5% CNC, (c) paint without CNC, (d) paint with 1.5% CNC.

As presented in Figure 2.6-a, which represents the varnish without CNC, the roughness is low, even at the submicron scale. At the opposite, as shown in Figure 2.6-b, the addition of 1.5% of CNC to a varnish formulation leads to a sharp increase in roughness. This reveals strong aggregation of CNC particles as the length of cellulose nanoparticles is only about 100 nm and the approximate aggregate size for this image is about 1 micron. Figure 2.6-c presents the surface of a paint formulation without CNC particles. As it can be seen,

roughness increases, but not as much as for the varnish formulation with CNC particles. Finally in Figure 2.6-d, the addition of both CNC and TiO_2 was found to increase significantly the size of the aggregates, much more defined than in Figure 2.6-b and Figure 2.6-c, indicating an interaction between TiO_2 and the CNC. It should be noted that it is very important to measure the surface roughness for quite small (10×10 μm in our case) areas, so that the surface irregularities at larger scale do not disturb the measurement of the degree of dispersion of nanoparticles. Thus, 10×10 μm images were chosen for characterization of the CNC dispersion in both varnish and paint formulations.

Four AFM characterizations (10×10μm) were performed on 10 samples for concentrations of CNC varying between 0 and 3% (0, 0.5, 1, 1.5, 2 and 3%) for varnish formulations (Figure 2.7), and between 0 to 2% (0, 0.5, 1, 1.5 and 2%) for paint formulations (Figure 2.8).

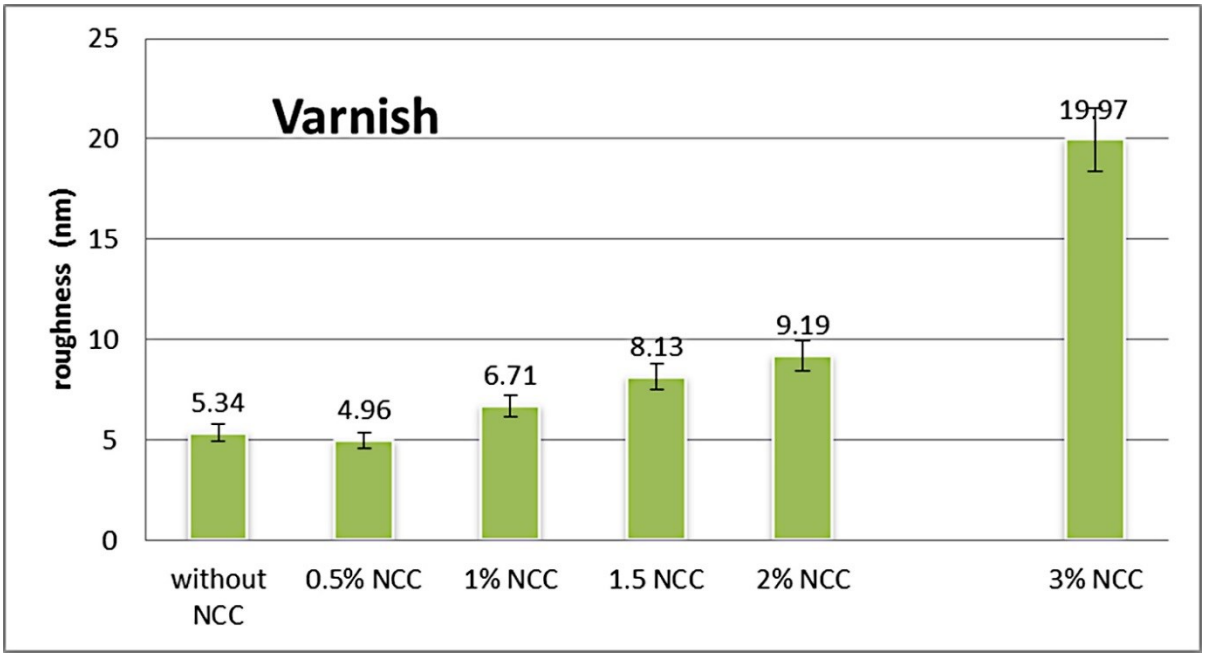

Figure 2.7. Varnish average roughness (Eq. 2.2) as a function of the CNC content.

The reason why CNC concentration was limited to 2% for paint formulations is that, above 2% in CNC content, the paint becomes highly viscous and it is impossible to spray the coating on the substrate without adding water.

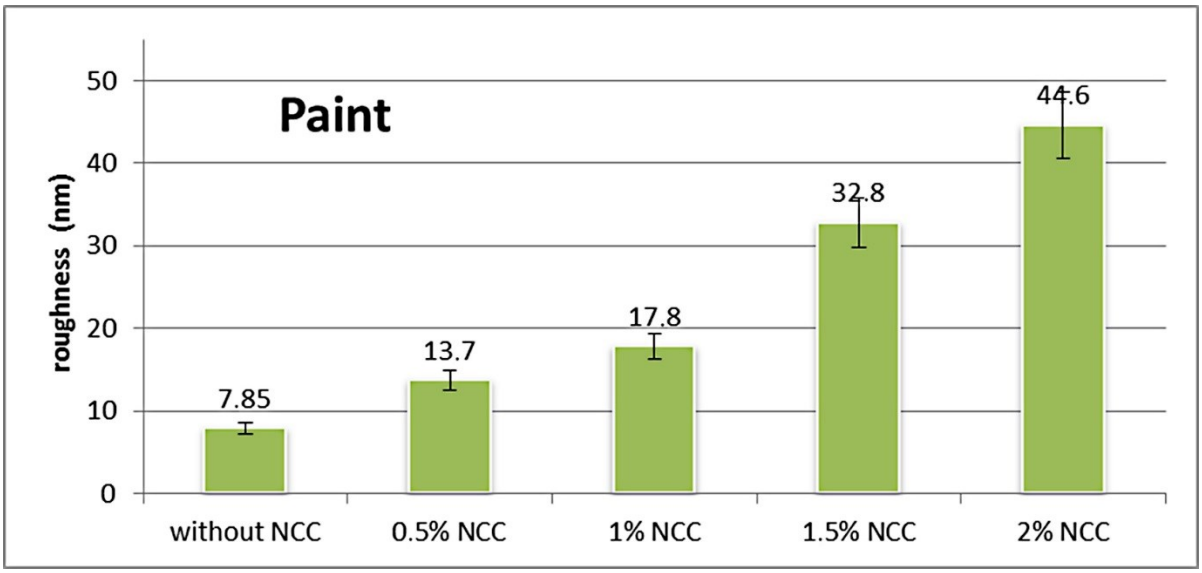

Figure 2.8. Paint average roughness (Eq. 2.2) as a function of the CNC content.

The average roughness measurements as a function of the CNC content were measured for the varnish (Figure 2.7) and the paint formulations (Figure 2.8). As mentioned previously, it is not possible to perform the same characterizations by SEM/TEM on sections of coatings due to the lack of contrast between the varnish and the CNC, both organic. Thus, AFM roughness measurements are considered as measures of dispersion quality of TiO_2 and CNC particles.

It is important to mention that even if the size of the CNC particles is about 100 nm (Figure 2.3) the surface roughness is much smaller as the CNC particles are not stacked at the surface of the coating but disperse in the coating film. Only part of the CNC sticks stand out of the surface. Figure 9 shows a schematic representation of the CNC and TiO_2 particles dispersion in the films. With no added micro or nanoparticles, the varnish film is

quite even and average roughness is about 5 nm, while with addition of 2% CNC it almost doubles (Figure 2.7) slightly superior 9 nm. The length of the CNC nanoparticles or rods is about 100 nm (Figure 2.3), so it could be argued that the CNC particles on the surface slightly protrude from the surface individually of in aggregates. Figure 2.9 shows a schematic representation of the CNC and TiO_2 particles dispersion in the films explaining the roughness values found. The presence of TiO_2 particles seems to increase the roughness, but as for the CNC particles, the roughness is not of the magnitude of the particle size of the TiO_2 particles.

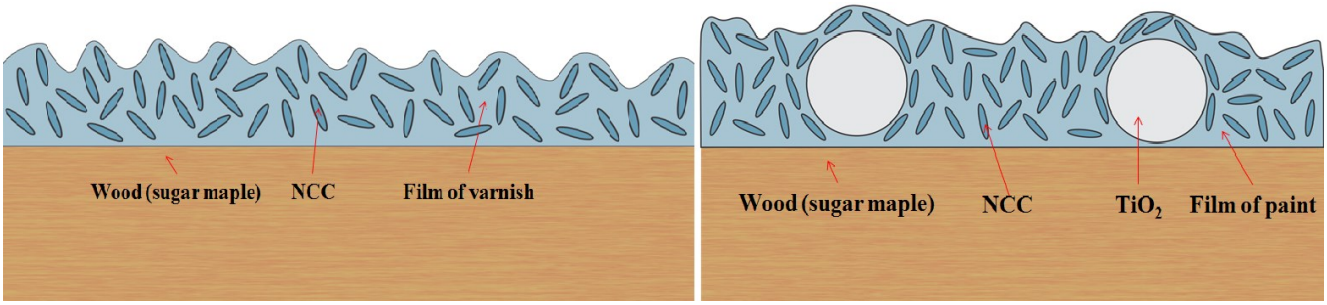

a) b)

Figure 2.9. Schematic (not to scale) representation of the (a) CNC-containing varnish layer and (b) CNC-containing paint layer.

2.5.3. Influence of the sonication on the CNC dispersion

The coatings analyzed so far revealed that the presence of CNC drastically changes the surface roughness and topology. This can be attributed to CNC instability in the medium (water) caused by the presence of the other ingredients and the mixing to disperse it within the formulation. Indeed, the CNC aqueous suspensions are very sensitive to pH and ionic strength, especially as to their liquid crystal states, in concentrated form [67]. Changes in these two parameters probably would affect the stability and the agglomeration state of the CNC suspensions. Moreover, the chemical affinity and surface characteristics of the CNC would have to be changed to better interact with the other components. For now, the mixing

aspect only is addressed. However, to optimize the dispersion of the CNC particles, CNC chemical surface modification is being addressed, as of now, in our laboratory.

Sonication impacts on the agglomeration state of the CNC and TiO_2 particles and should help to make the formulation more homogeneous in terms of surface roughness. SEM imaging was performed before and after sonication (Figure 2.10), for paints at 1% CNC content.

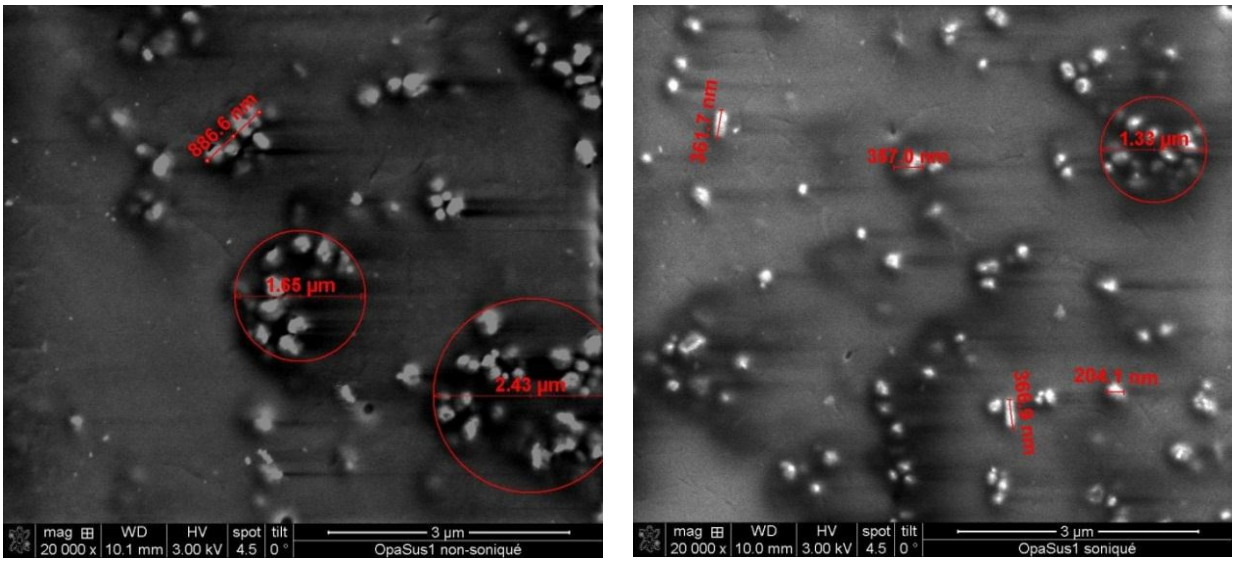

a) b)

Figure 2.10. SEM imaging for paints with 1% CNC (a) non-sonicated and (b) sonicated.

As presented in the SEM images in Figure 2.10, the aggregates are almost twice as small in the sonicated media than in the non-sonicated media. The roughness, after coating polymerization, was also measured by AFM. For sonicated samples, the roughness was found to be significantly lower (R_a=7.11 nm) than for the non-sonicated samples (Figure 2.10, 1% CNC), which is 17.8 nm. This experiment clearly shows that this roughness parameter is closely related to the degree of dispersion.

By comparing results found for the SEM and the AFM experiments for the paint formulations, it is possible to characterize the dispersion of CNC in the varnish, therefore the dispersion of organic nanoparticles in an organic matrix, which is very difficult to do by SEM, because there is no contrast between the two materials.

2.5.4. Abrasion resistance

Figure 2.11 presents the mass loss found for the paint and varnish formulations after 100 rotations. For the varnish, the abrasion resistance is improved by the addition of CNC particles. The maximum abrasion resistance is obtained for a CNC concentration of 2%. For a formulation with more CNC, 3%, the abrasion resistance was found to decrease slightly. As it was possible to see on the AFM images, roughness was found to increase significantly in this range of concentration (2-3%) for the varnish formulations. For these results, it is possible to conclude that the aggregation interferes with the mechanical properties but can be tolerated to a certain extent. As CNC particles possess a refractive index close to the one of most acrylic-acrylate resins [69], at low concentration it should not diffract light significantly, nor impede the polymerization process.

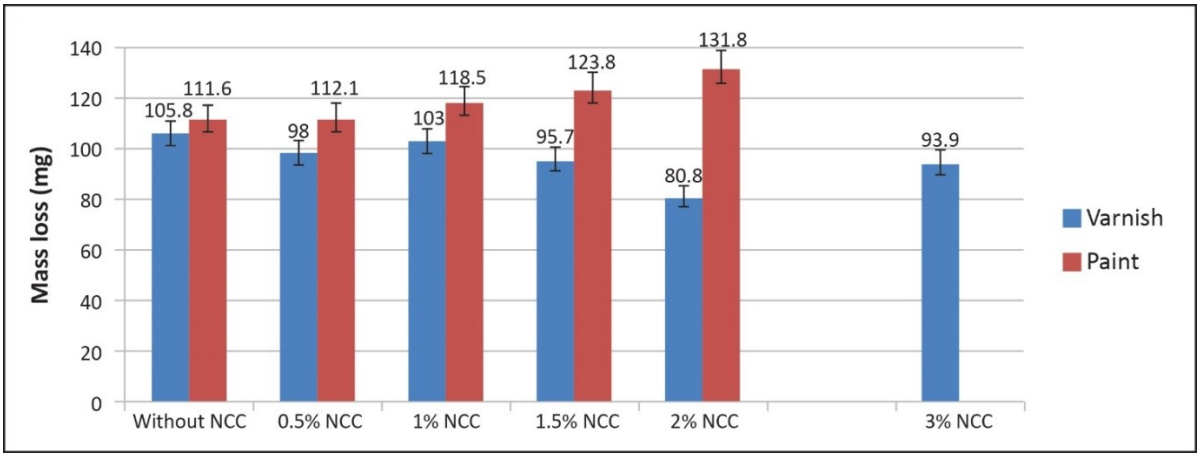

Figure 2.11. Mass loss of the paint and varnish coatings with different CNC concentrations.

Paint formulations show a totally different behavior. Even at low concentration, the addition of CNC decreases the abrasion resistance (higher mass loss). There is no optimum concentration such as for the varnish formulations. Many reasons could explain this negative result. First, as seen on the AFM images, roughness is important even at low CNC concentration for the paint formulations. High roughness increases light scattering decreasing the UV light penetration and the curing efficiency. Paint formulations already contain high particle content (TiO_2), adding CNC, as present on the AFM images seem to create a special aggregation phenomenon. Studying the interactions between the TiO_2 particles and the CNC particles would be beneficial to provide a better understanding of this phenomenon.

2.5.5. Scratch resistance

Figure 2.12 presents the scratch depth for the paint and varnish formulations after scratching by 10 N load.

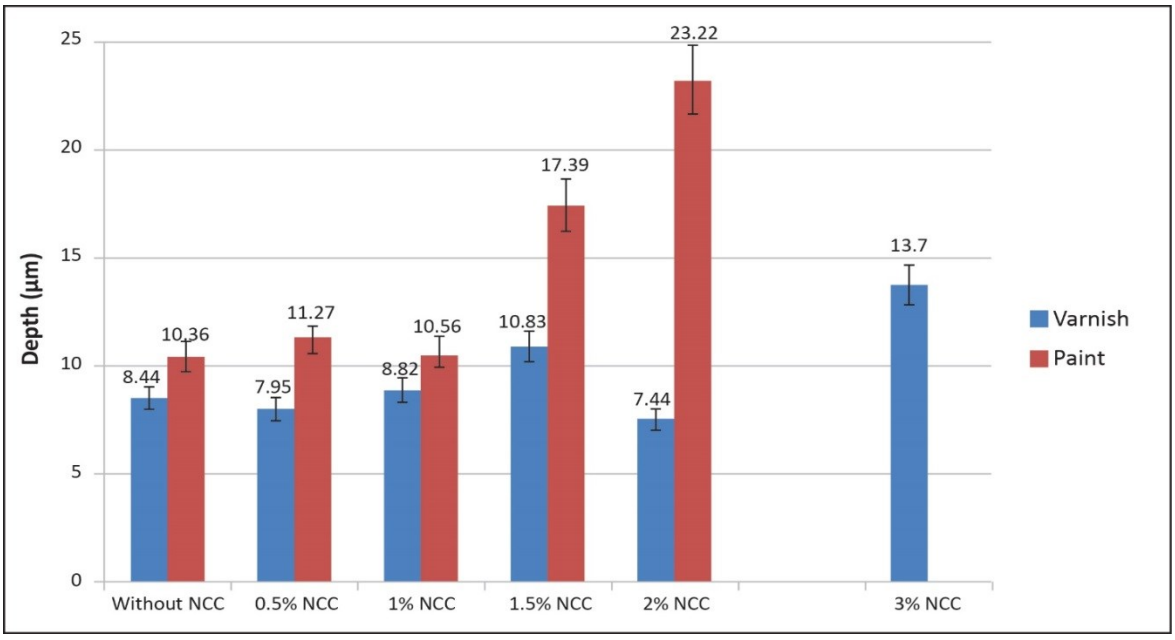

Figure 2.12. Depth after scratching of the paint and varnish formulations with different CNC concentrations.

There is some improvement for varnishes by the addition of CNC particles. The minimum depth (maximum resistance) is obtained for a CNC concentration of 2%, like the abrasion resistance, but, at CNC content over 2%, its decreases, because of the bad dispersion of particles in the varnish (Figure 2.7). In the case of paints, the depth practically did not change up to 1% of CNC particles, but at over 1% CNC content, it increases abruptly, like the roughness (Figure 2.8). So it can be concluded, that for both tests (abrasion and scratch resistances) we have improvement by the addition of 2% CNC particles in the varnishes, while properties remain at same level for the paints.

2.5.6. Multilayer coatings

We need opaque paint for some applications (kitchen furniture etc.). Addition of CNC particles can't improve mechanical resistance of paints because of aggregations with non-organic pigment (TiO_2). Pigment can be changed, but CNC could again create aggregation with new pigment too. One way to increase wear resistance is to make a multilayer coatings: first layer with paint on the wood to obtain opacity and white (or other) color, followed with one varnish layer to improve mechanical resistance. This technique is well known in car industry. Figure 2.13 presents the mass loss found for the multilayer coating after 100 rotations (all four green bars), as well as some other monolayer results. The mass loss of multilayer coatings is nearly equal to those of varnishes, so that the second (varnish) layer adheres to the first, and protects the wood.

There is no reason to repeat scratch resistance test for the multilayer coatings, because the maximum depth which registered for the varnishes is 13.7 μm (Figure 2.12, varnish with 3% CNC) and the varnish layer thickness is about 50 μm.

These multilayer coatings retain the white color of the paint, because of the highly transparent varnishes (Figure 2.2).

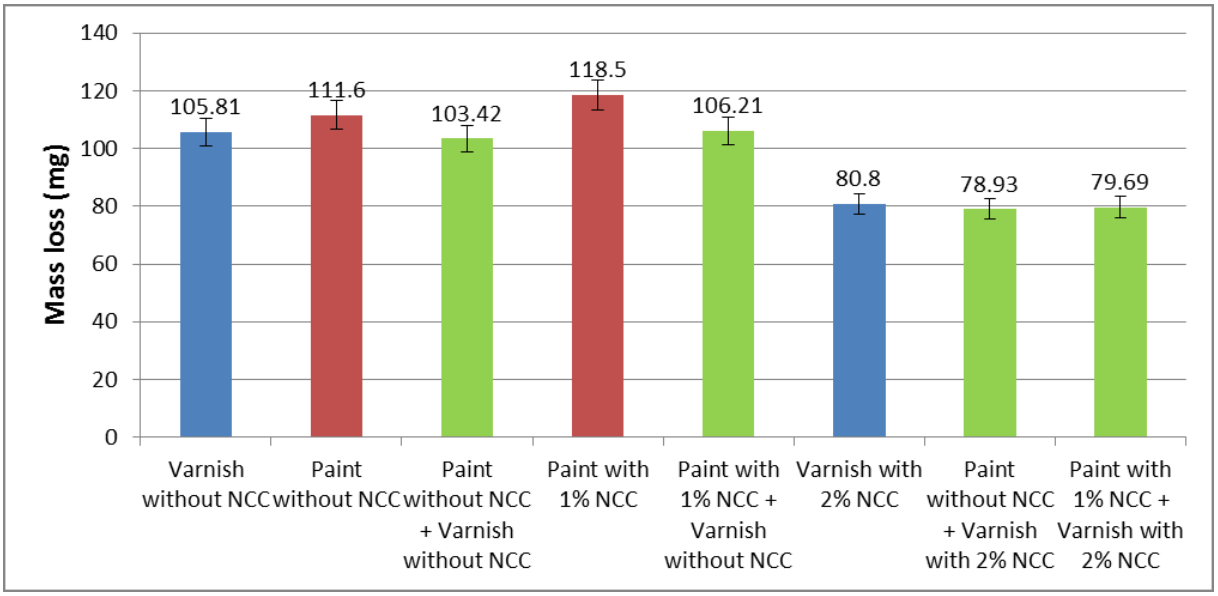

Figure 2.13. Mass loss of the multilayer coatings with different CNC concentrations, compared to that of single layer coatings.

2.6. Conclusions

In this chapter, UV-curable varnish and paint formulations containing CNC particles have been prepared. The surface roughness was measured by AFM and gives good indications of the degree of CNC dispersion and agglomeration for paints. It also gives indications of the degree of dispersion for the varnish formulations. This is an efficient method to evaluate the dispersion in cases where SEM cannot be employed as there is no contrast between the particles and matrix (organic composition). This method can easily be used to characterize the dispersion of other nanoparticles in other matrices and give results not only qualitative but also quantitative. In fact, the average of N measurements of roughness parameters, as obtained thanks to the AFM software, can easily and precisely be used to compare roughness parameters.

The average roughness of the painted surfaces is small, considering that wood is a rather rough substrate. This may be due to the high surface tension of the water, which, while evaporating, flattens all irregularities.

Still the presence of CNC can be detected by the topography of the varnish or paint surface. This is due to the sensitivity of the AFM technique, but it was found to have no effect on optical properties of the coating.

The impact of the CNC addition in the paint and varnish formulations was finally assessed. Varnish and paint formulations behaviors differ significantly in terms of abrasion and scratch resistance. For the varnish formulations, an optimum concentration (2%) was found. At the opposite, paint formulations were all negatively impacted by the addition of CNC particles. When the reinforced varnish was applied to an opaque paint layer, rather than the wood, the same reinforcement took place.

This work was performed with unmodified CNC. Surface–modified CNC and its influence on the dispersion will be introduced in a next paper.

Acknowledgments

The authors wish to thanks Arboranano, NanoQuebec, FQRNT (Québec, Canada) for funding this project, the FPInnovations' labs (Quebec and Pointe-Claire, QC, Canada) for providing the CNC samples and helping with the coating formulation, as well as Professors Carmel Jolicoeur and Bohuslav Kokta for help with funding application.

Chapitre 3. Modification of cellulose nanocrystals as reinforcement derivatives for wood coatings

3.1. Résumé

Les celluloses nanocristallines (CNC), un nanomatériau renouvelable émergent, ont été soumises à un greffage de chaînes carbonées afin d'améliorer leur dispersion et leur capacité à transférer leur propriété de rigidité à des matrices moins polaires, en particulier les revêtements acryliques pour le bois. Les modifications chimiques utilisées à cet effet doivent être simples, sans incidence sur la structure principale de la CNC et compatibles ou synergiques à la formulation UV-aqueuse ciblée. Ces modifications ont été réalisées en utilisant soit des bromures d'ammonium quaternaire alkylés ou du chlorure d'acryloyle. Ces nouvelles fonctionnalités chimiques, n'induisant pas de profonds changements structurels de la CNC modifiées, ont été mises en évidence par la résonance magnétique nucléaire, la spectroscopie infrarouge et l'analyse élémentaire en azote. Les dérivés de CNC se sont mieux dispersés dans le revêtement acrylique aqueux tel que suggéré par la microscopie à force atomique, avec une rugosité de surface moyenne réduite de 9 à 6 nm sur les revêtements contenant les CNC non modifiées et modifiées, respectivement. Pour les évaluations mécaniques, les revêtements comportant les différents dérivés de CNC ont été appliqués sur le bois d'érable à sucre, un matériau très apprécié comme bois d'intérieur ou de meubles en bois qui nécessitent une protection de surface efficace. Les tests d'abrasion ont indiqué que les CNC modifiées confèrent une résistance aux égratignures supérieures, avec une amélioration de 24 à 38% pour les revêtements contenant des CNC modifiées, sur ceux contenant la CNC non modifiée.

3.2. Abstract

Cellulose nanocrystals (CNC), an emerging renewable nanomaterial, was subjected to carbon chains grafting in order to improve its dispersion and its ability to transfer its rigidity properties into less polar matrices, especially acrylic wood coatings. Chemical modifications used to this purpose are required to be simple, not affecting the CNC main structure and compatible or synergistic to oligomer reticulation inside the targeted UV-waterborne formulation. Those modifications were carried out using either alkyl quaternary ammonium bromides or acryloyl chloride. These new chemical functionalities, not inducing deep structural changes in modified CNCs, were highlighted through nuclear magnetic resonance, infrared and nitrogen content analyses. CNC derivatives were better dispersed in aqueous acrylic coating as suggested by atomic force microscopy, with a mean surface roughness falling from 9 to 6 nm on the coatings containing unmodified and treated CNCs, respectively. For mechanical evaluations, the coatings including various CNC derivatives were applied on sugar maple wood, a much appreciated material as indoor timber or wooden furniture which requires an efficient surface protection. The abrasion tests indicated that the modified CNCs confer a higher scratch resistance, with an improvement from 24 to 38% for coatings containing CNC derivatives over those with unmodified CNC.

Keywords: Cellulose nanocrystal, Derivatives synthesis, Dispersion, Nanocomposites, Wood coating, Mechanical properties

3.3. Introduction

The durability improvement of wood products greatly calls for the development of protective coatings with higher performances. The use of various nanoparticles, including common inorganic metal oxides (ZnO, Al_2O_3, TiO_2, CeO_2, etc.) as mechanical reinforcement additives into coatings, represents a significant approach to reach this end [42, 57, 59, 70, 71]. However, difficulties encountered in incorporation of inorganic

nanoparticles in polymer matrixes (organic), such as incomplete dispersion and adhesion, suggest working with organic nanoparticles. That particularly applies to cellulose nanocrystals (CNC), a new renewable non-toxic product obtained after isolation of crystalline domains from cellulose acid hydrolysis. Indeed, as one of many advantageous characteristics, excellent mechanical reinforcement effects are known with CNC incorporation which has been the subject of a growing interest in nanocomposite materials with polymers [26, 35, 72-74]. This advantage is much more attractive since wood, compared with other natural sources of cellulose (cotton, hemp, bacteria, green algae, etc.), benefits from a long process experience of its controlled acid hydrolysis, as pulp, and, moreover, represents the most abundant, renewable and sustainable source of CNC [29, 75, 76]. Such CNC diversified applications would also permit to foresee a better development potential in the forest industry [72, 77]. Some applications, related to low polarity matrix, appear somewhat limited because of CNC surface hydroxyls and consequent hydrophilic nature, in acrylic waterborne coatings, for instance. Thus, to enhance its dispersion and therefore its mechanical reinforcement in a wide range of matrix polymers, CNC should be submitted to appropriate surface modifications.

Thanks to reactive surface of OH side groups, grafting of chemical species is possible to achieve in order to functionalize the CNC surface. In addition, the CNC obtained from sulfuric acid hydrolysis exhibits negative charges at the surface at neutral pH [73, 74, 78, 79], which are due to sulfate ester groups which are able to form ionic bonds with a matching reagent. Based on those reactive sites, some modification studies have been described as for the compatibilisation of CNC or cellulose with polymer composites referring to different application fields, as focused on by Emanuelsson and Wahlen [80], then Heux and Bonini [81]. In the same way, other authors have silylated CNC, resulting in an improved dispersion in polymers for biomedical and engineering contexts [82, 83]. Likewise, firstly activating CNCs surface with tempo-mediated oxidation, thereby creating carboxylic acids surface reactive groups and coupling those with alkylating amines, it was possible to create other CNC derivatives, for example leading to nanoplatelet gels, as stable mimetic nanomaterials [84, 85]. In another approach, the CNCs ability to establish ionic interactions have been put to good use in “green”, easy and safe synthesis processes of

stable selenium, nickel or titania nanoparticles, notably useful for medical diagnostics, energy conversion or catalytic applications [86-88].

In this communication, we report a preparation of cellulose nanocrystal derivatives by surface chemical modifications using alkyl quaternary amines or acryloyl chloride in simple conditions, the interest being to improve CNC dispersion in varnishes for wood and the mechanical properties of this matrix.

3.4. Experimental

3.4.1. CNC derivatives synthesis and characterization

CNC was provided under freeze-dried form by FPInnovations pilot plant (Celluforce, Windsor, Québec, Canada), from a sulfuric acid hydrolysis process of commercial bleached softwood kraft pulp source. In both following preparation approaches, the CNC used was previously dispersed in a solvent (deionized water or 1,4-dioxane according to involved method) by stirring at room temperature for 2 h. For the first modification method, in 60 mL of deionized water overall, various quantities of hexadecyltrimethylammonium bromide (HDTMA) or tetramethylammonium bromide (TMA) (Sigma-Aldrich, ≥99%) were mixed with 2 g of CNC, that is, from 0.1 to 14 mmol quaternary ammonium by weight of CNC. Each reaction mixture was vigorously stirred for 4 h at ambient temperature. In the second method, the reaction was based on the 1-methylimidazole (1 MIM) catalyzed esterification described by Connors and Pandit [89] and implying an alcohol and an anhydride. The expected result of this kind of grafting, with an ionic bond being created, should resist the environment of the aqueous liquid coating and replace most of the charged $-SO_2$ groups at the surface of the CNC with hydrophobic moieties, thus encouraging dispersion in the oily phase of the coating emulsion. In the present case, the synthesis consists in performing the reaction on the CNC (4 g) with acryloyl chloride (110.5 mmol, Sigma-Aldrich, ≥97%), being carried out with the catalyst 1-methylimidazole (6.1 mmol, Sigma-Aldrich, 99%) in 80 mL of 1,4-dioxane. The reaction was stirred overnight under nitrogen atmosphere at 50°C. This second kind of grafting should also

satisfy the same requirements as the precedent one, as well as creating an additional cure site with the acrylate phase, thus anchoring the CNC in the continuous cured. Both employed reaction types were performed in very simple conditions: at room temperature or around it, use of one reactant and mostly water as solvent, and, once, use of a moderate quantity of catalyst. All products from these methods were obtained after concentration of resulting mixtures by centrifugation at 1500 g for 15 min (Thermo IEC), surpernatants removal, and five washing cycles with 420 mL of warm deionized water to remove excess of unreacted CNC, quaternary ammonium salts or acryloyl chloride. Finally, after the last surpernatant removal, powdered products were recovered by freeze-drying. In this way, various treated CNCs were obtained according to the type, the length and the ratio of the used reactant in regarding the substrate. For all products, as molar weight of CNC is not exactly defined, usual definition of yield is not applicable in this context. Thus, to have an indication of crude quantitative results from preparations, we defined mass yield as the ratio of product weight to the CNC weight (Figure 3.1 and Figure 3.2).

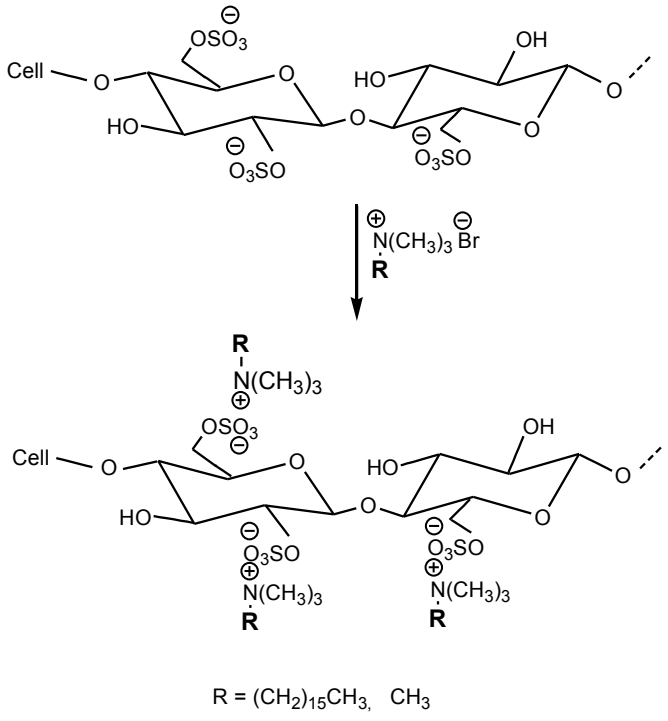

Figure 3.1. Reaction between CNC and quaternary ammoniums salts (hexadecyltrimethyl- or tetramethyl- ammonium bromide).

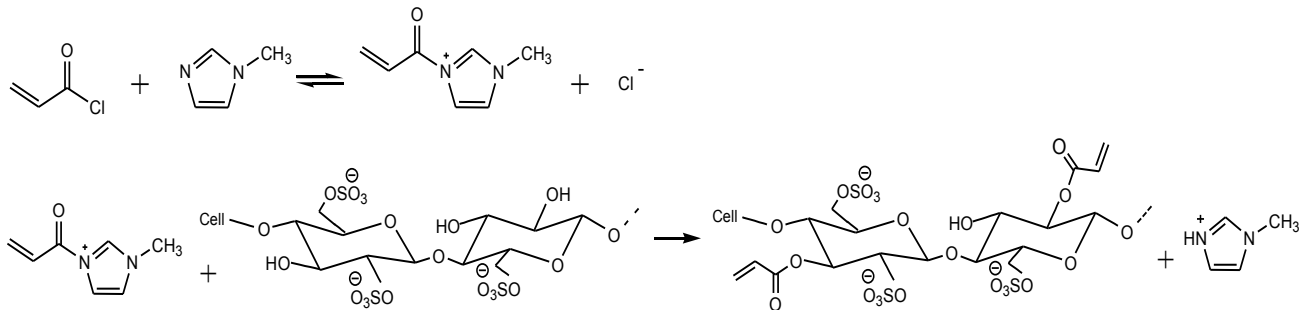

Figure 3.2. Reaction of 1 MIM catalyzed esterification based on the description proposed by Connors and Pandit [89]. The acryloyl chloride reacts with 1 MIM to form a N-acryloyl-N'-methylimidazolium ion, which then reacts irreversibly with the alcohol group from CNC. 1 MIM also reacts as the proton scavenger during the reaction of the imidazolium ion with the CNC.

Attenuated Total Reflectance Fourier Transform Infrared (ATR-FTIR) spectroscopy measurements from unmodified CNC and its synthesis derivatives were carried out using a Perkin Elmer Spectrum 400 Series instrument. Data were collected from 600–4000 cm^{-1} wavelength range with 64 scans for each sample. Concerning only samples with HDTMA-modification, to appreciate the qualitative intensity of the CH aliphatic bands, a flat baseline correction was done between 2750 and 3000 cm^{-1} and the spectra were normalized to the OH group [90], which were not likely to be modified in this case after reaching moisture equilibrium of samples, as checked by constant mass. The solid state CP/MAS ^{13}C NMR analyses were run with a Bruker Avance 300 spectrometer at a frequency of 75 MHz. All spectra were recorded using the technique of cross-polarization and rotation with magic angle spinning with 7 mm tubes. The samples were spun at 4000 Hz. The time of contact for cross-polarization was adjusted to 1 ms and 3000 scans were recorded. Nitrogen content of derivatives from synthesis i.e. the grafted CNC, with quaternary ammonium salts were determined by a Perkin Elmer 2410 Nitrogen Analyzer.

3.4.2. Preparation of nanocomposite coatings and application

The base resin, Bayhydrol UV 2282, is an UV-curing polyurethane acrylate dispersion (about 39 wt%) in water, used especially for wood coating and purchased from Bayer Material Science. To this resin, for obtaining the neat formulation, a photoinitiator and additives (defoamer, surfactant, dispersant and thickener) were added and mixed one by one, each 5 min, through a high speed disperser (Dispermat, VMA-Getzmann GmbH D-51580 Reichshof), glass beads being also added to improve the shear rate. Water (6 wt%) was added to adjust the viscosity of the UV-waterborne formulation. CNCs were dispersed into the neat formulation at a loading of 2 wt% at the same time as glass beads addition with a higher shear for 10 min. After glass beads removal by filtration, the formulation was coated (thickness of 127±20 μm) by spraying (pressure-fed HTi piston pump Kremlin) on wood. Coating films were dried for 10 min at 60°C in a ventilated oven to remove water. In order to verify complete water removal, an ATR-FTIR evaluation of each coated film was done over drying time, while focusing on the area decrease of the OH groups, with the C=O band at 1724 cm^{-1} being used as invariant band (from urethane) to normalize the spectra. According to the area stabilization, 10 minutes were defined as a sufficient drying time. Finally, all samples were cured on a UV-line (Sunkiss-Ayotte Techno-Gaz Inc.) under a medium pressure mercury lamp (≈ 600 W/cm) at a speed of 5 m/min. The UV-dose received by the samples measured using a radiometer was around 570 mJ/cm^2 and temperatures ranged from 25 to 30°C. The components of resulting dried coatings, their percent and theirs suppliers are given in *Table 3.1*.

About the substrate selection for coating application, sugar maple (*Acer saccharum* Marsh.) represents a common species in North America and an important commercial hardwood, notably for furniture, flooring, indoor joinery, paneling, etc. The wood samples were sawn into blocks with a size of 96 mm × 96 mm × 15 mm in the longitudinal, tangential and radial directions, respectively. Samples were stored in a conditioning room at 20ºC and 65% relative humidity until constant mass, for a final wood moisture content at equilibrium of 12%. Before each application, they were sanded with 150 grit abrasive paper. This sanding procedure contributed to the removal of the surface weak boundary layer as well as some of the wood extractives prior to coating application.

Table 3.1. Composition of cured basic and nanocomposites coatings.

Function	Component	Chemical composition	Percent (wt%)	
			Basic coating	Coating + CNCs
UV-curable resin	Bayhydrol UV 2282 (1)	Water dispersible urethane acrylate	95.1	93.1
Defoamer	Foamex 822 (2)	Emulsion based on polyether and polyethersiloxane	0.4	0.4
Surfactant	Byk 348 (3)	Polyether modifier polydimethylsiloxane	1.0	1.0
Dispersant	Disperbyk 190 (4)	Block copolymer of high molecular weight	1.3	1.3
Rheology modifier	Acrysol RM-2020 NPR (5)	Polyurethane	0.2	0.2
Photoinitiator	Irgacure 819 DW (6)	Aqueous dispersion of bis-acyl-phosphine oxide	2	2
Nanoparticle	CNC	-(1,4)-D-glucopyranose polymer	-	2

Suppliers: (1): Bayer Material Science

(2): Evonik Degussa GmbH

(3): BYK-Chemie

(4): BYK-Chemie

(5): Rhom and Haas

(6): BASF Resin – Inks and OPV

3.4.3. Evaluation of CNC particles characteristics

Particle size of CNCs was measured at 25°C by photon correlation spectroscopy (PCS) on a Malvern Zetasizer Nano ZS (Malvern Instruments Ltd). To avoid excess light scattering in the spectrometer, the samples were diluted to 0.05 wt% CNC in the presence of 5 mM NaCl. Samples were filtered with 0.45 µm or 0.7 µm GF/F Whatman syringe filters prior to measurement. No significant loss of CNC was measured by gravimetry after filtration. Because PCS is a light-scattering method, the measured CNC particle size values quoted are the z-average hydrodynamic diameters of equivalent spheres and do not represent actual physical dimensions of the rod-like CNC particles. However, they are valid for comparison purposes.

The wettability of CNC particle before and after chemical modification was examined through water contact angle measurements using a First Ten Ångstroms 200 dynamics contact angle analyzer. To sample CNC particle films, CNCs were dispersed at 2 wt% in deionized water by stirring for 2 h. Then, 10 mL of each suspension were let to dry for ten days at ambient temperature in open dishes of 60-mm diameter until a constant mass, synonymous of moisture equilibrium with the room housing the contact angle analyzer (23°C, 50% RH).

For analysis, with a sticker minimizing the film deformation after contact with water, each dried film was horizontally maintained flat on the carrier-sample of the apparatus. Sessile drops of distilled water (70 µL) were deposited on films and measurements were immediately recorded as a function of time.

To evaluate surface roughness of films containing CNCs, observations by atomic force microscopy (AFM) were carried out using a NanoScope V, fitted with a Hybrid XYZ scanner (Veeco Instruments Inc). AFM measurements were performed under ambient air conditions in tapping mode (tip radius is 8 nm). The resolution was set to 256 lines for all observations. Surface roughness was calculated in 10 × 10 μm scan areas, using the classical mean surface roughness parameters.

3.4.4. Evaluation of optical and mechanical properties

The effect of CNC particles on the gloss and haze of coatings was determined with a haze-gloss apparatus from BYK Gardner. This instrument simultaneously determines gloss at three different geometries, 20°, 60° and 85°, as well as haze. Gloss and haze measurements were performed on coating films applied onto wood. These tests were performed according to ASTM standards D523 and E430.

Abrasion resistance of topcoat nanocomposites was evaluated with a rotary platform abraser (Taber Industries, model 5150). S-42 sandpaper strips as abrasives were attached to the periphery of CS-0 resilient rubber wheels. Mass loss was determined after 100 rotations. The tests were performed according to ASTM D4060 standard.

Pull-off tests were used to measure the adhesion strength between wood and dried/UV-cured coating film. Experiments were performed with a testing machine (Qtest Elite, MTS) according to ASTM D4541 standard. A 20-mm diameter aluminum dolly was glued onto the coating surface with an epoxy resin. After 24 h of drying at room temperature, the test area was isolated with a cutting tool. Then the dolly was pulled away from wood sample by applying a force perpendicular to the surface test. The strength required to pull away the coatings from wood sample was recorded. Each test was repeated at least on ten wood samples in order to take into account the variability in wood.

3.5. Results and discussion

3.5.1. Isolation and nitrogen percent analysis of treated CNCs

Following the aqueous washing and drying steps, the yield values from CNC modification are reported in

*Table 3.**2***, in the same time as the nitrogen content data exclusively from modification with quaternary ammoniums salts.

Regarding the treatment with quaternary ammoniums salts, the nitrogen content allowed to calculate the grafting percent as following:

$$\%\ \text{grafting} = \text{nitrogen content} \times \frac{100}{\text{weight percentage of nitrogen in grafted group}}$$

Molar weights : HDTMA = 284 g/mol; TMA = 74 g/mol; N = 14 g/mol

Table 3.2. Mass yields, nitrogen and grafting percents (standard deviations, SD, are given for 5 experiments) after modifications using various quantities of hexadecyltrimethyl-, tetramethyl- ammonium bromide or acryloyl chloride (HDTMABr, TMABr or C_3H_3ClO, respectively) by weight of CNC. Nitrogen is % weight of nitrogen on dry CNC content.

Substrate, reactant or product	Mass yield (%) ± SD		Nitrogen content (%) ± SD		Grafting percent (wt%) ± SD	
CNC	-		0		-	
HDTMABr	-		3.92	±0.08	-	
HDTMABr (0.1 mmol)-treated CNC	72	±2	0.14	±0.01	2.8	±0.1

HDTMABr (0.2 mmol)-treated CNC	90	±3	0.27	±0.01	5.5	±0.2
HDTMABr (0.35 mmol)-treated CNC	88	±1	0.32	±0.02	6.5	±0.1
HDTMABr (1.4 mmol)-treated CNC	84	±3	0.68	±0.03	13.8	±0.5
TMABr	-		9.54	±0.17	-	
TMABr (7 mmol)-treated CNC	23	±2	0.40	±0.01	2.1	±0.2
TMABr (14 mmol)-treated CNC	18	±3	0.64	±0.01	3.4	±0.6
C_3H_3ClO (28 mmol)-treated CNC	16	±2	-		-	

Table 3.2 shows, on one hand, substantial yields of modifications in spite of small amount of reactant quantities. That would be in accordance with known high reactivity from quaternary ammoniums salts. The nitrogen content, which presently refers as an indicator of anchored nitrogeneous alkyl chains, increases according to the quantity of used ammoniums salts but not always similarly to grafting percent evolution. Indeed, the nitrogen content is a bit misleading since the length of the alkyl chain is much larger in grafted materials. So for the nitrogen content, the percentage in grafted weight is much higher with HDTMA than with TMA (cases of CNCs treated with 1.4 mmol of HDTMABr and with 14 mmol of TMABr).

3.5.2. NMR and infrared characterizations of treated CNCs

In Figure 3.3, spectra of products from CNC modification with ammonium salts, in comparison with the unmodified CNC, show the appearance of three signals at 24, 30 and 58 ppm. The 30 ppm broad signal and the 24 ppm small signal are respectively assigned to the $-(CH_2)_n-$ and the terminal $-CH_3$ from alkyl chains, whereas the signal at 58 ppm is attributed to CH_3-N from alkylammoniums [91-93]. The other signals at 66, 75/72, 89/84 and 105 ppm coming respectively from C-6, C-2/C-3/C-5, C-4 and C-1 atoms from cellulose remain unchanged and confirm that the CNC structure was unacffected by the modifications [94, 95].

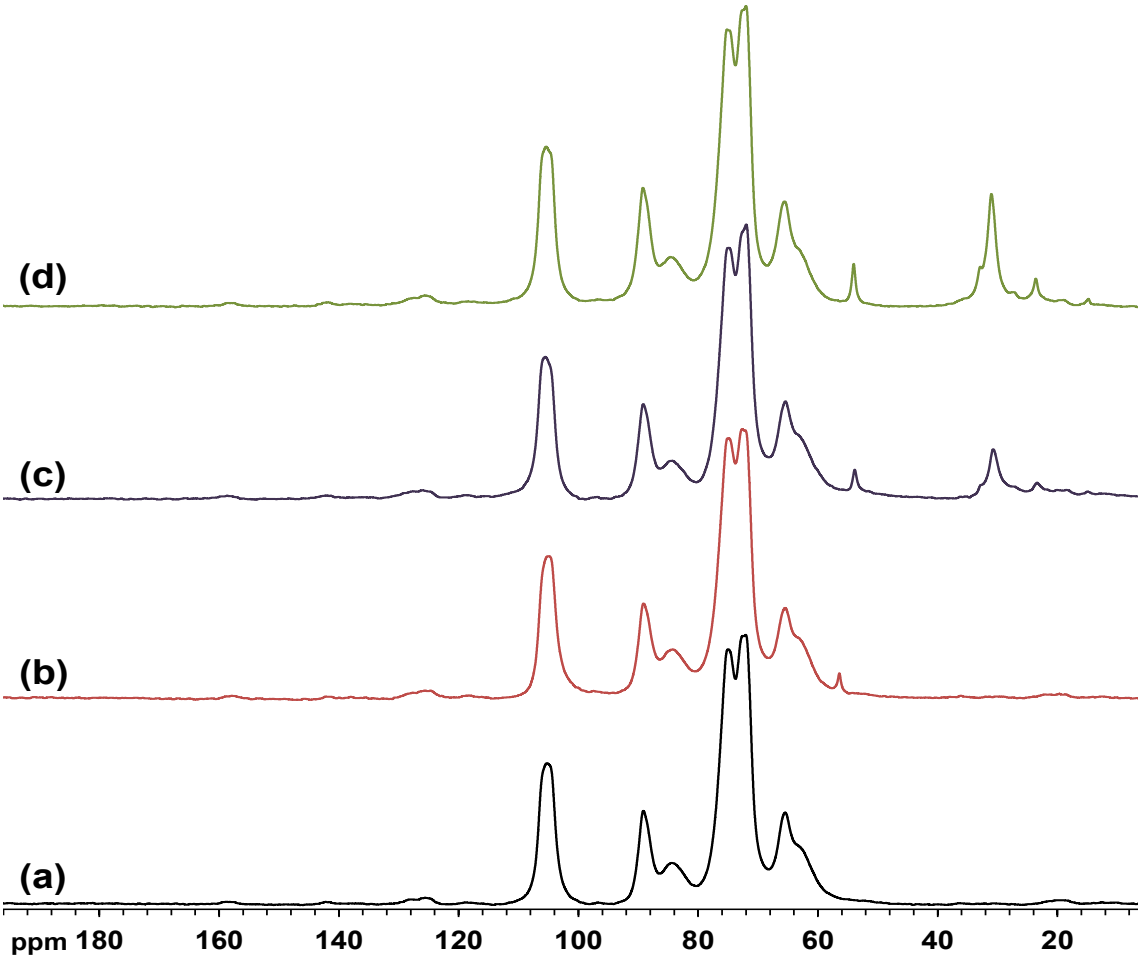

Figure 3.3. Solid state ^{13}C NMR spectra of untreated CNC (a) and its derivatives from modification with 14 mmol TMABr (b), 0.35 mmol HDTMABr (c) and 1.4 mmol HDTMABr (d) by weight of CNC.

Finally, these ^{13}C NMR spectra analyses confirm successful anchoring of alkylammonium groups on CNC surface after reaction with different quaternary ammoniums bromide, and that is much more obvious, since signal intensities are higher according to longer sizes and greater amounts of involved quaternary salts. Besides, similar observations were also reported by Wen et al. [93] about the ^{13}C NMR spectra of a montmorillonite in which were intercalated dodecyltrimethylammonium cations at different concentrations. As regards the product from the CNC reaction with the acryloyl chloride, the corresponding ^{13}C NMR spectrum showed no change in comparison with the untreated CNC spectrum, which suggests the possible modifications on CNC would be rather imperceptible because of short grafted acryloyl groups (C_3). That is equally observed in Figure 3.3 for the TMABr-treated CNC whose short anchored groups (C_4) were detected only thanks to carbons bounded to nitrogen, but not to methyl groups.

Success in modification was likewise confirmed by data from IR analysis, excepted for the products from treatment with TMABr and acryloyl chloride for which no spectral particularities were recorded, no doubt due to very short grafted groups, as mentioned above. Figure 3.4 and Figure 3.5 sharply indicates the increase of signals intensity at 2900 cm^{-1} (CH aliphatic) in accordance with the anchored groups size from HDMTABr. Even though the preserving in CNC structure after modification was again verified referring to no other spectral changes, it appears a decrease in the small band at 1640 cm^{-1} in parallel with the increase of the aliphatic chains. In fact, the band at 1640 cm^{-1} is assigned to OH bending of adsorbed water, since the cellulose-water interaction makes very difficult the removal of adsorbed water on cellulose molecules during the drying stage [96, 97]. Thus, the hydrophobic properties due to aliphatic chains from CNC derivatives would reduce this interaction and the remaining amount of adsorbed water after the aqueous washing and drying steps of preparation.

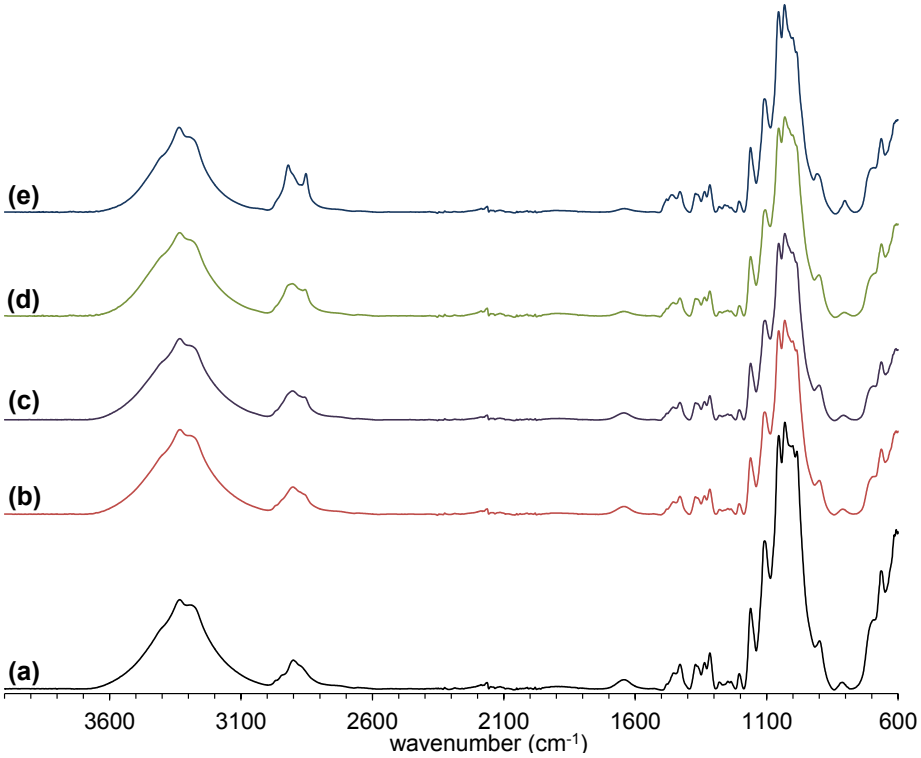

Figure 3.4. ATR-FTIR spectra of untreated CNC (a) and its derivatives from modification with HDTMABr at 0.10 mmol (b), 0.20 mmol (c), 0.35 mmol (d) and 1.4 mmol (e) by weight of CNC.

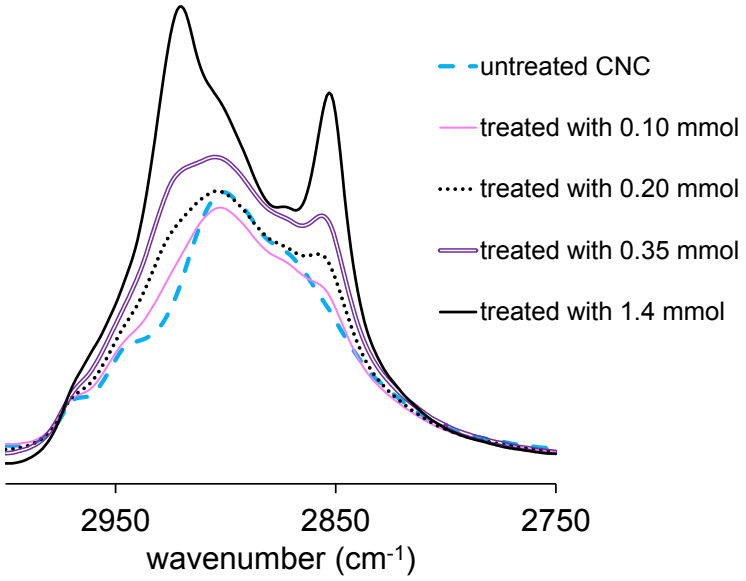

Figure 3.5. ATR-FTIR spectra in hydrocarbon domain (2750 – 3000 cm^{-1}) of CNC and its derivatives from modification with HDTMABr according to different reaction quantities by weight of CNC.

3.5.3. Size, dispersion and wettability of CNC particle derivatives

The PCS zetasizer technique applied to this study does not recognize the fiber-like nature of CNC (0.05 wt% in water) and gives a value equivalent to a hydrodynamic volume size. From the particle size distribution profile, the mean size of each CNC nanoparticle sample is presented in Figure 3.6. The unmodified particle mainly measures around 140 nm, which is compatible with literature about CNC from wood [36, 98]. Although the CNC particle size does not really change after surface modifications, its derivatives seem to become slightly larger possibly due to grafted and anchored groups. The particle derivatized with the longer chain reactant, HDTMABr, shows the largest apparent size (around 230 nm). Additionally, this observation based on the particle size also confirms the grafting of alkyl groups on CNCs, including the derivatives obtained by reaction with TMABr and acryloyl chloride for which chemical characterizations were ambiguous before.

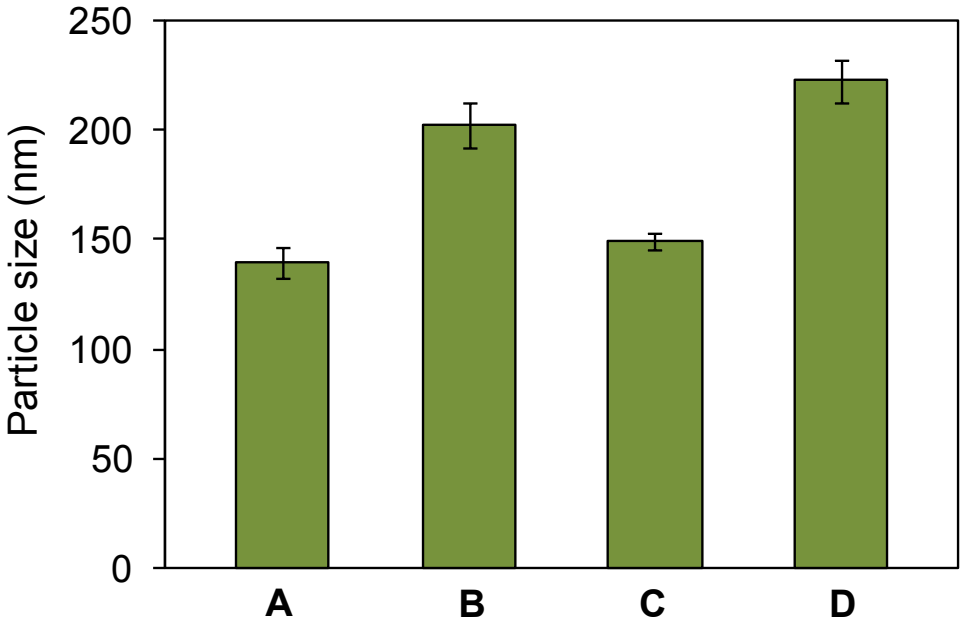

Figure 3.6. Particle size of CNC (A) and its derivatives from modification with 28 mmol acryloyl chloride (B), 14 mmol TMABr (C) and 0.35 mmol HDTMABr (D) by weight of CNC. Each bin is an average of measurements on five derivatives from the same synthesis method.

Prepared formulations from dispersion with CNC or its derivatives at 2 wt% were coated, dried and UV-cured onto sugar maple wood. *Table 3.3* and Figure 3.7 indicate an overall decrease of the final cured coating surface roughness induced by each CNC derivative, compared to unmodified CNC. This decrease of surface roughness, more pronounced for the particle derivative having the longer anchored group, may be associated to an improved dispersion. That means the dispersion was improved according to the bigger apparent size of the particle. In other words, the grafted alkyl groups from particle derivatives reduced the aggregation phenomenon of particles during the dispersion especially in this hydrophobic coating. Furthermore, particle derivatives having been vigorously sheared with glass beads during the dispersion step, this final improved dispersion shows that chemical bonds (including ionic bonds) by which were grafted alkyl groups remained intact.

Table 3.3. Surface roughness of basic and nanocomposites coatings loaded with 2 wt% of CNC or its derivatives from modifications. Each value is an average of measurements on ten varnished wood.

Basic and nanocomposites coatings	Surface roughness (nm) ± SD	
Neat coating	5.3	±0.9
+ unmodified CNC	9.2	±1.6
+ C_3H_3ClO (28 mmol)-modified CNC	6.4	±1.0
+ TMABr (14 mmol)-modified CNC	7.8	±1.3
+ HDTMABr (0.35 mmol)-modified CNC	5.9	±0.9

In the order to highlight hydrophobic properties of CNC particle derivatives, a direct method for powder or fibers, such as Wilhelmy balance technique, could have been suitable. However, the nanometric size of CNC particle caused the clogging of crucible (carrier-sample) during the analysis, and that made therefore this method ineffective.

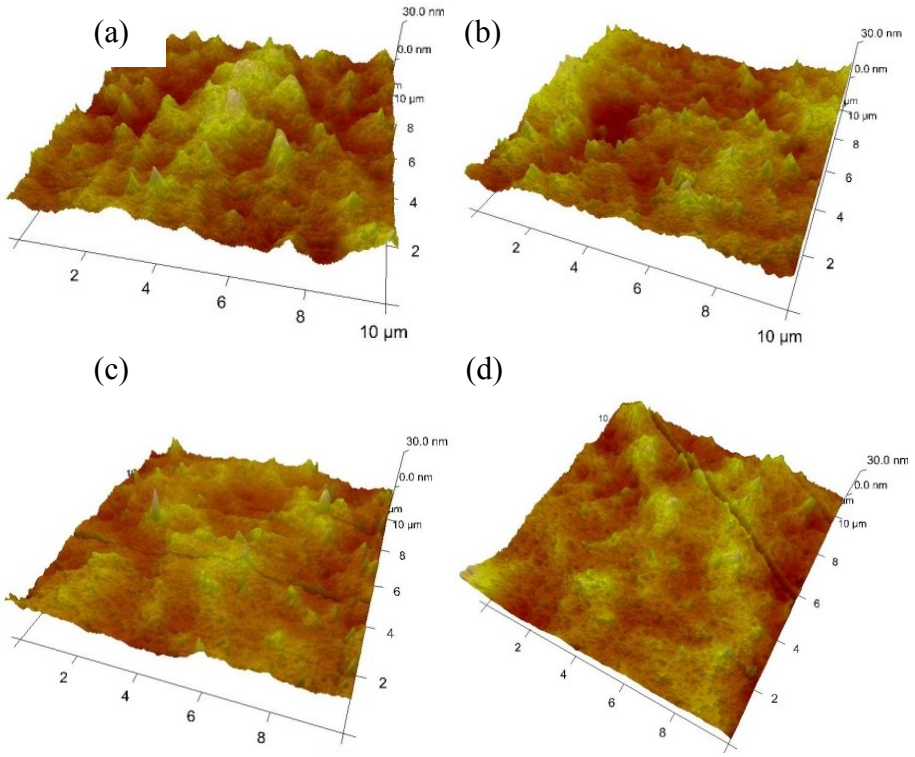

Figure 3.7. Ten micron AFM height images of the wood topcoat containing 2wt% of CNC (a) and its derivatives from modification with 14 mmol TMABr (b), 28 mmol acryloyl chloride (c) or 0.35 mmol HDTMABr (d), by weight of CNC.

Likewise, method of the partition coefficient between water and octanol, or the hydrophilic-lipophilic balance (HLB) value determination, was ineffective too because of the non-solubilization of CNC (neither in water nor in organic phase) permitting to quantify the distribution. Hence, it appeared interesting to appreciate water wettability on solid films made of CNC exclusively. Knowing that CNC particles are generally dispersed at 0.05–5 wt% in solvents [73], a solid film formed from 10 mL of a 2% CNC aqueous suspension, being left to dry in a 60 mm diameter dish at room temperature, appeared homogeneous and relevant for wettability measurements. In Figure 3.8, before anything else, it can be noticed that the angle measured at the first contact time of water with the unmodified CNC was higher than which is known from literature around 20-40° [99, 100]; this difference is due to the non-perfect drying of our CNC films intentionally obtained after water evaporation under ambient air conditions until reaching the moisture equilibrium of the room related to the contact angle measurement, in contrast with the heat-dried films (~ 60-

105°C) referring to lower angles. In fact, since the properly dried CNC films have a very high porosity of > 98% [101], it seems important to minimize the moisture variation of films during their sticking/adjustment on the carrier-sample, the analysis time and its repetition on other sites of the same film. In spite of not favoring more representative angles data, all films from the present experiment were analyzed under the same conditions taking account precise changes between the native and the modified CNCs.

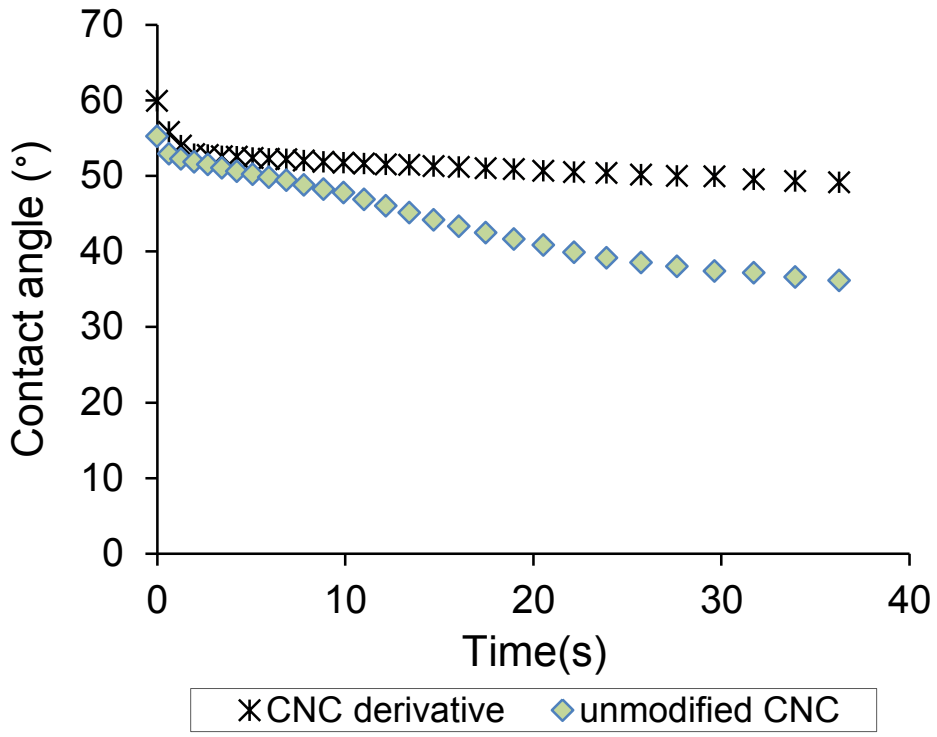

Figure 3.8. Dynamic contact angle of dried films made of unmodified CNC or its derivative from modification with 0.35 mmol HDTMABr by weight of CNC. Each curve is an average of wettability measurements on five samples.

Thereupon, Figure 3.8 shows a higher initial value (60°) for the film of modified CNC with 0.35mmol HDTMABr which is also shown to be more stable and repellent to water, in comparison with the unmodified CNC, since its water contact angle is stable over time. Despite the slight difference (at t = 0) next to the unmodified CNC probably due to the low grafting percent (6.5 wt%, from 0.35 mmol of reactant by weight of CNC) of aliphatic

chain previously mentioned in *Table 3.2*, the derivative was less prone to water uptake as seen over time; otherwise, a derivative from a higher amount of HDTMABr (1.4 mmol) in water suspension lead to a non-compact and crystalline film after evaporation. Accordingly, the result wettability as regards the HDTMABr (0.35 mmol)-modified CNC is coherent to alkyl groups anchoring which confers a less hydrophilic character to the CNC particle.

3.5.4. Haze and gloss measure of nanocomposite coatings

Haze of the different coated films on wood did not show a wholesale change with the addition of the CNC and its derivatives (Figure 3.9). There appeared little difference in the case with additives (haze values of 377 to 388) than without their presence (values of 352). The three derivatives slightly favored a haze decrease, in comparison with the unmodified CNC. Therefore, the involved modifications led to a, albeit small, relative improvement in visible light transmission of CNC-based coatings.

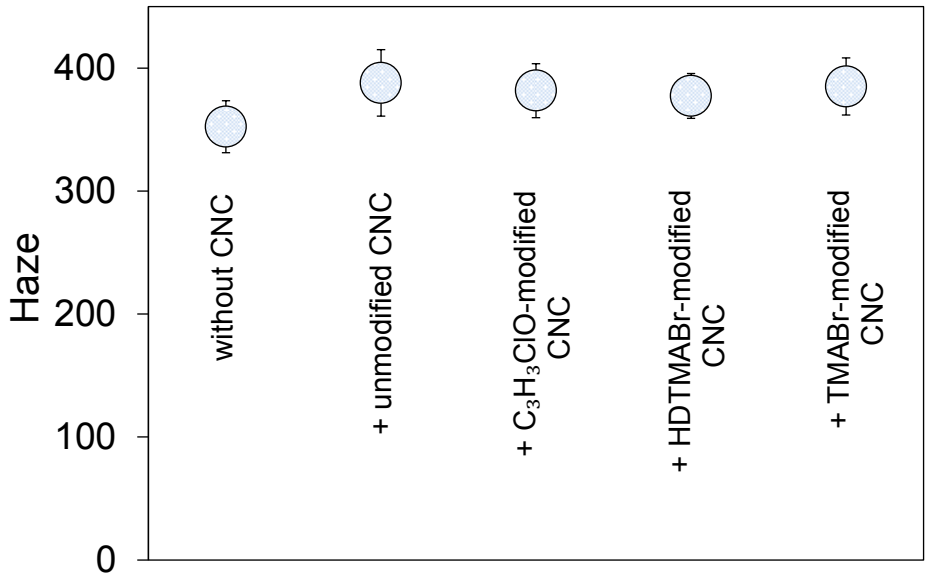

Figure 3.9. Haze of the films coated onto wood and containing, no CNC, and 2 wt% of CNC and its derivatives from modification with 14 mmol TMABr, 28mmol acryloyl chloride or 0.35 mmol HDTMABr by weight of CNC. Each circle is an average of five different measurements on a topcoat repeated on ten samples for the same derivative.

The 60° gloss levels presented in Figure 3.10 indicated that the CNC derivatives modified by HDTMABr and C_3H_3ClO conferred better aspect to the film than the unmodified CNC, this last one resulting in a reduced effect after its addition in the basic coating. In other words, these modifications made possible the retention of the high original gloss (~ 90) of the coating even after the CNC addition, which is also coherent with the precedent results from surface roughness.

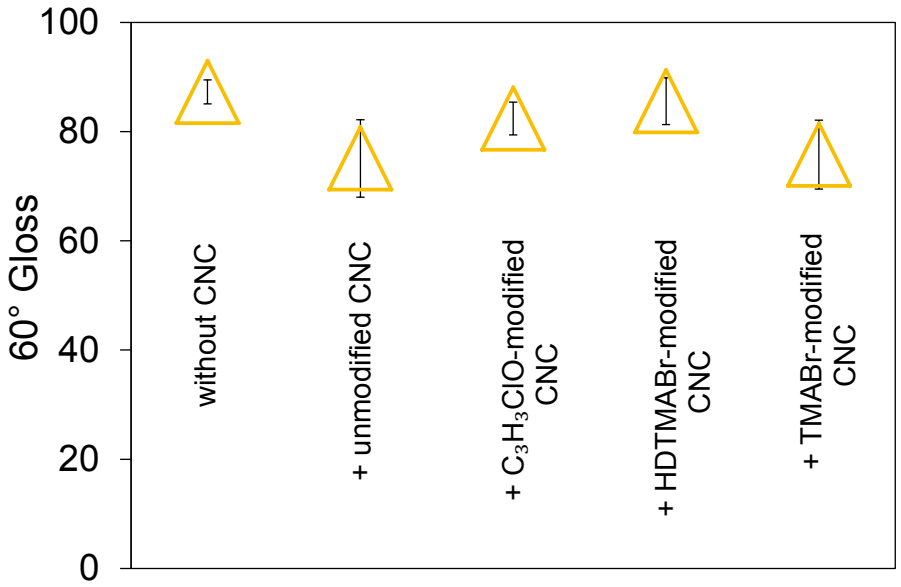

Figure 3.10. Gloss of the films coated onto wood and containing no CNC, and 2 wt% of CNC and its derivatives from modification with 14 mmol TMABr, 28 mmol acryloyl chloride or 0.35 mmol HDTMABr by weight of CNC. Each triangle is an average of five different measurements on a topcoat repeated on ten samples for the same derivative.

3.5.5. Mechanical properties from CNC derivatives in coating

According to ASTM D4060 standard, results of an abrasion resistance test having been performed on topcoat nanocomposites on sugar maple samples are shown in Figure 3.11. All CNC particles, including the unmodified one, induced globally a lesser mass loss of their varnish matrixes and hence, a better abrasion resistance, compared to varnish without nanoparticles. The particles modified with 0.35 mmol HDTMABr and those with 28 mmol

acryloyl chloride were those imparting the highest coating resistance to abrasion, respectively 66 and 67 mg, versus 81 mg mass loss when the unmodified CNC is involved and 106 mg when there was no addition of nanoparticle. Those results correspond to, with an addition of 2 wt% CNC, a 24 to 38% improvement. That is significant since equivalent improvements, 26 and 32% for waterborne epoxy coatings, were recently highlighted using superior loadings in unmodified CNC, respectively of 5 and 11.6 wt% [77].

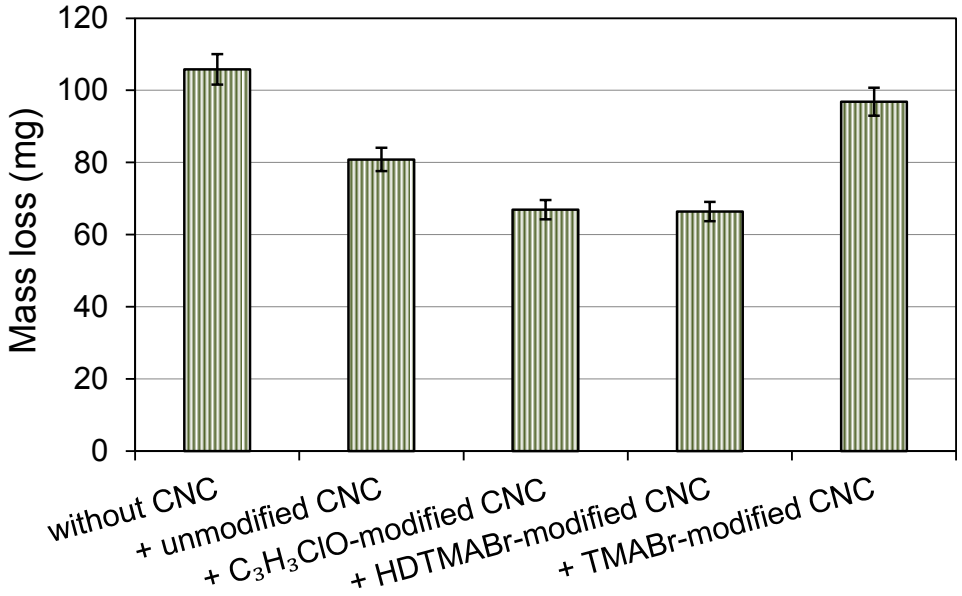

Figure 3.11. Mass loss after abrasion resistance test on sugar maple samples coated with basic and nanocomposite coatings containing 2 wt% of CNC and its derivatives from modifications with 28 mmol acryloyl chloride, 0.35 mmol HDTMABr or 14 mmol TMABr by weight of CNC. Each bin is an average of measurements on ten coatings containing the same particle.

On the other hand, the profile of enhanced abrasion resistances was compatible with previous corresponding levels of dispersion, except for the derivative with 14 mmol TMABr which is worse than the unmodified particle in abrasion test. Another worthy result is the performance of the CNC modified with acryloyl chloride which, after the derivative by 0.35 mmol HDTMA, shows the second best resistance and dispersion in spite of its very small amount of grafted group. As the used coating is made of acrylic oligomers, it is probable that the grafted group from the acryloyl chloride is more compatible with this

matrix with which it could form additional bonds by UV cure free radical process, to enhance abrasion resistance.

In the development of wood coating, it is also important to check the adhesion of coating applied to timber, since the addition of nanoparticles could lower this value. According to ASTM D4541 standard, pull-off tests were performed to measure the adhesion strength between maple sugar samples and the coating with CNC and its derivatives, and results are given in Figure 3.12. The unmodified CNC and its derivatives slightly decreased the adhesion of coating on wood. This could be due to a higher viscosity of liquid coatings, which could limit adhesion (diffusion) of coating into wood. Indeed, as wood fibers are hydrophilic and porous, formulations containing either more hydrophobic additives (HDTMABr-modified CNC) or lesser dispersed additives (unmodified and TMABr-modified CNCs) also could have a reduced penetration into upper layers of wood. This could be partially reversed by using a less viscous base formulation with lower molecular weight acrylates.

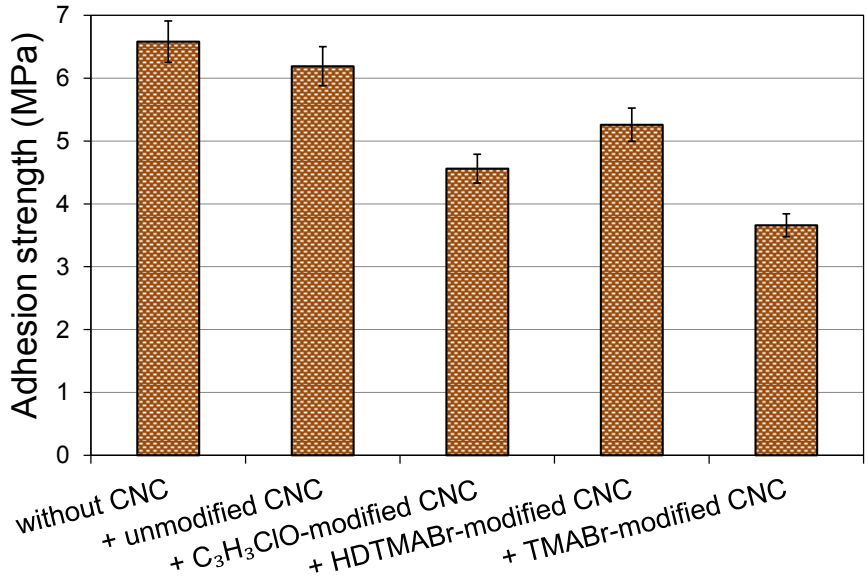

Figure 3.12. Adhesion strength of basic and nanocomposite coatings varnished on sugar maple samples and containing 2 wt% of CNC and its derivatives from modifications with 28 mmol acryloyl chloride, 0.35 mmol HDTMABr or 14 mmol TMABr by weight of CNC. Each bin is an average of measurements on ten coatings containing the same particle.

3.6. Conclusions

Modification of CNC as reinforcement derivatives was performed in simple conditions by chemical reactions with various alkyl quaternary ammonium bromides or acryloyl chloride. NMR, IR and nitrogen content analyses of products attested that the anchoring or grafting of alkyl groups was achieved on CNC surface without affecting its structure. The influence of type and extent of those surface modifications was revealed important in nanoparticles dispersion improvement. The less hydrophilic properties of CNC particle derivatives were shown from water wettability measurements. Additionally, based on the gloss and haze measurements, the modified nanocellulose fibers ensure maintaining of aesthetic properties of coatings. Finally, added derivatives in acrylic wood coating remained intact in spite of vigorous dispersion and resulted in enhanced abrasion resistance of the coating. The lower recorded interfacial adhesion between the nanocomposite coatings and wood seem to recommend the use of low molecular weight acrylates and probably some adjustments in reaction ratios between reactants and CNC in order to adjust the behavior of derivatives in regard the wood fibers. This simple applied study shows it is possible to valorize CNC in a wide range of matrix polymers, especially in wood coatings.

Acknowledgments

The authors would like to gratefully acknowledge the support of Arboranano, NanoQuebec, the Fonds Québécois de Recherche sur la Nature et les Technologies (Quebec, Canada) to this work, and the providing of CNC samples by FPInnovations' labs (Quebec City and Pointe-Claire, Quebec, Canada).

Chapitre 4. Mechanical properties of UV-waterborne varnishes reinforced by cellulose nanocrystals

4.1. Résumé

Il existe plusieurs cas dans la littérature de composites de nanocellulose-thermoplastique, mais il y a peu d'études sur les revêtements renforcés par des celluloses nanocristallines (CNC). L'objectif général de cette recherche est de développer des revêtements UV-aqueux renforcées par les nanoparticules pour les applications de bois, et étudier leur effet principalement sur les propriétés d'usure des revêtements composites. Les CNC ont été mélangées à des formulations de revêtements dans le but d'améliorer leurs propriétés mécaniques. L'un des aspects clés de la technologie des nanocomposites reste la dispersion des nanoparticules dans la matrice ainsi que leur affinité avec la matrice. Pour quantifier la dispersion, des méthodes efficaces de caractérisation sont nécessaires pour faire apparaître les particules de taille nanométrique. Dans cet article, une nouvelle méthode de caractérisation basée sur la microscopie à force atomique (AFM) a été utilisée pour caractériser ces revêtements nanocomposites, en mesurant la nano-rugosité de la surface, qui est clairement corrélée avec la qualité de la dispersion et des propriétés mécaniques. Les CNC ont été modifiées soit par les bromures d'ammonium quaternaire alkylés ou le chlorure d'acryloyle. Les propriétés mécaniques (résistances à l'abrasion et égratignure, la dureté et l'adhérence) ont été analysées et comparées à celles des vernis de référence sans nanoparticules. L'ajout de la CNC modifiée dans les revêtements UV-aqueux a entraîné une augmentation de 30-40% de la résistance à l'usure (abrasion et égratignure), sans perte de l'apparence.

4.2. Abstract

There are many instances in the literature of nanocellulose-thermoplastic composites, but there are few studies on coatings reinforced by cellulose nanocrystals (CNC). The overall objective of this research was to develop organic nanoparticles reinforced UV-water-based coatings for wood applications and to study the effect mainly on wear properties of the final composite coatings. CNC was mixed in the varnishes to improve the mechanical properties of the coatings. One of the key aspects in the technology of nanocomposites remains the dispersion of the nanoparticles within the matrix as well as its affinity with the matrix. To quantify the dispersion, efficient methods of characterization are needed in order to reveal the nanosized particles. In this paper, a novel characterization method based on atomic force microscopy (AFM) was employed to characterize such nanocomposite coatings, by measuring surface nano-roughness, which is clearly correlated with quality of dispersion and mechanical properties. CNC was modified by either alkyl quaternary ammonium bromides or acryloyl chloride. The mechanical properties (abrasion and scratch resistances, hardness and adhesion) were analyzed and compared to the reference varnish without nanoparticles. The modified CNC addition in UV-water-based coatings results in a ca 30 - 40% increase in wear resistance (abrasion and scratch), without any loss of appearance.

Keywords: Cellulose nanocrystals, CNC, coating, dispersion, surface modification, mechanical properties, wear resistance.

4.3. Introduction

4.3.1. Waterborne coatings

Water-based UV-cured coatings are increasingly used in the wood industry, in view of their performance, very low volatile organic content, hardness and fast setting (fast curing) properties. UV-aqueous technology is an attractive alternative since it combines the benefits of UV technology, and those of the water-based technology. First of all the

photopolymerization is very fast (a few seconds) and is accompanied by little or no VOC emissions. Second, the use of water as single solvent reduces the viscosity of formulations to promote homogeneous sprayable applications in environmentally friendly and secure conditions [102]. Finally, aqueous coatings promote good adhesion to wood [103]. The UV-aqueous technology also has additional advantages, compared to 100% solids UV coating since the polymerization of the UV-aqueous coatings is insensitive to atmospheric oxygen and generally coatings produced using this technology have excellent chemical and thermal resistance [102, 104]. The aqueous coatings are thin, about 100 μm, only two layers or coats, relative to commercial coatings, which for parquets for instance, may have up to 7 coats. Several additives can be used to improve the mechanical properties, such as aluminum oxide or silica [42, 57] while use of other nanoscale metal oxides (Al_2O_3, SiO_2, TiO_2, ZnO, $CaCO_3$, etc.) have been cited in the literature, in organic varnishes or in aqueous media. These additives are used in order to strengthen the coating for indoor use such as in flooring, or protect the coating from UV radiation attack, in the case of use outdoors. Nanoaluminium oxide is used to strengthen coatings, such as in study of Bautista [105], where addition of 5% nanosized SiO_2 to UV cured acrylics decreased weight loss by abrasion about 25%. Bauer et al. added functionalized nanoalumina and nanosilica to acrylic coatings [106], where about 10% added such nanoparticles increased abrasion resistance 40%. Distribution of nanoparticles was characterized with AFM [61, 106]. In another work of Bauer et al., it was shown that nanoalumina particles, at equivalent loading, were three times as efficient as microalumina particles, as far as abrasion resistance was concerned [62]. Adequate dispersion of nanoparticles is always a challenge, in view of their very high specific surface. In order to evaluate the use of an innovative organic-based renewable nanoscale reinforcement, we use organic nanoparticles, cellulose nanocrystals (CNC), as film reinforcement in our study. There are several publications in the literature of nanocellulose-thermoplastic composites, but there are few studies on coatings reinforced by CNC [107] and none which uses CNC as modified as in the present study [108] (*Chapitre 3*).

4.3.2. CNC

Cellulose is the most abundant organic material on earth (more than 50% of the biomass). Cellulose is the main component of plants and in particular of the cell walls. Cellulose microfibrils, which themselves are associated in layers, form the walls of plant fibers. The presence of hydrogen bonds between the anhydroglucose molecules of the different cellulose chains, results in a highly crystalline material. Many products in everyday life are cellulose derivatives, such as cellulose acetate, nitrates, esters and ethers, some of which are paint components. CNC, which is a new product, is also called 'cellulose whiskers'. These CNC are bio-based and have high aspect ratio, as opposed to inorganic nanoparticles which are usually spherical or plate-like. Generally, the CNC is extracted from the wood by a process of acid hydrolysis (H_2SO_4), with strict control of conditions of time and temperature [31]. The action of the acid removes the amorphous parts of the microfibrils to release only the highly crystalline particles of the original cellulose microfiber. When this level is reached, the hydrolysis is terminated by rapid dilution of the acid. A combination of centrifugation and extensive dialysis is used to completely remove the acid, and, for certain processes, ultrasonic treatments complete the process for dispersing the individual nanoparticles of the cellulose and produce an aqueous suspension [32]. The CNC nanoparticles have the following properties: specific surface area of 600 m^2/g, a Young's modulus of 150GPa and a tensile strength of 10GPa [35]. There are also other types of sources for CNC: cotton CNC, green algae CNC etc. [28-30, 109], as well as from other sources, such as bacterial CNC.

CNC was found to be rather a good reinforcing filler when mixed with aqueous latex matrices [35, 65]. Landry et al. have shown that the addition of small concentrations of CNC particles to clear clay-based coatings improves their mechanical properties (abrasion and scratch resistance, hardness) [42]. While it is still difficult to incorporate and properly disperse inorganic nanoparticles in an organic polymer matrix [110], it could possibly be easier to use organic nanoparticles, with proper surface modification. The research hypothesis assumes that CNC as such, and possibly with appropriate modification of its surface, will show high dispersion and stability in the resulting nanocomposite coatings, which are, in this case, transparent coatings (varnishes). Thus in this study, we compare the

mechanical properties of varnishes with either chemically modified (more hydrophobic) CNC [108] (*Chapitre 3*) with those of varnishes with unmodified (hydrophilic) CNC or without CNC.

4.3.3. CNC dispersion characterization

The choice of the mixing technique plays an important role in the dispersion state of the nanoparticles [42]. There are several types of equipment commonly used in the industry, among those: high speed mixer, three-cylinder mill and ball mill [42]. In our study a high speed mixer was used, since it is most appropriate to our system (varnish with CNC) as determined by our previous studies on varnishes with inorganic nanoparticles. The main challenge of mixing CNC particles into a host matrix is to achieve a homogeneous dispersion in order to maximize the macroscopic effects on the mechanical reinforcement. We used atomic force microscopy, AFM, to study the quality of CNC dispersion by measuring surface roughness. Farrokhpay conducted a literature review on the new assessment techniques of painted surfaces and obtained quantitative results on the surface roughness characterization by AFM [40]. Thometzek et al. also used TEM (transmission electron microscopy) and AFM to quantify the surface quality of paintings and correlated the degree of hydrophobicity of the particles with the quality of the dispersion [41]. In this paper we used our own characterization method based on surface roughness measurement by AFM to qualify CNC dispersion in varnishes [38] (*Chapitre 2*). Classical dispersion quality analysis by TEM is difficult to apply in this case because of the lack of contrast between the CNC and the continuous organic phase and the difficulty in obtaining free-standing varnish films.

4.4. Materials and experimental procedure

4.4.1. The composition of the formulation

The formulation used in this work is composed of the following components: the resin (or binder), photoinitiator and additives such as defoamer, dispersant, surfactant and thickener. These chemicals were added in order to minimize foaming, optimize the surface tension and help CNC dispersion. The typical compositions of the UV-aqueous formulation are presented in *Table 4.1*.

Table 4.1. Typical compositions of the formulation (see Table 4.2 for details).

Component	Chemical structure	Commercial name
Resin	Polyurethane-acrylate	Bayhydrol UV 2282
Defoamer	Ether poly dimethylsiloxane	Foamex 822
Surfactant	Polyether siloxane copolymer	Byk 348
Dispersant	Solution of block copolymer of high molecular weight	Byk 190
Photoinitiator	Bis-acyl phosphine oxide	Irgacure 819DW
Thickener	Polyurethane	RM 2020
Solvent	Deionized water	_

The resin selected is Bayhydrol UV 2282 (Bayer Material Science), a polyurethane acrylate (PUA) oligomer emulsified in water that was primarily developed for applications on wood. The photoinitiator used in this research is a bisacylphosphine oxide (Irgacure 819DW, BASF Resins - Inks and OPV), dispersed in water (45% w/w).

4.4.2. CNC

CNC used in this project has been prepared by FPInnovations (Canada). To the best of our knowledge there are no publications on the manufacturing process of the type of CNC used in this paper, CNC, since it is a proprietary industrial process, with patent pending.

Prior to shipping the CNC to our lab, the following treatment was done on the CNC by FPInnovations. Samples of the suspension of the CNC were sonicated using a Sonics Vibra-cell 130 W 20 kHz ultrasonic processor with a 6 mm diameter probe: typically, 15 ml of a suspension of 2-3% CNC weight were placed in a plastic tube of 50 ml and sonicated at 60% of maximum power until an energy input of more than 3600 J/g CNC is reached. This was performed in an ice bath to prevent the degradation caused by the rapid heating of the suspension [111].

In water suspension (0.05% w/w), with the specific material used in this study, the characteristic dimensions of CNC are: 6-10 nm (diameter) and 100-130 nm (length). This latter dimension of CNC was measured through dynamic light scattering with a Zetasizer Nano ZS (Malvern Instruments Ltd).

Cellulose fibers that remain after this treatment are almost entirely crystalline and as such are called "crystalline". The precise physical dimensions of the crystallites depend on several factors, including the nature of cellulose hydrolysis conditions and specific origin.

The aqueous CNC suspension was then concentrated in a Labconco RapidVap (Labconco, Kansas City, USA) up to 14% w/w. Such high CNC concentration is required to adjust the CNC loading within the formulation and avoid excessive dilution.

4.4.3. Surface modification of cellulose nanocrystals

Since CNC has an anionic surface at neutral pH, it is possible to modify its surface with hydrophobic cationic surfactants. A similar technique was used by Nipelö et al. to modify hydrophilic silica nanoparticles for coatings [112].

CNC was chemically modified by the following three different surfactant molecules (Figure 4.1), for further use in the formulations (in later discussions, unmodified CNC will be noted CNC). HDTMA and TMA were used to treat the CNC fiber with an hydrophobic coating while acryloyl chloride was reacted with hydroxyl groups to provide an anchoring group with acrylic reactive sites in the coating [108] (*Chapitre 3*). A proprietary hydrophobic grade CNC, modified by FPInnovations, was also used as a reference.

CNC: unmodified CNC

CNC-HDTMA: hexadecyltrimethylammonium bromide (HDTMA-Br)

CNC-TMA: tetramethylammonium bromide (TMA-Br)

CNC-Acryloyl: acryloyl chloride (C_3H_3ClO)

CNC-FPI: proprietary hydrophobic modification by FPInnovations

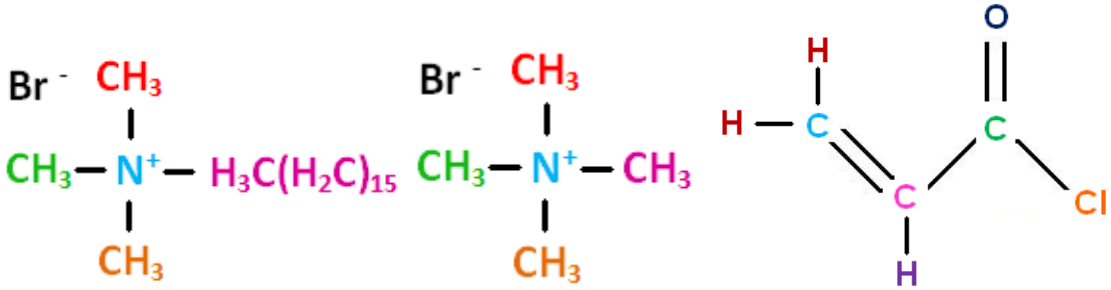

a) b) c)

Figure 4.1. Chemical formula of hydrophobic cationic molecules: a) HDTMA, b) TMA and c) acryloyl chloride.

The purpose of comparing 3 types of surface modified CNC: CNC-HDTMA, CNC-TMA and CNC-Acryloyl, with a commercial hydrophobic CNC, CNC-FPI, is to assess whether such surface modifications help in obtaining desirable properties in the coatings where the CNC are dispersed as reinforcing agents.

In the following study, these 5 types of CNC were added at concentrations into the liquid coatings as to have a final concentration of 2% in the cured, dry films.

More details about these modifications have been presented in another paper [108] (*Chapitre 3*), where advantage was taken of the anionic nature of the nanoparticle, whereas these sites were coupled to cationic hydrophobic surfactants. The amount of cationic reactant was adjusted to give a reasonably hydrophobic surface. Tests with too much of these surfactants resulted in an intractable nanopowder akin to powdered Teflon.

4.4.4. Preparation of formulations and samples

4.4.4.1. Dispersion method

A high-speed mixer (Dispermat, VMA-Getzmann GMBH D-51580 Reichshof) was used to disperse CNC in the varnish formulations. This equipment can produce shear rates comparable to those of industrial mixers. The high speed mixer consists of a vertical rotary axis with a propeller plate with tooth saws at its periphery, rotating at high speed in a vessel containing the formulation to be dispersed (Figure 4.2).

4.4.4.2 Preparation of formulations

The protocol followed for varnish preparation with CNC (stirring speed: 400 rpm) is presented below:

1. Addition of defoamer to the resin (in a metal container), with 4 min mixing.
2. Addition of surfactant to the above mixture, stirring for 4 min.
3. Addition of dispersant to the above mixture, stirring for 4 min.

4. Addition of the required amount of deionized water in the above mixture, stirred for 4 min.

5. Addition of CNC gel (14% w/w in water) gradually with 320 g of beads (glass) in the above mixture, stirring for 10 min (the chemically modified CNC was used in powder form, not gel).

6. Addition the rheological agent, stirring for 4 min.

7. Addition of photoinitiator, stirring for 6 min.

8. Removal of beads by filtration.

An example of varnish formulation with 2% CNC is presented in *Table 4.2*.

Results are presented, in various figures, as a function of

- Unmodified, hydrophilic CNC in concentrations of 0.5, 1, 1.5, 2 and 3% (w/w).
- 2% CNC (w/w), in 5 different types: unmodified hydrophilic CNC; CNC-HDTMA; CNC-FPI; CNC-Acryloyl; CNC-TMA.

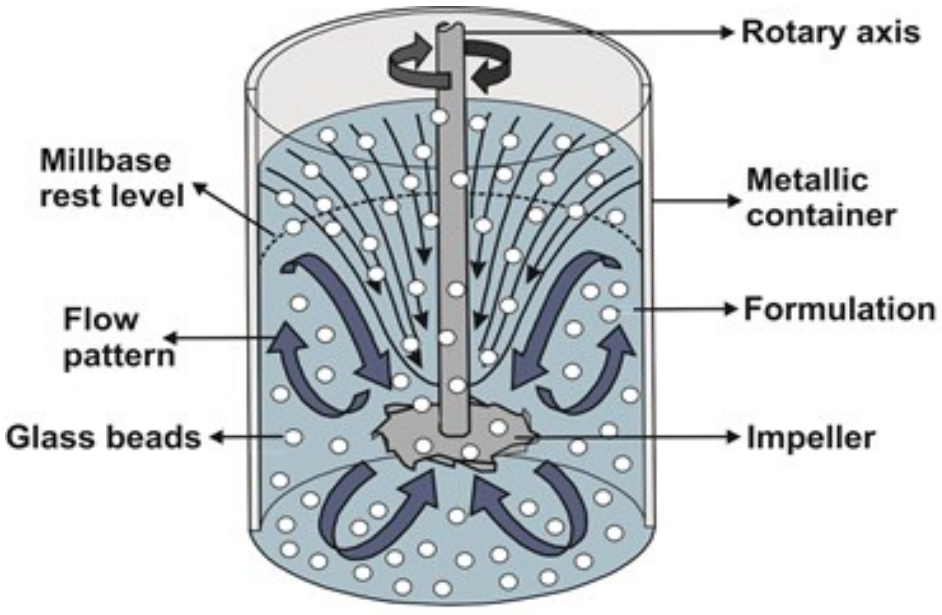

Figure 4.2. Principle of dispersion of high-speed mixer.

Table 4.2. List of chemicals for varnish formulation with 2% CNC (402.98 g).

	mass (g)	% dry (w/w)
- Resin	**366.23**	94.34
- Defoamer	**2.48**	0.41
- Surfactant	**1.53**	0.96
- Dispersant	**4.96**	1.29
- Deionized water	**1.87**	-
- CNC (14% in water)	**22.21**	2.00
- Rheological agent	**1.65**	0.21
- Photoinitiator	**2.05**	0.89
Total	**402.98**	

4.4.4.3 Preparation of the samples

Formulations were applied on sugar maple (*Acer saccharum*) on tangential face. The dimensions of the wood samples were 96 × 96 × 15 mm (Figure 4.3). Coatings were applied by spraying. After application (thickness: ~ 127 ±15 µm in liquid state), samples were put in a convection oven for 10 minutes at 60°C to gradually evaporate the water. During this step, the coating passes from a milky white liquid state to a transparent solid state. Film cure is then carried out using a UV oven (ATG 160305 from Ayotte Techno-Gaz, Inc.) equipped with a medium pressure mercury lamp (600 W/cm, model UV Mac 10, Nordson, OH, USA). This is a radical polymerization-type cure or crosslinking. The intensity of incident light measured with a radiometer was in the order of 570 mJ/cm^2 and the perceived temperature during curing is between 25 and 30°C. After curing, surfaces of varnishes were slightly sanded with 150 grit sandpaper, in the direction of wood grain.

These steps have to be repeated once again to get a coating ~ 100 μm thickness. These aqueous coatings are thin, about 100 μm, only two layers or coats, relative to commercial coatings, which for parquets for instance, may have up to 7 coats.

In Figure 4.3 it may be noted that there is no visual difference between the different samples. Thus, the CNC addition does not change the optical properties of the varnish, at least as perceived by human eye. More details about optical properties of these varnishes will be presented in a subsequent paper.

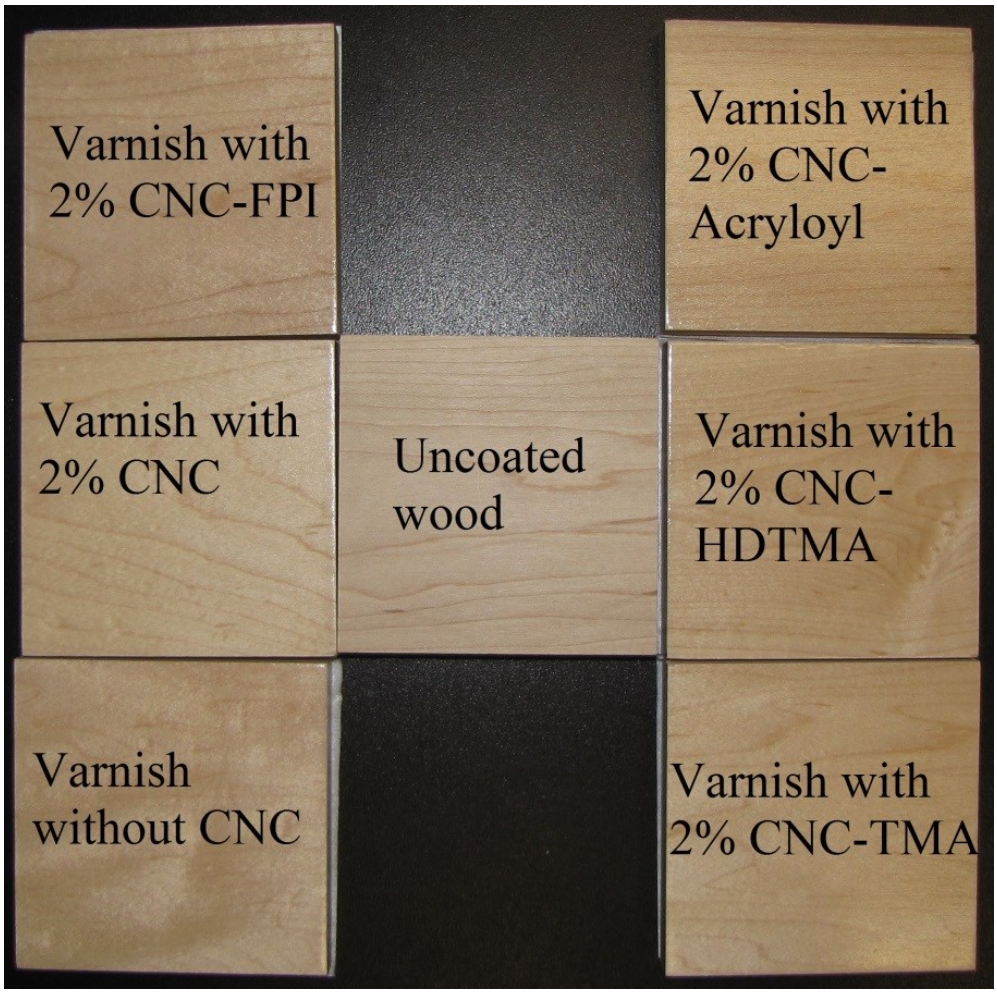

Figure 4.3. Wood samples with and without varnish coatings; with and without CNC in the coating: with modified and unmodified CNC in the coating.

4.4.5. Experimental methods

4.4.5.1 Atomic force microscopy

AFM observations were carried out using a NanoScope V (Veeco Instruments Inc., Santa Barbara, USA), fitted with a Hybrid XYZ scanner. AFM measurements were done under ambient air conditions in tapping mode. The sensitivity of the tip deviation and the scanner resolution was 0.3 nm. The resolution was set to 256 lines by 256 pixels for all observations. Surface roughness was calculated in 10×10 μm scan areas, using the classical mean surface roughness parameter R_a. The parameters were calculated by the Research Nanoscope 7.2 software:

$$R_a = \frac{1}{n}\sum_{i=1}^{n}\left|Z_i - Z_{ave}\right| \qquad (4.1)$$

where R_a is the mean roughness, the arithmetic average of the absolute values of the surface height deviations, Z_i is the current Z value, Z_{ave} is the average of the Z values within the given area and n is the number of points within the given area : 65536 in our case. The experimental value for each type of coating was obtained from the average of 12 measurements.

4.4.5.2 Contact angle

In order to see whether modified CNC had an effect on the hydrophobicity of coatings, contact angles measurements were performed. Water contact angles have been taken right after deposition of the water drop on the coated wood surface at laboratory temperature (23°C). The angle was calculated by software FTA200 Dynamic Contact Angle Analyzer (First Ten Angstroms, Inc., Portsmouth, USA). The experimental value for each type of coating was obtained from the average of 5 measurements.

4.4.5.3 Viscosity

Viscosity was measured using DV2T Viscometer at at 27°C (Brookfield engineering laboratories, inc., Middleboro, USA). The experimental value for each type of coating was obtained from the average of 5 measurements.

4.4.5.4 Adhesion test

To maximize the effectiveness of coatings, it is important that the adhesion of the coating on the wood is maximized, or at least that addition of CNC does not interfere in this respect. The drying of a varnish applied to the wood is accompanied by an increase in the work of adhesion [103]. This increase is accompanied by a decrease in the wood/varnish interface energy.

The adhesion strength of the varnishes was evaluated with the pull-off method according to ASTM D4541. 20-mm diameter aluminum dollies (Figure 4.4) were glued to the cured topcoat films with a two component epoxy adhesive, Araldite 2011 (Ciba-Geigy Corporation, MI, USA), which needed to cure for 24 h before testing. In order to test only the area bonded under the dollies, a circular groove was machined around these (Figure 4.4).

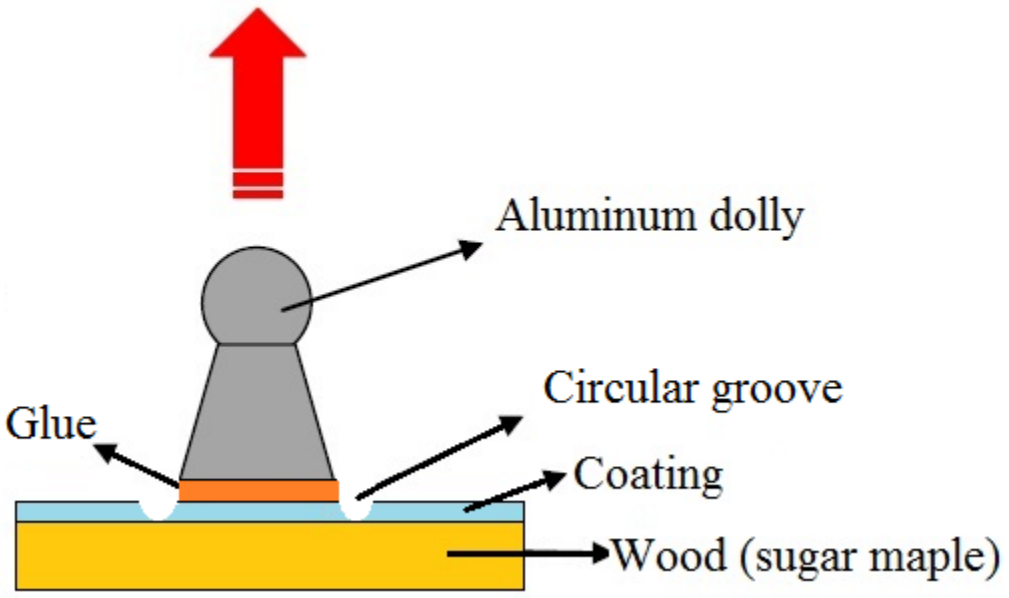

Figure 4.4. Diagram of the adhesion measurement set-up.

The dollies were pulled vertically away with a MTS Systems Corporation Alliance universal testing instrument, model RT/50, with a load cell of 5 kN mounted on the

crosshead. The force was applied normal to the surface with a speed of 2 mm/min to the loading fixture. The experimental value for each sample was obtained from the average of 12 measurements.

4.4.5 Hardness

The hardness of dried/UV-cured coatings was determined by measuring the damping number of a pendulum oscillating on the coating according to the standard ASTM D4366 (Pendulum hardness tester, BYK-Garner). The hardness value corresponded to the damping number of the pendulum from 6° to 3° (König pendulum). The experimental value for each type of coating was obtained from the average of 15 measurements.

2.5.6 Abrasion resistance

The abrasion resistance was measured using a Taber Rotary Platform Abraser (Taber Abraser ® 5135, Taber Industries, North Tonawanda, USA), according to ASTM D 4060. Two vertical discs of 500 g each, trimmed sandpaper type S-42, rub the sample of varnish on wood, the latter being driven by rotation (Figure 4.5). The abrasion resistance is expressed as weight loss caused by the passage of the abrasive surfaces, after 100 cycles of rotations, with the following relationship:

$$M_{loss} = M_0 - M_{100} \qquad (4.2),$$

where M_{loss} is the mass loss of the sample after a cycle of 100 revolutions, M_0 is the initial mass of the sample and M_{100} corresponds to the mass of the sample after a 100 cycle of rotations. The mass loss of a composite coating type corresponds to the average mass loss of 10 samples.

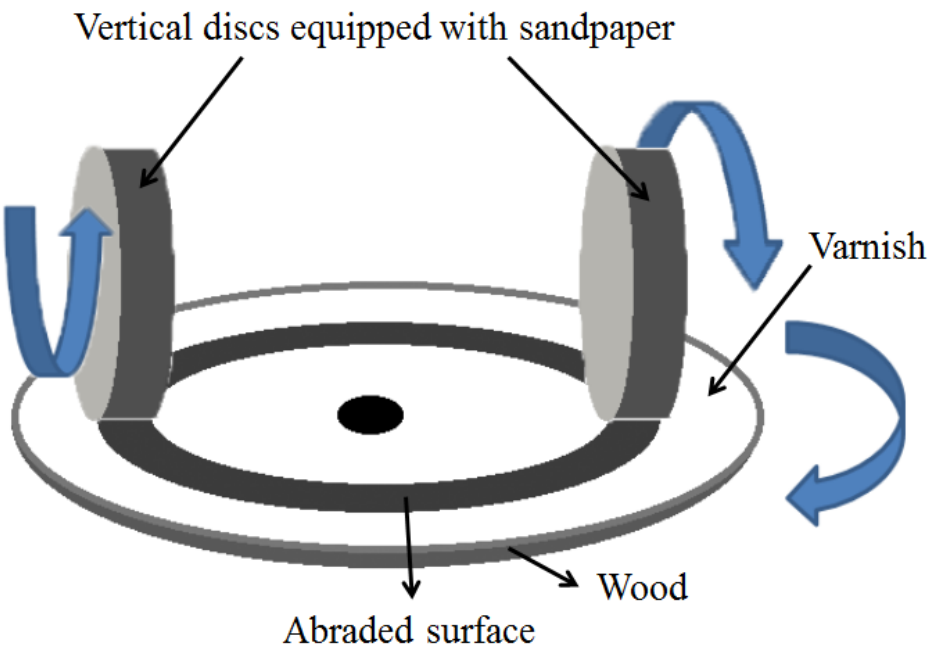

Figure 4.5. The abrasion resistance set-up using the Taber Abraser.

2.5.7 Scratch resistance

To measure the scratch resistance, the surface must be scraped with a standard load for all samples. This test was performed according to ASTM D7027 standard, using a Multi-finger Scratch / Mar Tester, model 710, (TABER Industries, North Tonawanda, NY, USA). The samples were scratched with a 10 N load, followed by depth profiling with a profilometer (DekTak 150, Veeco Instruments Inc., Santa Barbara, USA). The experimental value for each type of coating was obtained from the average of 15 measurements.

4.5. Results and discussion

4.5.1. Coating with unmodified CNC

We characterized surface dispersion degree of nanoparticles in varnishes, as first studied by measuring surface roughness using AFM [38] (*Chapitre 2*), since, as discussed above, standard x-ray techniques such as SEM and TEM did not give useful images, for lack of contrast. In Figure 4.6 are shown the surface roughness measurement results on the effect of hydrophilic, i.e. unmodified CNC addition in the varnish, as a function of CNC concentration. First, before coating application, the wood was sanded: its surface roughness is in the order of microns, since its cellular structure precludes a further lowering of the roughness, even with further sanding with increasingly fine sandpaper. Once coated with the cured water based varnish (2 coats), the roughness is reduced about a thousandfold, to about 5 nm (Figure 4.6).

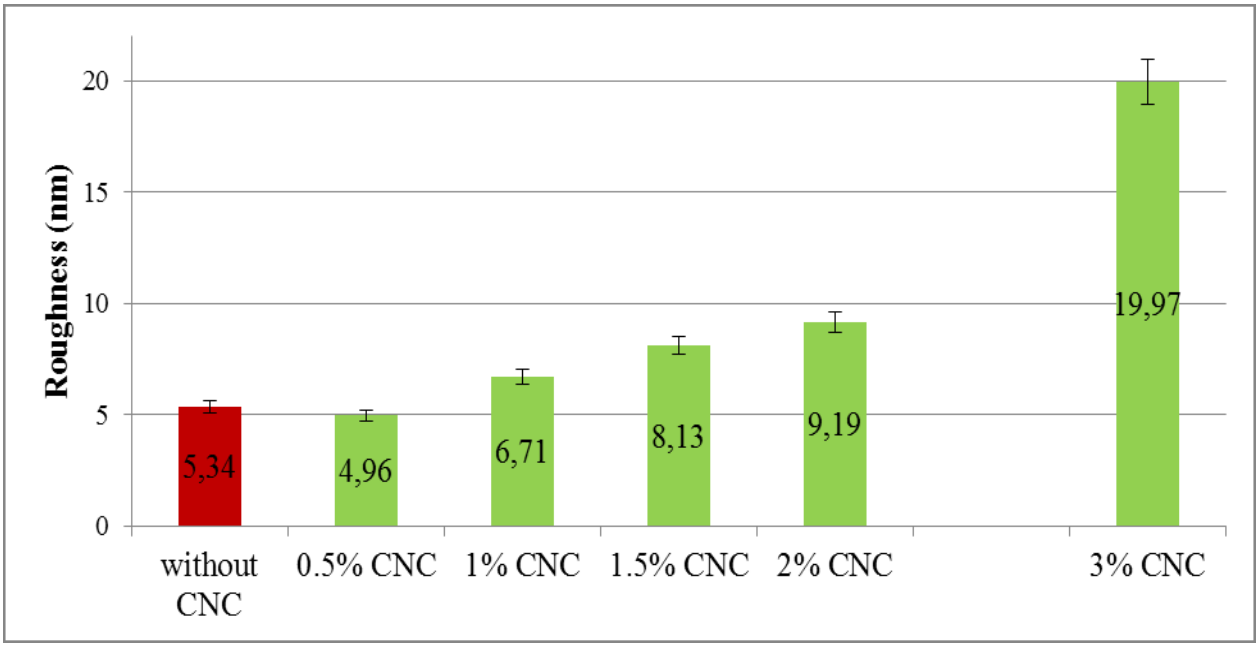

Figure 4.6. Surface roughness of varnishes without and with added hydrophilic CNC.

This is so because the AFM or any mechanical surface topography characterization apparatus detects only the cured coating surface, which is self-smoothing after liquid coating application, due to the high surface tension in the liquid phase. Thus there is no direct effect of the wood surface on the surface of the coating even if it is only between 30-100 μm thick: high gloss can be obtained [108] (*Chapitre 3*). Addition of 0.5% of CNC has no effect on the surface roughness. However, when more than 2% CNC is added into the varnishes, there is a significant increase in the surface roughness (around 20 nm). It may originate from the relatively decreasing quality of dispersion of CNC, which can be due to formation of CNC agglomerates. It is important to mention that the poor dispersion of nanoparticles may limit the possible improvement of the mechanical resistance, as well as other properties, such as surface properties, i.e. optical, paramount for appearance of coatings. This is discussed later in the text. One may object that the AFM only characterizes the surface roughness and potential agglomeration of CNC, not in the bulk, but in paints and varnishes, surface appearance is paramount, and any additive must preserve surface appearance. In this case, addition of untreated CNC does not affect the appearance, since even at 3% level of CNC in coating, a roughness of 20 nm is not perceived by the human eye.

These water-based coatings are self-smoothing, but addition of too much CNC interferes with this property. This may be related to increased viscosity. As shown in Figure 4.7, the addition of more than 1.5% CNC drastically increases viscosity, but it is still possible to spray the varnishes with up to 3% added CNC. Since varnishes with more than 2% CNC have shown significantly worse dispersion (Figure 4.6), no additional experiments were performed on coatings containing higher percentage of CNC than 2%, in the following text.

4.5.2. Effect of surface modification of CNC

In order to improve the CNC dispersion level within the coating, CNC particles were surface modified by three different surfactant molecules [108] (Figure 4.1) and a proprietary hydrophobic grade of CNC, modified by FPInnovations, was selected as control sample.

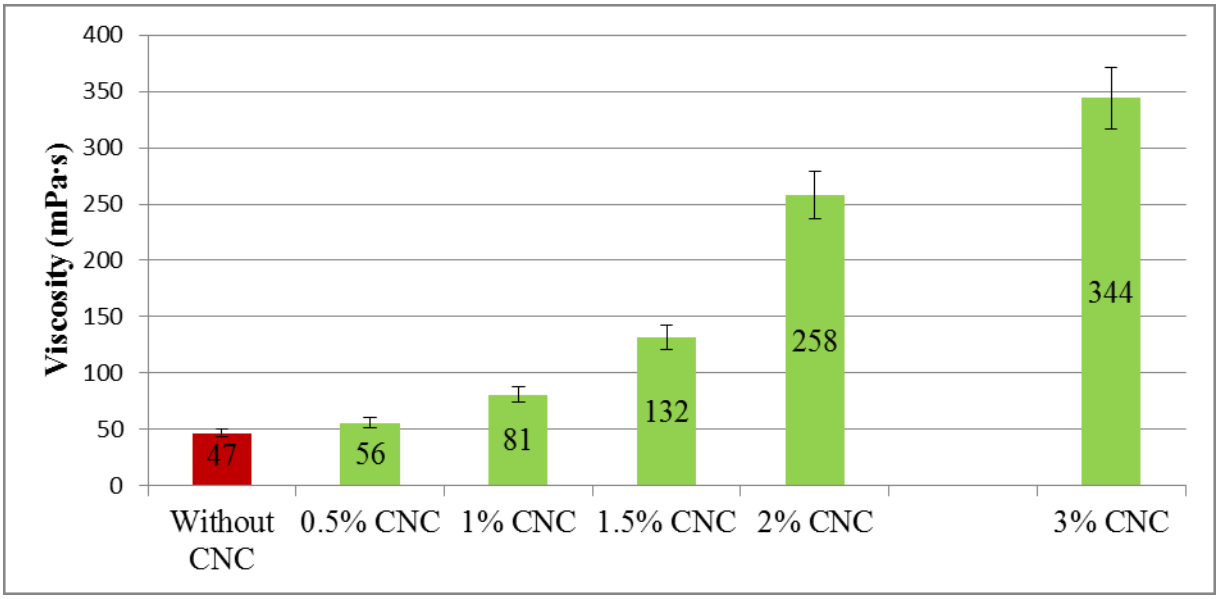

Figure 4.7. Viscosity of varnishes formulations without and with addition of hydrophilic CNC.

The aim of these modifications was to obtain more hydrophobic nanoparticles, which would disperse better in water-based coatings. Indeed a water-based emulsion, such as the coatings used here, is a dispersion of oily resin droplets in water, the latter playing the role of a carrier and a lubricant. Once the water has evaporated, only the hydrophobic phase remains. Our system is an emulsion, a so-called latex two-phase system, which means that the thinner or carrier is hydrophilic (water) and the resin is hydrophobic. To have a good dispersion of CNC in the hydrophobic resin, increasing its hydrophobicity is expected to have a positive effect [113]. For instance Tigges et al. use hydrophobized ZnO nanoparticles for better dispersion in emulsions [114] while Nobel et al. mention the advantages of using hydrophobic nanoparticles in coatings [115]. To compare hydrophobicity level of coatings with and without CNCs (modified and non-modified), we measured contact angles (Figure 4.8) on cured coatings with different CNC grades added. The coatings with more hydrophobic CNCs are more hydrophobic, as water contact angles are increased. There is no significant difference of this property between the four grades of hydrophobic CNC. Other measurements on surface properties of these surfactant-treated CNCs are given in a previous publication [108] (*Chapitre 3*).

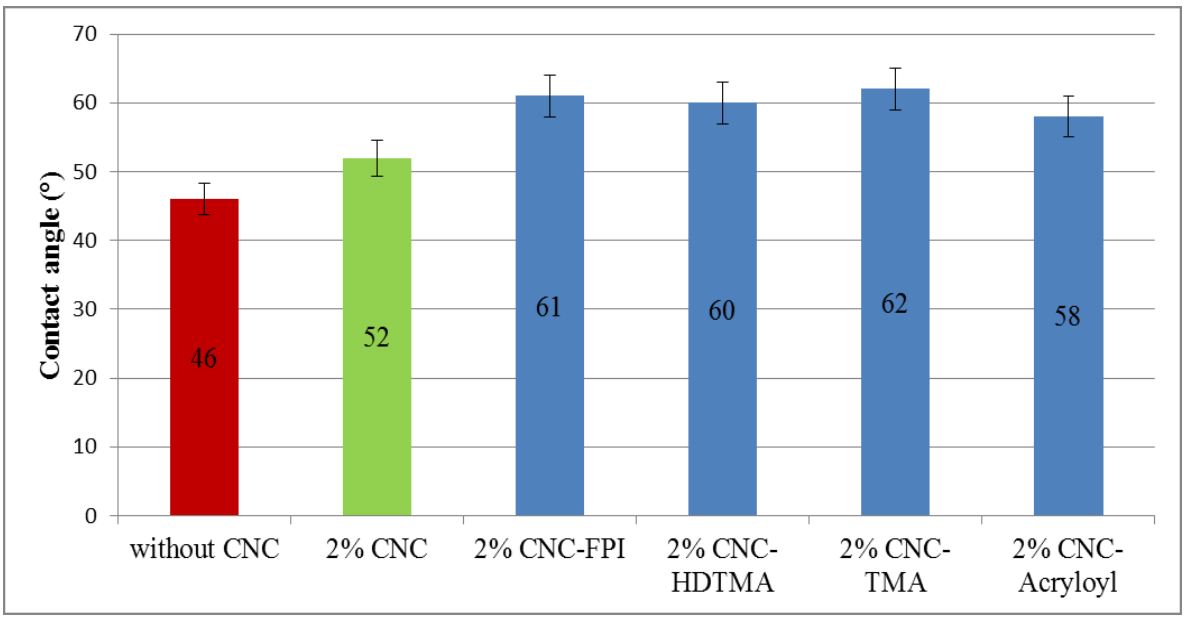

Figure 4.8. Contact angle for coatings on wood without and with CNC (unmodified and modified).

To study dispersion properties of varnishes with added modified CNCs, additional roughness measurements were performed by AFM [38] (*Chapitre 2*), on cured coatings with no CNC and 2% CNC (w/w), in 5 different types, as described in experimental section: unmodified (hydrophilic) CNC; CNC-HDTMA; CNC-FPI; CNC-Acryloyl; CNC-TMA; (Figure 4.9). The surface roughness of coatings incorporating modified CNCs are significantly lower, about 30%, than that of coatings containing same amount of hydrophilic (unmodified) CNCs. Surface roughness of coatings containing modified CNCs, especially those modified by HDTMA, acryloyl chloride, and hydrophobic CNC from FPInnovations are approximately at the same level as for coatings without nanoparticles. This means that the dispersion level of these hydrophobic CNCs is better, at least at the surface, where it is more important, for the final appearance of the coating. Possibly, more CNC could be incorporated, although high viscosity could become a hurdle to favor the spraying of the formulation. This also shows that having hydrophobic nanoparticles is desirable when working with an emulsion [110].

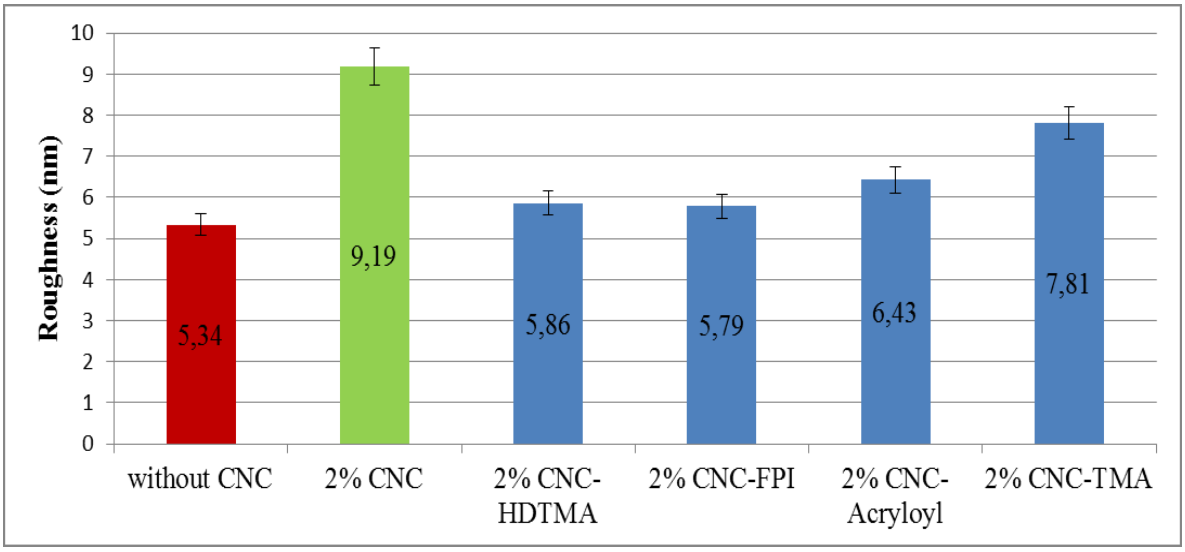

Figure 4.9. Surface roughness of varnishes without and with 2% unmodified and modified CNC.

4.5.3. Mechanical properties of coatings

4.5.3.1 Adhesion

To study the mechanical properties of these coatings, pull-off tests were performed (Figure 4.4). It is important that CNC addition (modified or not) does not worsen the adhesion characteristics of coatings. This study reveals that the adhesion strength of coatings with or without addition of CNC is practically at the same high level (Figure 4.10). However, it was noticed that coating with 2% CNC modified with HDTMA presents slightly higher adhesion strength compared with coatings containing CNC modified with TMA and hydrophobic CNC modified by FPInnovations. Since the hydrophobic CNC has been modified by FPInnovations by proprietary process, it is not possible to determine why it has less adhesion strength. Still, this shows that the higher viscosity (Figure 4.7) of CNC-based coatings does not interfere significantly with coating adhesion (Figure 4.10).

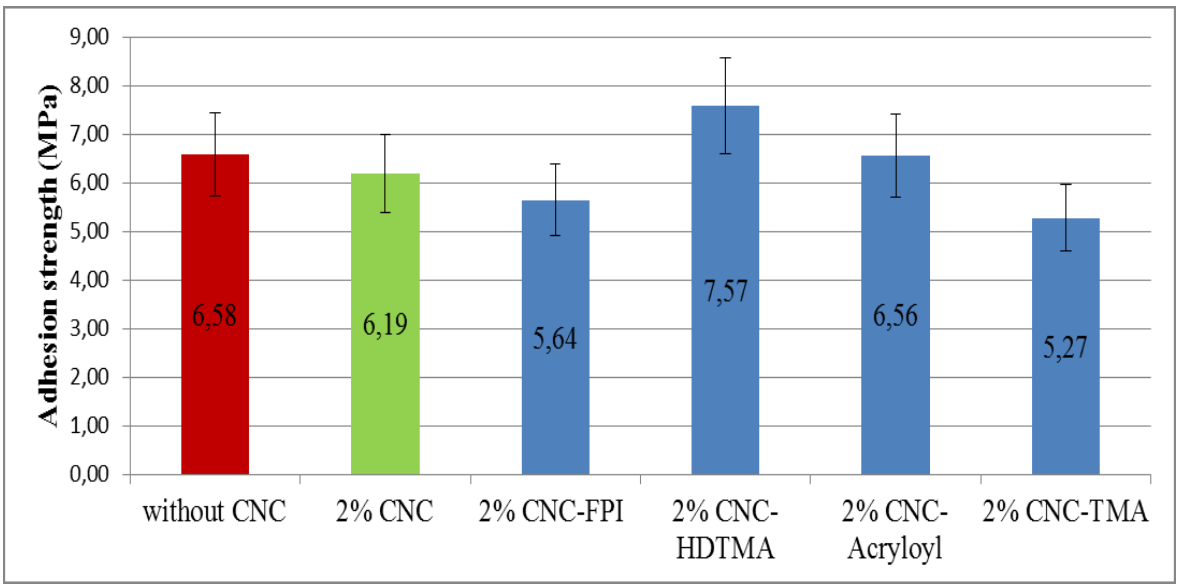

Figure 4.10. Adhesion strength of cured varnishes without and with 2% unmodified and modified CNC.

4.5.3.2 Hardness

Hardness is an important property of coatings, which is related to durability and long term performance. Any particle or nanoparticle added to the coating would be expected to enhance this property and the system should behave as a true composite. Figure 4.11 shows König hardness of UV-cured waterborne nanocomposite coatings with and without CNC (unmodified and modified): higher oscillations show that material is harder. This test reveals no significant difference between hardness of coatings with different types of CNC. This is not so surprising since the particles are not covalently bonded to the continuous phase, but simply dispersed within. However, we hoped that the acryloil choride residue on the nanoparticle would have coupled to the acrylates in the continuous phase resulting in an increased hardness, but it failed to do so.

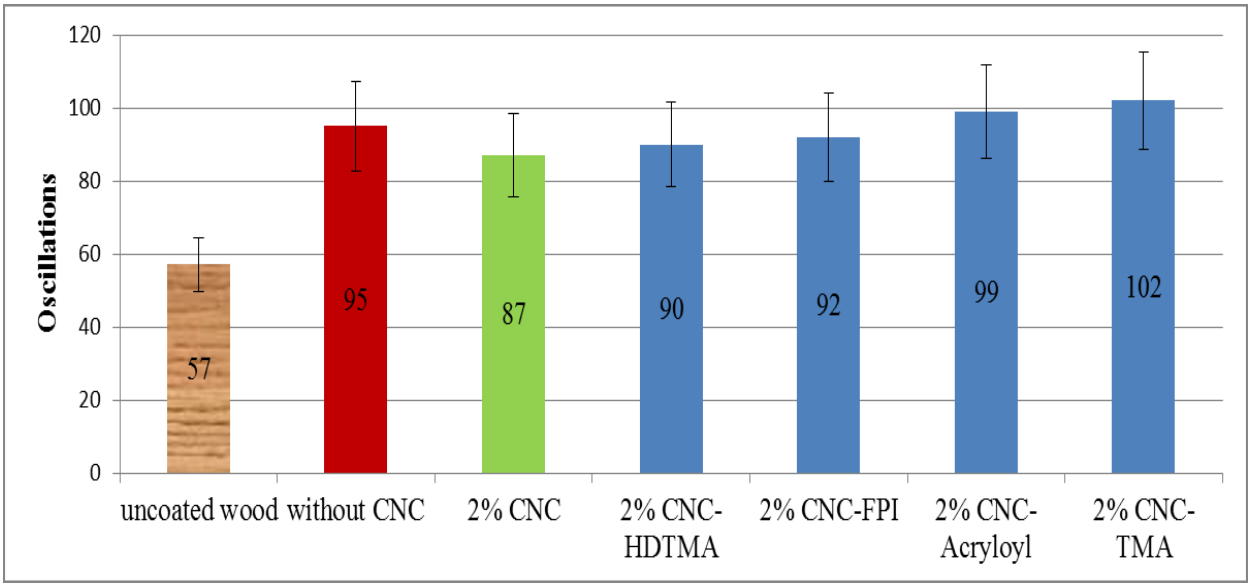

Figure 4.11. König hardness of uncoated wood and coated with UV-cured waterborne nanocomposite coatings with 2% unmodified and modified CNC.

4.5.3.3 Wear properties

Exploring wear and damage resistance of these nanocomposite coatings is the main purpose of this study. UV coatings are known for their outstanding wear properties, as they cure to a hard finish. To evaluate these characteristics, abrasion (Figure 4.12) and scratch (Figure 4.13) resistance experiments were performed on the various coatings applied on wood.

Both tests revealed that CNC-reinforced varnishes, even with 2% unmodified CNC added, showed improved mechanical resistance. More detailed results about mechanical properties of varnishes (and paints) with hydrophilic CNC were presented in our other publication [38] (*Chapitre 2*). Addition of 2% CNC-HDTMA, CNC-Acryloyl and CNC-FPI improved the mechanical resistance of UV-cured waterborne coatings even further, up to 30-40% (Figure 4.12), as a lower amount of material was abraded from the surface following the test. In comparison to the results found with CNCs, a significantly lower resistance to abrasion can be noted following nanosilica addition at 2% level to coating formulation. However, much larger amounts of alumina than CNC, up to 40%, can be added to coatings [106].

The scratch resistance was improved about 20-30% for the same CNC-reinforced varnishes (Figure 4.13), as depth of scratches decreased with addition of the same hydrophobic CNC. Addition of CNC-TMA did result in improving the scratch resistance, which can be due to its lower dispersion state in the varnish (Figure 4.9).

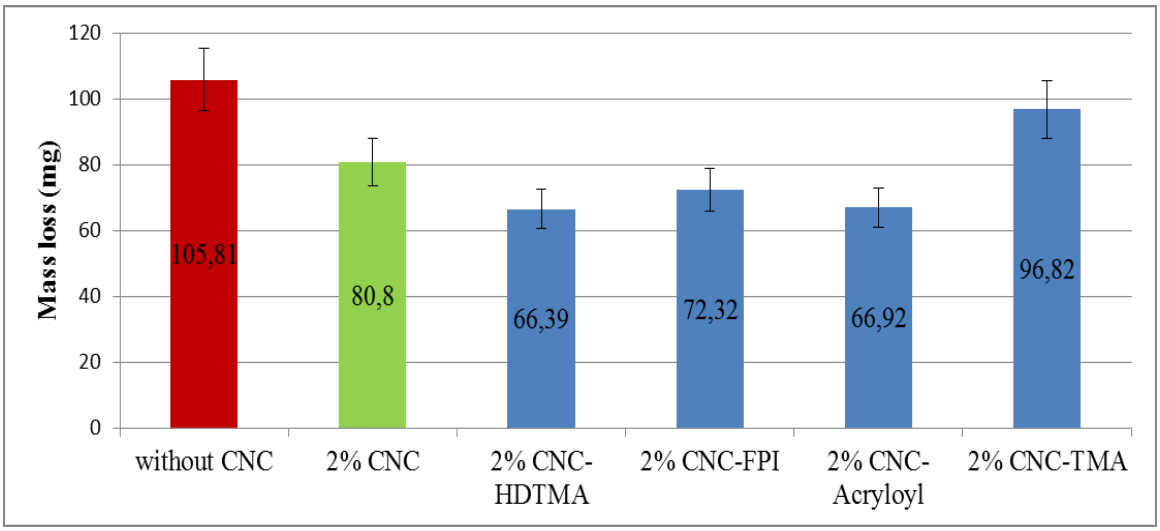

Figure 4.12. Mass loss after abrasion resistance test of wood coated with varnishes without and with 2% unmodified and modified CNC.

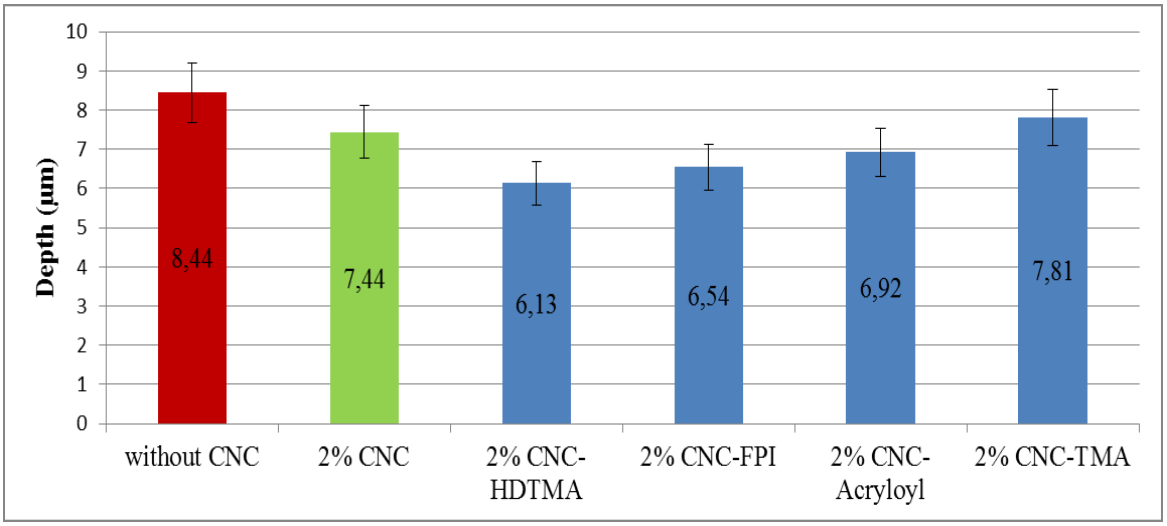

Figure 4.13. Depth of scratches after scratching the varnishes without and with 2% unmodified and modified CNC.

If we relate dispersion level (Figure 4.9) with mechanical resistance (abrasion and scratch: Figure 4.12, Figure 4.13) some correlations can be shown. It turns out that the varnishes which have good CNCs dispersion are much more resistant. So we can note that efficient dispersion is key in improving the mechanical resistance of the resulting nanocomposite varnish. It is reasonable to think that the CNC chemical modification did not change mechanical or structural characteristics of CNC itself, and helped to make the CNCs more compatible with the coating matrix, which should favor its dispersion [108] (*Chapitre 3*). Similarly, Bauer et al. obtained increased abrasion resistance of UV cured acrylates with the use of hydrophobized silica and alumina nanoparticles [62, 106, 110]. These results also suggest that characterization of dispersion with AFM, although being a surface phenomenon, does reflect the quality of the dispersion in the bulk, which is related to bulk wear and scratch resistance.

Not all nanoparticle addition gives positive results. In another study by Sow et al. [6], UV-waterborne varnishes reinforced with inorganic nanoparticles of alumina and silica evidenced increased mass loss upon abrasion, as compared to varnishes without nanoreinforcement, indicating a decrease of mechanical resistance of coatings, possibly because particles were not hydrophobized, which could have created weak interfaces between the filler and the matrix. In addition, hardness of above mentioned coatings was decreased by about 50% [57], despite an increase in adhesion strength. In contrast, our results show an increase of mechanical resistance, due to the presence of CNCs. We believe that varnish strengthening is due to proper CNCs dispersion within the organic varnishes due to right hydrophobic / hydrophilic balance of modified CNCs, as well as its intrinsic features (high aspect ratio, Young's modulus). Furthermore we may speculate that geometrical characteristics of CNCs may serve as nanostrusses, which can reinforce the binder matrix, like metallic fixtures for the modern high resistance buildings, but at the nanolevel.

4.6. Conclusions

In this study, the influence of addition of nanoparticles of CNC on the properties of water-based UV-cured coatings for wood products was studied. It was shown that it is possible to improve the quality of the dispersion of CNC in coatings using simple chemical reactions made on the surface of CNC. Dispersion was characterized by measuring the surface roughness by AFM. For these varnish formulations, an optimum concentration of CNC (2%) was found. Varnishes with 2% CNC-HDTMA, CNC-Acryloyl and CNC-FPInnovations gave approximately the same roughness as reference coating (without CNC nanoparticles), which suggests a good CNC dispersion state. The impact of the CNC addition in the paint and varnish formulations was assessed. Hardness and adhesion tests show that addition of CNC does not worsen mechanical characteristics of neat varnishes while in the case of CNC-HDTMA these were even improved. The effect of CNC on varnish formulations behavior differs significantly in terms of abrasion and scratch resistance. The property which is of greatest interest, wear resistance, was increased by 40% with addition of 2% of surface-modified CNC with HDTMA. From all tests done in this study we can conclude that varnishes with 2% CNC-HTDMA and CNC-Acryloyl are the most efficient. In the next paper we will examine properties of those varnishes (and corresponding paints) following accelerated aging and weathering.

Acknowledgements

Thanks to the Fonds de Recherche Nature et Technologie du Québec, the Conseil de Recherches en Sciences Naturelles et Génie du Canada and Arboranano for funding this research as well as FPInnovations' pilot plant for the production of CNC.

Chapitre 5. Characterization of cellulose nanocrystals dispersion in varnishes by back scattering of laser light

5.1. Résumé

Les celluloses nanocristallines ont été mélangées dans la formulation de revêtement pour améliorer les propriétés mécaniques des revêtements. L'un des aspects clés de la technologie des nanocomposites reste la dispersion de nanoparticules dans la matrice. Pour quantifier la dispersion, des méthodes efficaces de caractérisation sont nécessaires. Dans cette étude, une nouvelle méthode de caractérisation basée sur la microscopie à force atomique (AFM) et la rétrodiffusion de la lumière laser (He-Ne 632,8 nm) est appliquée pour caractériser ces revêtements nanocomposites. La distribution angulaire de l'intensité lumineuse rétrodiffusée a été représentée par une distribution de Gauss et son écart-type a été utilisé pour les analyses de la rugosité de surface. Une forte corrélation entre la nano-rugosité de surface du revêtement et la distribution angulaire (demi-largeur de l'étalement angulaire) de la lumière du laser rétrodiffusée a été constatée. Cette caractérisation laser est plus rapide et peut se faire sans contact direct sur une surface plus large que celle de l'AFM, et peut nous donner une idée sur les propriétés mécaniques des revêtements. Cette méthode peut avancer notre compréhension fondamentale de la dispersion des nanoparticules dans les revêtements et pourrait être utile pour l'assurance de qualité dans l'industrie.

5.2. Abstract

Cellulose nanocrystals were mixed into the coating formulation in order to improve the mechanical properties of the coatings. One of the key aspects in the technology of nanocomposites remains the dispersion of the nanoparticles within the matrix. To quantify the dispersion, efficient methods of characterization are needed. In this study a new characterization method based on atomic force microscopy (AFM) and back scattering of laser light (He-Ne 632.8 nm) is applied to characterize such nanocomposite coatings. The angular distribution of backscattered light intensity was approximated by Gaussian distribution and its standard deviation was used for the surface roughness analyses. A strong correlation between surface nano-roughness of coatings and angular distribution (half-width of the angular spread) of backscattered laser light was found. This laser characterization is faster and may be done without direct contact over a wider surface than AFM, and may give us an idea about mechanical properties of coatings. This method can advance our fundamental understanding of dispersion of the nanoparticles in coatings and could be of use in quality control service in industry.

Keywords: Cellulose nanocrystals, CNC, UV-water-based coatings, optical properties, wood, gloss, haze, roughness, scattering, dispersion

5.3. Introduction

5.3.1. Waterborne coatings

The overall objective of this research is to develop nanoparticles reinforced UV-water-based coatings for wood applications, and to study the effect, mainly on wear properties, of the final composite coatings. The formulation of varnishes is one of the most important steps for industrial uses, together with its application and drying. Water-based UV-cured

coatings are increasingly used in the wood industry, in view of their advantages, such as very low volatile organic content (VOC), hardness and fast setting (fast curing). First of all, the photopolymerization is very fast (few seconds) and is accompanied by little or no VOC emissions. Second, the use of water as single solvent reduces the viscosity of formulations to promote their homogeneous sprayable application in environmentally friendly and secure conditions [102]. Finally, aqueous coatings are known for their good adhesion to wood [103]. The UV-aqueous technology has other advantages, compared to 100% solid UV coating, since the polymerization of the UV-aqueous coatings is insensitive to atmospheric oxygen. Generally, coatings produced using this technology have excellent chemical and thermal resistance [102, 104]. The final properties of those coating are governed by the nature of the constituents. A varnish formulation is generally composed of three component groups: binder, solvent (water in this case) and additives. Each component group is made up of a wide range of products with specific properties and compatibilities. The binder or resin is the main element of a varnish formulation. Its role is to give to the coating its main physico-chemical characteristics, and once dried it forms a continuous dry film that adheres to the substrate. The solvent in this type of formulations is deionized water. Antifoaming agent, surfactant, dispersant, rheological agent and photoinitiator are the additives in water-based coatings and each one has its own important role even if they are in small quantities in those formulations. Here the role of the photoinitiator is of special importance. It is needed for the polymerization of coatings with a UV light source.

However, their mechanical performance is generally not as good as that of UV-curable high solid content coatings. The aqueous coatings are thin (about 100 μm, containing only two layers or coats), relative to commercial coatings, which for parquets for instance, may have up to 7 coats. In order to increase these properties, we use Cellulose nanocrystals (CNC), as film reinforcement in our study to evaluate their efficiency as organic-based renewable nanoscale reinforcement. We also modified CNC by different organic molecules and used in our coatings [108] (*Chapitre 3*).

5.3.2. CNC

Cellulose is the main component of wood, and in particular, of the cell walls. There are hydrogen bonds between the anhydroglucose molecules of different cellulose chains, resulting in a highly crystalline material. There are many products in everyday life made of cellulose derivatives, such as cellulose acetate, nitrates, esters and ethers, some of which are paint components. One of these products is CNC which have high aspect ratio (as opposed to inorganic nanoparticles, which are usually spherical or plate-like) and also are bio-based, non-toxic and recyclables. Generally, the CNC is extracted from the wood by a process of acid hydrolysis (H_2SO_4), with strict control of conditions of time and temperature [31]. The action of the acid removes the material of amorphous polysaccharide type. There remains the highly crystalline fiber of the original cellulose. When this level is reached, the hydrolysis is terminated by rapid dilution of the acid. A combination of centrifugation and extensive dialysis is used to completely remove the acid, and, for certain processes, ultrasonic treatments complete the process for dispersing the individual cellulose particles and produce an aqueous suspension [32]. CNC was found to be good reinforcing filler when mixed with aqueous latex matrices [35, 65]. Landry et al. have shown that the addition of small concentrations of CNC particles to clear clay-based coatings improves their mechanical properties (abrasion and scratch resistance, hardness) [42]. One of the reasons to choose CNC as a reinforcement agent in our study is that it is an organic nanoparticle. It is still difficult to incorporate and properly disperse inorganic nanoparticles in an organic polymer matrix [110]. The research hypothesis assumes that CNC as such, and possibly with appropriate modification of its surface, will show high dispersion and stability in the resulting nanocomposite coatings, which are, in this case, transparent coatings (varnishes). But there are some difficulties with dispersion characterizations of organic nanoparticles in such organic varnishes.

5.3.3. CNC dispersion characterizations

The choice of the mixing technique plays an important role in the dispersion state of the nanoparticles in varnishes. There are several types of equipment commonly used in the

industry, among those: high speed mixer, three-cylinder mill and ball mill [42]. In our study a high speed mixer was used, since it is most appropriate to our system (varnish with CNC). But whatever methods we use, efficient methods of characterization are needed to quantify the dispersion. There are many different methods to characterize nanoparticles dispersion in the matrix. The most widely used method to analyze the dispersion state of nanoparticles in dry films is electron microscopy, scanning (SEM) or transmission (TEM). However, in this project, it is difficult to do so as the polymer matrix (resin) and the CNC particles are both organic which leads to a very low contrast between the resin and the particles. Farrokhpay conducted a literature review on new assessment techniques of painted surfaces and obtained quantitative results on the surface roughness characterization by AFM [40]. Thometzek et al. also used TEM (transmission electron microscopy) and AFM to quantify the surface quality of paintings and correlated the degree of hydrophobicity of the particles with the quality of the dispersion [41]. In our previous research, we used AFM to study the quality of CNC dispersion by measuring surface roughness [38] (*Chapitre 2*). Correlation between surface roughness and the light scattering is well known [116]. In this paper another characterization method, based on the back scattering [116, 117] of laser light (He-Ne, 632.8 nm), is used to qualify the CNC dispersion in varnishes. This is a new method in coatings testing and our general aim is to bring the power of optical resources and methods to the domain of coatings.

5.4. Materials and experimental procedure

5.4.1. The composition of the formulation

The formulation used in this work is composed of the following components: the resin (or binder), solvent (deionized water), photoinitiator and other additives such us defoamer, dispersant, surfactant and thickener. These chemicals were added in order to minimize foaming, optimize the surface tension and help CNC dispersion. The typical compositions of the UV-aqueous formulation are presented in *Table 5.1*.

Table 5.1. Typical compositions of the formulation (see Table 5.2 for details)

Component	Chemical structure	Commercial name
Resin	Polyurethane-acrylate	Bayhydrol UV 2282
Defoamer	Ether poly dimethylsiloxane	Foamex 822
Surfactant	Polyether siloxane copolymer	Byk 348
Dispersant	Solution of block copolymer of high molecular weight	Byk 190
Photoinitiator	Bis-acyl phosphine oxide	Irgacure 819DW
Thickener	Polyurethane	RM 2020
Solvent	Deionized water	_
CNC	_	_

The photoinitiator is an essential element in a UV curing formulation since it initiates the radical polymerization reaction by absorbing ultraviolet light. The photoinitiator used in this research is a bisacylphosphine oxide (Irgacure 819DW, BASF Resins - Inks and OPV), dispersed in water (45 w/w %).

Then, in the basic formulations, CNC was added in concentrations of 0.5, 1, 1.5, and 2% (w/w).

5.4.2. Characteristics of CNC used in this study

CNC used in this project has been prepared by FPInnovations (Canada). To the best of our knowledge there are no publications on the manufacturing process of the CNC, since it is a proprietary industrial process, with patent pending [34]. Samples of the suspension of the CNC were sonicated using a Sonics Vibra-cell 130 W 20 kHz ultrasonic processor with a 6 mm diameter probe: typically, 15 ml of a suspension of 2-3% CNC weight were placed in a plastic tube of 50 ml and sonicated at 60% of maximum power until an energy input of more than 3600 J/g CNC is reached. This was performed in an ice bath to prevent the degradation caused by the rapid heating of the suspension [111]. Following this process, the resulting CNC nanoparticles have the following properties: specific surface area of 600 m^2/g, a Young's modulus of 150 GPa and a tensile strength of 10 GPa [35]. Cellulose fibers that remain after this treatment are almost entirely crystalline and as such are called "crystalline". The precise physical dimensions of the crystallites depend on several factors, including the nature of cellulose hydrolysis conditions and specific origin.

In water suspension (0.05% w/w), with the specific material used in this study, the characteristic dimensions of CNC are: 6-10 nm (diameter) and 100-130 nm (length) [108] (*Chapitre 3*). These dimensions of CNC were measured through dynamic light scattering with a Zetasizer Nano ZS (Malvern Instruments Ltd.) and TEM.

The aqueous CNC suspension was then concentrated in a Labconco RapidVap (Labconco, Kansas City, USA) up to 14% w/w. Such high CNC concentration is required to adjust the CNC loading within the formulation and avoid excessive dilution.

5.4.3. Surface modification of CNC

Since CNC has an anionic surface at neutral pH, it is possible to modify its surface with hydrophobic cationic surfactants. A similar technique was used by Nipelö et al. to modify hydrophilic silica nanoparticles for coatings [112].

CNC was chemically modified by two different cationic surfactant molecules: hexadecyltrimethylammonium bromide (HDTMA-Br), tetramethylammonium bromide (TMA-Br), while CNC was also modified by acryloyl chloride (C_3H_3ClO), for further use in the formulations (in later discussions, unmodified CNC will be noted as CNC). A proprietary hydrophobic grade CNC, modified by FPInnovations, was also used as a reference. Acryloyl chloride reacted with hydroxyl groups. More details about these modifications have been presented in another paper [108] (*Chapitre 3*), where advantage was taken of the anionic nature of the nanoparticle, as these sites were coupled to the cationic ones of the hydrophobic surfactants. Thus the nanoparticles were coated with a hydrophobic molecular coating. The amount of cationic reactant was adjusted to give a reasonably hydrophobic surface. Tests with too much of these surfactants resulted in an intractable nanopowder akin to powdered Teflon.

In later discussions, modified CNC will be noted by following short format:

CNC-HDTMA: CNC modified by hexadecyltrimethylammonium bromide (HDTMA-Br)

CNC-TMA: CNC modified by tetramethylammonium bromide (TMA-Br)

CNC-Acryloyl: CNC modified by acryloyl chloride (C_3H_3ClO)

CNC-FPI: CNC modified by proprietary hydrophobic modifier in FPInnovations.

5.4.4. Preparation of the samples

5.4.4.1. Preparation of formulations; dispersion method

A high-speed mixer (Dispermat, VMA-Getzmann GMBH D-51580 Reichshof) was used to disperse CNC in the varnish formulations. This equipment can produce shear rates comparable to those of industrial mixers. The high speed mixer consists of a vertical rotary axis with a propeller plate with tooth saws at its periphery, rotating at high speed in a vessel containing the formulation to be dispersed.

Since in our formulation there are different types of products, it is very important to follow the order of additions. The formulations should always be prepared the same way, to be comparable. Here is the protocol of formulations preparation with CNC. At the beginning the stirring speed is 400 rpm. The protocol followed for varnish preparation with CNC is presented below:

1. Addition of defoamer to the resin (in a metal container), with 4 min mixing.
2. Addition of surfactant to the above mixture, stirring for 4 min.
3. Addition of dispersant to the above mixture, stirring for 4 min.
4. Addition of deionized water (solvent) in the above mixture, stirred for 4 min.
5. Addition of CNC gel (14% in water) gradually with 320 g of beads (glass) in the above mixture, stirring for 10 min (the chemically modified CNC was used in powder form, not gel).
6. Addition of the rheological agent, stirring for 4 min.
7. Addition of photoinitiator, stirring for 6 min.
8. Removal of beads by filtration.

An example of varnish formulation with 2% CNC is presented in *Table 5.2*.

Table 5.2. List of chemicals for varnish formulation with 2% CNC (402.98 g).

	mass (g)	% dry (w/w)
- Resin	**366.23**	94.34
- Defoamer	**2.48**	0.41
- Surfactant	**1.53**	0.96

- Dispersant	**4.96**	1.29
- Deionized water	**1.87**	-
- CNC (14% in water)	**22.21**	2.00
- Rheological agent	**1.65**	0.21
- Photoinitiator	**2.05**	0.89
Total	**402.98**	

5.4.4.2. Preparation of the samples

Formulations were applied on sugar maple (*Acer saccharum*) on tangential face. The dimensions of the wood samples were 96 × 96 × 15 mm (Figure 5.1). Coatings were applied by spraying. After application (thickness: 127 ± 15 μm in liquid state), samples were put in a convection oven for 10 minutes at 60°C to gradually evaporate the water. During this step, the coating passes from a milky white liquid state to a transparent solid state. Film cure is then carried out using a UV oven equipped with a medium pressure mercury lamp (600 W/cm). This is a radical polymerization-type cure or crosslinking. The intensity of incident light measured with a radiometer was in the order of 570 mJ/cm^2 and the perceived temperature during curing is between 25 and 30°C. After curing, surfaces of varnishes were slightly sanded with 150 grit sandpaper, in the direction of wood grain. These steps have to be repeated once again to get a coating ~ 100 μm thickness.

In Figure 5.1 it may be noted that there is no visual difference between the different samples. Thus, the CNC addition does not change the optical properties (color, gloss, etc.) of the varnish, at least as perceived by human eye. More details about optical properties of these varnishes will be discussed later in this paper.

Figure 5.1. Samples with and without coatings.

5.4.5. Optical properties of coatings

5.4.5.1. Gloss and haze

The effect of the CNC on the gloss and haze of the coatings was determined with a haze-gloss apparatus from BYK Gardner. This instrument simultaneously determines gloss and hazeat three different geometries, 20°, 60° and 85°. These tests were performed according to ASTM standards D523 and E430. In our research we used 20° to measure gloss and for haze as shown on Figure 5.2. Gloss is generally defined as the amount of light that is reflected in the specular direction (i.e. at an angle that is equal to the light incident angle, Figure 5.2-a). The haze is given by the ratio of the scattered intensity at an angle off the specular direction (Figure 5.2-b) [118]. Commercial gloss meters (like apparatus from BYK Gardner etc.) have a detector with finite dimensions in the order of 1–10 mm, which implies that the beam of light measured during a gloss measurement with a standard gloss

meter will also contain some scattered light and will not only consist of purely specular reflected light [118, 119]. This is the reason why we have decided to use a dedicated optical setup (see in next section) to have a higher angular resolution of backscattered optical power. The experimental value for each type of coating was obtained from the average of 12 measurements.

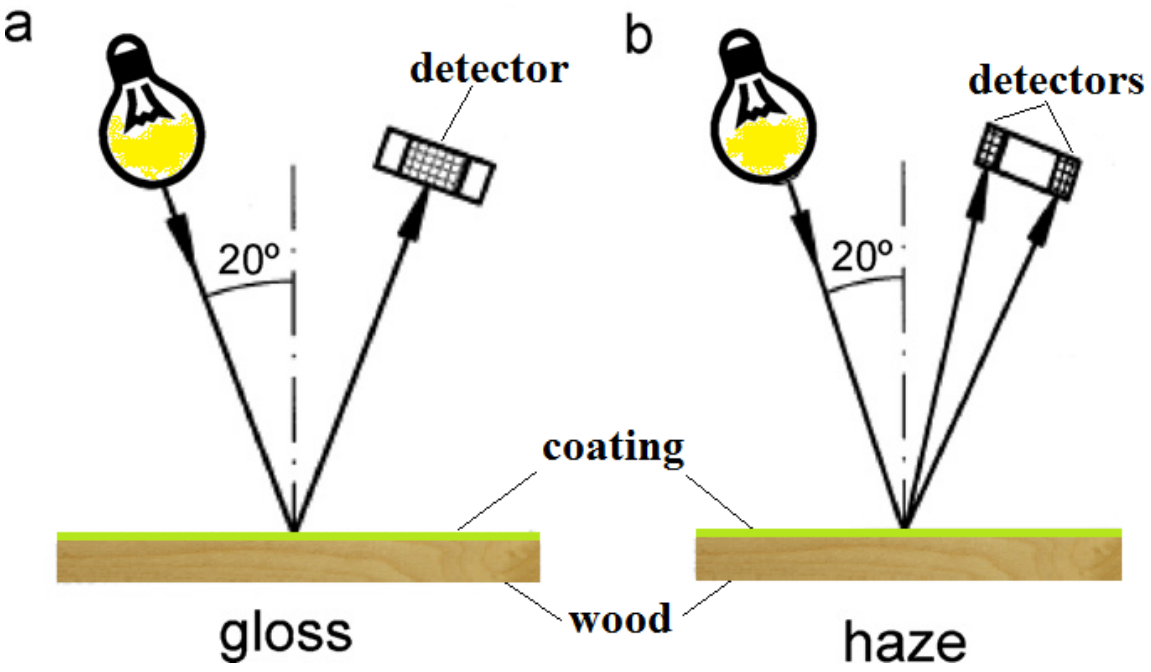

Figure 5.2. Principle of a) gloss and b) haze measurements of coatings.

5.4.5.2. Optical setup

The backscattering of He-Ne laser light from coatings was measured by an optical setup (Figure 5.3) and the obtained results (see hereafter) were compared with the surface characterization data obtained by AFM. The same geometry of gloss and haze measurement was used (Figure 5.2) to construct the optical setup (incidence angle is 20°). The beam of He-Ne laser, operating at 632.8 nm (red), was used to probe the coating sample, which was in the center of the main fixed optical table. The diaphragm and photodetector were all mounted on a rotating horizontal base. A dielectric mirror was used to obtain the desired

angle of incidence. A linear polarizer and half-wave plate were used to control laser beam polarization on samples (s and p polarizations [120]). To measure the angular dependence of the scattered light, the rotating base turned over -30° to 30° from initial position of photodetector, which is 20° from normal of sample's surface (position of specular reflection). Our experiments show (not presented here) that the wood fibrils' orientation in combination with laser beam polarization is important. We have chosen the vertical orientation of wood fibrils and the s-polarized laser light scattering in the horizontal plane (the photodetector's movement plane) to gather as much as possible scattering data information. All results presented in this paper correspond to above specified configuration.

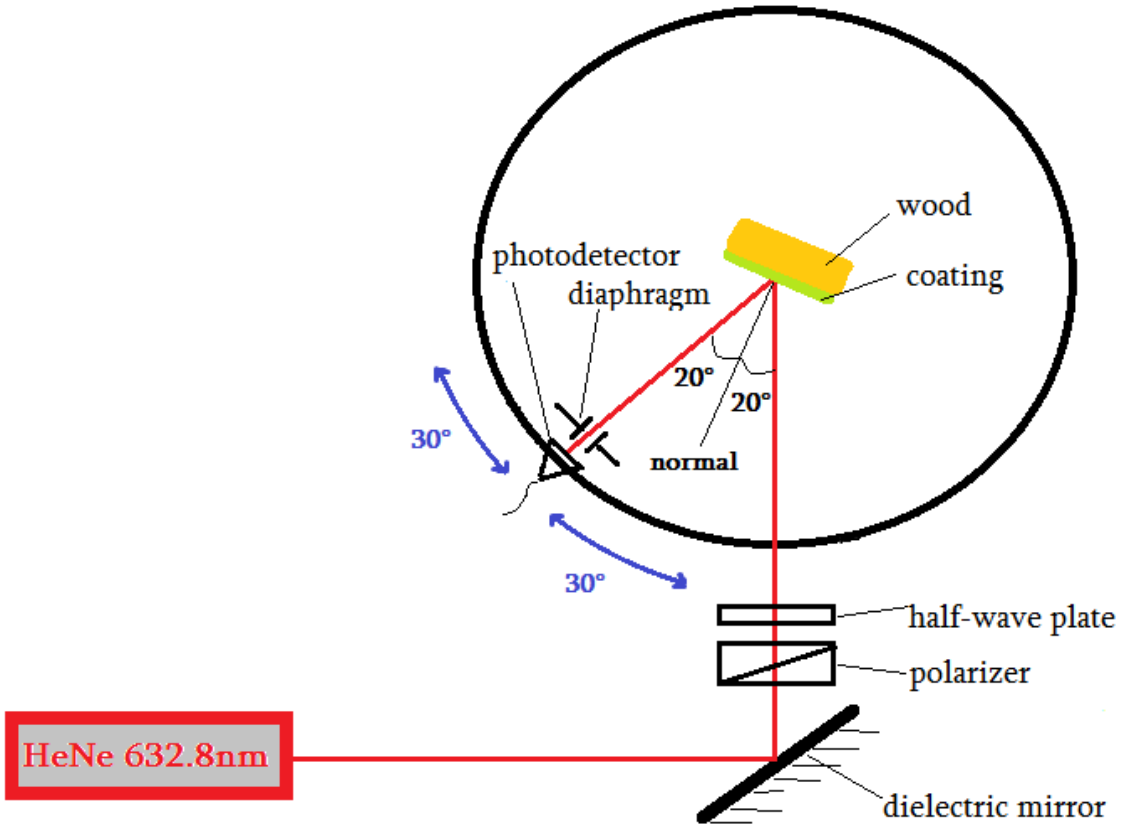

Figure 5.3. Optical setup for measuring the backscattering from coatings.

5.4.5.3. Index matching

To minimize the wood surface scattering effect (due to air-surface defects), an index matching liquid was added on the coating and covered with transparent glass. This index matching was done by using certified refractive index liquid 1-lodonaphthalene with 1.70 refractive index (Cargille-Sacher Laboratories Inc., Cedar Grove, NJ, USA) because our coating have refractive index 1.69, measured by Mline (Metricon Corporation, Pennington, NJ, USA).

5.4.5.4. AFM

AFM observations were carried out using a NanoScope V (Veeco Instruments Inc., Santa Barbara, USA), fitted with a Hybrid XYZ scanner. AFM measurements were done under ambient air conditions in tapping mode. The sensitivity of the tip deviation and the scanner resolution was 0.3 nm. The resolution was set to 256 lines by 256 pixels for all observations. Surface roughness was calculated in 10×10 μm scan areas, using the classical mean surface roughness parameter R_a. The parameters were calculated by the Research Nanoscope 7.2 software:

$$R_a = \frac{1}{n}\sum_{i=1}^{n}\left|Z_i - Z_{ave}\right| \qquad (5.1)$$

where R_a is the mean roughness, the arithmetic average of the absolute values of the surface height deviations, Z_i is the current Z value, Z_{ave} is the average of the Z values within the given area and n is the number of points within the given area : 65536 in our case. The experimental value for each type of coating was obtained from the average of 12 measurements.

5.5. Results and discussion

5.5.1. Characterization of coatings by AFM

We characterized surface dispersion degree of nanoparticles in varnishes, as first studied by measuring surface roughness using AFM, since the standard common techniques such as SEM and TEM did not give useful images, for lack of contrast [38] (*Chapitre 2*). In Figure 5.4 are shown the surface roughness measurement results on the effect of hydrophilic, i.e. unmodified CNC, addition in the varnish as a function of CNC concentration.

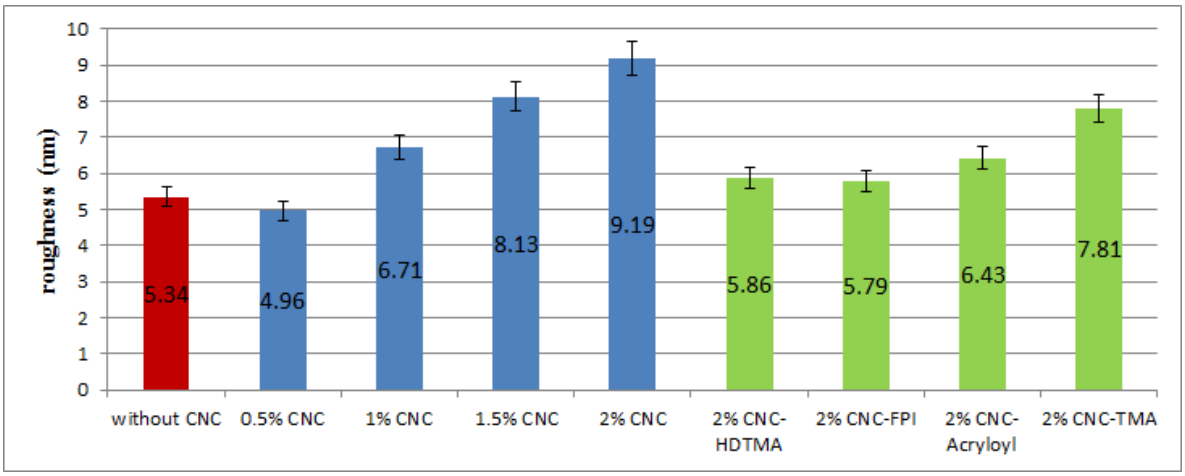

Figure 5.4. Surface roughness of varnishes without and with modified and unmodified CNCs.

Addition of 0.5% of CNC has no effect on the surface roughness. However, when 2% CNC is added into the varnishes, there is a significant increase in the surface roughness (around 5 nm). It may originate from the relatively decreasing quality of dispersion of CNC, which can be due to formation of CNC agglomerates. To improve the dispersion of nanoparticles in varnishes we modified CNC with 3 different molecules [108] (*Chapitre 3*) and also we used hydrophobic CNC from FPInnovations, to compare results with industrial product too. The surface roughnesses of coatings incorporating modified CNCs are significantly lower, about 30%, than that of coatings containing the same amount of hydrophilic (unmodified)

CNCs (Figure 5.4). Surface roughness of coatings containing modified CNCs, especially those modified by HDTMA, acryloyl chloride, and hydrophobic CNC from FPInnovations are approximately at the same level as for coatings without nanoparticles. This means that the dispersion level of these hydrophobic CNCs is better, at least at the surface, where it is more important, for the final appearance of the coating. Surface roughness of coatings with 2% CNC modified by TMA is higher than that from the other hydrophobic CNCs, this means that CNC-TMA is too hydrophobe and dispersion degree is low, which have impact on mechanical properties too [10] (*Chapitre 4*).

5.5.2. Characterization of coatings by haze and gloss

Haze of the different coated films on wood did not show a noticeable change with the addition of the CNC and its derivatives (Figure 5.5). There appeared very little difference between coating without CNC (haze value is 353.4) and nanocomposite coatings (haze values of 373 to 390).

The coatings with modified CNC slightly favored a haze decrease, in comparison with the coatings with unmodified CNC. But they are all in same level, so we can't really mention appearance differences between these coatings at least with this technique. It is clear that to have more information about surface we need other methods, more precise.

On Figure 5.6 a slight decrease of gloss of the coating can be noticed following addition of more and more unmodified CNC (0.5-2%). The gloss levels presented on Figure 6 indicated that the CNC derivatives modified by HDTMA, Acryloyl and CNC-FPI conferred better aspect to the film than the unmodified CNC, this last one resulting in a reduced effect after its addition in the basic coating.

Gloss level of coating with CNC-TMA is equal to gloss level of coating with unmodified CNC. In other words, these modifications (except CNC-TMA) made possible the retention of the high original gloss (~ 90) of the coating even after the CNC addition, which is also coherent with the precedent results from surface roughness (Figure 5.4). However this weak difference is not remarkable for human eye (Figure 5.1).

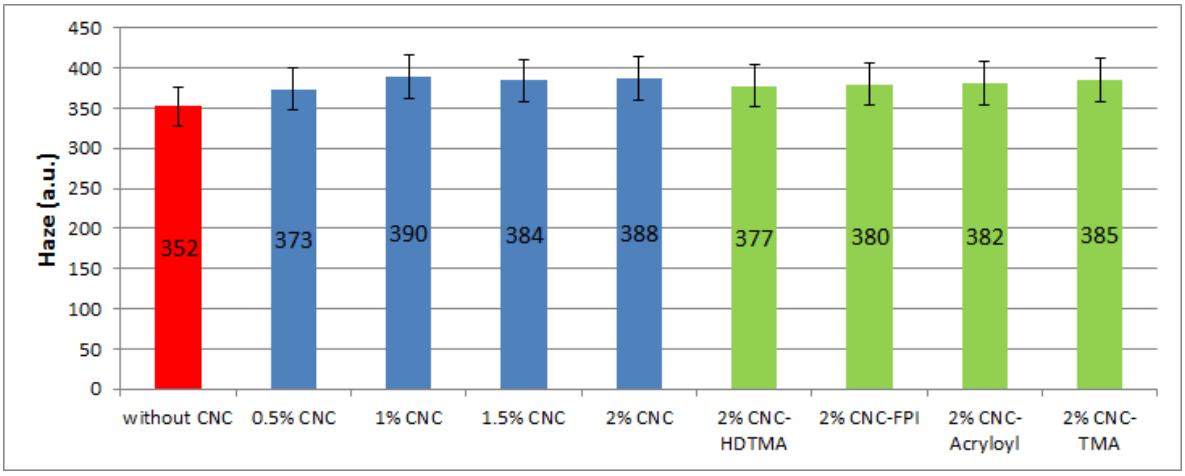

Figure 5.5. Haze of varnishes without and with modified and unmodified CNCs, measured by haze-gloss apparatus.

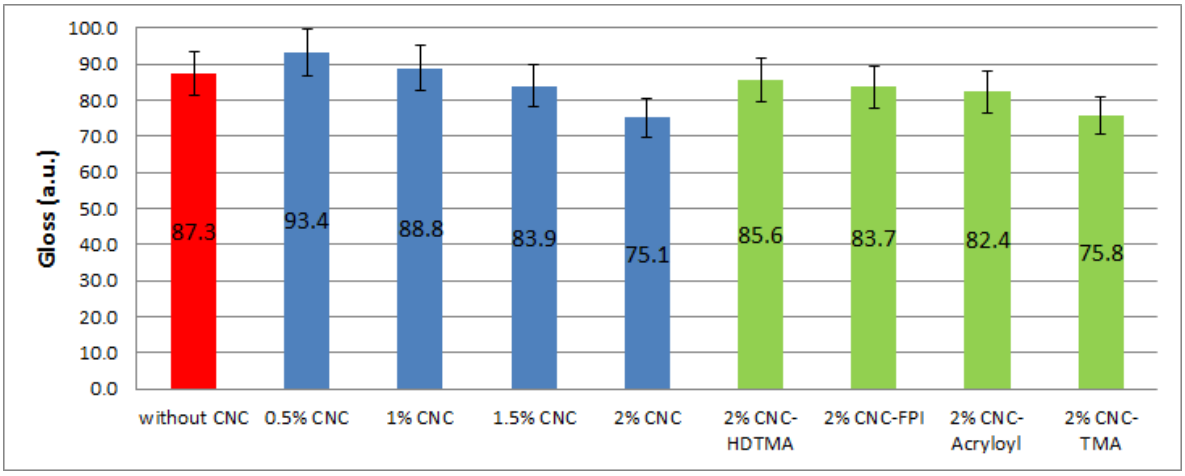

Figure 5.6. Gloss of varnishes without and with modified and unmodified CNCs.

5.5.3. Characterization of coatings by optical setup

To study more detailed optical characteristics of varnish coatings we have used the optical setup shown in Figure 5.3. Typical measure by using this setup provides graphs (raw data, but with same arbitrary units) like shown on Figure 5.7. As we can see, the addition of CNC (modified or unmodified) in initial varnishes increases not only the roughness of coatings (Figure 5.4) but also the angular spread of light backscattering (Figure 5.7).

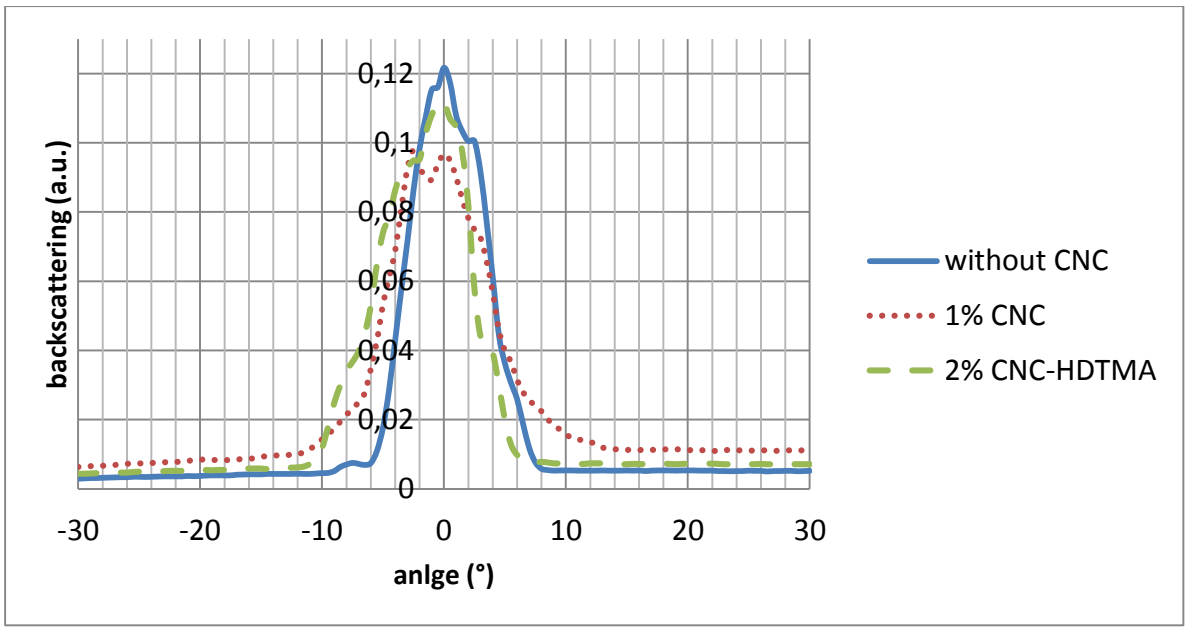

Figure 5.7. Backscattering of the probe beam (from a CW He-Ne laser, operating at 632.8 nm) from coatings with and without modified and unmodified CNC measured by the optical setup shown on Figure 5.3.

To properly compare the angular spreads we have fitted experimental data by theoretical distribution. We know, that to perfectly accurate calculations and explanations of all backscattering effects from the coatings surfaces we need complex functions as well described in many of classical books about scattering of light **[116, 117]**. But since the aim of our study requires much simpler mathematical representation of angular distribution, we have chosen normal (or Gaussian) distribution:

$$p(\theta) = \frac{1}{\sqrt{2\pi}\sigma} e^{-\frac{\theta^2}{2\sigma^2}} \qquad (5.2)$$

where θ is the angle, and the parameter σ is its standard deviation; its variance is therefore σ^2.

On Figure 5.8 coating without CNC and its theoretical fit are shown. As we can see here Gaussian distribution is close enough to our experimental data.

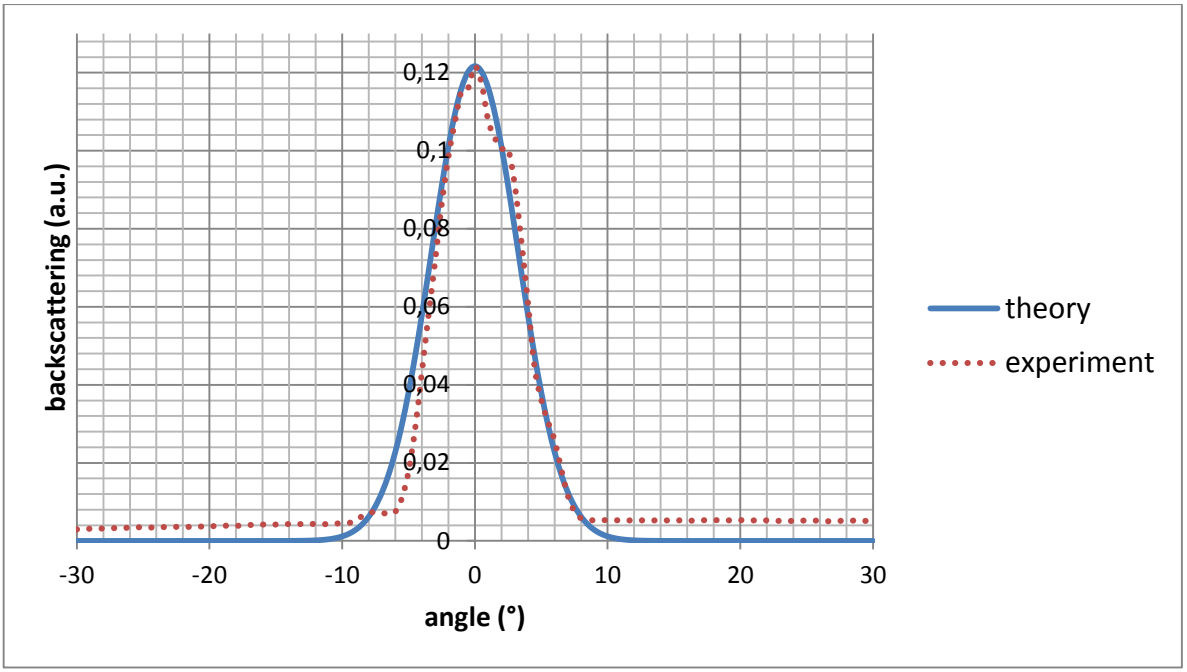

Figure 5.8. Backscattering of the probe beam (from a CW He-Ne laser, operating at 632.8 nm) from coating without CNC (red dashed line) and its corresponding theoretical fit according to equation 2 (blue solid line).

To discriminate the contribution of the air-varnish interface, we have used an index matching liquid. Liquid was added on the two types of coatings: varnish without CNC and varnish with 2% CNC and covered with transparent glass slide. Same measures were done for these samples and results are normalized with mirror (we put mirror in place of the sample on Figure 5.3). On Figure 5.9 it can be noticed that after index matching and normalization, the backscattering from both of coatings (without and with 2% CNC) is almost the same as the backscattering of mirror, which means that when we have eliminated the effect of surface roughness, it practically stops scattering. On Figure 5.9 it is very hard to distinguish the at results of backscattering by index matched coatings since they are very close to the peak of mirror (after normalization), see the inset showing a zoom on the central part of graph.

To quantitatively compare all type of coatings by using this optical setup we calculated half-width of peaks (angular width at half-intensity) after normalization with mirror and theoretical fit by using the equation (5.2). On Figure 5.10 it can be noticed that the addition

of CNC increases the half-width of angular spread gradually in a manner similar to the tendency had been observed with the surface roughness (Figure 5.4). Addition of modified CNCs: CNC-HDTMA, CNC-FPI and CNC-Arcyloyl, provides half-width of the same value as for the coating without CNC, this also being similar to the case of roughness studies (Figure 5.4).

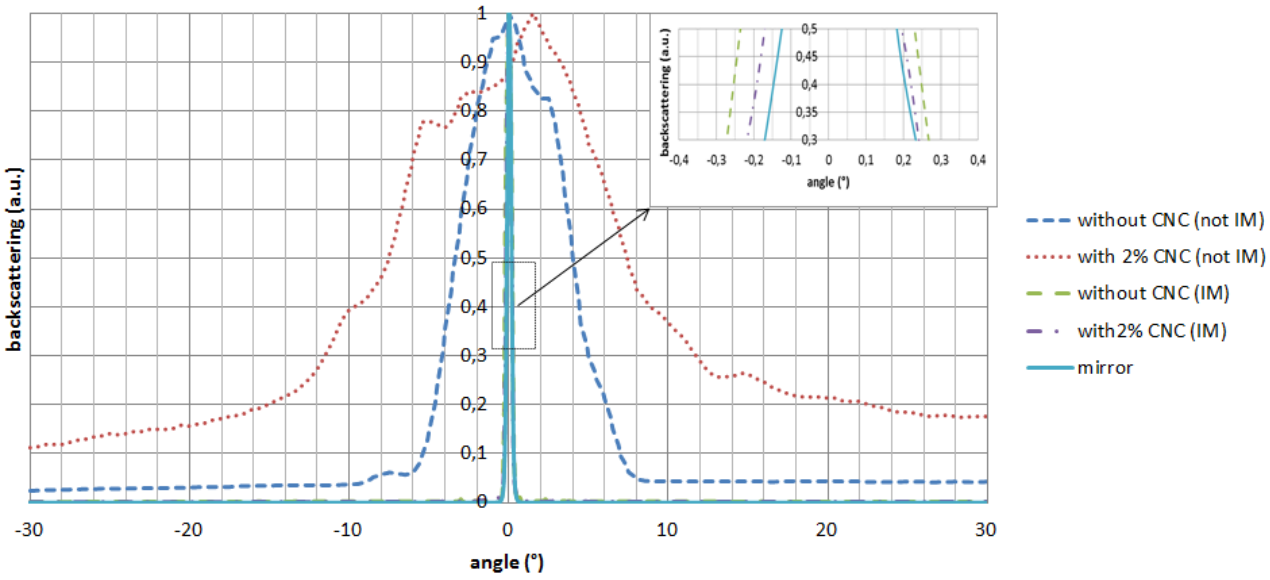

Figure 5.9. Backscattering of He-Ne from coatings without and with 2% CNC before and after index matching (IM).

We built correlations between surface roughness and half-width of angular distributions of scattering observed in Figure 5.10. Here we can see almost linear dependence between surface roughness and half-width of angular spread. Surely that theoretically cannot be linear just because the half-width of angular spread has a theoretical maximum (180°) but roughness has not. The surface roughness R_a is much smaller then probe wavelength (λ), which allows us apply Rayleigh scattering model [117, 120]. According to this model, the half-width of angular spread ($\Delta\theta$) widens with decrease of λ. Theoretical relation between R_a and $\Delta\theta$ was found based on above mentioned considerations, theoretical and

experimental results from other references ([116-119]) and our empirical data from all type of coatings that we made:

$$\Delta\theta(R_a) = \pi\left(1 - e^{-\frac{2\pi^4}{5}\frac{R_a}{\lambda}\left(\frac{n^2-1}{n^2+2}\right)^2}\right) \qquad (5.3)$$

where R_a is surface roughness, λ is wavelength of laser light (632.8 nm) and n is refractive index of coatings (as already mentioned $n = 1.69$). The coefficient $2\pi^4/5$ was found by approximation.

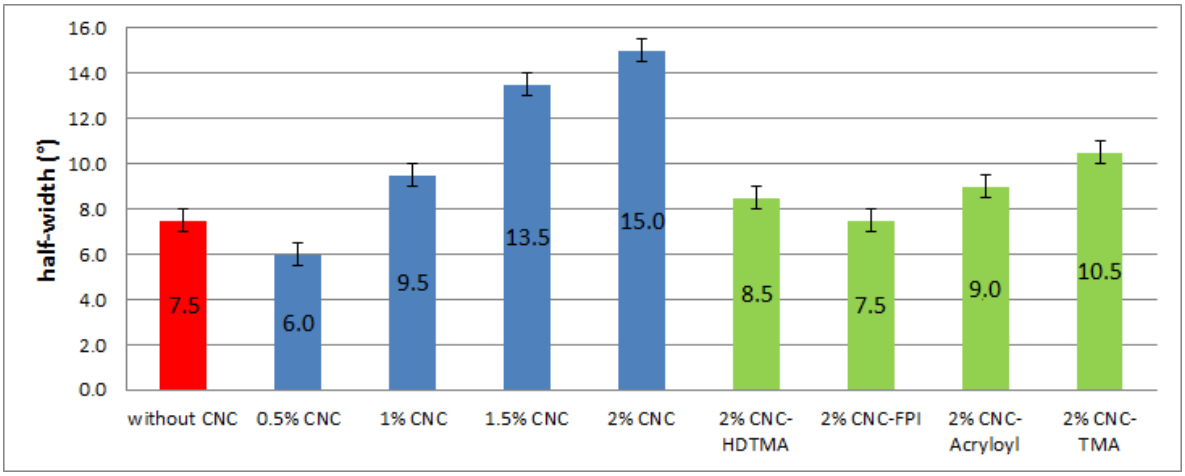

Figure 5.10. Half-width of angular spread of backscattering from varnishes without and with modified and unmodified CNCs.

In our case roughness is at nanoscopic level and in this particular range of values (Figure 5.4) this correlation (eq. 5.3) can be interpreted as linear dependence (Figure 5.11).

We have made coatings with modified CNC only in concentration of 2%. Reason of this comes from mechanical properties of coatings, since it was shown that 2% is the best concentration for this coating, which can improve their mechanical resistance about 40% [10] (*Chapitre 4*). In a previous report (about mechanical properties of this coatings [10]), a strong correlation between mechanical resistance and surface roughness has been shown;

coatings with well dispersed CNC are more resistant and coatings with badly dispersed CNC, i.e. with high roughness, even show a decrease in the mechanical resistance (CNC-TMA). This shows the importance of dispersion of nanoparticles in varnishes, for mechanical properties optimization. Dispersion was characterized by AFM [38] (*Chapitre 2*), which is not a simple technique, as it takes time, is not largely available and is not a cost effective approach for quality control. The method described in this paper could represent the next step to characterize nanocomposite coatings in a fast, easy and cheap fashion. The other advantage of this method is that it can be used in a much more mobile setup than AFM.

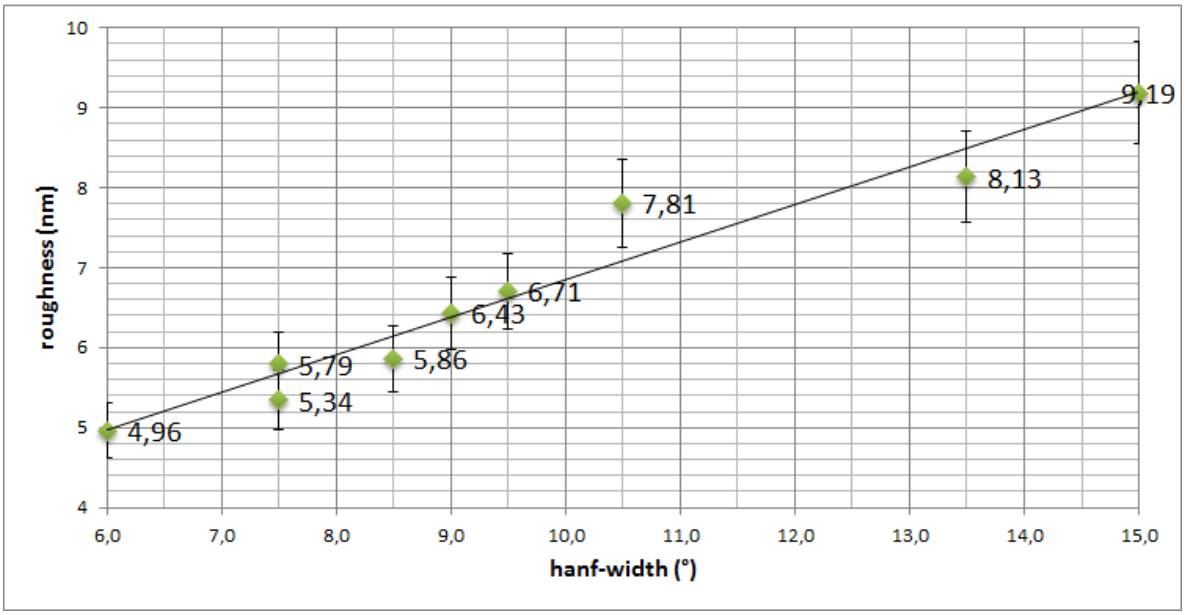

Figure 5.11. Correlations between surface roughness and half-width angular spread.

In other words, if we have some type of coatings and we added some nanoparticles, resulting in an increase in the backscattering from surface, then a worse dispersion and a decrease of mechanical resistance could be inferred. This method is aimed at being a fast and easy way to perform–preliminary evaluation of optical and mechanical properties of coatings, to facilitate upcoming works.

5.6. Conclusions

In this paper, UV-curable varnishes containing CNC particles have been prepared. The surface roughness of coatings on wood was measured by AFM and gives good indications of the degree of dispersion of CNC in coatings. This is an efficient method to evaluate the dispersion in cases where SEM cannot be employed as there is no contrast between the particles and matrix (organic composition).

Optical properties of coatings were measured by traditional standard methods (gloss and haze) as well as by using special optical setup. Data obtained from optical setup give us much more detailed information about interaction of light with coating. Theoretical fit by Gaussian distribution to experimental data was done to properly calculate and compare half-width of angular distributions. Results were compared with surface roughness data from AFM and a strong linear correlation between them was found.

Thanks to these results it is possible to evaluate in a preliminary way the mechanical properties of coatings, compare the influence of addition of different type of CNCs in different concentrations.

This characterization method can be used for other type of coatings with other nanoparticles too. The practical application of our results can be the quality control service in industrial level by using our procedure and the analogy of our experimental setup in smaller form factor.

Acknowledgments

We thank Arboranano, NanoQuebec, FQRNT (Québec, Canada) for funding this project as well as FPInnovations' pilot plant and Dr. Gregory Chauve for the production of CNC.

Chapitre 6. Effect of addition of cellulose nanocrystals to wood coatings on color changes and surface roughness due to accelerated weathering

6.1. Résumé

Une formulation aqueuse d'acrylate polyuréthane translucide cuite sous rayonnement ultra-violet a été soumise à vieillissement accéléré pendant 1200 h, sur un substrat de bois, avec et sans cellulose nanocristalline (CNC) ajoutée dans les revêtements. Lors des travaux antérieurs, l'addition de la CNC a amélioré plusieurs propriétés mécaniques du revêtement, sans modifier d'autres propriétés souhaitables telles que la transparence optique, la couleur et la brillance. Des mesures de nanorugosité ont été effectuées avec la microscopie à force atomique sur une surface recouverte ainsi vieillie. La rugosité de surface a augmenté 8-10 fois après le vieillissement. Des mesures de couleur et luminosité ont été effectuées périodiquement, chaque 100 h, au cours du vieillissement. Les tests ont été faits aussi pour un revêtement multicouche, soit un vernis sur un revêtement opaque sur bois. L'ajout de CNC non modifiée, donc hydrophile, dans les revêtements transparents n'a pas affecté la stabilité de la couleur des revêtements, mais en fait a augmenté la stabilité de leur couleur, tandis que l'effet des CNC modifiées (hydrophobes) est un peu moindre. L'ajout de CNC dans les revêtements non seulement augmente les propriétés mécaniques, mais augmente également la stabilité de la couleur du bois ainsi peint.

6.2. Abstract

An aqueous ultraviolet cured polyurethane acrylate transparent resin formulation was submitted to accelerated weathering during 1200 h, on wood substrate, with and without added Cellulose Nanocrystals (CNC) in coatings. In previous work addition of CNC improved several mechanical properties of the coating, without changing other desirable properties such as optical transparency, color and gloss. Measurements of nanoroughness were performed with atomic force microscopy on coated weathered surfaces. Surface roughness increased 8-10 times following weathering. Color and lightness measurements were done periodically, each 100 h, during the weathering. Testing was also done for a multilayer coating, varnish on an opaque coating on wood. Addition of un-modified, i.e. hydrophilic, CNC to transparent coatings did not downgrade the color stability of coatings, but actually increased their color stability, while the effect on hydrophobically modified CNC was somewhat less. Thus addition of CNC to coatings not only increases mechanical properties but also increases color stability of coated wood.

Keywords: Cellulose nanocrystals, CNC, UV- water-based coatings, wood, weathering, color stability

6.3. Introduction and literature review

6.3.1. Effect of UV / humidity on color of wood surfaces

Wood is known to change color rapidly, especially when stored outside. All organic polymers are sensitive to UV light, and a material made up of lignin and cellulose like wood is no exception. Since wood inside the living tree is not exposed to UV light, nature did not evolve any resistance mechanism to protect wood from UV. That is not the case for wood bark, which is quite resistant to light degradation. Cellulose and lignin have been shown to be rapidly, at the wood surface, attacked by UV light [121].

George et al. (2005) showed that the wood color change due to UV attack was due to lignin deterioration and, somewhat less, to cellulose hydrolysis [122]. During UV exposure, wood is bleached, lignin removed, and surface concentration of cellulose increases. Evans et al. (1996) showed that lignin degradation was noticeable, even after 400 h exposure, on wood surfaces as assessed by IR spectroscopy, when exposed to bright solar radiation, and reached 62% of deterioration after 30 days exposure [121]. The same authors also characterized holocellulose, a term referring to both highly crystalline cellulose and amorphous hemicellulose, degradation at the surface, as its mean molecular mass (cupriethylenediamine method [123]) was reduced by a factor of four after 29 days exposure. Tolvaj and Faix (1995) interpreted the color changes upon such degradation as due to appearance and transformation of oligomeric chromophores from lignin hydrolysis, especially during the first 50 h of exposition to UV, as well as formation of unconjugated carbonyl and carboxyl groups [124]. A good review was done by Teaca et al. (2013) on the subject [125].

Color changes upon exposure to UV radiation are usually discussed in terms of variations of the color coordinates in the model used, e.g. the CIELAB (or CIE L*a*b*) system. The CIELAB system presents color coordinates in the color space determined by three dimensions, i.e. L*, a*, b*. ΔL* is the variation of the lightness (dark to light), Δa*: (green (-) to red (+)), Δb* (blue (-) to yellow (+)) and ΔE* is the overall color difference. For instance in Teaca et al. (2013) [125], exposition of a softwood sample to artificial weathering with UV light for 140h gave a positive ΔE, lightened the wood tone with a positive ΔL*, increased redness with a positive Δa* and increased yellow tone with positive Δb*. These color changes were attributed to formation of quinones after lignin deterioration and depolymerization. Auclair observed very similar results: these results were obtained in dry conditions on Sugar Maple (*Acer saccharum*), with a UV curing waterborne urethane acrylate coating [9]. Very different results were obtained with addition of 'rain' cycles during artificial accelerated weathering: Δa* and Δb* rapidly went towards the green and the blue tones, respectively. This may be due to the water rinsing away the molecules arising from hydrolysis [9], exposing new surfaces and even, possibly, apparition of fungi. Also the same author showed that effects of natural outdoor weathering were similar to the latter.

As for the coatings as such without wood, Singh et al. (2010) showed that polyurethane coatings rapidly became yellow in sunlight, although chromatic values were not assessed [126]. Auclair did show that coating's color change over 400 h weathering was much less than that of wood [9].

6.3.2. Effect of UV / humidity on color of coated wood

For varnished, painted or otherwise coated wood, it is difficult to compare color results in the literature because of varying substrate (species), coatings, coating thickness, UV intensity and absence / presence of humidity / water with artificial ageing or weathering. Still, after ageing, Chang and Chou (1998) showed that in wood, with a transparent coating, color changes were mainly due to changes in wood rather than coating [127]. Irmouli et al. (2012), with different transparent coatings on different woods, found that additives in the coating did not increase much their performance and that changes in overall hue were at par with changes in brightness [128]. They showed that UV coating on wood have a very variable effect depending on whether the coating was acrylate or epoxy-based and substrate was different (oak and pine). All coated wood showed extensive color changes after 840 h UV accelerated weathering. Value of ΔE reached about 25 after 700 h artificial UV ageing on spruce with transparent epoxy acrylate film. Teaca et al. (2013) show similar changes in ΔE of wood modified with epoxydized soybean oil, at about 140 min wood irradiation time, with also a darkening of the surface at same time (negative ΔL*), and increase in Δa* (towards the red) and Δb* (towards the yellow) [125]. In opaque films, the films are much more robust and changes in color are much lower due to the pigment which back-scatters light, with no light reaching the wood substrate.

In general, transparent coatings do protect wood, for a while, but still there are color changes and these are due to wood surface degradation.

6.3.3. Effect of addition of nanoparticles in coatings

Since wood is sensitive to weathering, it is usually coated with varnishes, which are transparent or with paints or stains, which are opaque. Of course opaque coatings are better at protecting wood from UV light because the (usually TiO_2) pigments scatters or absorbs light. Varnishes are still popular since the appearance of wood is preserved. Evans et al. advocate the large scale use of nanotechnology for wood preservation [129]. The same reasoning can be applied to wood surface protection. Accordingly, some of the pigments can be nanosized. Advantages of these are usually a better performance with a lighter loading, with usually, adhesion and dispersion issues. In addition, in varnishes, the small size of the nanoparticles allows for their being invisible, but at low loadings, like 2-3% in weight. Previous results from our group on the effect of nanoparticles in coatings on wood showed that addition of such nanoparticles did increase performance as to wear resistance and resistance to weathering [42, 57, 70, 130]. In maple wood coated with waterborne urethane–acrylate coatings, addition of 2% nanosized ZnO in coating stabilized color over 400 h accelerated UV weathering. Otherwise with no additives, the coatings deteriorated with, at 400 h UV weathering time, values of ΔL^* of -6, Δa^* of +3 and Δb^* of about 10 [70].

Previous work of Poaty et al. (2014) has shown that addition of Cellulose Nanocrystals, CNC, to wood coatings at 1-2% w/w level clearly gave better mechanical results for the coating (varnish) especially as for resistance to wear. Results were better for CNC treated with cationic hydrophobic surfactants, like hexadecyltrimethylammonium bromide [108] (*Chapitre 3*). This last research was done to investigate if such a renewable–based product could compare with inorganic strengthening agents as an additive to coatings.

CNC is obtained, in this case [31], from a cellulose fiber suspension via an acid process. Following this process, the resulting CNC nanoparticles have properties such us: a specific surface area of $600 m^2$ / g, a Young's modulus of 150 GPa and a tensile strength of 10 GPa [35]. In water suspension (0.05% w/w), with the specific material used in this study, the characteristic dimensions of CNC are: 6-10 nm (diameter) and 100-130 nm (length) [108] (*Chapitre 3*). However, little is known about CNC behavior towards UV light degradation. Results of Evans et al. (1996) [121] show that wood is degraded by UV, mostly through

UV absorption by lignin, which suggest that CNC, which is extracted from wood, could also be degraded by UV in coatings.

In this work, color changes were assessed on varnished wood after 1200 h exposure to artificial UV light and rain, with coatings similar to those of Poaty et al. (2014) [108] (*Chapitre 3*). Coatings contained CNC, 1-2% w/w, some of which were treated to increase quality of dispersion.

6.4. Experimental section

6.4.1. Varnish formulation

CNC was from FPinnovations and Celluforce (Montréal, Québec, Canada). There were four grades used in this study, described in a precedent study [108] (*Chapitre 3*). One was the CNC as furnished by supplier. Second was the same CNC, treated with hexadecyltrimethylammonium bromide (HDTMA) in order to make it more hydrophobic and dispersible. A third grade was furnished by FPinnovations, which was hydrophobized by a proprietary process at FPInnovations. Finally, a fourth grade was treated with acryloyl chloride, to make it more hydrophobic and, possibly, to anchor it with acrylates moieties in the coating. Our previous study confirmed that these treatments did improve dispersion of the CNC in the coating. In the following text and figures, these four materials will be referred to as: CNC, CNC-HDTMA, CNC-FPI and CNC-Acryloyl, respectively.

Coating was a waterborne coating formulated as in Poaty et al. (2014) [108] (*Chapitre 3*). These UV-curable clear and opaque coatings were prepared from a water-based emulsified polyurethane acrylate resin, a defoaming agent, a surfactant, a dispersant, a thickener, CNC and a photoinitiator. Opaque formulations also include titanium dioxide (TiO_2) (*Table 6.1*).

The resin, the main component of the coating, selected is Bayhydrol UV 2282 (Bayer Material Science), a polyurethane acrylate (PUA) oligomer emulsified in water that was primarily developed for applications on wood. The photoinitiator used is a bis-acyl phosphine oxide (Irgacure 819DW, BASF Resins - Inks and OPV) dispersed in water (45

wt %). Titanium oxide (TiO_2) was used as a pigment. After trials, it was found that ~ 30% (dry weight) of TiO_2 gives an opacity of 80%.

Table 6.1. Summary of the different components used in the paint and varnish formulations

Component	Chemical structure	Commercial name
Resin	Polyurethane-acrylate	Bayhydrol UV 2282
Defoamer	Ether poly dimethylsiloxane	Foamex 822
Surfactant	Polyether siloxane copolymer	Byk 348
Dispersant	Solution of block copolymer of high molecular weight	Byk 190
Photoinitiator	Bis-acyl phosphine oxide	Irgacure 819DW
Thickener	Polyurethane	RM 2020
Solvent	Deionized water	_
Pigment	TiO_2	_
CNC	Cellulose	_

Then, in the basic formulations, CNC was added in concentrations of 0.5, 1, and 2% (w/w).

6.4.1.1. Coating formulations preparation; dispersion method

The choice of the dispersion method plays an important role in the final dispersion state of nanoparticles [42]. Several types of apparatus are commonly used in the industry, among those: high speed mixer, three-cylinder mill and ball mill. Although the last two methods lead to very high shear rates and high degree of dispersion, high-speed mixer (Dispermat, VMA-Getzmann GMBH D-51580 Reichshof) was preferred as it is the one of most commonly encountered in the industry. The mixer used can produce shear rates comparable to those of industrial mixers.

To achieve good TiO_2 dispersion, ultrasonication was used; after high speed mixing, the formulation was transferred to a 1 L Erlenmeyer flask and placed in a cooling bath containing ethylene glycol maintained at 5°C. An ultrasonic probe of 750 Watts (Ultrasonic processor, Cole Palmer) and a thermometer were immersed in the aqueous formulation. The ultrasonic frequency used for the dispersion was set to 20 kHz. The ultrasonic treatment was carried out for 2 min by setting the maximum temperature attainable in the formulation at 40°C [57].

6.4.2. Wood samples preparation

Waterborne coatings were prepared according to Vardanyan et al. (2014) and Poaty et al. (2014) [10, 108] (*Chapitre 3, 4*). Formulations were applied on black spruce (*Picea Mariana*) on tangential face. The dimensions of the wood samples were 130 × 60 × 9 mm. Coatings were applied by spraying [10, 38] (*Chapitre 2, 4*). After application (thickness: ~ 127 μm in liquid state), samples were put in a convection oven for 10 minutes at 60°C to gradually evaporate the water. During this step, the coating goes from a milky white liquid state to a transparent solid state. Film cure is then carried out using a UV oven (ATG 160305 from Ayotte Techno-Gaz, Inc.) equipped with a medium pressure mercury lamp (600 W/cm, model UV Mac 10, Nordson, OH, USA). This is a radical polymerization-type cure leading to 3D crosslinking. The intensity of incident light measured with a radiometer was in the order of 570 mJ/cm^2 and the perceived temperature during curing was between

25 and 30°C. After curing, surfaces of varnishes were lightly sanded with 150 grit size sandpaper in the direction of wood grain. These steps have to be repeated once again to get a dry coating ~ 100 μm of thickness.

6.4.3. Accelerated weathering

The accelerated weathering tests were performed in a Xenon arc Weather-O-meter Ci3000+ (Atlas Material Testing Technology, USA) according to ASTM G155 and ASTM D6695 (Xe-WOM CAM 7 cycles). The radiation source was a Xenon arc lamp of 4500 W equipped with borosilicate filters. The coatings applied on wooden panels were cyclically exposed to UV-A radiation (λ=340 nm) at 63ºC (temperature on black panel) and relative humidity of 50% for 102 minutes and water spray for 18 minutes at the same irradiation conditions. The irradiance intensity was 0.35 W m^{-2} nm^{-1}. The duration of the exposure test was 1200 h while the panels were automatically rotated around the xenon lamp. For the panels where surface roughness was measured, exposition time was also 1200 h. The panels exposed consisted of 2 samples of each formulation of the nanocomposites coatings including the control of acrylic solid-color stain on wood.

The color measurements were done according to ASTM D2244. Chromatic coordinates L*, a*, b* of the CIELAB color system were measured with a colorimeter (BYK-Gardner Color Guide 45/0) provided with a light source type D65. During the weathering test, 10 measurements of lightness (L*) and color (a* and b*) were made periodically on each sample every 100 h, five parallel and other five perpendicularly to the application direction of the coating.

Color changes are evaluated in terms of:

$$\Delta E = \sqrt{(L_2 - L_1)^2 + (a_2 - a_1)^2 + (b_2 - b_1)^2} \qquad (6.1)$$

where ΔE is the overall color change, as function of a*, b* and L* color components changes (Δa*, Δb* and ΔL*), as determined by CIE.

6.4.4. Atomic force microscopy

AFM observations were carried out using a NanoScope V (Veeco Instruments Inc., Santa Barbara, USA), fitted with a Hybrid XYZ scanner. AFM measurements were done under ambient air conditions in tapping mode. The sensitivity of the tip deviation and the scanner resolution was 0.3 nm. The resolution was set to 256 lines by 256 pixels for all observations. Surface roughness was calculated in 10×10 μm scan areas, using the classical mean surface roughness parameter R_a. The parameters were calculated by the Research Nanoscope 7.2 software:

$$R_a = \frac{1}{n}\sum_{i=1}^{n}\left|Z_i - Z_{ave}\right| \tag{6.2}$$

where R_a is the mean roughness, the arithmetic average of the absolute values of the surface height deviations, Z_i is the current Z value, Z_{ave} is the average of the Z values within the given area and n is the number of points within the given area : 65536 in our case. The experimental value for each type of coating was obtained from the average of 12 different measurements.

6.5. Results and discussion

6.5.1. Weathering of varnishes with added CNC: color and appearance

6.5.1.1. Color changes: ΔE

The overall change in color index, ΔE, of UV-cured varnishes is shown in Figure 6.1, with varying amounts to CNC added, on wood, over a period of 1200 h. This time of exposure is the same for all the color measurements which follows. Only one representative curve is given, fitted to a simple third order polynomial, and one series of error bars. Error and curves are very similar for all series of points, and not shown otherwise figures would be unreadable. This is also done on Figure 6.2-Figure 6.8. Horizontal axis time units are in

increments of 100 h. ΔE is a compound index of the color variation of the sample, as shown in Eq. 6.1, of color coordinates Δa*, Δb* and ΔL*.

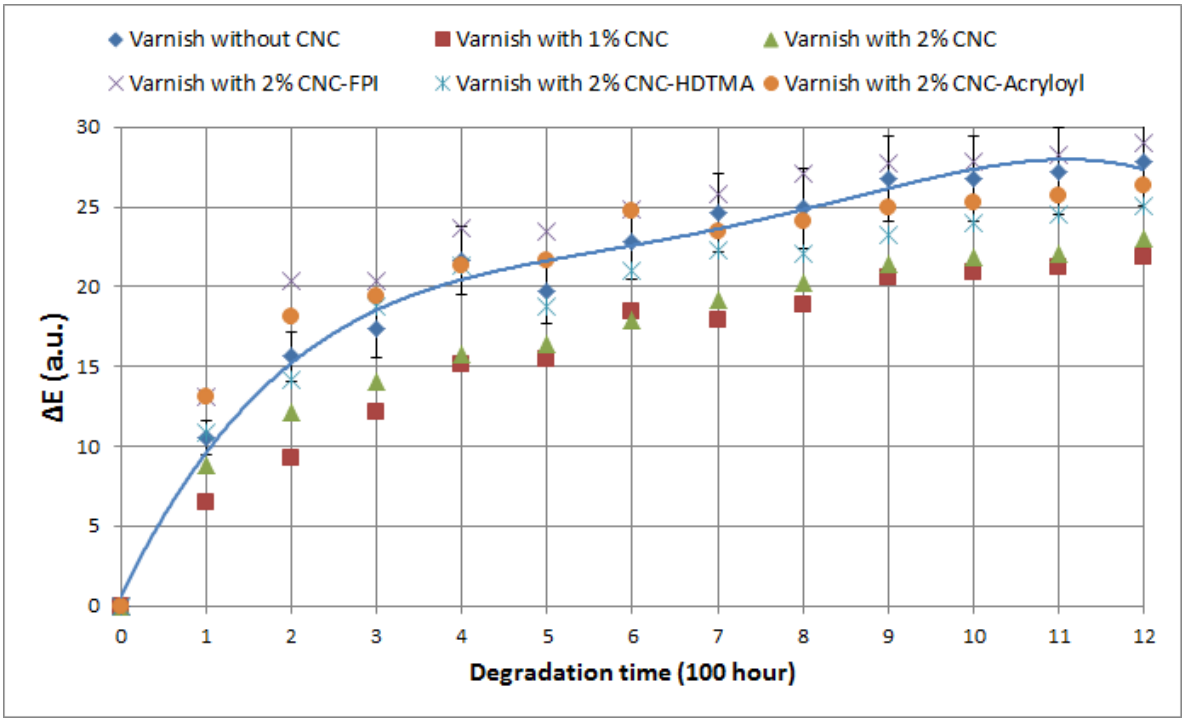

Figure 6.1. Change in overall color index, ΔE, of UV-cured varnishes on wood with varying amounts of CNC added.

In this case, the change is rapid in the first 200 h, and then much slower up to 1200 h in UV chamber, where ΔE reaches about 28. As shown in literature review, wood is known to be quite susceptible to color change following UV exposure. As discussed in introduction, most likely, the color change is due to wood color change, not that of the varnish. As cited in introduction, Irmouli et al. obtained a similar ΔE, about 25, after 700 h artificial UV ageing on spruce with a transparent epoxy acrylate film [128]. The wood coated with the varnish with 2% CNC-FPI changes the most; while the wood coated with varnish filled with 1-2% unmodified CNC performs the best, giving a 20% decrease in E, with other grades giving results in between these two extremes. The increase in performance, with addition of CNC, is modest but it is achieved with a low amount of CNC, 2% by weight in

the film. However, since the change is non-linear, alternatively, it could be said that the weathering variations of the best coating formulation at 1200 h is equivalent to that of the worst at only 300 h, which a fourfold difference. The surface modification performed on hydrophobic species of CNC increased its performance in the coating, due to better dispersion, in mechanical testing of coatings [108] (*Chapitre 3*). Whereas, in this case, for weathering, it is not so and this is in contrast with previous published results where most surface treatments on CNC increased its performance when used in coatings [108] (*Chapitre 3*). Addition of CNC increases color stability of coating, possibly due to scattering of UV light, but treating the CNC to make it more hydrophobic seems to decrease its UV resistance, or its ability to scatter light.

6.5.1.2. Color changes: Δa, Δb* and ΔL**

Going into the details of the specific components of ΔE, graphs of Δa* and Δb* (Figure 6.2Figure 6.3), as a function of time, shows a similar pattern: a rapid change of color in the first 200h followed by a gradual decline of the slope. The changes in Δa and Δb are respectively towards the red and the yellow, with the same intensity of changes. The color drift is about complete in about 200 h, except for Δa*, which still changes after 500 h. This could be due to a saturation effect, in the sense that most chromophores are created or degraded during the first 100 h, or that they make up a UV screen, slowing down further degradation. However, for ΔL*, there is no leveling off after 200 h and the coatings continues to darken even after 1200h (Figure 6.4). This is why there is also a continuous change in the overall color parameter, ΔE. In Figure 6.1, ΔE variation is highest for varnishes without CNC, or with commercial hydrophobic CNC, but lightest for varnish with 2% hydrophilic, unmodified CNC, with about the same pattern for the individual color components, Δa*, Δb* and ΔL*, (Figure 6.2Figure 6.4). Since the chemically modified CNC were modified with aliphatic cationic salts, it is unlikely they absorbed or diffused UV light. It was observed in other work that these unmodified CNC are not as well dispersed as modified ones [38, 108] (*Chapitre 2, 3*). It is possible that the degree of dispersion plays a role in these different results, because it changes surface roughness, and level of back-scattering [116].

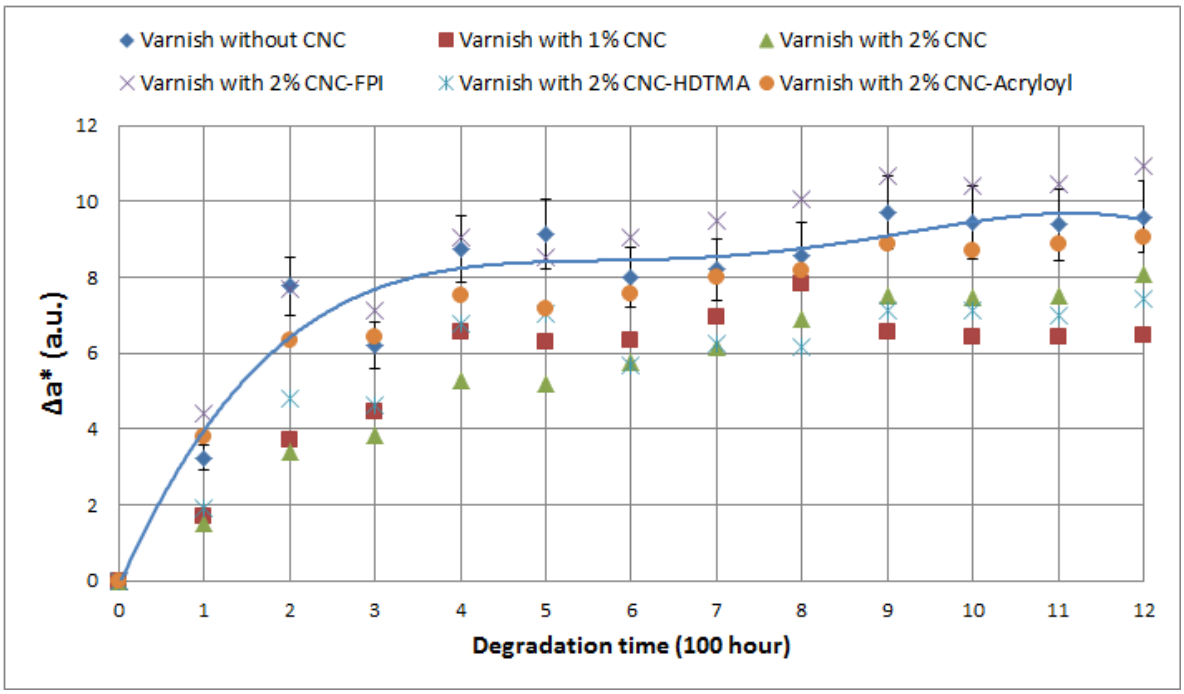

Figure 6.2. Change in a color coordinate index, Δa*, of UV-cured varnishes on wood with varying amounts of CNC added.

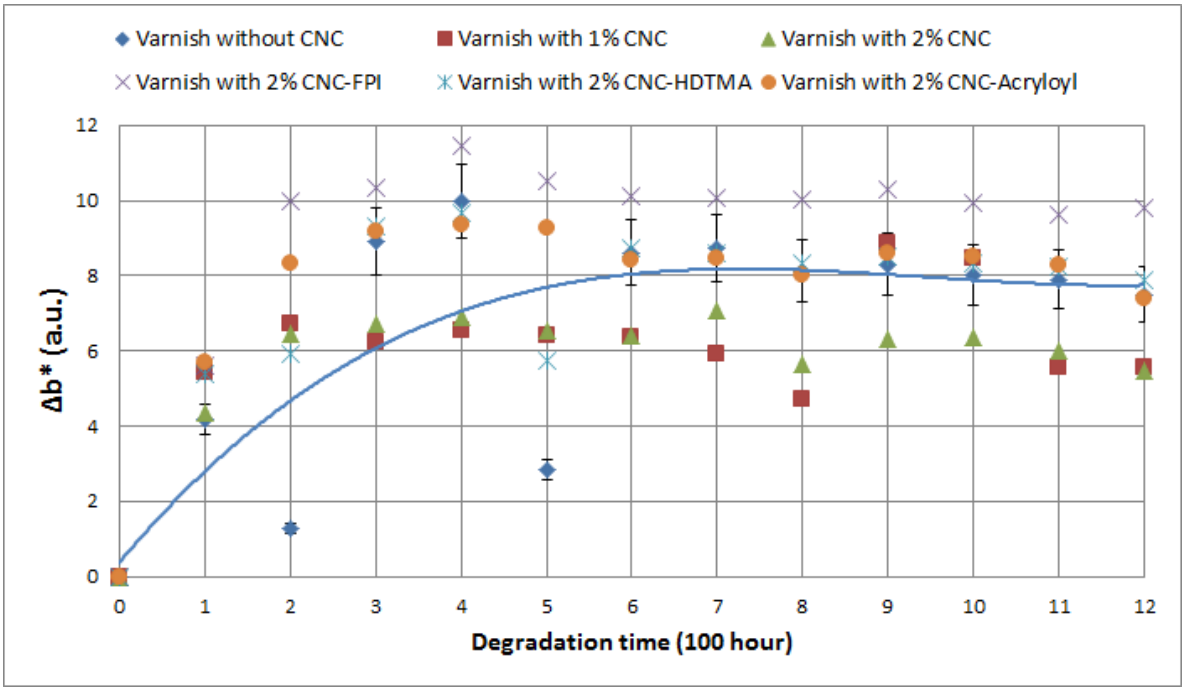

Figure 6.3. Change in a color coordinate index, Δb*, of UV-cured varnishes on wood with varying amounts of CNC added.

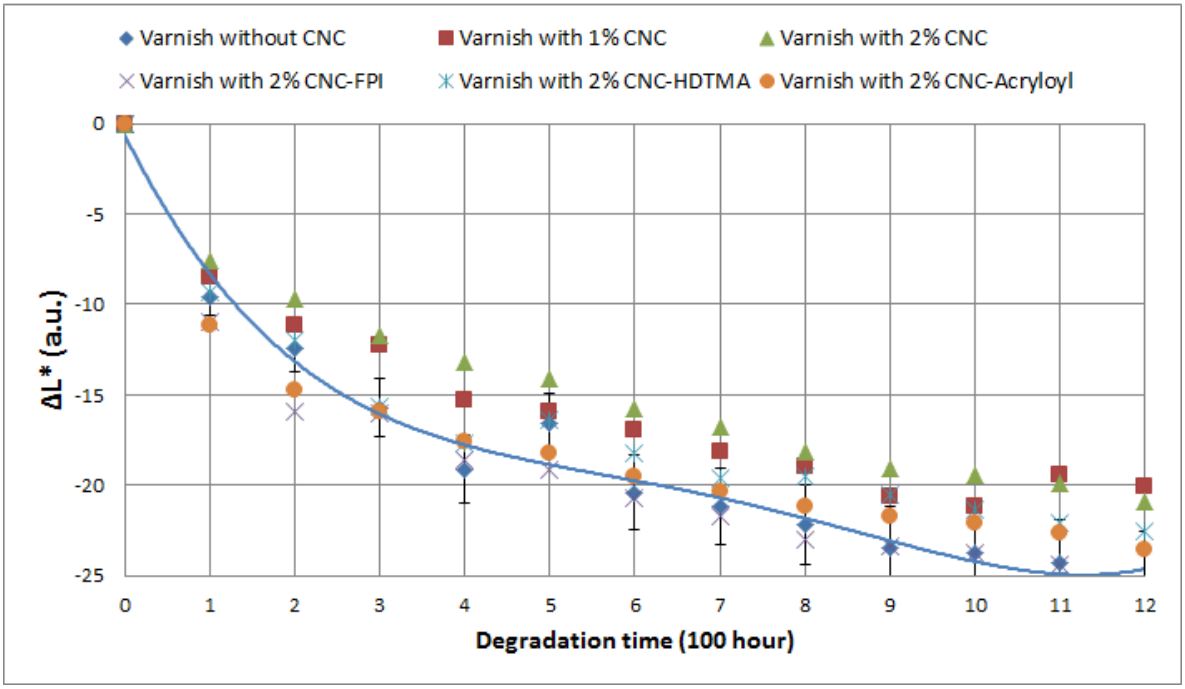

Figure 6.4. Change in a color coordinate index ΔL of UV-cured varnishes on wood with varying amounts of CNC added.

6.5.1.3. Comparison with other UV absorbers

In previous papers, efficiency of nanosized inorganic particles in coatings was evaluated [70]. Inorganic nanoparticles, as ZnO (2% w/w) and ZnO combined with some organic UV absorbers totally stabilized ΔL* and Δa* in wood waterborne urethane-acrylate coatings, after 400 h of UV weathering, a better performance than CNC additives. Our intent is not to protect wood with CNC, as is done with ZnO, but to evaluate whether it does not lower the weathering properties of the coating it strengthens.

6.5.2. Weathering of paints with added CNC: color and appearance

As mentioned in the literature review, the color changes upon weathering of paints on wood are much less than those for varnishes. Actually, there is no effect of wood in this case: the paint could be on any surface. In this case, the only nanoparticle added to the paint was neat

CNC, without treatment, since this gave best results in varnishes. In previous results [10] (*Chapitre 4*), CNC and modified CNC failed to increase mechanical properties of paints, since paints already contain a large amount of pigments and any addition of more of a non-resinous component, i.e. a filler, decreases the degree of polymerization and cure of main resin component, with a negative effect on mechanical properties. As for weathering, the same variables than for varnishes, ΔE, Δa*, Δb* and ΔL*, are shown in Figure 6.5-Figure 6.8, for painted wood surfaces, as a function of weathering time. The overall color change ΔE is shown in Figure 6.5, as a function of time. There is no effect of CNC on this variable. Thus the TiO_2 pigment, which is quite abundant in this paint (about 30% by weight), scatters UV, with little additional effects due to the presence of the CNC in the coating.

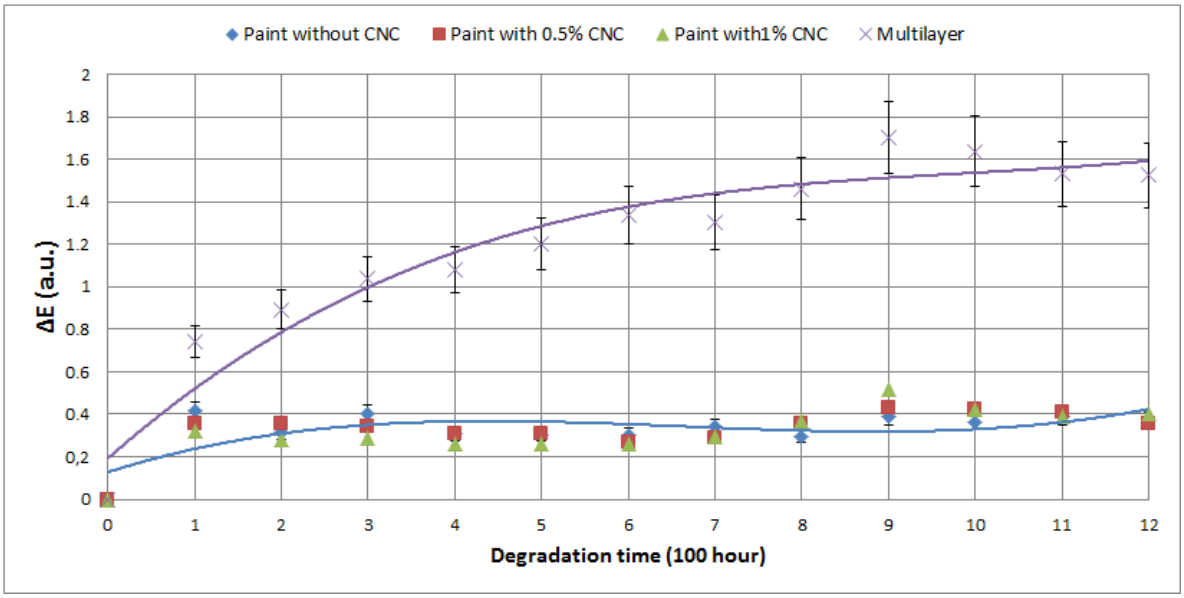

Figure 6.5. Change in a color coordinate index, ΔE, of UV-cured paints on wood with varying amounts of CNC added.

In addition, we did try to add a varnish coating on the paint (with no CNC in this top layer of varnish) to see whether we could reproduce some of the defects of the varnish in preceding section. This approach offers a way to evaluate weathering of varnish independently of wood beneath. What we observe is a small increase in ΔE, (Figure 6.5, multilayer curve) but the variation it much less than with transparent coating on wood.

Therefore, this is clear evidence that the color changes in weathered varnished wood surface is due to UV light going through the varnish and attacking the wood.

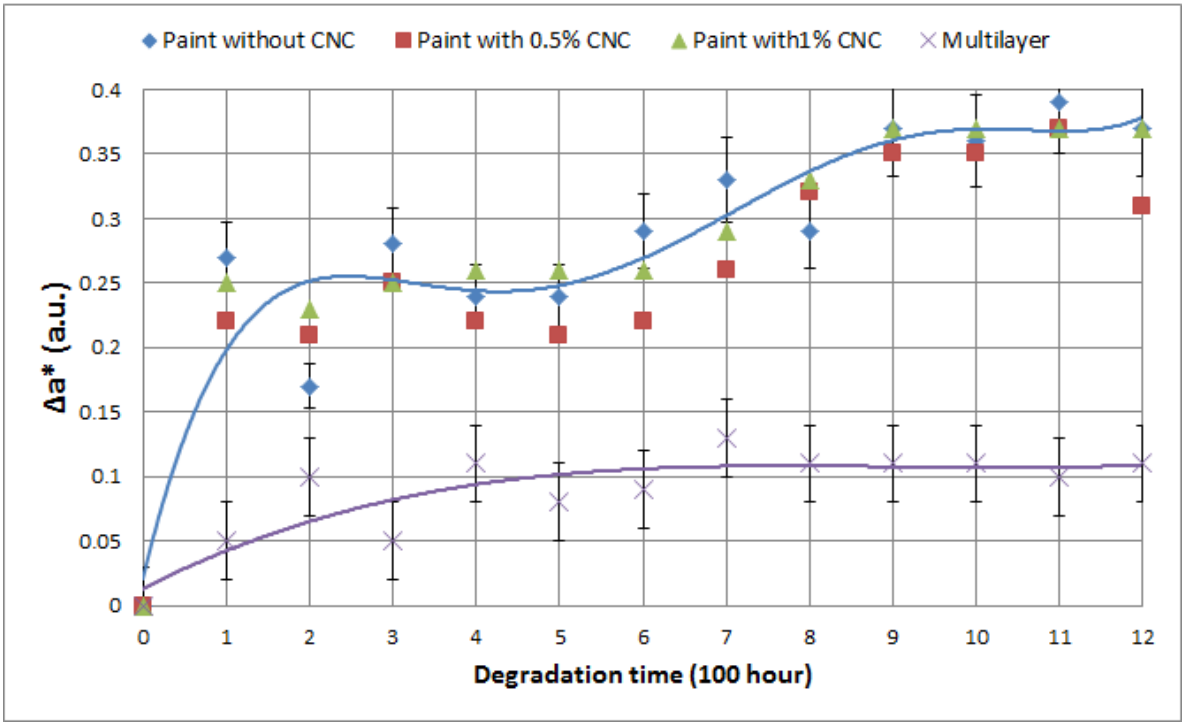

Figure 6.6. Change in a color coordinate index, Δa, of UV-cured paints on wood with varying amounts of CNC added.

To see to which color component this color drift is due to, we present Δa* and Δb* results in Figure 6.6 and Figure 6.7**.** For the paints, there is positive variation, as a small increase towards the red, of Δa*, while Δb* is stable, and so is ΔL* (Figure 6.8). Thus it is the slight drift in Δa* which mainly determines the value of ΔE: it is probably due to slight hydrolysis of the coating's resin at the surface. The variations are still very small compared to those of varnished wood, which is actually variations in color of the substrate, wood, not the coating.

For the multilayer coating, with varnish over the paint, results show there is a noticeable drift in color as to ΔE and mostly due to changes in Δb* (towards the yellow) and ΔL*. There is no change in Δa*. Thus this does not agree with the hypothesis of the preceding

paragraph about resin hydrolysis. The color trend between the opaque white coating and the transparent coating is different, one towards the red and the other, about three times stronger, towards the yellow. The white pigment does scatter UV while the transparent coating is not protected, although the color change is slight. It can also be noted that color change (ΔE) of such multilayer coating is slightly higher than just paint coating (Figure 6.5). This is so because of top varnish layer (ΔE=1.50) and its means that we can evaluate varnish degradation level, because the paint practically does not degrade. So this confirms again that the main part of color change in case of varnish coating (Figure 6.1) originates from wood.

Still, one wonders what happens at the immediate surface of the coating, where it does take a few nanometers for the UV light to be scattered. To inquire about this, some AFM surface measurements were done following the accelerated weathering.

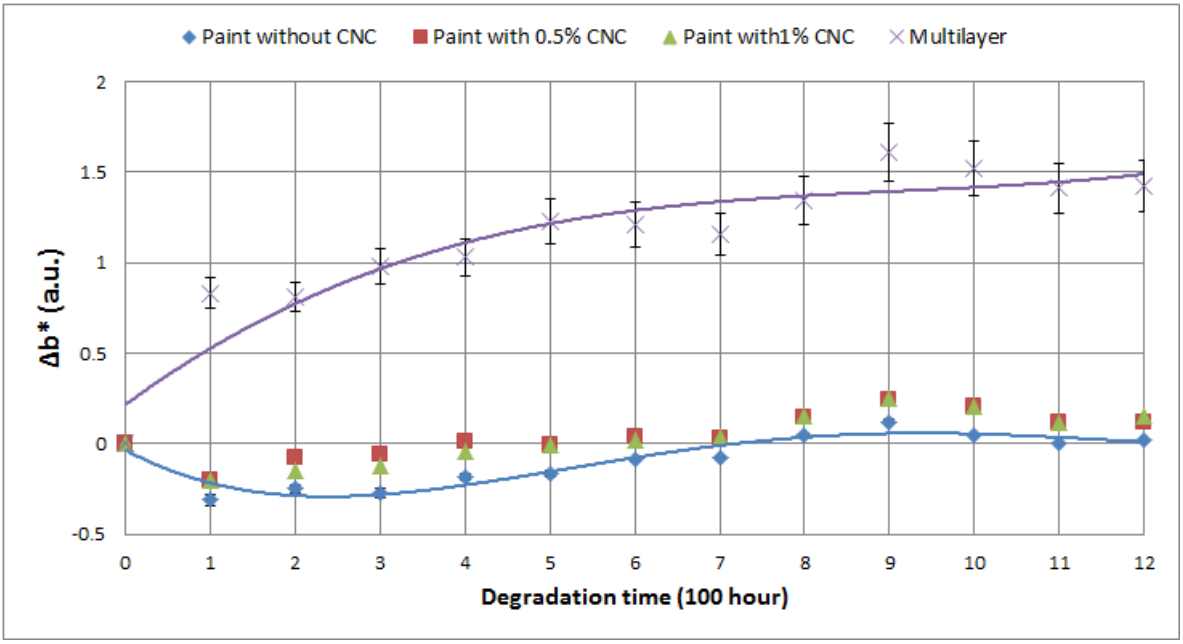

Figure 6.7. Change in a color coordinate index, Δb*, of UV-cured paints on wood with varying amounts of CNC added.

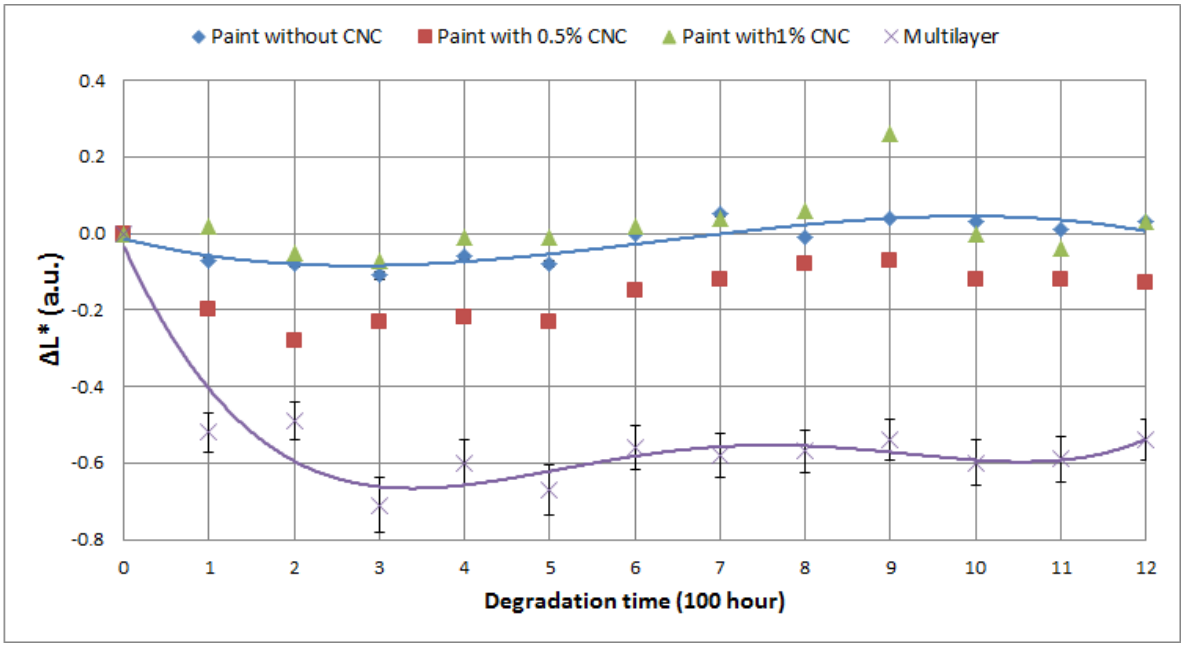

Figure 6.8. Change in a color coordinate index, ΔL*, of UV-cured paints on wood with varying amounts of CNC added.

6.5.3. Changes in roughness following weathering: AFM profiles

As the paint or varnish ages under the UV radiation, one would expect it to crack and become pitted: accordingly, these changes do occur and are reflected in the average surface roughness obtained from the AFM data.

For the wood samples with only varnish, Figure 6.9, the surface roughness nearly doubles with addition of CNC to coating formulation. It does decrease with addition of CNC's treated with cationic salts or acryloil chloride, not quite to the level of the coating without CNC. This roughness is very low, much too small to affect appearance of the film. Upon weathering, the surface roughness went from 5-10 nm to 40-50 nm with about no variation irrespective of the type of varnish (the standard deviation is rather large). This is in contrast with the color measurements, which vary with CNC additives, or mechanical properties which also vary with type of CNC added [10] (*Chapitre 4*).

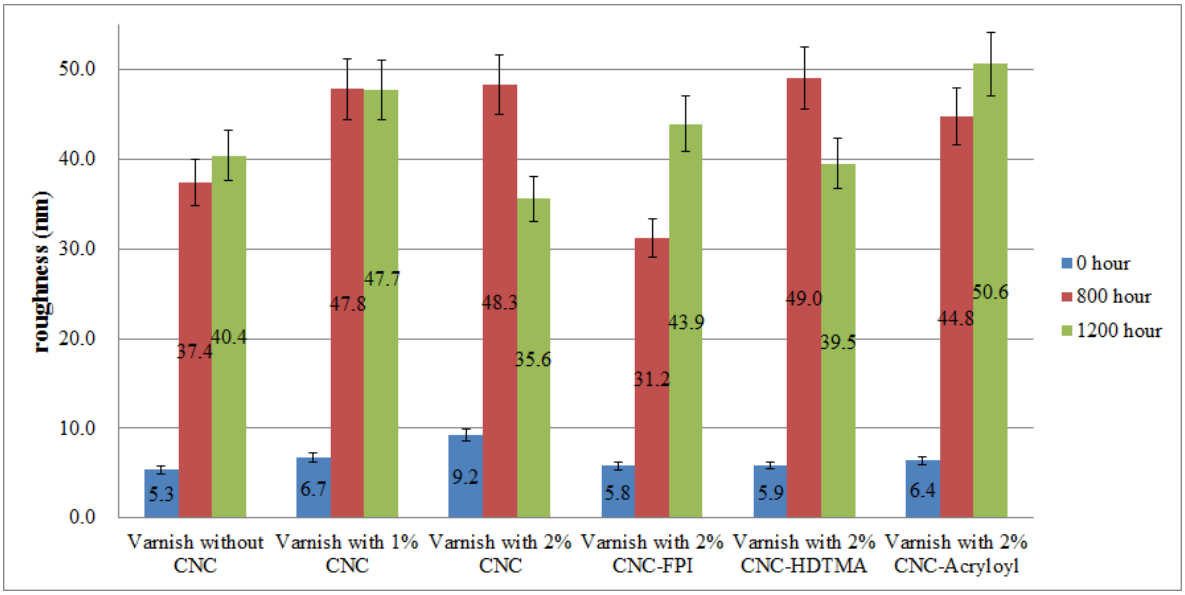

Figure 6.9. Change in roughness of UV-cured varnishes on wood with varying amounts of CNC added as a function of time.

For panels with paint, the initial roughness is higher and increases towards 100 nm after weathering, but there was also little difference (Figure 6.10) after 1200 h exposition to UV of all samples, with or without CNC, which had increased their surface roughness from about 8-18 nm to about 100-120 nm. The roughness is higher for these samples compared to the ones with varnish, since, in the paint, the TiO_2 pigment does increase the initial surface roughness [38] (*Chapitre 2*), and even more so after weathering. However for the painted samples with added varnish (Figure 6.10, multilayer curve), the increase was much less, and corresponded to those of the wood with only varnish. This also suggests that any reflection from the wood, or paint surface of the UV light does not affect further the coating since the transparent coating on the wood or paint was affected in the same way.

Figure 6.11 gives a general idea of the surface degradation of the samples after 1200 h accelerated weathering. Thus, the painted surface is quite affected by the UV in the first nanometers, and this is in contrast with the color measurements which show minimal effect in the bulk of the paint.

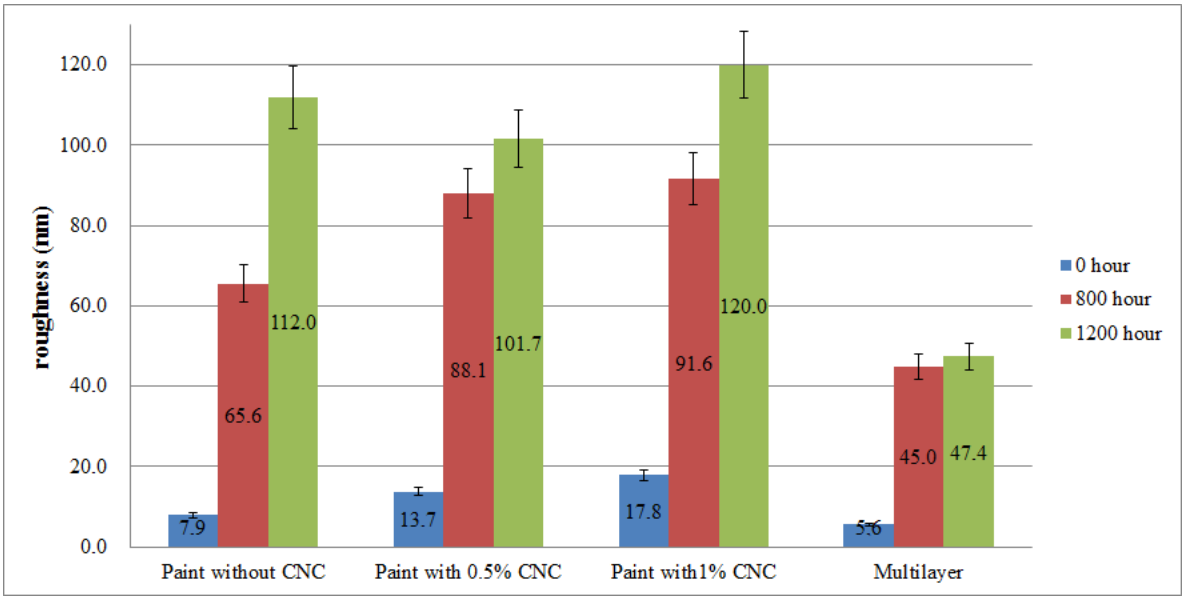

Figure 6.10. Change in roughness of UV-cured paints on wood with varying amounts of CNC added as a function of time.

This suggests that this attack from the UV radiation on the coating occurs in the top 100 nm of the surface, and the presence of TiO_2 does not protect the paint in the first 100 nm. This may be due to the fact the TiO_2 microparticles actually scatters most of UV, so light passes through the degraded layer twice, while for varnishes most of UV light does so only once, eventually reaching the wood.

Since sometimes it is difficult to note real changes of color by just looking at numbers like ΔE, Figure 6.12 has been added. It is the actual representation of the change in color of varnishes on wood. Here we can remark that varnish with 2% CNC (Figure 6.12a) is more stable during 1200h of UV degradation than varnish without CNC (Figure 6.12b). There is also a fluctuation in color, according to the structural regions of wood (earlywood and latewood). Although after 100 h of degradation color significantly changed in both cases, the changes were more abrupt in case of varnish without CNC. This data reflects previously seen results in Figure 6.1, where ΔE=10.50 for varnish without CNC and ΔE=8.86 for varnish with 2% CNC.

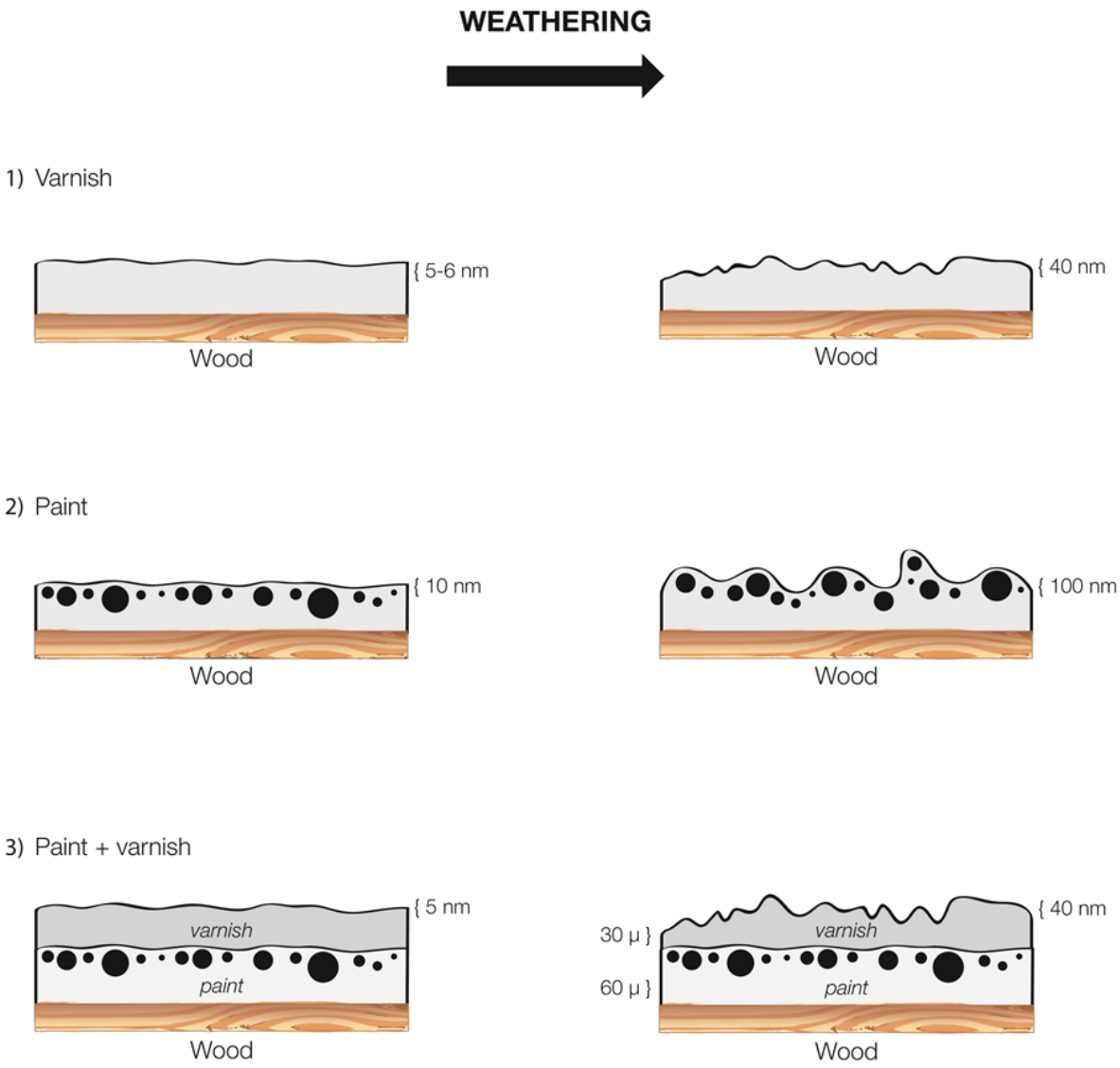

Figure 6.11. Schematic interpretation of effect of UV light weathering on surface texture, from AFM, on various varnished and painted wood surfaces (drawing not to scale as to particle size / roughness / thickness).

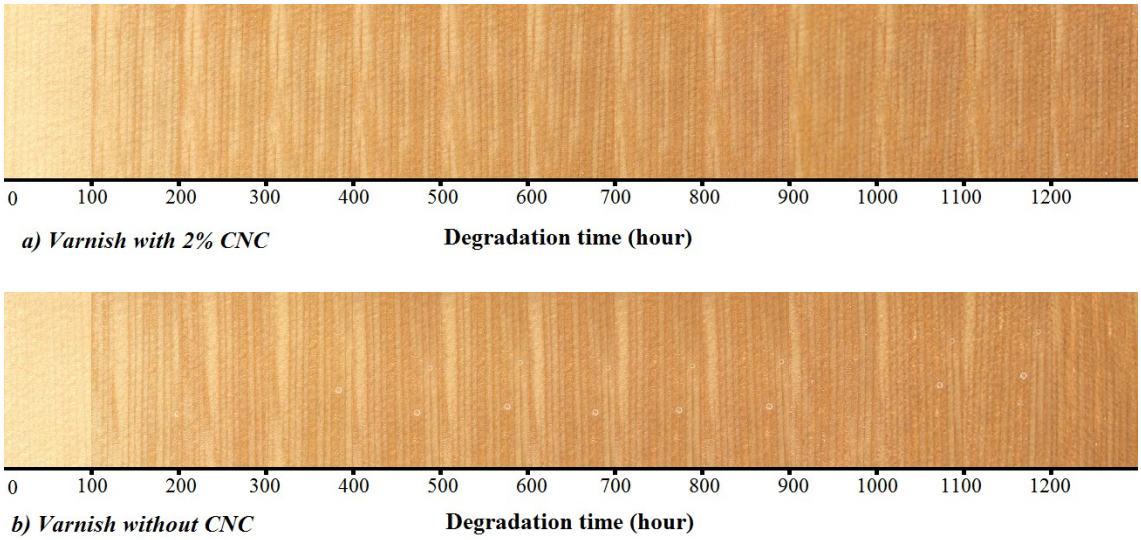

Figure 6.12. Visual representation of the change in color of varnishes: a) with 2% CNC and b) without CNC.

6.6. Conclusions

Addition of CNC, an organic product, to wood coatings does not lower color stability of the coatings, transparent or opaque, on wood, when those are exposed to UV light but actually increases the weathering performance of the varnished wood surface.

This added stability appears to be best for resistance to color drift towards the yellowing, in varnishes, but as to the other color components, the effect of CNC is still noticeable.

In paints, addition of CNC has no effect on the small color changes, with UV weathering. AFM measurements performed on the weathered surfaces show that the first 40-100 nm of the surface of both varnishes and paints are degraded by UV light.

Acknowledgements: Thanks to the Fonds de Recherche Nature et Technologie du Québec, the Conseil de Recherches en Sciences Naturelles et Génie du Canada and Arboranano for funding this research as well as FPInnovations' pilot plant and Dr. Gregory Chauve for the production of CNC.

Conclusions générale

Le secteur forestier a toujours été très majeur au Québec et généralement partout au Canada. L'industrie des lambris extérieurs et autres composantes en bois pour portes et fenêtres est très importante au Québec. Ces industries utilisent une quantité importante de revêtements. Les revêtements aqueux, bien qu'avantageux pour l'environnement et la santé des travailleurs et utilisateurs présentent encore plusieurs lacunes de performance. Le présent projet consiste à augmenter la performance de revêtements UV-aqueux pour le bois, en utilisant la ressource forestière. Les nanoparticules sont connues pour leur difficulté de dispersion, plus particulièrement dans les milieux aqueux. Puisqu'il est difficile d'intégrer les nanoparticules inorganiques dans une matrice polymère (organique), ce sera possiblement plus facile d'utiliser des nanoparticules organiques. Nous avons remplacé les nanoparticules étudiées précédemment par de la cellulose nanocristalline (CNC), un produit canadien et québécois, issu de la forêt.

L'originalité de cette thèse consiste en l'ajout de la CNC dans les revêtements pour améliorer leurs résistances mécaniques, qui n'a jamais été fait avant.

L'objectif principal du projet est la formulation des revêtements aqueux nanocomposites (renforcés par la CNC) opaques et transparent pour le bois à usage extérieur et intérieur, et étudier l'effet des nanoparticules essentiellement sur les propriétés d'usure des revêtements.

Les conclusions principales de cette étude sont :

1. Tout d'abord bien sûr c'est le développement des revêtements UV-aqueux pour le bois renforcés par la CNC, ce qui n'a jamais été fait avant. Les CNC ont été mélangées à la formulation de revêtements dans le but d'améliorer les propriétés mécaniques des revêtements secs. Les formulations de revêtements ont été pulvérisées sur des planches d'érable à sucre, qui ont été ensuite placées dans un four pour évaporer l'eau et cuire le revêtement par rayonnement UV. Une analyse élémentaire a été faite pour mesurer la quantité de pigment blanc de TiO_2 dans les agrégats de peinture.

2. L'un des aspects clés de la technologie des nanocomposites reste la dispersion de nanoparticules dans la matrice. Pour quantifier la dispersion, des méthodes efficaces de caractérisation sont nécessaires. Dans cette étude, une nouvelle méthode de caractérisation basée sur la microscopie à force atomique (AFM) et la rétrodiffusion de la lumière laser (He-Ne 632,8 nm) est appliquée pour caractériser ces revêtements nanocomposites. La distribution angulaire de l'intensité lumineuse rétrodiffusée a été représentée par une distribution de Gauss et son écart-type a été utilisé pour les analyses de la rugosité de surface. Une forte corrélation entre la nano-rugosité de surface du revêtement et la distribution angulaire (demi-largeur de l'étalement angulaire) de la lumière du laser rétrodiffusée a été constatée.
3. Les CNC ont été soumises à un greffage de chaînes de carbonés afin d'améliorer leur dispersion et leur capacité à transférer leur propriété de rigidité à des matrices moins polaires, en particulier les revêtements acryliques pour le bois. Ces modifications ont été réalisées en utilisant soit des bromures d'ammonium quaternaire alkylés ou du chlorure d'acryloyle. Ces nouvelles fonctionnalités chimiques, n'induisant pas de profonds changements structurels de la CNC modifiés, ont été mises en évidence par la résonance magnétique nucléaire, la spectroscopie infrarouge et l'analyse élémentaire en azote. Les dérivés de CNC se sont mieux dispersés dans le revêtement acrylique aqueux tel que suggéré par la microscopie à force atomique, avec une rugosité de surface moyenne réduite de 9 à 6 nm sur les revêtements contenant les CNC non modifiées et modifiées, respectivement.
4. Les propriétés mécaniques (résistances à l'abrasion et égratignure, la dureté et l'adhérence) ont été analysées et comparées à celles des vernis de référence sans nanoparticules. L'ajout de la CNC modifiée dans les revêtements UV-aqueux a entraîné une augmentation de 30-40% de la résistance à l'usure (abrasion et égratignure), sans perte de l'apparence. Lorsque le vernis a été appliqué sur une couche de peinture opaque, plutôt que sur du bois, le même renforcement a eu lieu.
5. Les formulations aqueuse d'acrylate polyuréthane translucide cuite sous rayonnement ultra-violet a été soumis à vieillissement accéléré pendant 1200 h, sur un substrat de bois, avec et sans CNC ajoutée dans les revêtements. Des mesures de nanorugosité ont été effectuées avec l'AFM sur une surface recouverte vieillies. La rugosité de surface a augmenté 8-10 fois après le vieillissement. Des mesures de couleur et luminosité ont été

effectuées périodiquement, chaque 100 h, au cours du vieillissement. L'ajout de CNC non modifiée, donc hydrophile, dans les revêtements transparents n'a pas affecté la stabilité de la couleur des revêtements, mais en fait il a augmenté la stabilité de leur couleur, tandis que l'effet des CNC modifiées (hydrophobes) est un peu moindre.

Donc, au final, on peut en toute confiance conclure que grâce à l'ajout de la CNC (seulement 2%), les revêtements UV-aqueux (opaque et transparent) peuvent protéger le bois contre l'abrasion, l'égratignure et dégradation aux UV.

Comme travaux futurs, nous recommandons deux axes principaux:

1. Axe théorique – simulations mathématiques pour caractériser la dispersion des nanoparticules de la CNC dans le volume des revêtements. Avec une analyse plus profonde, en utilisant les propriétés de polarisations de la lumière, cela peut être vérifié. Ainsi, on pourrait se demander si les nanoparticules sont orientées dans les revêtements?

2. Axe pratique – conception et préparation d'une appareil optique mobile pour mesurer la rétrodiffusion de la lumière, qui va indiquer la qualité des revêtements.

3. Aussi ça serait intéressent d'essayer de préparer des revêtements avec d'autres types de CNC, et faire des mesures similaires pour comparer les résultats.

4. Un autre aspect intéressant serait d'examiner et trouver les longueurs d'ondes UV qui dégradent les revêtements et le bois, et ensuite faire le test de dégradation aux UV avec les lasers, au lieu des lampes UV …

5. Les mesures AFM, mises en évidence dans ce travail, montrent que les surface de telles nanopeintures ont une surface nano-texturée. Au lieu d'essayer de minimiser cette texture comme nous l'avons fait, on pourrait, au contraire, essayer d'encourager l'agrégations des nanoparticcules pour créer une surface nanotexturée qui pourrait avoir des propriétés surperhydrophobes.

6. Il faudrait 'teindre' les CNC, ou greffer des atomes opaques aux rayons-X sur ces CNC, pour pouvoir confirmer les résultats d'AFM, au niveau de la masse des nanorevêtements.

Nous pensons que cette thèse, bien que comportant des chapitres sous forme de publications, donne une idée générale des revêtements nanocomposites pour le bois, leur formulation, les méthodes de tests, en alliant la chimie, la physique et les sciences du bois.

Annexe A. Nanocomposite coatings

A.1. Introduction

This chapter will review the techniques for synthesis and characterization of coatings containing nanoparticles for various substrates (i.e. nanocoatings and bio-based nanocoatings). The discussion will focus mainly on coatings developed for wood substrates, although coatings can also be applied to other types of substrates requiring functional surface properties. There are several terms to describe different types of coatings: stains, varnishes, paints, lacquers, and glazes. Here we will use the general term coating and adapt the specific terms to address specific situations. This chapter will introduce some aspects of the chemistry and physics of coatings reinforced with nanoparticles. There is a large variety of coatings for wood and one can categorize them as a function of their chemical, physical, and optical properties (Figure A.1Figure A.2). According to the formulation, these can be water-based or solvent-borne, high solid contents, UV-cured or even powders. Considering a particular application, they can be designed for exterior or interior use; they can also be transparent or opaque and can incorporate several combinations of these characteristics. The main objective of coatings incorporating nanoparticles reinforcement is better resistance to wear, UV degradation and water ingress, all of which must be done without affecting visual characteristics such as brilliance, color and transparency. The starting hypothesis is that nanoparticles, when combined with existing coating formulation, may display improved performance when compared to a similar coating containing microparticles.

Overall, the global coatings market is estimated at 30 million tons per year and is worth about 120 billion US dollars [131]. Any additive which makes an inroad into this huge market and very competitive environment is thus very welcome. Moreover, technology in this field is changing rapidly due to market and environmental pressures. In recent years there has been significant emphasis on the development of water-based and so-called ‘green’ formulations and coatings [131]. There is, especially in Europe, a massive shift

towards waterborne coatings, as they are perceived as environmentally friendly. This is even further encouraged by government regulations related to issues such as volatile organic compound (VOC) emissions [132].

In the field of thermoplastic composites, nanoparticle additives have been the subject of active research for many years, whereas this is a rather new avenue for coatings. Due to their relatively low thickness (around 30 microns), paints and coatings are not thought of as composites, even in the presence of filler microparticles such as pigments. Pigments may reinforce the coatings, but their main intended contributions are opacity and UV-absorption functions, properties for which they are designed in the first place.

Figure A.1. Parquet floor with Al_2O_3 UV-cured coatings resistant to wear and scratching.

Figure A.2. Building with UV-resistant coatings (Maibec Inc., Québec, Canada).

A.1.1. Wood surface characteristics

Wood is a porous, hydrophilic, and anisotropic material which is widely used because of its availability in a great variety of species and surface textures (grain), elegant appearance, and ease of processing. It is by far the most widely used biosourced material in the world. It is eco-friendly, is an efficient carbon sink and comes from a renewable resource. Most wood products, except those used for structural purposes, are coated during processing for protection against humidity and wear. Wood is especially sensitive to ultraviolet light (UV) degradation, as one of its main polymeric constituents is lignin, an unsaturated molecule which readily absorbs light in the UV range, resulting in its degradation. In its natural configuration, wood is shielded and protected from such degradation by the layer of bark surrounding the soft core of the tree. When used indoors, wood must also be protected against wear by a protective coating, especially when used in flooring applications. Coatings are usually more hydrophobic than the wood itself. Initial roughness of the substrate, even after careful sanding, is in the sub-millimeter (<mm) range, while the roughness of the coating once dried, is found in the nanometer (nm) range. The coating in a liquid state will therefore penetrate the porous structure of wood through wicking and will reticulate upon drying, thus imparting adhesion of the coating to the substrate. The

thickness of this boundary layer can be variable, while the dried coating is usually about 30–60 μm thick.

Most solid additives are surface-treated to enhance dispersion and avoid aggregation, and since coatings are usually hydrophobic, many additives are treated to present hydrophilic properties. The scientific literature on nanocomposite coatings is not very abundant, although a few interesting reports have recently been published. Bauer and Mehnert worked on UV-cured acrylate coatings incorporating nanosilicate reinforcement [110]. These coatings were shown to cure through very rapid radical polymerization initiated by UV light, and are nowadays widely used. In this study, the surface of the nanosilicate particles was treated with trialkoxysilanes to enhance adhesion in the continuous phase. With respect to neat coatings, increase in hardness, resistance to scratch and abrasion, as well as good optical properties were reported. Allen et al. reported on the addition of nanometric TiO_2 particles to acrylic coatings, resulting in increased UV-light stability over time [133]. Fufa et al. [134] and Weichelt et al. [135] used ZnO nanoparticles in an organic matrix to enhance weather resistance of various formulations.

A.1.2. Appearance of coatings

In Figure A.3, one can see the thickness of a coating relative to the total thickness of a wood surface. As previously mentioned, coatings are usually 30–60 μm thick, and some substrates may have as much as five to ten layers of coatings displaying various properties, usually starting with a stain or primer, followed by multiple paint layers and finished with a topcoat consisting of a tough lacquer or varnish. Several characterization assays can be done on the coating, regardless of the substrate of interest. The interpenetration zone can be found between the coating and the substrate, where the coating, while in the liquid state, diffuses in the substrate, and where the adhesion mechanism takes place. This interphase zone can be as thick as 30 μm for a wooden substrate. In Figure A.3, the particular structure of wood consisting of cells of about 30 μm in diameter can be seen, comprising an empty space called the lumen and the cell wall. When wood is cut and processed through a sanding step, some of these cells are damaged. The liquid coating can thus penetrate the

structure for a few μm, cure and better adhere to the surface. It is, however, improbable that it will penetrate the cell wall itself, which is made up of a dense array of cellulose and lignin molecules.

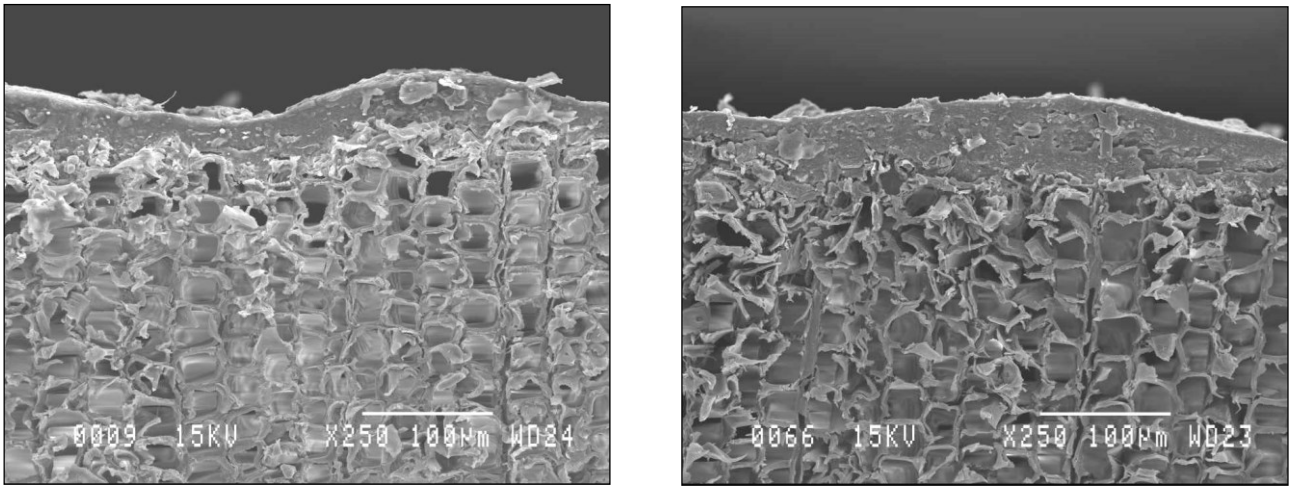

a) b)

Figure A.3. SEM micrographs (250× magnification) of (a) a pristine, and (b) an artificially aged coating (acrylic stain without nanoparticles) [8].

A.2. Coating formulations

A.2.1. Chemical components

Generally, the chemical mixture of an uncured paint or varnish is called a formulation. This formulation is comprised of multiple constituents, each contributing to the specific properties desired for the dried coating. In order to understand the chemical composition of a coating, a list of components for a typical UV-cured aqueous coating formulation (excluding water) follows [132, 136, 137]:

1. The binder is the main element of a paint formulation. It gives the coating its principal physicochemical characteristics. Once cured and dried, the binder forms a

continuous dry film which adheres to the substrate. It is often a mixture of reactive oligomers, having urethane or acrylic reactive sites.

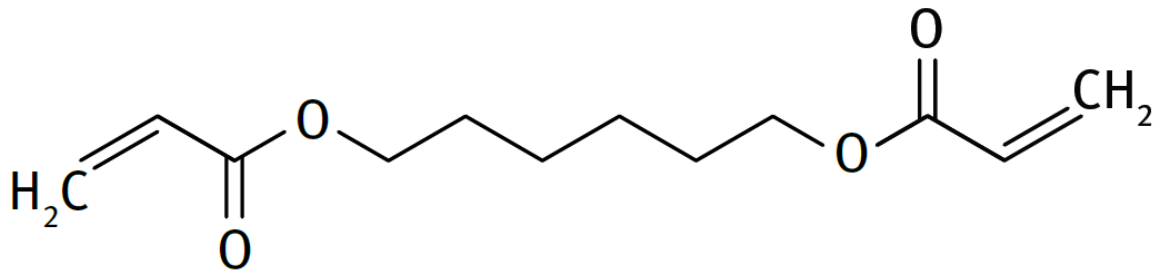

Figure A.4. Example of a reactive monomer in UV-cured coatings: 1,6-hexanediol diacrylate.

2. An antifoaming agent, usually a liquid with low surface tension, insoluble in the medium into which it is introduced and with a positive spreading coefficient.
3. A surfactant, lowering the surface tension of aqueous formulations and fostering better spreading of the formulation onto the substrate.
4. A dispersant, used to distribute the pigment evenly (for example TiO_2, Al_2O_3 and others) and nanoparticles (nanoclays, as aluminosilicates) simultaneously.
5. A photoinitiator, an essential element for a UV-curing formulation. This chemical, which initiates the radical polymerization reaction by absorbing ultraviolet incident light, can be a phosphine, a ketone or a benzophenone.

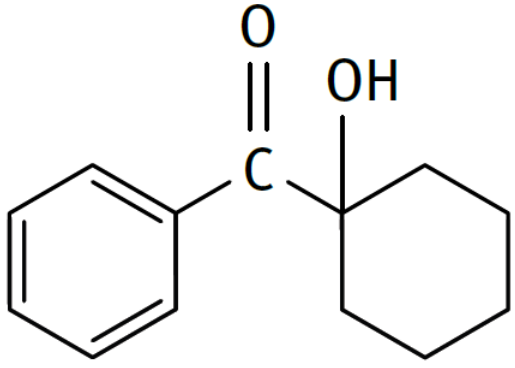

Figure A.5. Example of a photoinitiator: an α-hydroxyketone.

6. A rheological agent (thickener), introduced in order to adjust the viscosity of the aqueous UV-formulation.
7. A pigment (if the coating is opaque) such as titanium oxide (TiO_2), which is well known for white pigmentation. In the cured formulation called a film, it can reach a concentration of approximately 30% (dry weight), giving an opacity of 80% which is usually sufficient for complete opacity requirements. For outdoor applications, the role of the pigment, for example zinc oxide, is to absorb UV light, thereby protecting the substrate and paint against wear and degradation.
8. A film strengthening agent to which various nanoparticles can be added, such as alumina or cellulose nanocrystals (CNC), up to 10% in weight for a dry film. This amount is restricted for rheological reasons in order to avoid high viscosity due to nanoparticle content.

All of these components have to be added in a definite order and quantity, and usually require strong agitation. The formulation has to remain stable without phase separation over a reasonable period of time for obvious practical reasons.

A.2.2. Mixing techniques

For nanocomposite coatings, the final morphology is dependent on both the mixing technique and the equipment used. High levels of shear are required, while making sure the temperature of the formulation remains low and constant. The addition of nanoparticles, even at concentrations as low as 1% (in final cured coating), can increase viscosity noticeably [138].

Figure A.6 shows different qualities of nanoclay dispersions, achieved with four different types of mixers for the same formulation. It has been shown that a three-roll milling process, followed by bead milling, leads to the best dispersion of nanoclays [7, 42, 136]. This can be explained by the gap between the rollers which can be optimized, leading to high shear throughout the formulation. One should be aware that it might be difficult to find appropriate equipment for laboratory scale setup, since most mixers are designed for factory requirements. This hinders research by requiring industrial size formulations, as

well as problems cleaning the equipment while switching formulations. Component mixing is usually performed following a precise procedure, and the results obtained may vary depending on the type of mixer, which can be a conventional paddle agitator, a high speed mixer (similar to a household blender) or a roller mixer.

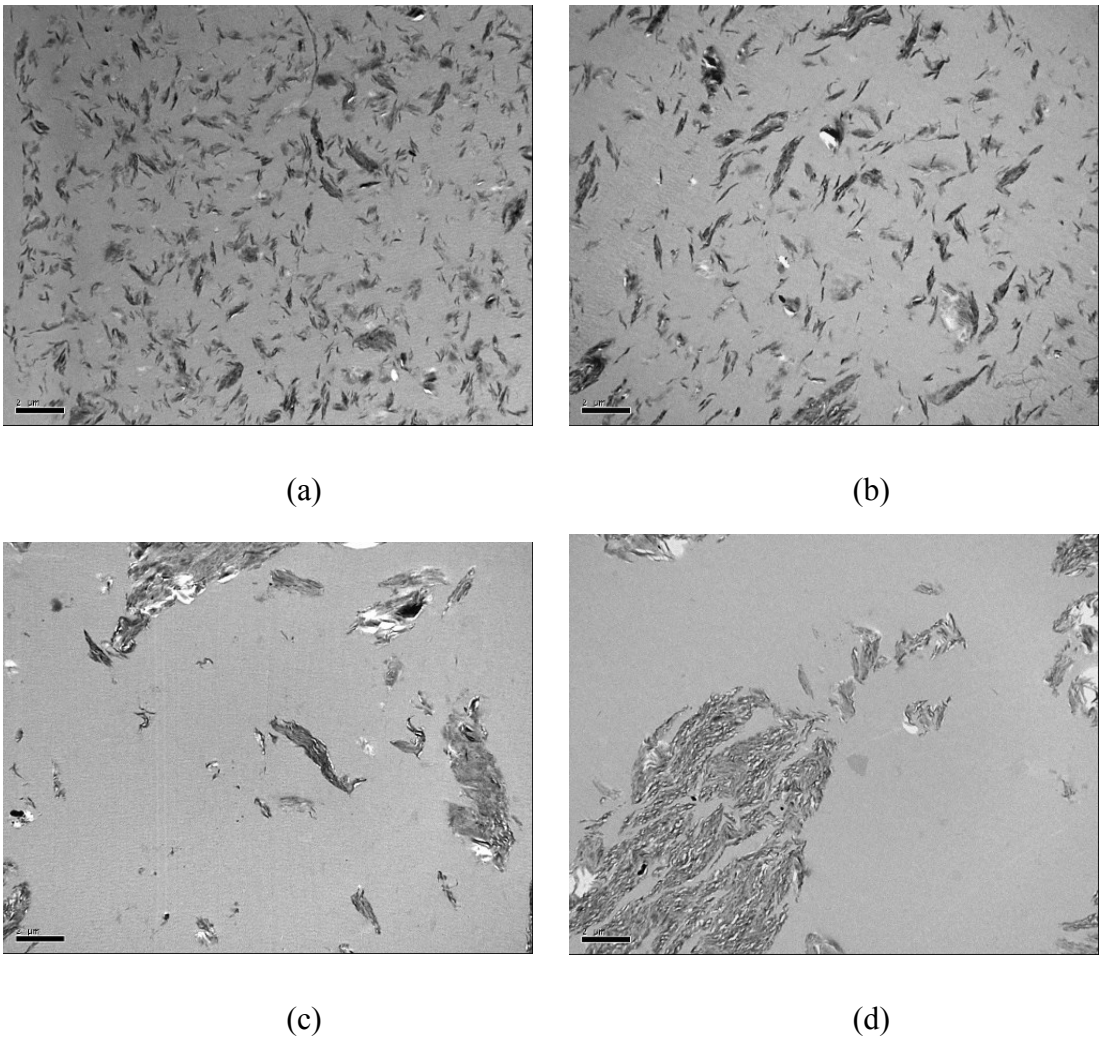

(a) (b)

(c) (d)

Figure A.6. Transmission electron microscopy images of the formulation prepared with 10 %wt of nanoclay by (a) three-roll milling, (b) bead milling, (c) ball milling, and (d) high-speed mixing (bar = 50 nm) [136].

While mixing, the role of the antifoaming agent is to prevent the formation of large bubbles, which otherwise could interfere with the film forming abilities of the coating.

Once the mixing process is over, the shelf life of the solution must be characterized to determine the time required for the insoluble components of the formulation to precipitate.

A.2.3. Application and curing

Another factor impacting on the final result of a coating is the application technique and equipment used. Results can vary widely for the same formulation, depending on the technique used for application. Coatings may be sprayed if their viscosity is compatible with spraying equipment. This technique is especially suitable for irregular or uneven, as well as large surfaces. Application with rollers or mechanical brushes is usually appropriate for even and small surfaces. For example, a coating can be applied, dried, and then polymerized with high intensity UV light to tailor the properties of the paint. As seen in Figure A.7, the samples are put on a conveyor belt and irradiated with UV light in a closed chamber. For thicker coatings, this process can be repeated several times.

Figure A.7. A semi-industrial UV-curing oven (AyotteTechno-gas, Québec, Canada).

A.3. Nanoparticle additives

Most paints contain microparticles, mostly to make them opaque, add color, or in the case of transparent finishes such as those ones for flooring applications, to increase wear resistance. Since these additives are ground prior to usage, a significant fraction of the semicroparticles is actually nanoparticles. These nanoparticles may be added to a formulation in powder form, which is often a source of problems since the aggregates are difficult to break up. A better way to incorporate these nanoparticles is to have a concentrated suspension or slurry of nanoparticles. Moreover, the nanoparticles can be surface-treated to prevent such aggregation and foster better dispersion and adhesion to continuous phase.

A.3.1. Nanoclays

Nanosize additives such as aluminosilicates, also known as nanoclays, can be exfoliated to generate a nanothin layer which reinforces the coating (Figure A.6). In order to achieve this functionality, the surface must be treated with cationic surfactants, which adhere to the anionic nanoclay surface to make it hydrophobic [42], and hence more dispersible. Examples of such surfactants are hexadecyltrimethylammonium bromide (HDTMAB) and tetramethylammonium chloride (TMAC). These compounds can be added to a concentrated aqueous suspension of nanoclay, and subsequently washed to remove unreacted hydrophobic cationic surfactant [139]. The use of these materials is more widespread than one might think: for instance cationically modified cellulose materials are widely used as conditioners in formulations such as shampoos and detergents.

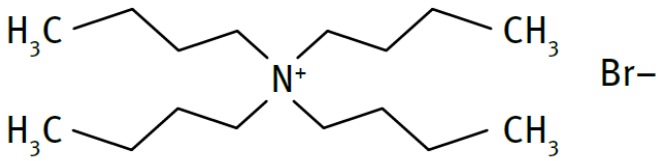

Figure A.8. Example of a cationic surfactant: a tetraalkyl ammonium bromide.

A.3.2. Inorganic oxides: titanium, aluminum and zinc oxides

Oxides are added to coating formulations to provide either resistance to UV degradation [8, 70] or mechanical resistance to abrasion in applications such as flooring [42, 138]. Oxides used in paints and coatings are: ZnO, TiO_2, SiO_2, and CeO_2, some of which can be modified chemically, for instance with 3-aminopropyltrimethoxysilane, to achieve better dispersion. Alternatively, dispersants such as polyacrylates may be added to the formulation to achieve similar results. It is also possible to use organic compounds which will act as UV absorbers, and ultrasound may also be used to encourage dispersion.

A.3.3. Organic compounds: nanocrystalline cellulose and carbon nanotubes

Cellulose, the most abundant organic polymer in the biosphere, is the main constituent of wood and is a homopolysaccharide composed of β-1-4 glucopyranose units [140, 141]. Each repeating unit of cellulose contains three hydroxyl (–OH) groups. These hydroxyl groups and their ability to form hydrogen bonds play a major role in directing the crystal packing and also governing the physical properties of cellulose. In cellulosic plant fiber, cellulose is present in an amorphous state, but also associates into crystalline domains through both intermolecular and intramolecular hydrogen bonding [142, 143]. The characteristics of cellulose, including good mechanical properties, low density, biodegradability, and availability from renewable resources, have become increasingly important in the context of sustainable development.

One of the promising new applications for cellulose is in nanotechnology as a reinforcing material. As cellulose has a natural nanostructure, different methods are used to benefit from this configuration, leading to various forms of nanocellulose (namely nanocrystalline cellulose or cellulose nanocrystals (CNC), or in some publications (NCC)) and microfibrillated cellulose (MFC). Cellulose fibrils consist of different hierarchical microstructures commonly known as nanosized microfibrils. These nanosized fibrils are comprised of a crystalline and an amorphous part, the crystalline region being named nanocrystalline cellulose (CNC) or nanowhisker. In comparison with MFC, CNC has received more attention and been the focus of more intensive research.

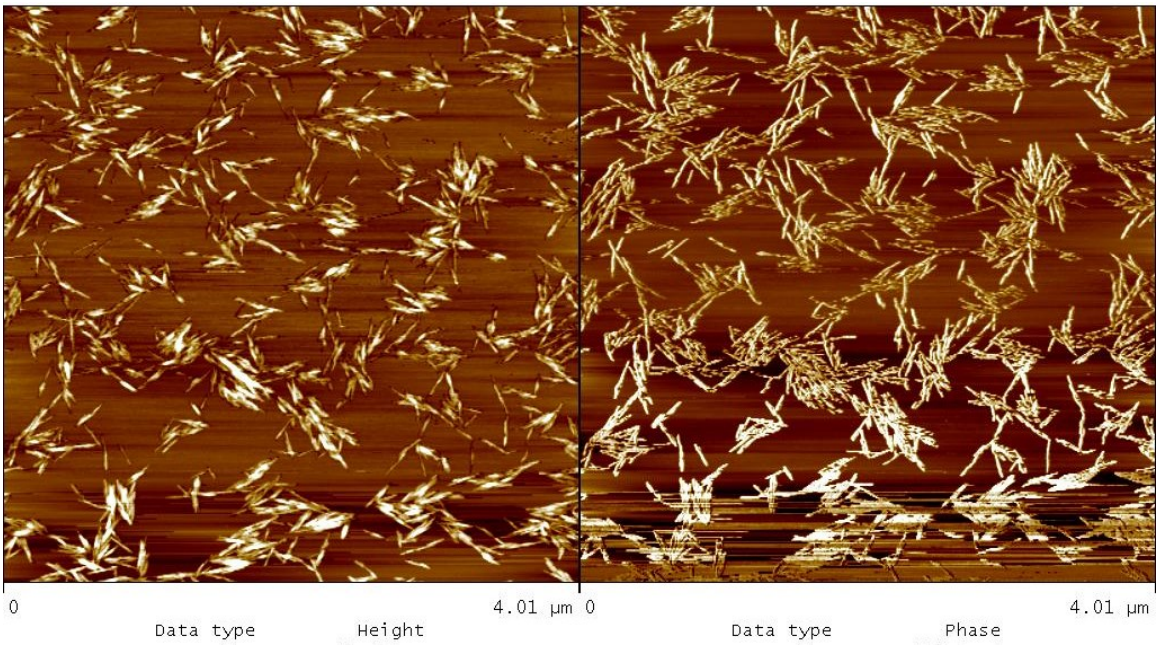

Figure A.9. Height and phase AFM images of unmodified CNCs.

CNC is obtained by the acid hydrolysis of cellulose under conditions where the amorphous regions are selectively hydrolyzed (Figure A.9). For wood-based CNC, the remaining crystalline regions are 3–10 nm in diameter, 100–300 nm long and retain the natural cellulose I crystalline structure [78, 144]. Among its interesting characteristics, CNC is abundant and renewable. It also exhibits low density in comparison to mineral fillers (around 1.566 g/cm^3), as well as a high form factor (about 70), a high specific area of 150 m^2/g, a length of 50–500 nm and width of about 3–5 nm [72, 78, 144]. Although neither as resistant to UV, nor as hard as the aforementioned metal oxides, these nanoparticles have several advantages. Displaying a tensile strength of about 8 GPa and an elastic modulus in the transverse direction of about 110 GPa, there is an interest in incorporating CNC into various polymer matrices to produce nanocomposites [73]. CNC has been shown to lead to remarkable reinforcing properties in polymer matrices such as styrene-acrylate latex [65], starch [145], polyhydroxybutyrate octanoate [146], and poly(ethylene oxide) [147]. In most cases, the reinforcing effect comes from the percolating network of CNC, together with good interfacial compatibility between matrix and filler.

Cellulose fibers can be classified as hydrophilic because of their high hydroxyl content (3 per anhydroglucose unit (AGU)). Therefore, when used as reinforcing fibers in non-polar polymer matrices, the durability and mechanical performance of the resulting composites are limited by poor fiber-matrix adhesion. Many studies currently focus on the improvement of CNC dispersibility and compatibility in different solvents or matrices, which is essential to the production of nanocomposites. However, most nanoparticles are difficult to disperse and modify at the surface of a solvent due to their high specific surface.

The experiences of various groups in dispersing CNC in water based adhesives and coatings have shown that the hydrophilic nature of CNC can cause problems, especially when working with a polar matrix. The poor dispersibility of CNC when incorporated in large amounts results in a high degree of agglomeration, leading to the deterioration of the mechanical properties of adhesives and coatings. Besides the problem of incompatibility with polymer matrices, most conventional nanocelluloses are characterized by hydrogen bonding-induced aggregation of their nanosized rod-like and fibrillar structures. These strong hydrogen bonds prevent cellulose from melting, dissolving, and being easily processed.

To provide CNC with ease of processability and extend its applications in nanocomposite coatings, its surface properties could be modified to inhibit self-aggregation and improve dispersion, as well as interfacial adhesion in various coatings. Concurrently, the intrinsic structure of the nanocrystals (i.e. the original crystalline structure) should not be destroyed during CNC modification. There is a growing research focus on the modification of CNC because of its increasing potential applications in various technologies.

Chemical functionalization of CNC has been mainly conducted to (1) introduce stable negative or positive electrostatic charges on the surface to obtain better dispersion (CNC obtained after sulfuric acid hydrolysis has labile sulfate moieties which are readily removed under mild alkaline conditions), and to (2) tune its surface energy characteristics to improve compatibility, especially when used in conjunction with nonpolar or hydrophobic matrices in nanocomposites. The main challenge for the chemical functionalization of CNC is to conduct the process in such a way that it only changes the surface, while preserving the

original morphology to avoid any polymorphic conversion and to maintain the integrity of the crystal.

A quick review of the literature demonstrates that the surface of CNC can be modified by different methods. For example, the modification of CNC by hexadecyltrimethylammonium (HDTMA), a quaternary ammonium hydrophobic cation, leads to the addition of $–CH_2$, N–C and $–CH_3$ groups to the surface (Figure A.10). This is a similar process to the one used to intercalate and exfoliate nanoclays (as mentioned in this section, 450), since this material has hydrophilic and anionic surface characteristics. A study of the morphology of modified and unmodified CNC, performed using atomic force microscopy (AFM), showed interesting results. As seen previously in Figure A.9, the individual crystals can be seen in unmodified CNC.

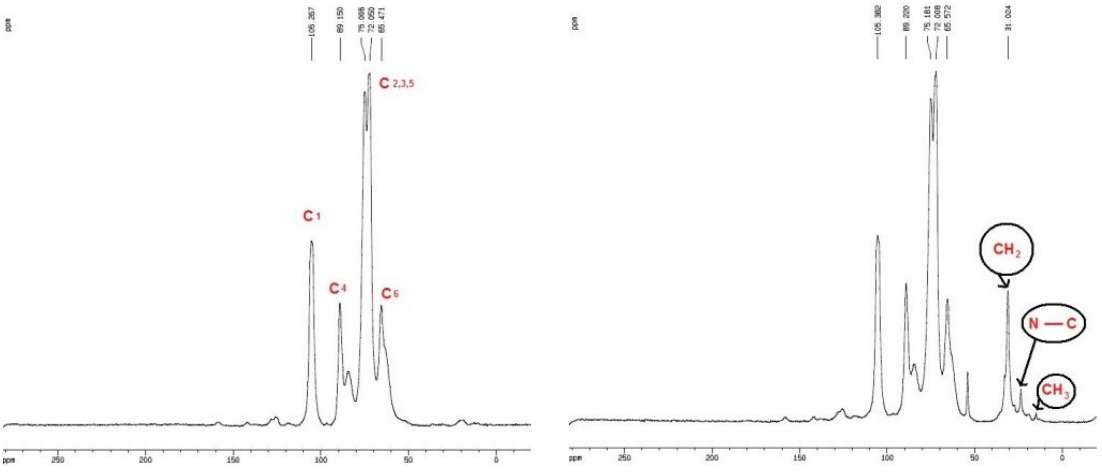

Figure A.10. Solid-state NMR spectra of (a) unmodified CNC, and (b) CNC modified by hexadecyltrimethylammonium (HDTMA) [108] (*Chapitre 3*).

On the other hand, AFM images taken from re-dispersed, modified and dry-frozen CNC in water showed highly aggregated CNCs, making it difficult to differentiate individual CNC crystals (Figure A.11). This high level of aggregation is thought to be caused by the lack of surface charges and hydrogen bonds leading to strong interactions between CNC particles.

Precise dimensional measurements of CNC revealed that the modification did not change the size of CNC particles (Figure A.12).

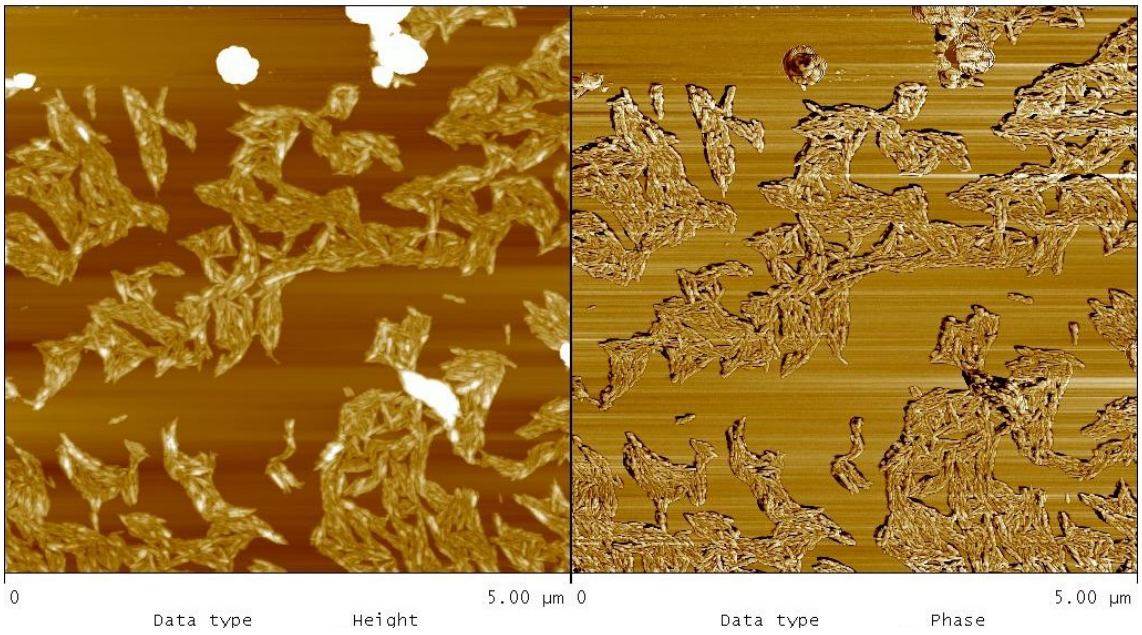

Figure A.11. Height and phase AFM images of CNCs modified by hexadecyltrimethylammonium (HDTMA).

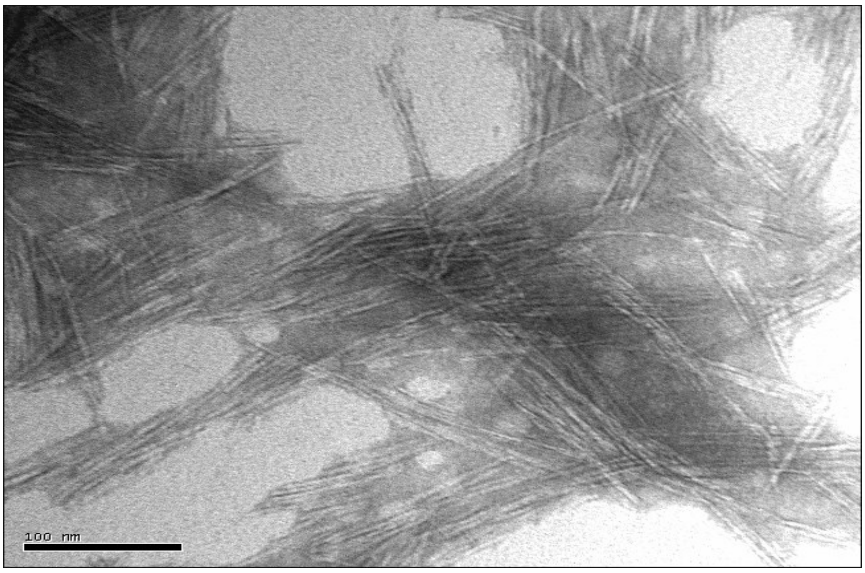

Figure A.12. Transmission electron microscope micrograph of CNC.

A.4. Coating characterization

A.4.1. Mechanical properties

A great number of methods can be used to characterize coatings, and the use of a particular method is usually related to an application of interest. For example, coatings designed for outdoor use require resistance to hostile weather conditions, water, humidity, UV light, and fungi, which must be characterized and quantified. This can be done either in situ in natural outdoor settings, or in special accelerated weathering chambers equipped with intense UV light and humidity control. For products intended for indoor use, such as parquet floors, resistance to wear, scratching and hardness must be measured. There are a large number of standard ASTM tests to assess these parameters. The hardness of a coating film can be measured by monitoring the damping time of a pendulum oscillation according to ASTM D4366 "Standard Test Methods for Hardness of Organic Coatings by Pendulum Damping Tests". As an example, the following measurements of abrasion resistance can be combined with gloss measurements: as the surface is abraded with a metal wool pad, the coating becomes matt and loses its gloss. Addition of nano- and micro- alumina and silica in different forms has the potential to increase gloss retention dramatically (Figure A.13).

Abrasion resistance can be determined with a Taber Rotary Platform Abraser™, in which mass loss can be measured after a specific number of rotations of abrasive paper maintained with constant pressure on the coated surface, following the ASTM D4060 standard. The adhesion of a coating can be measured according to the ASTM D4541 standard, where an aluminum stub is glued to the coating surface and is pulled off using a standard protocol. If the coating is entirely pulled off with substrate fibers from the surface clinging to it following the test, the coating has fulfilled the cohesive failure criterion. If no fibers are left on the surface and the stub remains smooth, then the coating fails the adhesion criterion, resulting in adhesive failure. All these tests for coatings can be performed after exposition to accelerated weathering following a 400–2000 h exposure to strong UV light, combined in some cases with humidity and/or rain. Accelerated weathering tests can be done in a special chamber where the samples are irradiated with UV-A light, (λ = 340 nm) with

irradiance intensity in the order of 0.35 $Wm^{-2}nm^{-1}$, according to ASTM G155 and ASTM D6695 standards.

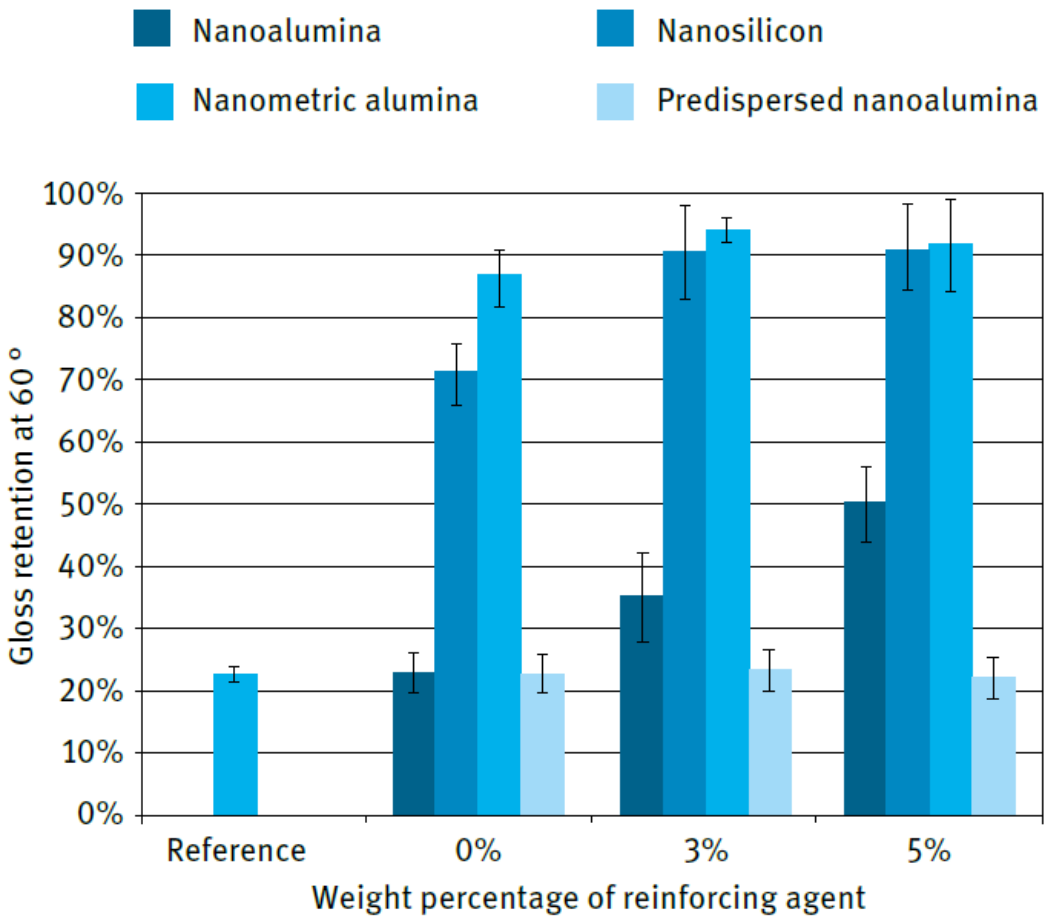

Figure A.13. Gloss retention of coatings with added micro- and nanoparticles, after abrasion with steel wool (modified from [6]).

In several cases following this treatment it was found that the T_g of the coatings actually increased and their mechanical resistance diminished as the coatings became brittle due to weathering.

A.4.2. Optical properties

Optical properties such as color, gloss and haze can be measured according to ASTM standards D523 and E430, with an instrument that simultaneously determines the gloss at three different angles (20°, 60°, and 85°), as well as the haze.

Color

To quantify the color of a coating, the CIE L*a*b* system is used in order to provide standard values recognized worldwide. Using this method, a color is defined by a point located in a 3D plot (Figure A.14), where the luminance (L*), varies from 0 (black) to 100 (white), and where a* and b* refer to the two series of complementary colors, respectively red–green and blue–yellow (Figure A.14).

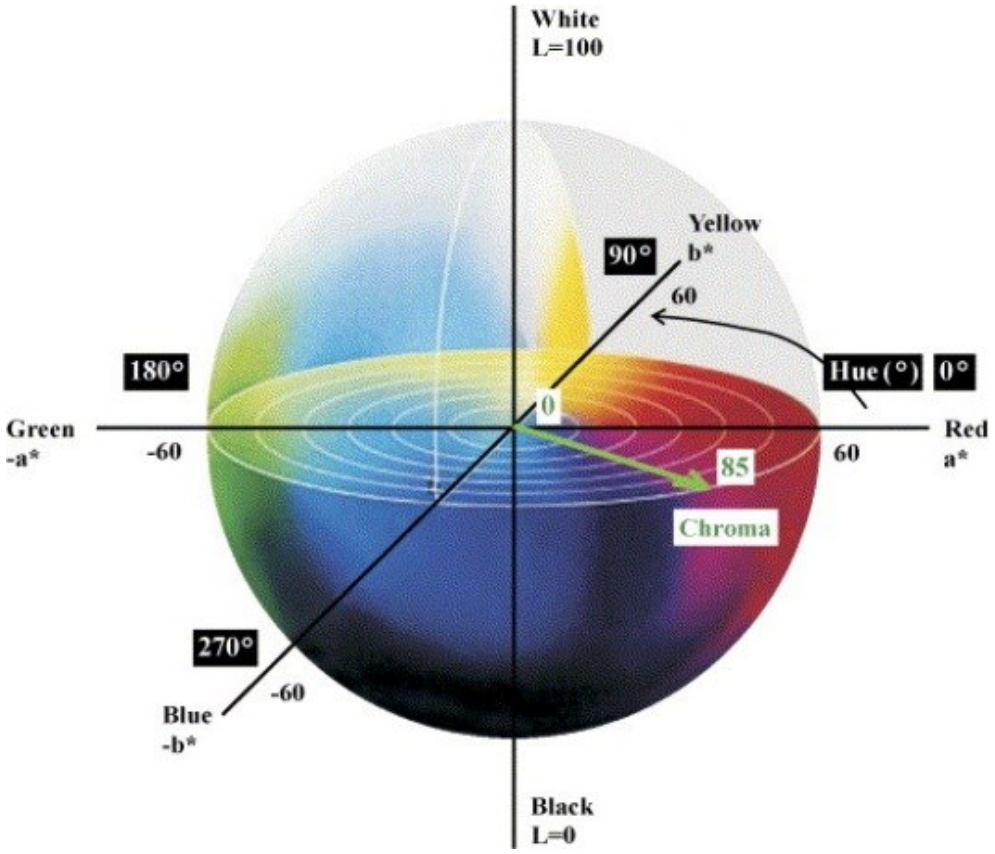

Figure A.14. The CIE L*a*b* color space (BYK-Gardner).

With these three coordinates, any color can be reproduced in the CIE L*a*b* referential. The measurement is usually done with a handheld meter according to ASTM E1347 and D2244 (Figure A.15).

Figure A.15. Colorimeter (BYK-Gardner).

If one is looking for color uniformity or changes, any point within these coordinates can be combined in an overall color index as:

$$\Delta E = \sqrt{(L_2 - L_1)^2 + (a_2 - a_1)^2 + (b_2 - b_1)^2} \qquad \text{(A.1)}$$

where the ΔE values correspond to the absolute difference in the color and brightness parameters. One should note that a ΔE of 5 or lower cannot be detected by the human eye.

For instance, Figure A.16 shows an overall color change, ΔE, following accelerated UV aging on a coating. There is a strong initial change in color followed by a slow drift of the values measured, while the presence of nano-TiO_2 increases color stability. A typical accelerated aging apparatus is shown in Figure A.17.

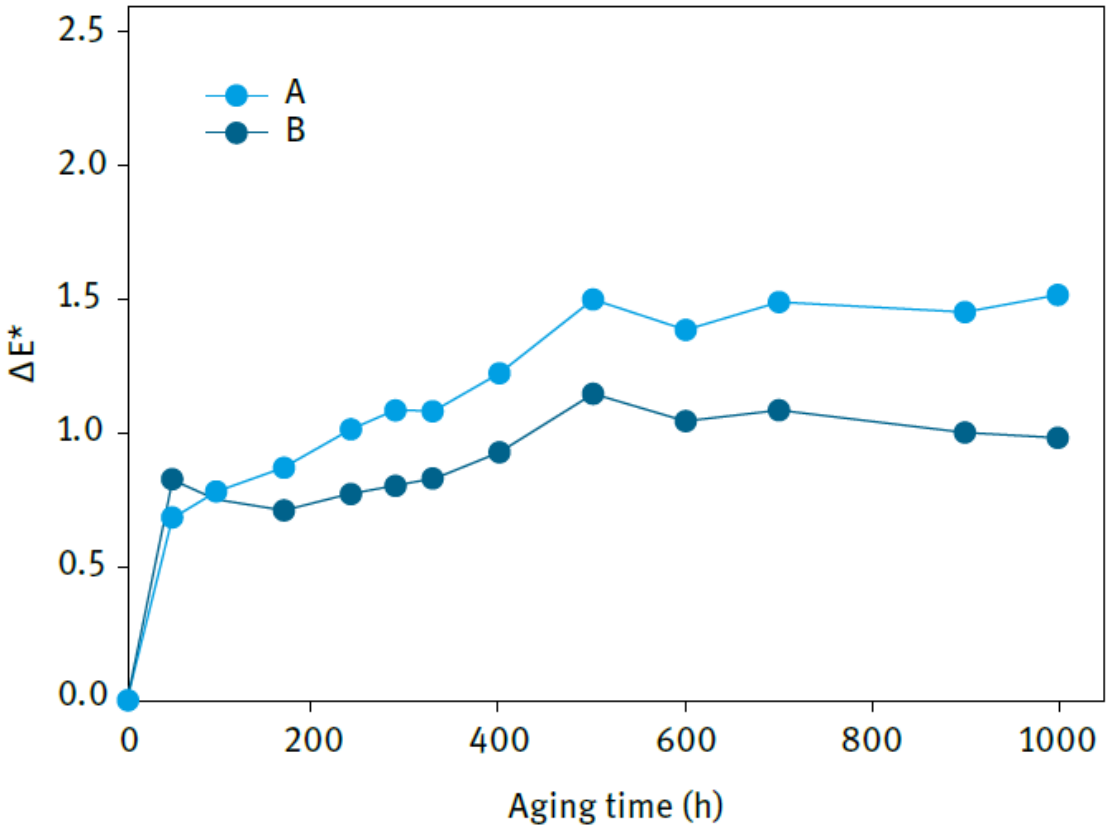

Figure A.16. Overall color change (ΔE) following up to 1000 hours of accelerated UV aging treatment in an acrylic-based waterborne solid-color opaque coating (curve A), and with the addition of nano-TiO_2 rutile (10 nm, curve B) [8].

A.4.3. Atomic force microscopy and surface roughness

Once sanded, wood has a typical roughness in the micron range. When a coating is applied, this value falls about a thousandfold to the nanometer range, even with coating thicknesses as low as 30 microns (Figure A.18). This is important, since excessive surface roughness can lead to deleterious optical effects such as loss of gloss. When adding particles to the formulation, surface roughness is bound to increase and can lead to light dispersion effects (Figure A.18).

Figure A.17. An example of an accelerated UV aging system (Atlas Inc., USA).

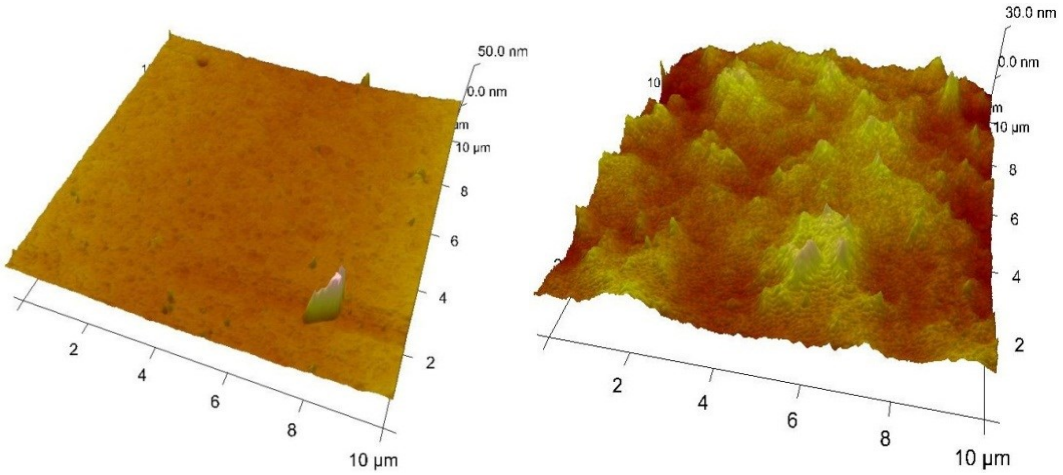

a) b)

Figure A.18. AFM images of (a) a varnish without CNC, and (b) a varnish with 1.5% CNC.

A.4.4. X-ray imaging and particle aggregation

Several types of nanoparticles can be mixed into coating formulations. These are often clays (Figure A.19) or oxides, as these have desirable properties such as specific colors, UV absorption capabilities, and increased hardness. The quality of the dispersion can be characterized by x-ray imaging with transmission electron spectroscopy. The nanoparticles can be surface-treated in order to facilitate dispersion, since dispersion of the particles remains problematic, especially if the material is supplied in powder form, encouraging the formation of aggregates.

Since CNC is an organic material, it is rather difficult to obtain good contrasts for a coating in TEM images [7].

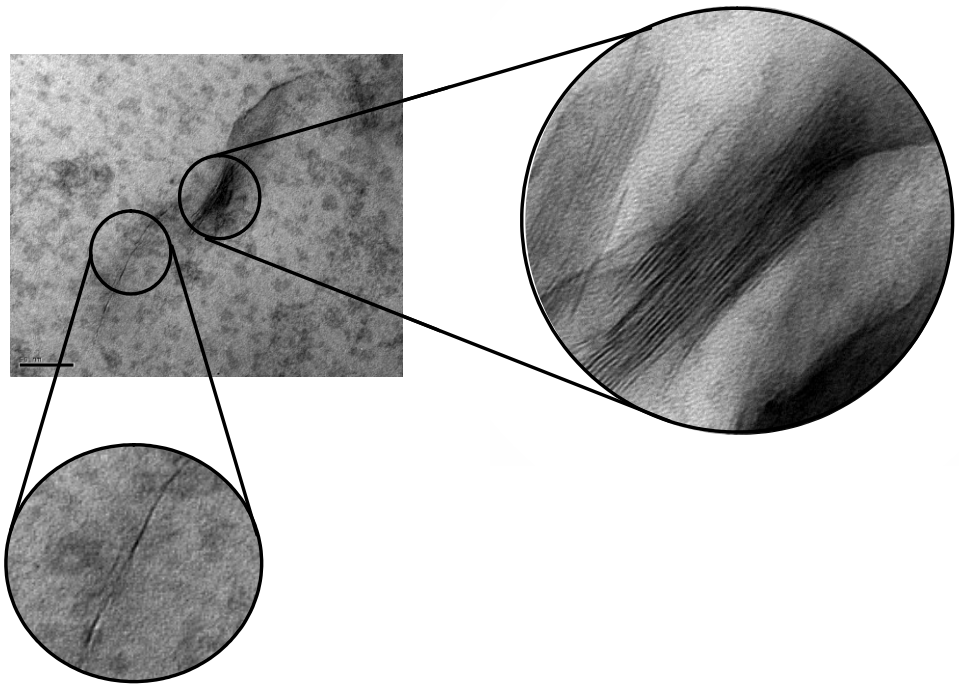

Figure A.19. Presence of clay aggregates and single clay platelets (1% weight) in a formulation prepared by bead milling (bar = 50 nm) [7].

A.4.5. Weathering and artificial aging

This is an important part of testing of coatings intended for outdoor use. All of the tests and standards mentioned so far in this chapter can be carried out before and after weathering and compared to investigate the durability of the coating. Generally, a loss of properties and shift in colors can be observed after weathering. However, in some cases, values of glass transition temperature (T_g), modulus, and hardness of coatings can actually increase after weathering, due to cross-linking of macromolecules within the thickness of the coating. This increase happens at the expense of resistance to impact and scratches: in other words, as it ages, the coating becomes more fragile and displays glass-like properties.

However, a better method of testing a coating is one which reproduces realistic service conditions. For that scenario, the samples are usually put outside in a sunny location for months or even years at a time. The conditions needed are described in European standards ISO 2810, EN 927-3, and ASTM D6763-08, among others. This process is rather lengthy and efforts are being made to come up with techniques giving faster results. There are artificial or accelerated aging techniques where the samples are put into an environmental chamber-like device (Figure A.17) and subjected to intense solar-like UV light emitted by a xenon lamp. Samples are usually submitted to these conditions for about 2 000 hours, often mixed with cycles of water spray. This treatment severely degrades unprotected samples and provides a rapid method of grading a series of coatings in a relative fashion in order to select the most efficient, which may then be subjected to expensive and lengthy supplementary tests. In addition, there are other tests to quantify the performance of coatings in special environments such as high humidity, where biofouling by fungi can be a concern, for example in bathrooms or humid and damp climates.

A.5. Bio-based coatings

The term “bio-based coatings” is intended to describe a formulation in which the chemicals used originate from biological products. However, it does not necessarily mean that these formulations are eco-friendly, ecological and the like. It is easy, especially in the marketing

field, to mix terms such as recyclable, recycled, degradable, natural basis, renewable, eco-friendly, bio-, carbon sink and other catchy terms. Each one of these descriptive terms refers to a specific set of properties. Perhaps a more useful concept would be that of 'sustainability', which means exactly what it states. For wood coatings, there is a long history of formulations going back as far as thousands of years. Indeed, small industries such as cabinet making and 'lutherie' (the making of string instruments) have developed excellent coatings, which have lasted literally hundreds of years, for example for the famous Stradivarius violins. These were based on natural products: linseed oil, soy, turpentine (solvent derived from pine trees), glycerin, shellac, beeswax, rosins, and natural gums [148]. They were thus formulated from natural bio-based products of agricultural origin or by-products from animal sources, as synthetic chemicals derived from petroleum, coal, and gas appeared only in the 20th century. These traditional coatings perform well indoors, but are slow to cure and dry, are not resistant to moisture and UV light, and reliable sources for these reagents are hard to find, especially for large volumes. Historically, the largest volume for traditional paints and varnishes were alkyd (oil-) types, based on fatty acids such as linseed oil and its esters, and glycerin. There were very few water-based coatings. The white pigment for many opaque coatings was often based on lead oxide, which is not used nowadays due to its toxic nature. Most of the traditional paints and varnishes were of the siccative type (oil-drying agent), based on bio-based unsaturated fatty acids (termed alkyl or oil-based paints) and alcohols, which cure via an oxidation-based free radical mechanism. Nowadays many coatings are of a different nature, being water-based (emulsion), UV-cured or having a high solid content. There are currently huge efforts to replace some of the synthetic chemicals used in these formulations with bio-based ones, although they often require major modifications. As seen in the preceding sections, one can add bio-based materials such as CNC to coatings, but the main ingredient remains resin, which is usually petroleum-based. Efforts are being made to develop bio-based resins such as acrylated vegetable oils and their derivatives, e.g., epoxidized soybean oil as shown in the work of Rengasamy et al. [149]. There is still a debate as to whether soybean-based products should be classified as eco-friendly, since if they are to be used as chemical feedstock, this will also put pressure on food prices. There are also reports of

acrylated products derived from epoxidized linseed oil, which could be of interest for similar applications [150, 151].

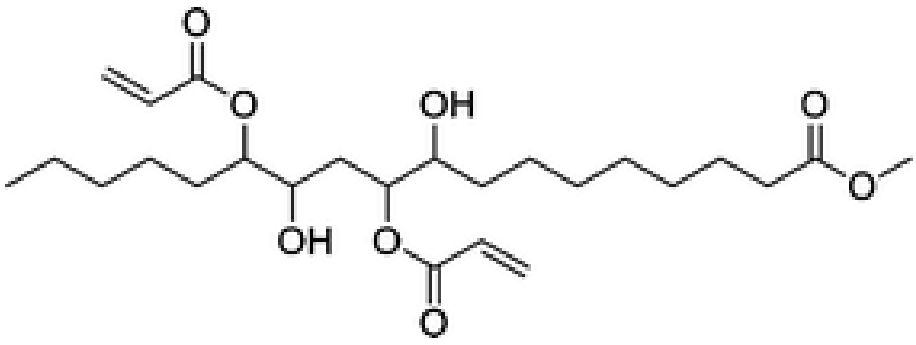

Figure A.20. Acrylated epoxidized fatty methyl ester [152].

Thus, for sustainable formulations, the main component of the resin constituents should be obtained from natural sources. However, the main resin system of UV-cured acrylates discussed in the preceding sections is a mixture of reactive monomers and oligomers, thus containing very little solvents and therefore, little volatile organic compounds (VOC). It remains to be seen whether bio-based materials can achieve the same ease of formulation as their synthetic counterparts. It is also possible to incorporate sugar-based polymers into basic paint chemicals. Lactide-based polymers can be incorporated into saturated polyesters and alkyl resins, thus lowering the carbon footprint of the raw materials by as much as 27% [152]. Many coating systems already contain cellulose-based materials, such as cellulose ethers as thickeners and cellulose nitrates.

A.6. Future developments

Among the present and future incentives for the development of new coatings are environmental concerns and performance. Bio-based materials will play an increasing role in paint and coating materials. The industry, especially in Europe, is incorporating new concepts into its production practices, such as “cradle-to grave design”, sustainability and

carbon footprint. These practices are implemented for marketing reasons and because they can lead to improved efficiency and product design, as seen for CNC and bio-based coatings. While governments and industries are not about to regulate the amounts of bio-based materials in formulations and products, they are rather active on the VOC reduction front. Some coatings such as high solid content, UV-curing and powder coatings already emit very little VOC. The French government has developed mandatory labeling for construction and decorative materials, enforced since January 2012, which classifies emissions according to 10 key chemicals emitted by a given material (Figure A.21).

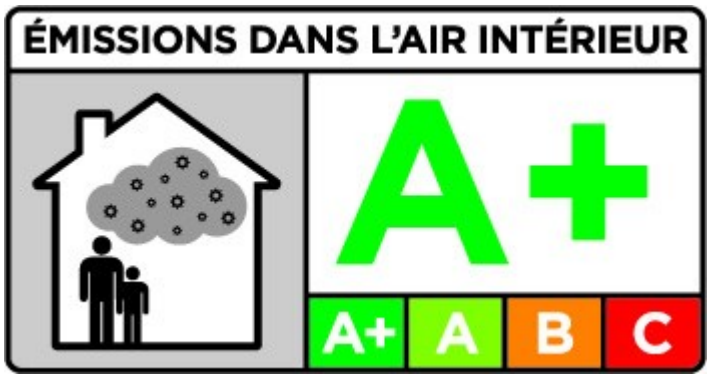

Figure A.21. Example of French material labelling for VOC regulations.

Other existing procedures for monitoring VOC emissions are based on the ISO 16000 series. Similarly, LEED (Leadership in Energy and Environmental Design) is a US based rating system for sustainable buildings. It sets limits on VOC emissions for coatings, among other things. There are also other improvements on the horizon: superhydrophobic coatings and self-cleaning coatings are being developed. Although they involve nanotechnologies, they currently do not involve bio-based products per se. There is also a large amount of concern about nanoparticles regarding toxicity issues. While unmodified CNC is deemed safe, there is a regulatory vacuum regarding the toxicity of other nanoparticles [153].

A.7. Summary

The technical literature is replete with thermoplastic nanocomposites, but as far as coatings are concerned, it is a rather new field. Coatings can be improved with the use of such technologies, but several issues will have to be addressed such as formulation stability, dispersion, cost effectiveness, chemical safety and long term performance of nanocoatings.

Acknowledgements

The authors acknowledge the financial support from Fonds de Recherches du Québec en Nature et Technologies (FRQNT), Arboranano and FPInnovations.

Annexe B. Affiches présentées dans le cadre des conférences et colloques

Caractérisation de la dispersion de la nanocellulose cristalline dans les revêtements par microscopie à force atomique

Vahe Vardanyan[1, 2], Bouddah Poaty[2], Bernard Riedl[2], Tigran Galstian[1], Grégory Chauve[3]

[1] Center for Optics, Photonics and Laser, Department of Physics, Engineering Physics and Optics, Université Laval, Pav. d'Optique-Photonique, 2375 Rue de la Terrasse, Québec, Canada G1V 0A6
[2] Département des sciences du bois et de la forêt, Faculté de foresterie, de géographie et de géomatique, Université Laval, 2425, rue de la Terrasse, Québec, QC, G1V 0A6 , Canada
[3] FPInnovations, 570, boul. Saint-Jean, Pointe-Claire, Montréal (QC) H9R 3J9, Canada

Résumé

Nous vivons à l'ère des nanotechnologies. Dans la littérature, il est souvent question des composites nanocellulose (NCC) -thermoplastiques, mais il n'y a rien sur les revêtements nanocomposites. Le problème majeur en nanotechnologie des composites est la dispersion optimale des nanoparticules: sans cette dispersion, il est difficile d'obtenir de bons résultats. Il nous faut donc une méthode efficace pour évaluer cette dispersion. Nous présentons ici une nouvelle technique de caractérisation de la dispersion, via une analyse de surface.

L'objectif de cette recherche est de développer des revêtements nanocomposites pour des applications sur le bois, bien que d'autres substrats soient possibles, et d'étudier l'effet du renfort NCC sur l'usure du revêtement. Ces expériences sont les premières qui concernent les revêtements avec nanorenfort NCC.

Matériaux et procédure expérimentale

Une formulation, donc la peinture /vernis liquide, comporte trois ou quatre groupes de composantes chimiques, soit la résine, le solvant, les pigments (peintures seulement) et additifs. Ces composantes sont données au tableau suivant.

Composante	Nature chimique	Nom commercial
Résine	Polyuréthane-acrylate	Bayhydrol UV 2282
Anti-mousse	Ether poly dimethylsiloxane	Foamex 822
Surfactant	Polyether siloxane copolymer	Byk 348
Dispersant	Solution de copolymères en blocs de haute masse molaire	Byk 190
Photoinitiateur	Bis-acyl phosphine oxide	Irgacure 819DW
Thickener	Polyuréthane	RM 2020
Solvant	Eau deionisée	-
Pigment	TiO_2	-

Un mélangeur à haute vitesse est utilisé pour mélanger les formulations, alors que des billes de verre ont été ajoutées pour augmenter le cisaillement et aide à la dispersion des nanoparticles et, le cas échéant, le pigment.

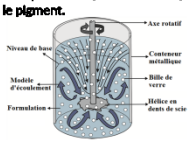

La NCC utilisée ici a été produite par la firme FPInnovations. Les dimensions moyennes sont de: 6-10 nm (largeur) and 100-130nm (longueur). Ceci a été obtenu par mesures de dispersion dynamique de la lumière à l'aide d'un Zetasizer Nano ZS (Malvern Instruments Ltd.). La figure ci-bas montre la dispersion de taille en solution aqueuse de la NCC.

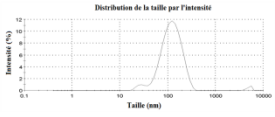

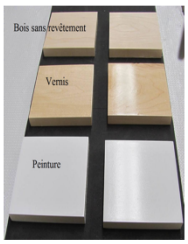

Résultats et discussion

Il existe différentes techniques pour évaluer la qualité de la dispersion. Le plus courant est d'effectuer des micrographies SEM /TEM, mais dans ce cas-ci, c'est contre-indiqué, puisque la matrice (résine) est organique et le renfort (NCC) aussi, ce qui donne une absence de contraste:

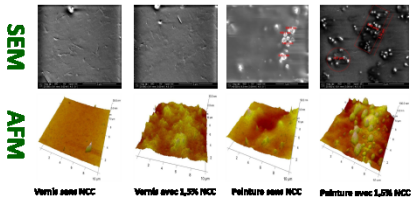

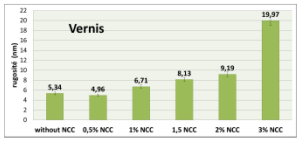

À la figure ci-haut, on peut constater que les valeurs moyennes de rugosité augmentent de façon mesurable avec l'augmentation de la concentration de NCC, au-dessus de 1% pour la peinture et 2% pour le vernis.

Ci-haut, dans les deux premières micrographies SEM, il n'y a aucune différence entre les vernis sans et avec NCC, alors que dans le cas des peintures, deux figures suivantes, il y a un contraste entre la résine et le pigment TiO_2 .

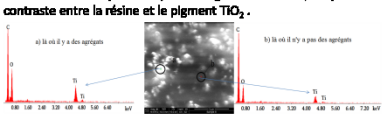

Pour s'assurer que les points blancs sont bien des microparticles de TiO_2, nous avons choisi deux points: a) là où il y a des agrégats et b) et où il n'y en n'a pas, et effectué une analyse chimique par fluorescence de R-X, une fonctionalité additionelle du SEM.

Une analyse similaire ne peut être faite sur le vernis, mais nous pouvons mesurer la rugosité de toutes les surfaces à l'AFM. Dans la première figure AFM ci-haut, sans NCC, la surface est très lisse, même au niveau submicron, alors que l'addition de 1, 5% de NCC mène à une importante augmentation de la rugosité, laquelle est un signe de formation d'agrégats.

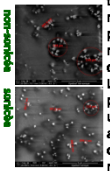

On peut aussi constater que la taille des agrégats est deux fois moindre dans les échantillons passés aux ultra-sons, par rapport aux échantillons de contrôle, dans les images SEM. La rugosité obtenue par a AFM pour les échantillons traités aux ultra-sons est de (Ra) 7,1nm, alors que c'est le double pour le contrôle. Cela confirme que la rugosité de surface est liée au degré de dispersion.

Conclusions

Nous pensons que cette rugosité, quand même très faible au niveau nanométrique, est une évidence de la qualité de la dispersion de la NCC, et ainsi, si nous avons une surface lisse au niveau nanométrique, la dispersion est bonne. Ceci a été démontré à l'aide de mesures SEM and AFM dans le cas des peintures, mais à l'aide de cette technique AFM, nous pouvons aussi évaluer la qualité de la dispersion pour les vernis, laquelle ne peut être évaluée par SEM, vu le manque de contraste entre la résine et la NCC, toutes deux à base de carbone. On peut alors prétendre que la rugosité est un indice de la qualité de la dispersion pour les peintures et vernis. Ceci est une méthode rapide pour évaluer des tels revêtements sur le bois, mais aussi sur d'autres substrats.

Cette méthode à la qualité additionelle de fournir des chiffres plutôt que des images, pour une évaluation quantitive et effectuer des corrélations avec les autres qualités qui nous intéressent soit la brillance et la résistance mécanique des revêtements, sur n'importe quelle surface, sans préparations et opérations au microtome ou autres perturbations de la surface

Les propriétés mécaniques des revêtements UV-aqueux renforcées par la nanocellulose cristalline

Vahe Vardanyan[1, 2], Bouddah Poaty[2], Gregory Chauve[3], Véronic Landry[4], Bernard Riedl[2], Tigran Galstian[1]

[1] Center for Optics, Photonics and Laser, Department of Physics, Engineering Physics and Optics, Université Laval, Pav. d'Optique-Photonique, 2375 Rue de la Terrasse, Québec, Canada G1V 0A6

[2] Département des sciences du bois et de la forêt, Faculté de foresterie, de géographie et de géomatique, Université Laval, 2425, rue de la Terrasse, Québec, QC, G1V 0A6 , Canada

3 FPInnovations, 570 boul. Saint-Jean, Pointe-Claire, Montréal (QC) H9R 3J9, Canada;

4 FPInnovations, 319 rue Franquet, Québec (QC), G1P 4R4, Canada;

Résumé

Le secteur forestier a toujours été très majeur au Québec et généralement partout au Canada. Le présent projet consiste à augmenter la performance de revêtements UV-aqueux pour le bois, en utilisant la ressource forestière. Dans ce but, nous pensons remplacer les nanoparticules étudiées précédemment par de la cellulose nanocristalline (NCC), un produit canadien et québécois, issu de la forêt.

L'objectif principal du projet est la formulation des revêtements aqueux nanocomposites NCC opaques et transparent pour le bois à usage extérieur et intérieur.

L'analyse de la dispersion a été faite par microscopie à force atomique (AFM) en mesurant la rugosité. L'analyse élémentaire a été faite pour mesurer le taux de TiO2 dans les agrégats en cas de peinture. Les résultats sont comparés avec les images de microscopie électronique à balayage (SEM).

Les propriétés optiques et mécaniques ont été mesurées et sont acceptables. La propriété qui nous intéresse particulièrement, la résistance à l'usure a été augmentée de 40% avec ajout de 2% de NCC modifiée en surface.

Matériaux et procédure expérimentale

Une formulation, donc la peinture/vernis liquide, comporte trois ou quatre groupes de composantes chimiques, soit la résine, le solvant, les pigments (peintures seulement) et additifs (dispersant, photoinitiateur etc.). La NCC été utilisée comme un argent de renfort à cause ces propriétés mécaniques très élevées. Les modifications chimiques de la NCC ont été faites par des molécules suivantes pour obtenir une NCC plus hydrophobe et donc améliorer la dispersion.

La bromure d'hexadecyltriméthyl ammonium (HDTMA)

La bromure de tetraméthyl ammonium (TMA)

La chlorure d'acryloyl (C_3H_3ClO)

Un mélangeur à haute vitesse est utilisé pour mélanger les formulations, alors que des billes de verre ont été ajoutées pour augmenter le cisaillement et aider à la dispersion des nanoparticules et, le cas échéant, le pigment. Les formulations sont appliquées par pulvérisation sur l'érable à sucre. Les échantillons sont cuits à l'aide d'un four UV.

L'analyse de la dispersion été effectuée par SEM, AFM et à l'aide d'un montage optique suivant.

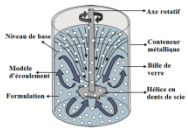

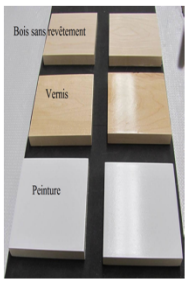

Résultats et discussion

Il existe différentes techniques pour évaluer la qualité de la dispersion. Le plus courant est d'effectuer des micrographies SEM /TEM, mais dans ce cas-ci, c'est contre-indiqué, puisque la matrice (résine) est organique et le renfort (NCC) aussi, ce qui donne une absence de contraste:

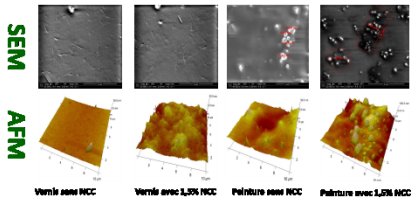

Dans les deux premières micrographies SEM, il n'y a aucune différence entre les vernis sans et avec NCC, alors que dans le cas des peintures, deux figures suivantes, il y a un contraste entre la résine et le pigment TiO_2. Dans la première figure AFM, sans NCC, la surface est très lisse, même au niveau submicronique, alors que l'addition de 1,5% de NCC mène à une importante augmentation de la rugosité, laquelle est un signe de formation d'agrégats.

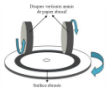

$$M_{perte} = M_0 - M_{180}$$

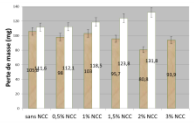

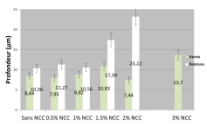

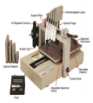

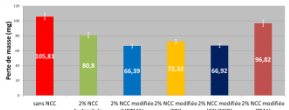

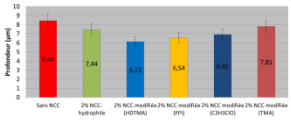

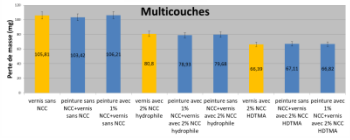

Conclusions

La dispersion dans un film solide est difficile à suivre par des méthodes conventionnelles (SEM-TEM), la microscopie à force atomique semble utile à ce titre: en effet la rugosité semble refléter la qualité de la dispersion et l'effet renfort. Nous pensons que cette rugosité, quand même très faible au niveau nanométrique, est une évidence de la qualité de la dispersion de la NCC, et ainsi, si nous avons une surface lisse au niveau nanométrique, la dispersion est bonne.

On peut améliorer la qualité de la dispersion de la NCC dans les revêtements à l'aide de réactions chimiques simples faites sur la NCC. Cela confirme que sa nature au départ hydrophile nuit à sa dispersion, en encourageant la formation d'agrégats. Ces modifications n'ont pas nui à la cristallinité de la NCC.

La propriété qui nous intéresse particulièrement, la résistance à l'usure, a été augmentée de 40% avec ajout de 2% de NCC modifiée en surface. Il est possible que la sonication améliore encore cette propriété.

Caractérisation de la dispersion de la nanocellulose cristalline dans les revêtements par rétrodiffusion de la lumière

Vahe Vardanyan[1, 2], Bouddah Poaty[2], Bernard Riedl[2], Tigran Galstian[1]

[1] Center for Optics, Photonics and Laser, Department of Physics, Engineering Physics and Optics, Université Laval, Pav. d'Optique-Photonique, 2375 Rue de la Terrasse, Québec, Canada G1V 0A6

[2] Département des sciences du bois et de la forêt, Faculté de foresterie, de géographie et de géomatique, Université Laval, 2425, rue de la Terrasse, Québec, QC, G1V 0A6 , Canada

Résumé

Nous vivons à l'ère des nanotechnologies. Dans la littérature, il est souvent question des composites nanocellulose (NCC) -thermoplastiques, mais il y a très peu travaux sur les revêtements nanocomposites. Le problème majeur en nanotechnologie des composites est la dispersion optimale des nanoparticules: sans cette dispersion, il est difficile d'obtenir de bons résultats. Il nous faut donc une méthode efficace pour évaluer cette dispersion. Nous présentons ici une nouvelle technique de caractérisation de la dispersion, via une analyse de surface par rétrodiffusion de la lumière en comparant avec la rugosité qui été mesurée par AFM.

L'objectif de cette recherche est de développer des revêtements nanocomposites pour des applications sur le bois, bien que d'autres substrats soient possibles, et d'étudier l'effet du renfort NCC sur l'usure du revêtement. Ces expériences sont les premières qui concernent les revêtements avec nanorenfort NCC.

Matériaux et procédure expérimentale

Une formulation, donc la peinture/vernis liquide, comporte trois ou quatre groupes de composantes chimiques, soit la résine, le solvant, les pigments (peintures seulement) et additifs (dispersant, photoinitiateur etc.). La NCC été utilisée comme un argent de renfort à cause ces propriétés mécaniques très élevées. Les modifications chimiques de la NCC ont été faites par des molécules suivantes pour obtenir une NCC plus hydrophobe et donc améliorer la dispersion.

Le bromure d'hexadecyltriethyl ammonium (HDTMA)

Le bromure de tetramethyl ammonium (TMA)

Le chlorure d'acryloyl (C_3H_3ClO)

Un mélangeur à haute vitesse est utilisé pour mélanger les formulations, alors que des billes de verre ont été ajoutées pour augmenter le cisaillement et aider à la dispersion des nanoparticules et, le cas échéant, le pigment. Les formulations sont appliquées par pulvérisation sur l'érable à sucre. Les échantillons sont cuits à l'aide d'un four UV.

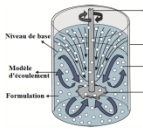

L'analyse de la dispersion été effectuée par SEM, AFM et à l'aide d'un montage optique suivant.

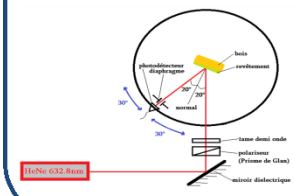

Résultats et discussion

Il existe différentes techniques pour évaluer la qualité de la dispersion. Le plus courant est d'effectuer des micrographies SEM /TEM, mais dans ce cas-ci, c'est contre-indiqué, puisque la matrice (résine) est organique et le renfort (NCC) aussi, ce qui donne une absence de contraste:

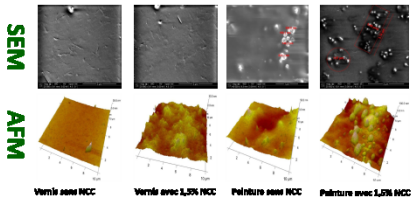

Dans les deux premières micrographies SEM, il n'y a aucune différence entre les vernis sans et avec NCC, alors que dans le cas des peintures, deux figures suivantes, il y a un contraste entre la résine et le pigment TiO_2. Dans la première figure AFM, sans NCC, la surface est très lisse, même au niveau submicron, alors que l'addition de 1,5% de NCC mène à une importante augmentation de la rugosité, laquelle est un signe de formation d'agrégats.

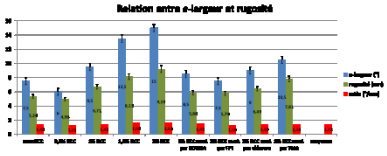

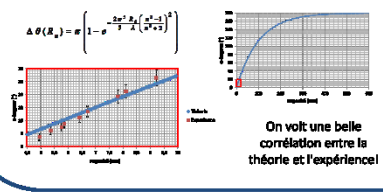

On voit une belle corrélation entre la théorie et l'expérience!

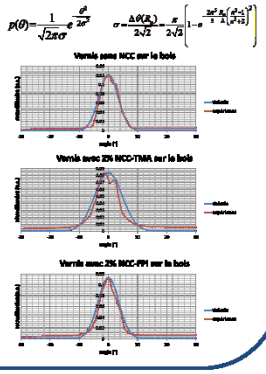

Conclusions

Nous pensons que cette rugosité, quand même très faible au niveau nanométrique, est une évidence de la qualité de la dispersion de la NCC, et ainsi, si nous avons une surface lisse au niveau nanométrique, la dispersion est bonne. Ceci a été démontré à l'aide de mesures SEM and AFM dans le cas des peintures, mais à l'aide de cette technique AFM, nous pouvons aussi évaluer la qualité de la dispersion pour les vernis, laquelle ne peut être évaluée par SEM, vu le manque de contraste entre la résine et la NCC, toutes deux à base de carbone. On peut alors prétendre que la rugosité est un indice de la qualité de la dispersion pour les peintures et vernis. Ceci est une méthode rapide pour évaluer des tels revêtements sur le bois, mais aussi sur d'autres substrats.

D'une autre côté nous avons trouvé une relation entre la rétrodiffusion de la lumière et la rugosité. Les données expérimentales ont été modélisées théoriquement et il y a une belle corrélation entre elles. Grace à ces méthodes on peut facilement caractériser la dispersion pas seulement qualitativement mais aussi quantitativement sur n'importe quelle surface, sans préparations et opérations au microtome ou autres perturbations de la surface.

Bibliographie

[1] J. Panno, *The cell: evolution of the first organism*, Infobase Publishing, New York, USA, 2009.

[2] W.F. Doolittle, *Uprooting the tree of life*, Scientific American, 282 (2000) 90-95.

[3] J.L. Bowyer, J.G. Haygreen, R. Shmulsky, *Le bois et ses usages*, Montréal: Centre collégial de développement de matériel didactique, 2005.

[4] R.M. Rowell, *Handbook of wood chemistry and wood composites*, CRC press, Boca Raton, USA, 2012.

[5] F. Bulian, J. Graystone, *Wood coatings: Theory and practice*, Elsevier, Oxford, UK, 2009.

[6] C. Sow, *Revêtements nanocomposites UV-Aqueux pour le bois à usage intérieur*, Thèse de doctorat, Université Laval, Québec, Canada, 2010.

[7] V. Landry, *Revêtements nanocomposites à haute teneur en solides cuits aux ultraviolets pour les couvre –planchers en bois*, Thèse de doctorat, Université Laval, Québec, Canada, 2009.

[8] M. Vlad Cristea, *Revêtements nanocomposites anti-UV pour le bois à usage extérieur*, Thèse de doctorat, Université Laval, Québec, Canada, 2011.

[9] N. Auclair, *Stabilité des couleurs des systèmes bois/vernis améliorée par des revêtements nanocomposites aqueux à usage extérieur*, Mémoire de maîtrise, Université Laval, Québec, Canada, 2010.

[10] V. Vardanyan, B. Poaty, G. Chauve, V. Landry, T. Galstian, B. Riedl, *Mechanical properties of UV-waterborne varnishes reinforced by cellulose nanocrystals*, Journal of Coatings Technology and Research, 11 (2014) 841-852.

[11] B. Müller, U. Poth, *La formulation des peintures et vernis*, Eurocol, Offranville, FR, 2004.

[12] I. Hosker, *Complete woodfinishing*, Guild of Master Craftsman Publications, Lewes, UK, 1993.

[13] W.C. Feist, *Weathering and protection of wood*, in: Proceedings - Annual Meeting of the American Wood-Preservers' Association, Kansas, USA, 1983, pp. 195-205.

[14] C. Decker, *Polymérisation sous rayonnement UV*, Ed. Techniques Ingénieur, 2000.

[15] C. Decker, K. Moussa, T. Bendaikha, *Photodegradation of UV-cured coatings II. Polyurethane–acrylate networks*, Journal of Polymer Science Part A: Polymer Chemistry, 29 (1991) 739-747.

[16] T. Jaworek, H.H. Bankowsky, R. Königer, W. Reich, W. Schrof, R. Schwalm, *Radiation curable materials–principles and new perspectives*, in: Macromolecular Symposia, John Wiley & Sons, 2000, pp. 197-204.

[17] C. Decker, *Kinetic study and new applications of UV radiation curing*, Macromolecular Rapid Communications, 23 (2002) 1067-1093.

[18] F. Masson, C. Decker, T. Jaworek, R. Schwalm, *UV-Radiation curing of waterbased urethane–acrylate coatings*, Progress in Organic Coatings, 39 (2000) 115-126.

[19] C. Decker, I. Lorinczova, *UV-radiation curing of waterborne acrylate coatings*, Journal of Coatings Technology and Research, 1 (2004) 247-256.

[20] C. Decker, F. Masson, R. Schwalm, *How to speed up the UV curing of water-based acrylic coatings*, Journal of Coatings Technology and Research, 1 (2004) 127-136.

[21] T. Brock, M. Groteklaes, P. Mischke, S. Kups, J. Gruninger, J.-C. Gruninger, *Manuel de technologie des peintures et vernis*, Eurocol éditions, Offranville, FR, 2002.

[22] J.-C. Laout, *Formulation des peintures: Physico-chimie et matières pulvérulentes*, Techniques de l'ingénieur. Génie des procédés, JC1 (2005) 1-23.

[23] R. Schwalm, *UV coatings: basics, recent developments and new applications*, Elsevier, Oxford, UK, 2006.

[24] R. Sun, *Cereal straw as a resource for sustainable biomaterials and biofuels: chemistry, extractives, lignins, hemicelluloses and cellulose*, Elsevier, 2010.

[25] U. Heinze, W. Wagenknecht, *Comprehensive cellulose chemistry: functionalisation of cellulose*, in: Wiley-VCH, Weinheim, 1998.

[26] B. Peng, N. Dhar, H. Liu, K. Tam, *Chemistry and applications of nanocrystalline cellulose and its derivatives: a nanotechnology perspective*, The Canadian Journal of Chemical Engineering, 89 (2011) 1191-1206.

[27] J.F. Revol, L. Godbout, X.M. Dong, D.G. Gray, H. Chanzy, G. Maret, *Chiral nematic suspensions of cellulose crystallites - phase separation and magnetic field orientation*, Liquid Crystals, 16 (1994) 127-134.

[28] J. Sugiyama, H. Chanzy, J.F. Revol, *On the polarity of cellulose in the cell-wall of valonia*, Planta, 193 (1994) 260-265.

[29] X.M. Dong, J.F. Revol, D.G. Gray, *Effect of microcrystallite preparation conditions on the formation of colloid crystals of cellulose*, Cellulose, 5 (1998) 19-32.

[30] L. Heux, E. Dinand, M.R. Vignon, *Structural aspects in ultrathin cellulose microfibrils followed by C-13 CP-MAS NMR*, Carbohydrate Polymers, 40 (1999) 115-124.

[31] J.F. Revol, H. Bradford, J. Giasson, R.H. Marchessault, D.G. Gray, *Helicoidal self-ordering of cellulose microfibrils in aqueous suspension*, International Journal of Biological Macromolecules, 14 (1992) 170-172.

[32] K. Fleming, D.G. Gray, S. Matthews, *Cellulose crystallites*, Chemistry-a European Journal, 7 (2001) 1831-1835.

[33] S. Beck, J. Bouchard, R. Berry, *Dispersibility in Water of Dried Nanocrystalline Cellulose*, Biomacromolecules, 13 (2012) 1486-1494.

[34] S. Beck, J. Bouchard, R. Berry, *Dried nanocrystalline cellulose of controllable dispersibility and method therefor*, numéro de brevet (USA): 8652636, 2014.

[35] W. Helbert, J.Y. Cavaille, A. Dufresne, *Thermoplastic nanocomposites filled with wheat straw cellulose whiskers. 1. Processing and mechanical behavior*, Polymer Composites, 17 (1996) 604-611.

[36] A. Dufresne, J.Y. Cavaillé, W. Helbert, *Thermoplastic nanocomposites filled with wheat straw cellulose whiskers. Part II: effect of processing and modeling*, Polymer Composites, 18 (1997) 198-210.

[37] I. Kvien, B.S. Tanem, K. Oksman, *Characterization of cellulose whiskers and their nanocomposites by atomic force and electron microscopy*, Biomacromolecules, 6 (2005) 3160-3165.

[38] V. Vardanyan, B. Poaty, G. Chauve, V. Landry, T. Galstian, B. Riedl, *Wear resistance of nanocomposite coatings*, in: P. Woodhead (Ed.) Anti-Abrasive Nanocoatings: Current and future applications (*Chapter 8*), Elsevier, 2014.

[39] F. Karakas, M.S. Celik, *Effect of quantity and size distribution of calcite filler on the quality of water borne paints*, Progress in Organic Coatings, 74 (2012) 555-563.

[40] S. Farrokhpay, *Application of Spectroscopy and Microscopy Techniques in Surface Coatings Evaluation*: A Review, Applied Spectroscopy Reviews, 47 (2012) 233-243.

[41] P. Thometzek, A. Ludwig, A. Karbach, K. Kohler, *Effects of morphology and surface treatment of inorganic pigments on waterborne coating properties*, Progress in Organic Coatings, 36 (1999) 201-209.

[42] V. Landry, P. Blanchet, B. Riedl, *Mechanical and optical properties of clay-based nanocomposites coatings for wood flooring*, Progress in Organic Coatings, 67 (2010) 381-388.

[43] A.J. Panshin, C. de Zeeuw, *Structure, identification, uses, and properties of the commercial woods of the United States and Canada*, in: Textbook of wood technology. Volume I., McGraw-Hill Book Co., New York, USA, 1970.

[44] L. Lecamp, C. Pavillon, P. Lebaudy, C. Bunel, *Influence of temperature and nature of photoinitiator on the formation kinetics of an interpenetrating network photocured from an epoxide/methacrylate system*, European Polymer Journal, 41 (2005) 169-176.

[45] M.J. Duer, *Solid state NMR spectroscopy: principles and applications*, John Wiley & Sons, Stanford, USA, 2008.

[46] J. Keeler, *Understanding NMR spectroscopy*, John Wiley & Sons, Stanford, USA, 2013.

[47] M.H. Levitt, *Spin dynamics: basics of nuclear magnetic resonance*, John Wiley & Sons, Stanford, USA, 2008.

[48] R.H. Fernando, L.P. Sung, *Nanotechnology applications in coatings*, American Chemical Society, Washington, USA, 2009.

[49] P.M. Ajayan, L.S. Schadler, P.V. Braun, *Nanocomposite science and technology*, John Wiley & Sons, Stanford, USA, 2006.

[50] H.S. Nalwa, *Handbook of organic-inorganic hybrid materials and nanocomposites*, Book News Inc., Portland, USA, 2003.

[51] S.S. Ray, M. Bousmina, *Polymer nanocomposites and their applications*, Department of Chemical Engineering, Université Laval, Québec, Canada, 2006.

[52] A.A. Asif, B. John, V.L. Rao, K.N. Ninan, *Surface morphology, thermomechanical and barrier properties of poly (ether sulfone)-toughened epoxy clay ternary nanocomposites*, Polymer International, 59 (2010) 986-997.

[53] S.H. Park, H.S. Lee, J.H. Choi, C.M. Jeong, M.H. Sung, H.J. Park, *Improvements in barrier properties of poly (lactic acid) films coated with chitosan or chitosan/clay nanocomposite*, Journal of Applied Polymer Science, 125 (2012) E675-E680.

[54] M.M. Jalili, S. Moradian, H. Dastmalchian, A. Karbasi, *Investigating the variations in properties of 2-pack polyurethane clear coat through separate incorporation of hydrophilic and hydrophobic nano-silica*, Progress in Organic Coatings, 59 (2007) 81-87.

[55] E. Amerio, P. Fabbri, G. Malucelli, M. Messori, M. Sangermano, R. Taurino, *Scratch resistance of nano-silica reinforced acrylic coatings*, Progress in Organic Coatings, 62 (2008) 129-133.

[56] Z. Ranjbar, S. Rastegar, *The influence of surface chemistry of nano-silica on microstructure, optical and mechanical properties of the nano-silica containing clear-coats*, Progress in Organic Coatings, 65 (2009) 125-130.

[57] C. Sow, B. Riedl, P. Blanchet, *UV-waterborne polyurethane-acrylate nanocomposite coatings containing alumina and silica nanoparticles for wood: mechanical, optical, and thermal properties assessment*, Journal of Coatings Technology and Research, 8 (2011) 211-221.

[58] M. Sangermano, N. Lak, G. Malucelli, A. Samakande, R. Sanderson, *UV-curing and characterization of polymer–clay nanocoatings by dispersion of acrylate-funtionalized organoclays*, Progress in Organic Coatings, 61 (2008) 89-94.

[59] M.V. Cristea, B. Riedl, P. Blanchet, *Effect of addition of nanosized UV absorbers on the physico-mechanical and thermal properties of an exterior waterborne stain for wood*, Progress in Organic Coatings, 72 (2011) 755-762.

[60] F. Bauer, V. Sauerland, H.-J. Glasel, H. Ernst, M. Findeisen, E. Hartmann, H. Langguth, B. Marquardt, R. Mehnert, *Preparation of scratch and abrasion resistant polymeric nanocomposites by monomer grafting onto nanoparticles, 3. Effect of filler particles and grafting agents*, Macromol. Mater. Eng., 287 (2002) 546-552.

[61] F. Bauer, H. Ernst, D. Hirsch, S. Naumov, M. Pelzing, V. Sauerland, R. Mehnert, *Preparation of Scratch and Abrasion Resistant Polymeric Nanocomposites by Monomer Grafting onto Nanoparticles*, 5, Macromolecular Chemistry and Physics, 205 (2004) 1587-1593.

[62] F. Bauer, R. Flyunt, K. Czihal, M.R. Buchmeiser, H. Langguth, R. Mehnert, *Nano/micro particle hybrid composites for scratch and abrasion resistant polyacrylate coatings*, Macromol. Mater. Eng., 291 (2006) 493-498.

[63] F. Bauer, R. Flyunt, K. Czihal, H. Langguth, R. Mehnert, R. Schubert, M.R. Buchmeiser, *UV curing and matting of acrylate coatings reinforced by nano-silica and micro-corundum particles*, Progress in Organic Coatings, 60 (2007) 121-126.

[64] S. Berndt, F. Wesarg, C. Wiegand, D. Kralisch, F.A. Müller, *Antimicrobial porous hybrids consisting of bacterial nanocellulose and silver nanoparticles*, Cellulose, 20 (2013) 771-783.

[65] V. Favier, H. Chanzy, J.Y. Cavaille, *Polymer Nanocomposites Reinforced by Cellulose Whiskers*, Macromolecules, 28 (1995) 6365-6367.

[66] V. Landry, P. Blanchet, *Coatings containing nanocrystalline cellulose, processes for preparation and use thereof*, numéro de brevet (USA): 20130061774, 2010.

[67] D. Klemm, F. Kramer, S. Moritz, T. Lindström, M. Ankerfors, D. Gray, A. Dorris, *Nanocelluloses: A New Family of Nature-Based Materials*, Angewandte Chemie International Edition, 50 (2011) 5438-5466.

[68] J. Cool, R.E. Hernandez, *Improving the Sanding Process of Black Spruce Wood for Surface Quality and Water-Based Coating Adhesion*, Forest Products Journal, 61 (2011) 372-380.

[69] V. Landry, A. Alemdar, P. Blanchet, *Nanocrystalline cellulose: morphological, physical, and mechanical properties*, Forest Products Journal, 61 (2011) 104-112.

[70] N. Auclair, B. Riedl, V. Blanchard, P. Blanchet, *Improvement of Photoprotection of Wood Coatings by Using Inorganic Nanoparticles as Ultraviolet Absorbers*, Forest Products Journal, 61 (2011) 20-27.

[71] M. Vlad-Cristea, B. Riedl, P. Blanchet, E. Jimenez-Pique, *Nanocharacterization techniques for investigating the durability of wood coatings*, European Polymer Journal, 48 (2012) 441-453.

[72] W. Hamad, *On the development and applications of cellulosic nanofibrillar and nanocrystalline materials*, The Canadian Journal of Chemical Engineering, 84 (2006) 513-519.

[73] R.J. Moon, A. Martini, J. Nairn, J. Simonsen, J. Youngblood, *Cellulose nanomaterials review: structure, properties and nanocomposites*, Chemical Society Reviews, 40 (2011) 3941-3994.

[74] W.J. Orts, J. Shey, S.H. Imam, G.M. Glenn, M.E. Guttman, J.-F. Revol, *Application of cellulose microfibrils in polymer nanocomposites*, Journal of Polymers and the Environment, 13 (2005) 301-306.

[75] J. Araki, S. Kuga, *Effect of trace electrolyte on liquid crystal type of cellulose microcrystals*, Langmuir, 17 (2001) 4493-4496.

[76] M. Roman, W.T. Winter, *Effect of sulfate groups from sulfuric acid hydrolysis on the thermal degradation behavior of bacterial cellulose*, Biomacromolecules, 5 (2004) 1671-1677.

[77] G. Schueneman, E. Mintz, L. Cross, *Polymer Matrix Nanocomposites via Forest Derived Nanomaterials*, (2012).

[78] J. Araki, M. Wada, S. Kuga, T. Okano, *Flow properties of microcrystalline cellulose suspension prepared by acid treatment of native cellulose*, Colloids and Surfaces A: Physicochemical and Engineering Aspects, 142 (1998) 75-82.

[79] B.G. Rånby, Fibrous macromolecular systems. *Cellulose and muscle. The colloidal properties of cellulose micelles*, Discussions of the Faraday Society, 11 (1951) 158-164.

[80] J.G. Emanuelsson, S.L. Wahlen, *Quaternary ammonium compounds and treatment of cellulose pulp and paper therewith*, numéro de brevet (USA): 4144122, 1979.

[81] C. Bonini, L. Heux, *Microfibrillated and/or microcrystalline dispersion, in particular of cellulose, in an organic solvent*, numéro de brevet (USA): 6967027, 2005.

[82] C. Goussé, H. Chanzy, G. Excoffier, L. Soubeyrand, E. Fleury, *Stable suspensions of partially silylated cellulose whiskers dispersed in organic solvents*, Polymer, 43 (2002) 2645-2651.

[83] A. Pei, Q. Zhou, L.A. Berglund, *Functionalized cellulose nanocrystals as biobased nucleation agents in poly (l-lactide)(PLLA)–crystallization and mechanical property effects*, Composites Science and Technology, 70 (2010) 815-821.

[84] I. Filpponen, D.S. Argyropoulos, *Regular linking of cellulose nanocrystals via click chemistry: Synthesis and formation of cellulose nanoplatelet gels*, Biomacromolecules, 11 (2010) 1060-1066.

[85] J. Yi, Q. Xu, X. Zhang, H. Zhang, *Temperature-induced chiral nematic phase changes of suspensions of poly (N, N-dimethylaminoethyl methacrylate)-grafted cellulose nanocrystals*, Cellulose, 16 (2009) 989-997.

[86] Y. Shin, I.-T. Bae, B.W. Arey, G.J. Exarhos, *Simple preparation and stabilization of nickel nanocrystals on cellulose nanocrystal*, Materials Letters, 61 (2007) 3215-3217.

[87] Y. Shin, J.M. Blackwood, I.-T. Bae, B.W. Arey, G.J. Exarhos, *Synthesis and stabilization of selenium nanoparticles on cellulose nanocrystal*, Materials Letters, 61 (2007) 4297-4300.

[88] Y. Shin, G.J. Exarhos, *Template synthesis of porous titania using cellulose nanocrystals*, Materials Letters, 61 (2007) 2594-2597.

[89] K.A. Connors, N.K. Pandit, *N-methylimidazole as a catalyst for analytical acetylations of hydroxy compounds*, Analytical Chemistry, 50 (1978) 1542-1545.

[90] B.H. Lomax, W.T. Fraser, M.A. Sephton, T.V. Callaghan, S. Self, M. Harfoot, J.A. Pyle, C.H. Wellman, D.J. Beerling, *Plant spore walls as a record of long-term changes in ultraviolet-B radiation*, Nature Geoscience, 1 (2008) 592-596.

[91] J. Baldock, J. Oades, A. Vassallo, M. Wilson, *Solid-state CP/MAS 13C NMR analysis of particle size and density fractions of a soil incubated with uniformly labeled ^{13}C-glucose*, Soil Research, 28 (1990) 193-212.

[92] M.I.B. Tavares, J. d'Almeida, S. Monteiro, *^{13}C solid-state NMR analysis of the DGEBA/TETA epoxy system*, Journal of Applied Polymer Science, 78 (2000) 2358-2362.

[93] X. Wen, H. He, J. Zhu, Y. Jun, C. Ye, F. Deng, *Arrangement, conformation, and mobility of surfactant molecules intercalated in montmorillonite prepared at different pillaring reagent concentrations as studied by solid-state NMR spectroscopy*, J. Colloid Interface Sci., 299 (2006) 754-760.

[94] J. Kunze, G. Scheler, B. Schröter, B. Philipp, *^{13}C High resolution solid state NMR studies on cellulose samples of different physical structure*, Polymer Bulletin, 10 (1983) 56-62.

[95] E. Princi, S. Vicini, N. Proietti, D. Capitani, *Grafting polymerization on cellulose based textiles: A ^{13}C solid state NMR characterization*, European Polymer Journal, 41 (2005) 1196-1203.

[96] J. Łojewska, P. Miśkowiec, T. Łojewski, L. Proniewicz, *Cellulose oxidative and hydrolytic degradation: In situ FTIR approach*, Polymer Degradation and Stability, 88 (2005) 512-520.

[97] J.I. Morán, V.A. Alvarez, V.P. Cyras, A. Vázquez, *Extraction of cellulose and preparation of nanocellulose from sisal fibers*, Cellulose, 15 (2008) 149-159.

[98] S. Beck-Candanedo, M. Roman, D.G. Gray, *Effect of reaction conditions on the properties and behavior of wood cellulose nanocrystal suspensions*, Biomacromolecules, 6 (2005) 1048-1054.

[99] C. Aulin, S. Ahola, P. Josefsson, T. Nishino, Y. Hirose, M. Österberg, L. Wågberg, *Nanoscale Cellulose Films with Different Crystallinities and Mesostructures ‐ Their Surface Properties and Interaction with Water*, Langmuir, 25 (2009) 7675-7685.

[100] T.A. Dankovich, D.G. Gray, *Contact angle measurements on smooth nanocrystalline cellulose (I) thin films*, Journal of Adhesion Science and Technology, 25 (2011) 699-708.

[101] J.T. Korhonen, M. Kettunen, R.H. Ras, O. Ikkala, *Hydrophobic nanocellulose aerogels as floating, sustainable, reusable, and recyclable oil absorbents*, ACS Applied Materials & Interfaces, 3 (2011) 1813-1816.

[102] C. Decker, F. Masson, R. Schwalm, *How to speed up the UV curing of water-based acrylic coatings*, Journal of Coatings Technology and Research, 1 (2004) 127-136.

[103] E. Liptakova, J. Kudela, J. Sarvas, *Study of the system wood-coating material - I. Wood-liquid coating material*, Holzforschung, 54 (2000) 189-196.

[104] A. Tauber, T. Scherzer, R. Mehnert, *UV curing of aqueous polyurethane acrylate dispersions. A comparative study by real-time FTIR spectroscopy and pilot scale curing*, Journal of Coatings Technology, 72 (2000) 51-60.

[105] Y. Bautista, J. Gonzalez, J. Gilabert, M.J. Ibáñez, V. Sanz, *Correlation between the wear resistance, and the scratch resistance, for nanocomposite coatings*, Progress in Organic Coatings, 70 (2011) 178-185.

[106] F. Bauer, H.J. Glasel, U. Decker, H. Ernst, A. Freyer, E. Hartmann, V. Sauerland, R. Mehnert, *Trialkoxysilane grafting onto nanoparticles for the preparation of clear coat polyacrylate systems with excellent scratch performance*, Progress in Organic Coatings, 47 (2003) 147-153.

[107] C.W. Miao, W.Y. Hamad, *Cellulose reinforced polymer composites and nanocomposites: a critical review*, Cellulose, 20 (2013) 2221-2262.

[108] B. Poaty, V. Vardanyan, L. Wilczak, G. Chauve, B. Riedl, *Modification of cellulose nanocrystals as reinforcement derivatives for wood coatings*, Progress in Organic Coatings, 77 (2014) 813-820.

[109] J.F. Revol, L. Godbout, X.M. Dong, D.G. Gray, H. Chanzy, G. Maret, *Chiral nematic suspensions of cellulose crystallites - phase-separation and magnetic-field orientation*, Liquid Crystals, 16 (1994) 127-134.

[110] F. Bauer, R. Mehnert, *UV curable acrylate nanocomposites: Properties and applications*, J. Polym. Res., 12 (2005) 483-491.

[111] S. Beck, J. Bouchard, R. Berry, *Controlling the Reflection Wavelength of Iridescent Solid Films of Nanocrystalline Cellulose*, Biomacromolecules, 12 (2011) 167-172.

[112] T. Nypelo, M. Osterberg, X.J. Zu, J. Laine, *Preparation of ultrathin coating layers using surface modified silica nanoparticles*, Colloid Surf. A-Physicochem. Eng. Asp., 392 (2011) 313-321.

[113] J. Bibette, F. Leal-Calderon, V. Schmitt, P. Poulin, *Emulsion science - Basic principles. An overview - Introduction*, Springer Tracts in Modern PhysicsSpringer Verlag, 181 (2002) 1-4.

[114] B. Tigges, M. Moller, O. Weichold, *ZnO nanoparticle-containing emulsions for transparent, hydrophobic UV-absorbent films*, J. Colloid Interface Sci., 345 (2010) 41-45.

[115] M.L. Nobel, S.J. Picken, E. Mendes, *Waterborne nanocomposite resins for automotive coating applications*, Progress in Organic Coatings, 58 (2007) 96-104.

[116] P. Beckmann, A. Spizzichino, *The scattering of electromagnetic waves from rough surfaces*, Norwood, MA, Artech House, Inc., 1987, 511 p., 1 (1987).

[117] C.F. Bohren, D.R. Huffman, *Absorption and scattering of light by small particles*, John Wiley & Sons, 2008.

[118] K. Dullaert, P. Steeman, J. Bolks, *A mechanistic study of the effect of pigment loading on the appearance of powder coatings: The effect of surface topography on the optical properties of powder coatings: Modelling and experimental results*, Progress in Organic Coatings, 70 (2011) 205-212.

[119] R. Alexander-Katz, R. Barrera, *Surface correlation effects on gloss*, Journal of Polymer Science-B-Polymer Physics Edition, 36 (1998) 1321-1334.

[120] M. Born, E. Wolf, *Principles of optics: electromagnetic theory of propagation, interference and diffraction of light*, Press Syndycate of the University of Cambridge, Cambridge, UK, 1999.

[121] P. Evans, P. Thay, K. Schmalzl, *Degradation of wood surfaces during natural weathering. Effects on lignin and cellulose and on the adhesion of acrylic latex primers*, Wood Science and Technology, 30 (1996) 411-422.

[122] B. George, E. Suttie, A. Merlin, X. Deglise, *Photodegradation and photostabilisation of wood–the state of the art*, Polymer Degradation and Stability, 88 (2005) 268-274.

[123] A. Martin, *Intrinsic viscosity of cellulose*, Industrial & Engineering Chemistry, 45 (1953) 2497-2499.

[124] L. Tolvaj, O. Faix, *Artificial ageing of wood monitored by DRIFT spectroscopy and CIE L* a* b* color measurements. 1. Effect of UV light*, Holzforschung-International Journal of the Biology, Chemistry, Physics and Technology of Wood, 49 (1995) 397-404.

[125] C.-A. Teacă, D. Roşu, R. Bodîrlău, L. Roşu, *Structural Changes in Wood under Artificial UV Light Irradiation Determined by FTIR Spectroscopy and Color Measurements* - A Brief Review, BioResources, 8 (2013) 1478-1507.

[126] R. Singh, N.S. Tomer, S.V. Bhadraiah, *Photo-oxidation studies on polyurethane coating: effect of additives on yellowing of polyurethane*, Polymer Degradation and Stability, 73 (2001) 443-446.

[127] S.-T. Chang, P.-L. Chou, P*hoto-discoloration of UV-curable acrylic coatings and the underlying wood*, Polymer Degradation and Stability, 63 (1999) 435-439.

[128] Y. Irmouli, B. George, A. Merlin, *Artificial ageing of wood finishes monitored by IR analysis and color measurements*, Journal of Applied Polymer Science, 124 (2012) 1938-1946.

[129] P. Evans, H. Matsunaga, M. Kiguchi, *Large-scale application of nanotechnology for wood protection*, Nature Nanotechnology, 3 (2008) 577-577.

[130] M. Vlad Cristea, B. Riedl, P. Blanchet, *Enhancing the performance of exterior waterborne coatings for wood by inorganic nanosized UV absorbers*, Progress in Organic Coatings, 69 (2010) 432-441.

[131] Anonymous, *Global coatings consumption projected to reach 10 billion pounds*, Paint & Coatings Industry, 28 (2012) 8.

[132] F. Bulian, J. Graystone, *Wood Coatings, Theory and Practice*, Elsevier, Amsterdam, The Netherlands, 2009.

[133] N.S. Allen, M. Edge, A. Ortega, C.M. Liauw, J. Stratton, R.B. McIntyre, *Behaviour of nanoparticle (ultrafine) titanium dioxide pigments and stabilisers on the photooxidative stability of water based acrylic and isocyanate based acrylic coatings*, Polymer Degradation and Stability, 78 (2002) 467-478.

[134] S.M. Fufa, B.P. Jelle, P.J. Hovde, P.M. Rørvik, *Coated wooden claddings and the influence of nanoparticles on the weathering performance*, Progress in Organic Coatings, 75 (2012) 72-78.

[135] F. Weichelt, R. Emmler, R. Flyunt, E. Beyer, M.R. Buchmeiser, M. Beyer, *ZnO-Based UV Nanocomposites for Wood Coatings in Outdoor Applications*, Macromol. Mater. Eng., 295 (2010) 130-136.

[136] V. Landry, B. Riedl, P. Blanchet, *Nanoclay dispersion effects on UV coatings curing*, Progress in Organic Coatings, 62 (2008) 400-408.

[137] B. Müller, U. Poth, *Coatings formulation*, Vincentz Network Hannover, (2006).

[138] C.E. Corcione, M. Frigione, *UV-cured polymer-boehmite nanocomposite as protective coating for wood elements*, Progress in Organic Coatings, 74 (2012) 781-787.

[139] E. Araújo, R. Barbosa, A. Rodrigues, T. Melo, E. Ito, *Processing and characterization of polyethylene/Brazilian clay nanocomposites*, Materials Science and Engineering: A, 445 (2007) 141-147.

[140] S. Eichhorn, C. Baillie, N. Zafeiropoulos, L. Mwaikambo, M. Ansell, A. Dufresne, K. Entwistle, P. Herrera-Franco, G. Escamilla, L. Groom, *Review: current international research into cellulosic fibres and composites*, Journal of Materials Science, 36 (2001) 2107-2131.

[141] T. Nishino, I. Matsuda, K. Hirao, *All-cellulose composite*, Macromolecules, 37 (2004) 7683-7687.

[142] D. Fengel, G. Wegener, *Wood: chemistry, ultrastructure, reactions*, Walter de Gruyter, Munich, Germany, 1983.

[143] D. Klemm, B. Heublein, H.P. Fink, A. Bohn, *Cellulose: fascinating biopolymer and sustainable raw material*, Angewandte Chemie International Edition, 44 (2005) 3358-3393.

[144] D. Bondeson, A. Mathew, K. Oksman, *Optimization of the isolation of nanocrystals from microcrystalline cellulose by acid hydrolysis*, Cellulose, 13 (2006) 171-180.

[145] M.N. Angles, A. Dufresne, *Plasticized starch/tunicin whiskers nanocomposite materials. 2. Mechanical behavior*, Macromolecules, 34 (2001) 2921-2931.

[146] D. Dubief, E. Samain, A. Dufresne, *Polysaccharide microcrystals reinforced amorphous poly (β-hydroxyoctanoate) nanocomposite materials*, Macromolecules, 32 (1999) 5765-5771.

[147] M.A.S. Azizi Samir, F. Alloin, J.-Y. Sanchez, A. Dufresne, *Cellulose nanocrystals reinforced poly (oxyethylene)*, Polymer, 45 (2004) 4149-4157.

[148] J. Nagyvary, *The chemistry of a Stradivarius*, Chemical and Engineering News, 66 (1988) 24-31.

[149] S. Rengasamy, V. Mannari, *Development of soy-based UV-curable acrylate oligomers and study of their film properties*, Progress in Organic Coatings, 76 (2013) 78-85.

[150] G. Wuzella, A.R. Mahendran, U. Müller, A. Kandelbauer, A. Teischinger, *Photocrosslinking of an Acrylated Epoxidized Linseed Oil: Kinetics and its Application for Optimized Wood Coatings*, Journal of Polymers and the Environment, 20 (2012) 1063-1074.

[151] Y. Xia, R.C. Larock, *Vegetable oil-based polymeric materials: synthesis, properties and applications*, Green Chemistry, 12 (2010) 1893-1909.

[152] B. van Leeuwen, P. Cordfunke, *Improved saturated polyester and alkyl coatings from renewable, bio-based building blocks*, Paint & Coatings Industry, 29 (2013) 32.

[153] M. Romany, D. Shuping, A. Hirani, W.L. Yong, *Cellulose nanocrystals for drug delivery*, in: ACS symposium series, Oxford University Press, Oxford, UK, 2009, pp. 81-91.